THE INFLUENCE OF MASS TRANSFER ON DESIGN CRITERIA IN LIQUID EXTRACTION

A thesis

submitted in partial fulfilment

of the requirements for the Degree

of

Doctor of Philosophy in Chemical Engineering

in the

University of Canterbury

by

A.A. Espie

University of Canterbury

1977

To my wife Jennyfer

" If a man will begin with certainties,

He shall end with doubts,

But if he will be content with doubts,

He will end in certainties. "

Francis Bacon.

ACKNOWLEDGEMENTS

Thanks must go to my supervisor, Dr E.E.Graham, for his helpful advice and criticisms during this project.

Thanks must also go to the technical staff of the Chemical Engineering Department for their assistance in constructing the apparatus. In particular Messrs Colin Campbell and Neville Foot deserve credit for meeting numerous requests made invariably at short notice.

The author was the recipient of a University Grants Committee Postgraduate Scholarship during this project and the project itself was funded by U.G.C.grants C73/23 and C73/44.

Finally thanks must go to my wife for her patience and support, and not least, for translating my handwriting into type.

CONTENTS

ABSTRACT

An investigation into dispersed phase holdup and the droplet size distribution in a counter-current flow packed column, and in particular, into the effects of mass transfer, has been performed using the toluene - acetone - water system in a 15cm ID column with a packed height of 1.40m of 1.6cm OD ceramic Raschig rings.

The holdup data, obtained as a function of flowrates, was qualitatively similar to that of other authors. The presence of a third component resulted in small reductions in holdup due to changes in physical properties except when transfer was out of the dispersed phase. Then, substantial coalescence resulted in reductions in holdup of up to 50%. The data were first analysed using the slip velocity model of Gayler et al (1953). This was approximately obeyed with the effects of continuous phase flowrate not being fully correlated. However, the model of droplet motion used to predict the slope of the slip velocity function was inadequate, especially when mass transfer induced coalescence was occuring. A new model of droplet motion was developed based on the integral volumetric flowrate of all droplet sizes.

The droplet size distributions were controlled by breakup criteria except when transfer was out of the dispersed phase. Then, the coalescence occuring meant that the distribution was an equilibrium between breakup and coalescence. A relatively large distribution was formed at the column inlet and breakup of this occured over more than 60% of the packed height. The impaction mechanism of Ramshaw and Thornton (1967) was important in the breakup of the larger droplets. As the droplet size decreased, restriction breakup by instability and force balance mechanisms became more important. The flow structure within the packing strongly influenced

the rate of breakup. These factors were confirmed using a computer simulation to reproduce the experimental distributions.

INTRODUCTION

Liquid-liquid extraction is a method of separating the components of a solution by distributing between two immiscible or partly miscible liquids. Although it has always been widely used in the laboratory as a separation technique, the industrial use of liquid-liquid extraction was initially limited to applications where distillation was impractical.

The first large scale use was in the petroleum industry in the 1930's for separating aromatics from kerosene, and in the coal tar industry for the recovery of phenols. Spectacular successes in the nuclear and pharmaceutical industries have resulted in a resurgence of interest in liquid-liquid extraction and it is now regarded as a separation technique in its own right. Applications of this technique are now very diverse and range from the traditional fields already mentioned through heavy chemical processes, metallurgical separations, food processing, and more recently, waste treatment. Hanson, (1971), contains a review of many of the most significant applications which are currently in use, or are being developed.

One popular type of contactor has been the packed column. This is a variation of the simple spray column and relies upon gravity both to interdisperse the phases, and to produce the counter-current flow. The simple spray column is a very inefficient device because of the unhindered backmixing that occurs in the continuous phase as a result of entrainment by the countercurrently moving dispersed phase. The introduction of some form of packing into the column can substantially reduce the backmixing and increase the mass transfer by increasing the interfacial area. The presence of the packing however, reduces the free cross-sectional area of the column, so reducing the capacity. Thus, packed columns have been popular for applications requiring only a few transfer units and moderate capacities.

Many other types of contactor have been developed for various applications. These vary in the manner of operation - stagewise or continuous; in the method of dispersing the phases - by gravity or by mechanical agitation; and in the method of producing counter-current flow - by gravity or by centrifugal force. A recent review has been done by Logsdail and Lowes, (1971).

There are two aspects to the design of a packed extraction column. The height of the column is determined by the height of a transfer unit, or HTU, and the number of transfer units, or NTU, required for a given separation. Methods for calculating these are presented in standard texts (Treybal, 1963). The HTU is found to be inversely proportional to the overall mass transfer coefficient and the interfacial area. The mass transfer coefficient is dependent on the droplet size distribution, and upon the flow regime prevailing in the contactor. The interfacial area is determined by the droplet size distribution and the holdup of the dispersed phase in the contactor.

The column diameter is determined by the desired capacity and the flooding characteristics of the packing. The holdup of dispersed phase in the column increases with increases in the phase flowrates until, at some critical point, entrainment in the continuous phase outlet occurs and the column floods. The behaviour of the holdup with changes in flowrates and the droplet size distribution, is therefore important. The holdup and droplet size distribution are thus important in determining both the height and diameter of a column.

The methods for calculating holdup and droplet size which are presented in standard texts are invariably based upon data obtained with pure mutually saturated phases. However, it is known that in some cases the presence of a third component can result in significantly different behaviour. Johnson and Bliss, (1946), reported that droplet sizes in industrial spray columns were larger when transfer of a solute was out of the dispersed phase. Similar results have been reported for

unsaturated phases in a packed column, (Gayler, Roberts and Pratt, 1953, Gayler and Pratt, 1953b), and for a rotating disc column, (Thornton and Pratt, 1953). The effect is reversed for holdup,with substantial reductions being reported when the transfer of a solute was out of the organic phase, (Gayler and Pratt, 1957b).

It was thus felt desirable to initiate a study of the influence of mass transfer on holdup and the droplet size distribution in a packed column. Such a study would improve the fundamental understanding of these parameters and could lead to improvements in the design techniques which are currently in use.

The objectives of this study were thus:

(1) To construct a packed liquid-liquid extraction column, to obtain data on,and elucidate the factors controlling holdup and the droplet size distribution in the column.

(2) To obtain data on the influence of mass transfer on the holdup and droplet size distribution.

SECTION I

EXPERIMENTAL EQUIPMENT AND PROCEDURE

CHAPTER ONE

EQUIPMENT

Chapter contents.

EXPERIMENTAL APPARATUS

The experimental apparatus consisted of a six inch diameter packed column with a closed loop pumping cycle. Water was used as the heavy phase, toluene as the light phase, with acetone being used as a solute. The feed and the solvent were pumped from storage tanks through flowmeters into the column. Flow through the column was countercurrent with the toluene dispersed. Phase separation occured in a settling zone at the top of the column. The interface position could be adjusted by controlling the heavy phase flow from the column. A small centrifical pump was used to return the heavy phase to the storage tanks while the light phase returned by gravity flow.

Figure 1 - 1 shows the line diagram of the apparatus.

I COLUMN

The column consisted of sections of six inch diameter thick-walled QVF glass tubing. An"equal-T" section was used at the bottom of the column to insert the light phase distributor into the packing. Use of twelve inch sections for the packing allowed easy variation of the packing height between zero and 1.4m. A further T section was used above the packing to provide a photographic chamber.

The heavy phase was fed into the column using a QVF feed section immediately above the photographic chamber. A stainless steel baffle placed beneath the inlet acted as a weir and deflected the jet of continuous phase that might otherwise have unduly effected droplet size distributions at the packing surface.

Two stainless steel probes were used to sample the phases at the top of the packing. These consisted of 5mm OD tube supported by a length of 16mm OD tube. A stainless steel cone was attached to the dispersed phase probe to provide sufficient area for droplet collection.

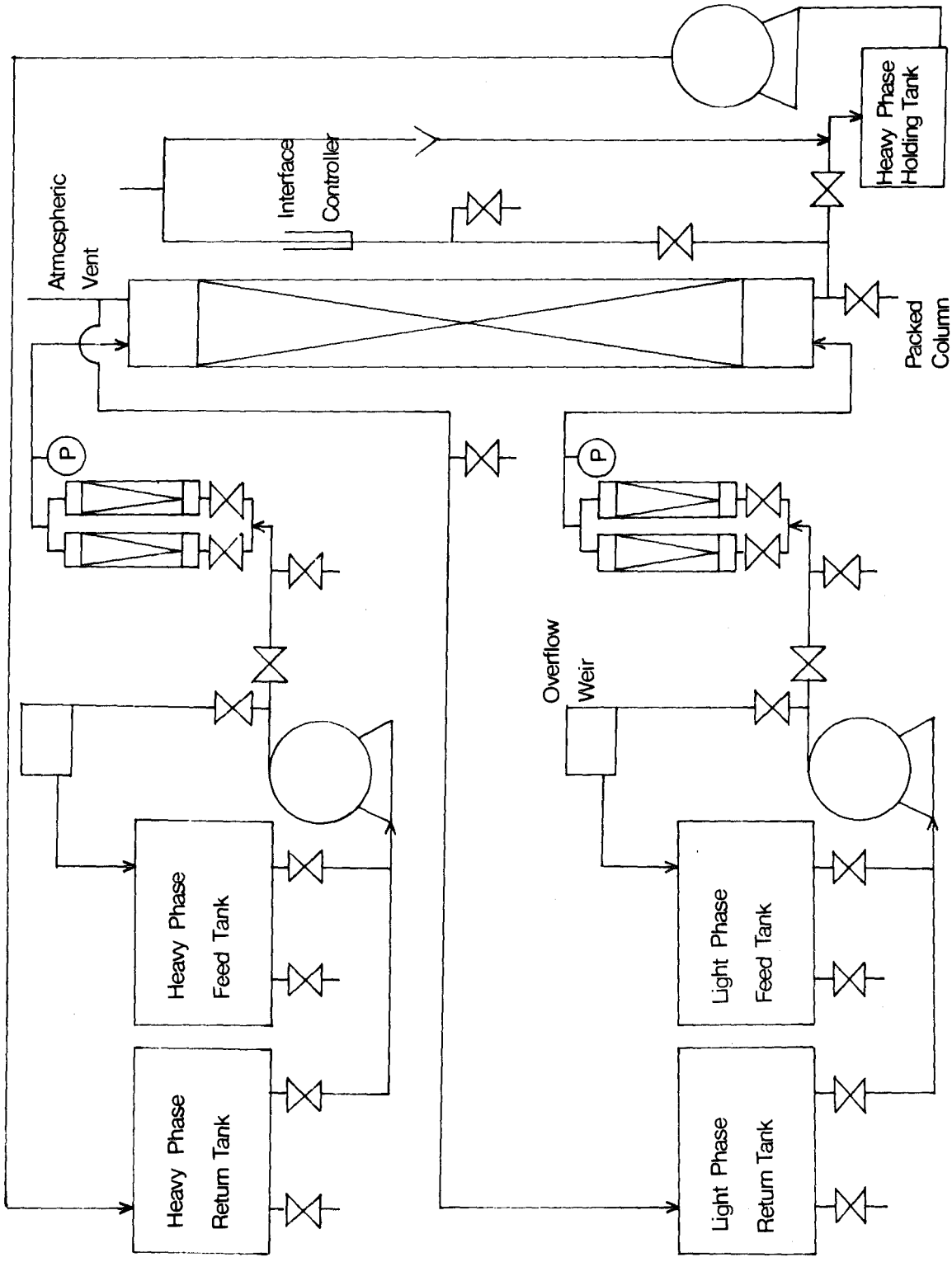

FIGURE 1 - 1 LINE DIAGRAM OF APPARATUS

The probes could be lowered through the photographic chamber to take a sample and withdrawn when photographs were taken. The point of entry at the top of the column was sealed with PTFE packed sliding joints. See figure 1 - 2.

The packing used was 16mm OD ceramic Raschig rings supplied by Crown Lynn Potteries Limited. This was supported by a stainless steel grid placed at the bottom of the T section. This consisted of 3mm diameter wire on a 10mm spacing welded into a 6mm thick stainless steel flange. No further support was used for the packing and a re-distributor for the dispersed phase was not found necessary.

Figures 1 - 3 and 1 - 4 show the column.

II PUMPS, PIPING, TANKS

Four 250 litre stainless steel tanks were used to hold the inlet and outlet streams. These were provided with two take-off points flush with the bottom of the tank. One was used as a drain, the other as an outlet. The tanks had flanged tops and could be sealed when necessary. The four were arranged as two pairs of one above the other. Liquid could be pumped from the bottom tank to the top one of a pair and could flow by gravity from top to bottom. However, liquid could not be pumped from one pair to the other, except through the column. It was possible to pump liquid from the top tank through an overflow weir back into the tank. This, however, was found to be insufficient to give good mixing in the tank. A $\frac{1}{4}$ HP induction motor with a 7.5cm diameter six-bladed turbine was used to prepare a tank of feed solution and to saturate the solvent when required. A 200 l high density polyethylene tank was used to hold the heavy phase outlet stream before it was pumped back to the storage tanks. Tests were carried out to check the effect of the liquids used on high density polyethylene and no leaching was detected.

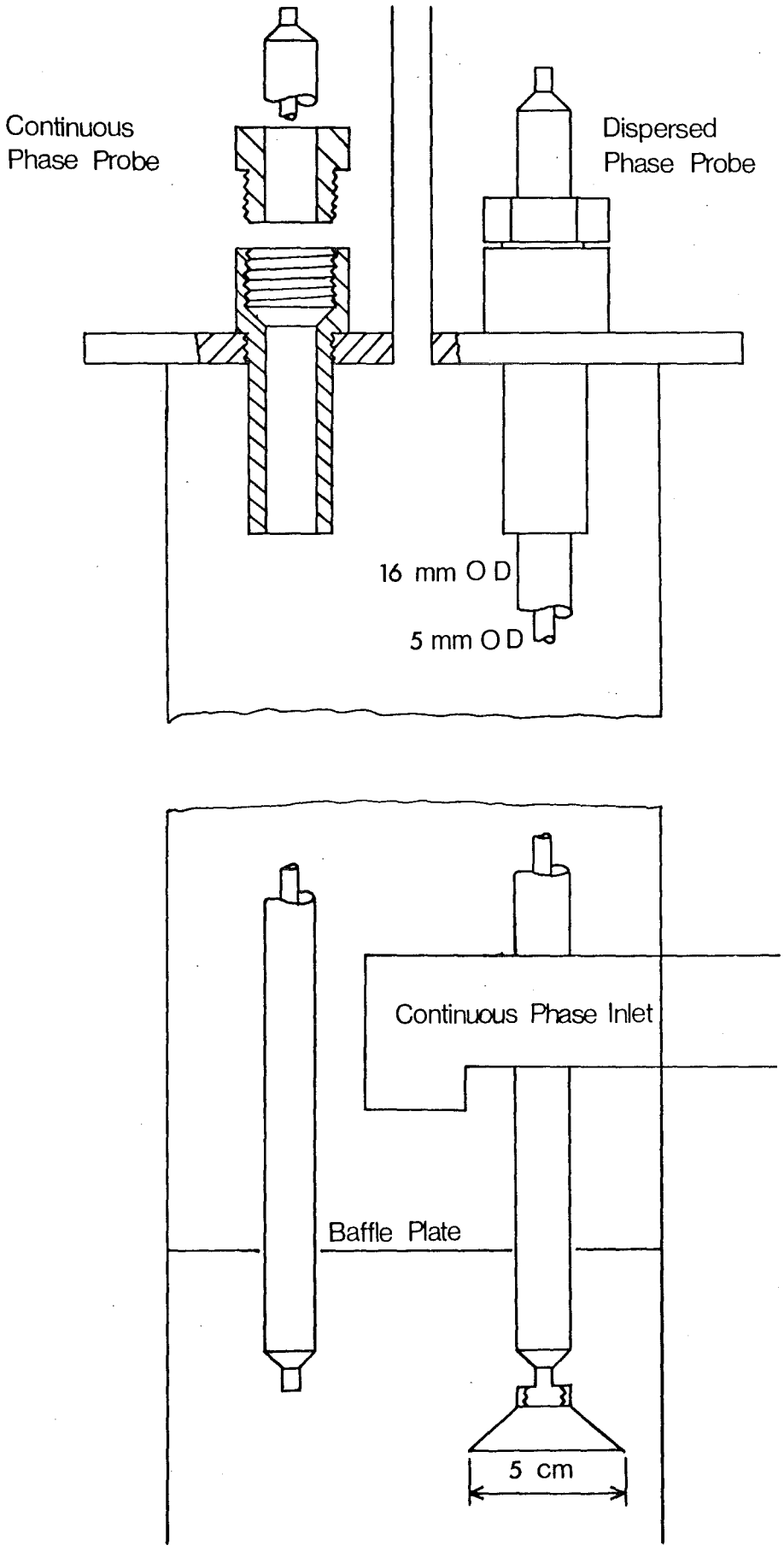

FIGURE 1 - 2 SAMPLING PROBES

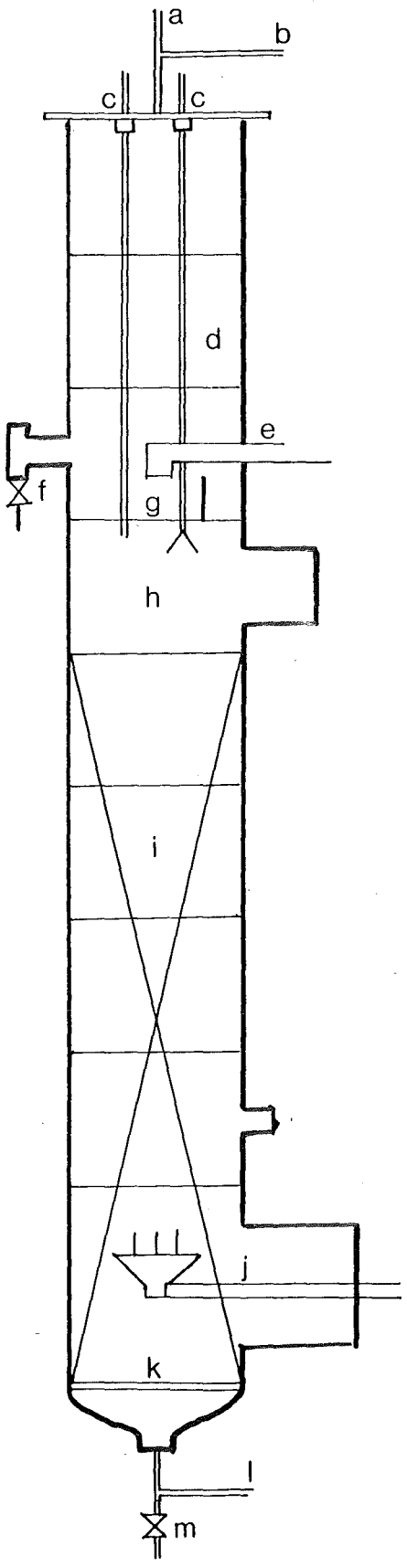

a Atmospheric vent

b Dispersed phase outlet

c Sampling probes

d Settling zone

e Continuous phase inlet

f Interface drain

g Baffle plate

h Photographic chamber

i Packing

j Dispersed phase distributor

k Packing support

l Continuous phase outlet

m Drain

FIGURE 1 – 3 GENERAL COLUMN ARRANGEMENT

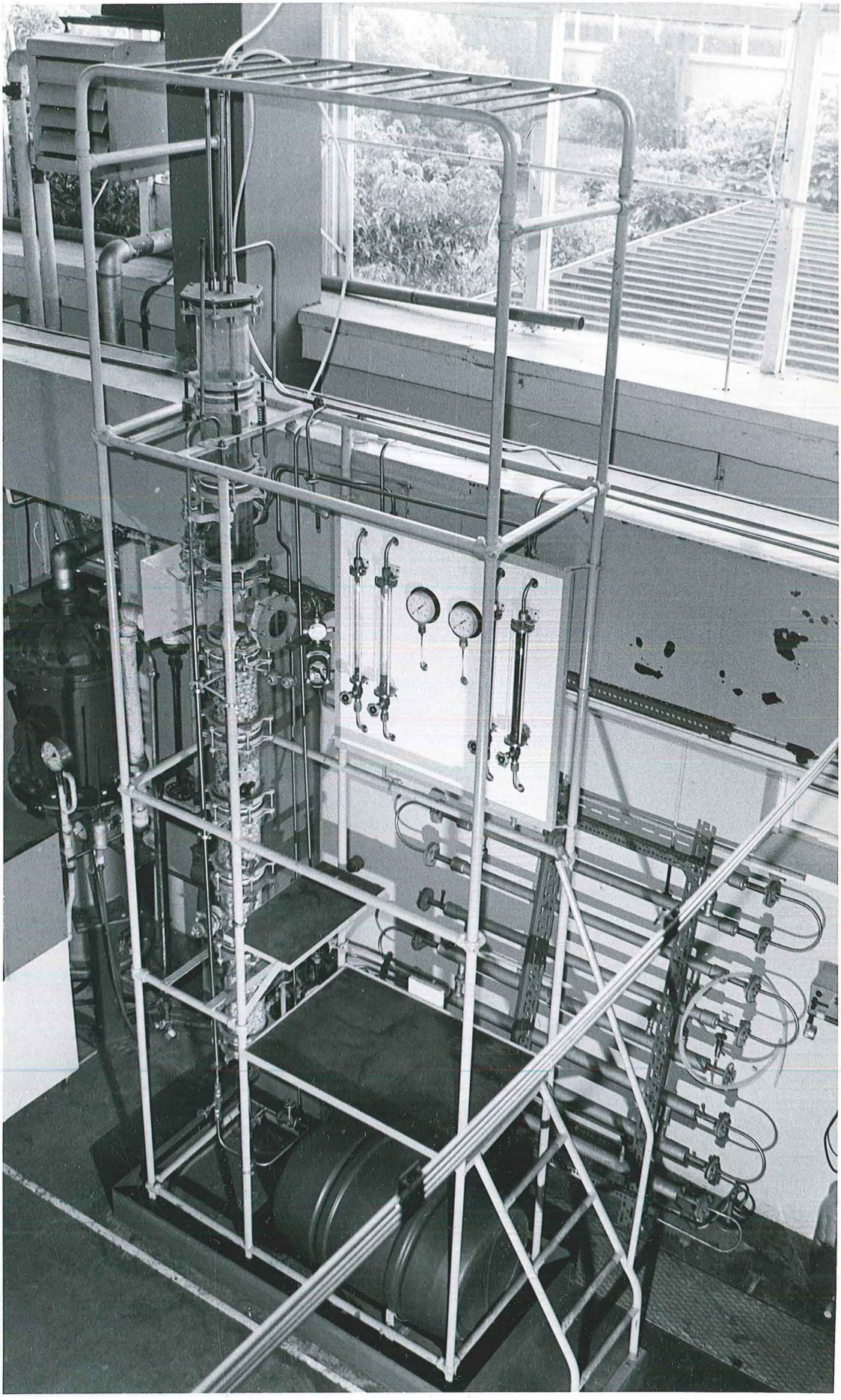

FIGURE 1 – 4 THE COLUMN

Two stainless steel centrifical pumps (Brown Brothers, model 3900) driven by $\frac{1}{4}$ HP electric motors were used to pump the feed and solvent through the column. These were sealed in explosion-proof casings to eliminate the risk of fires. The heavy phase outlet stream was returned to the holding tanks by a centrifical pump (Charles Austin model C25) driven by an induction motor. The body of the pump was made of rigid polypropylene and the impellor was made of a less dense grade of polypropylene. The impellor, however, proved very sensitive to even very small quantities of toluene, swelling to such an extent that the pump jammed. It was necessary to replace it with an impellor machined from stainless steel.

The pipework consisted of 13mm and 16mm OD stainless steel tubing. Connections between piping, tanks, pumps, and column were by flanged joints using PTFE sheathed asbestos gaskets. PTFE flexible couplings were used on the pump outlets to reduce the amount of vibration transmitted.

PTFE lined Saunders valves isolated the storage tanks from the pumps. Downstream of the pumps 13mm QVF glass valves directed flow to the column or through the overflow weir to the top tanks. Flowrates through the rotameters were regulated by commercial needle valves packed with PTFE. Stainless steel valves made in the department workshops were used to control the heavy phase outlet flow and hence interface position. QVF glass valves were used on sampling ports on inlet and outlet lines.

III FLOW METERING AND INTERFACE CONTROL

A metric 14 G and a 24 G rotameter supplied by the Rotameter Manufacturing Co. were used in parallel for each phase to meter flowrates. These were calibrated in place. Maximum flowrates were limited by pump capacity to 5.5 litres/min of heavy phase and 4 litres/min of light phase.

The interface position was controlled by adjusting the pressure drop across the heavy phase outlet. This stream split into two parts. One went directly into the holding tank and adjusting the valve on this line gave a coarse control. The second went through an inverted U arm, vented at the top, into the holding tank. The upper part of the U arm could move in a PTFE packed sliding joint and adjustment of the height of this gave fine control of the interface position.

IV DISTRIBUTOR

Trials were performed to find a distributor which gave as uniform a drop size distribution as possible. Initial trials were carried out with the distributors shown in figure 1 - 5a. These were most unsatisfactory and examination of the hydrodynamics showed it was not possible to generate a uniform population with them. The design suggested by Lewis, Jones and Pratt, (1951) figure 1 - 5b was next tried and proved satisfactory. The most uniform distribution of drops is obtained by adjusting the baffle within the cone to a pressure drop significantly higher than fluid inertial effects. In most cases, however, the distribution of drop sizes was sufficiently uniform without using the baffle. Nine nozzles of 4.8mm ID were chosen. This arrangement maximises the range of flowrates which lie between the jetting point and the transition point to sinuous flow, this region giving the most uniform droplet size distribution.

V PHOTOGRAPHY

A small T section was used at the top of the packing to provide a chamber for photography. The exposed end of this was sealed with plate glass enabling photographs to be taken with none of the refraction problems of photography through curved sections.

The camera used was an Asahi Pentax Spotmatic with Kodak HP4

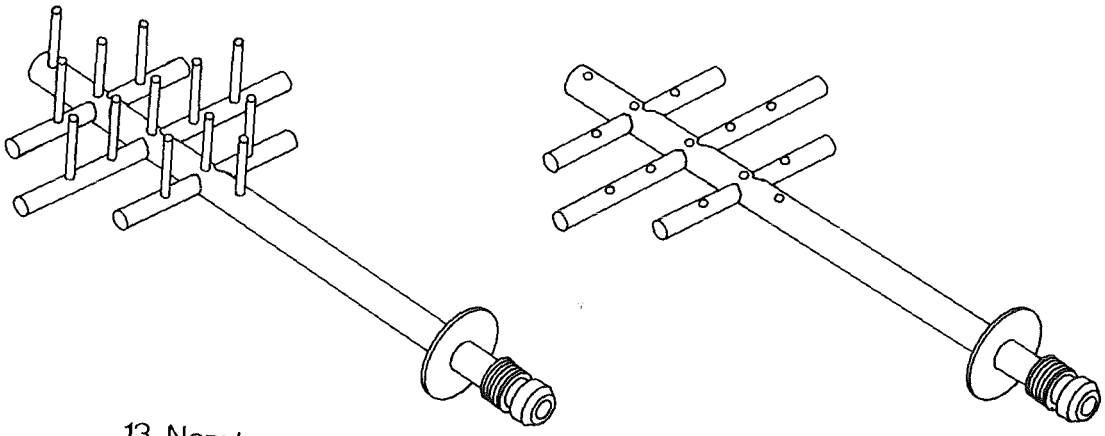

a Distributors 1 - A and 1 - B

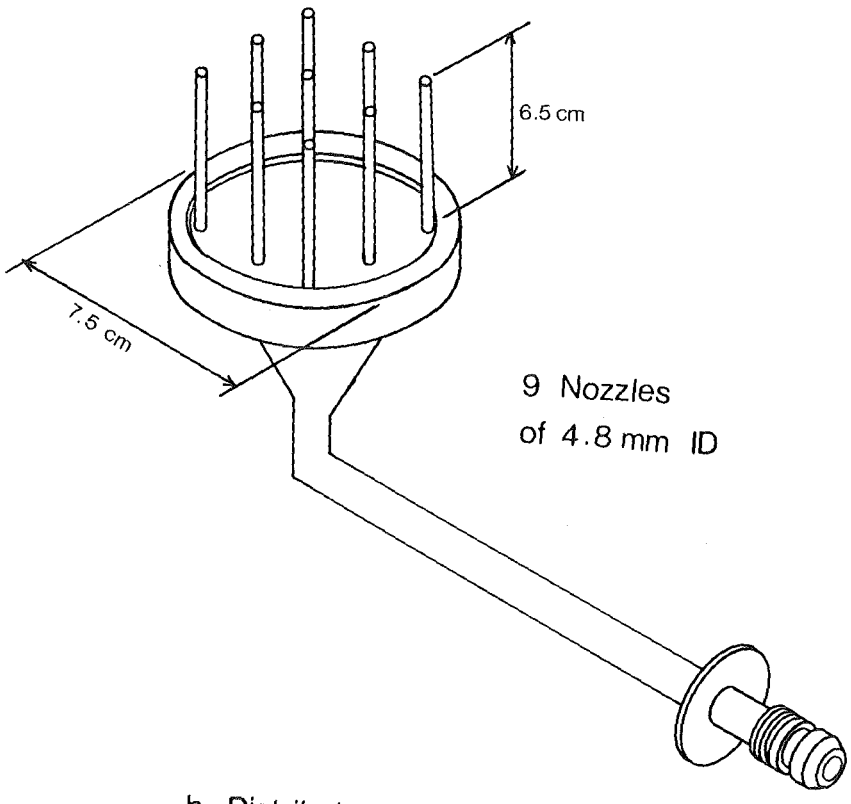

b Distributor 2

FIGURE 1 - 5 DISPERSED PHASE DISTRIBUTORS

negative film exposed at 1000 ASA for $\frac{1}{1000}$ sec. Light was provided by a 500W photo-flood lamp through a frosted glass screen at the rear of the column. The rest of the section was painted black to minimise reflections. A small stainless steel marker was bolted to the baffle at the top of the section and was present in all photographs, giving a scale factor when the images were magnified.

The arrangement is shown in figure 1 - 6.

In order to contrast the colourless toluene against the colourless water a non-surface active dye was added to the toluene. This was Oil Red A manufactured by Du Pont and Co.

VI PHYSICAL PROPERTIES

The density, viscosity, interfacial tension and when relevant, solute concentration were monitored for both phases.

Density was measured using standardised hydrometers, these being calibrated using a pyknometer. Viscosity was measured using an Ostwald capilliary viscometer, size A. This was not calibrated with a master viscometer and could be up to 3% in error due to surface tension effects. Surface tension was measured using a Fisher ring tensiometer with an expected accuracy of 4%. Refractive index was the property chosen to measure the solute concentration. This was measured with a Zeiss Abbie refractometer giving mole fraction data accurate to $\pm$.0005. The temperature of the phases was recorded but no attempt was made to control it.

VII MISCELLANEOUS

The pressure in the system could be monitored with pressure gauges on the inlet lines downstream of the rotameters.

The pressure drop across the distributor could be measured using a manometer giving a toluene over water reading. This was usually

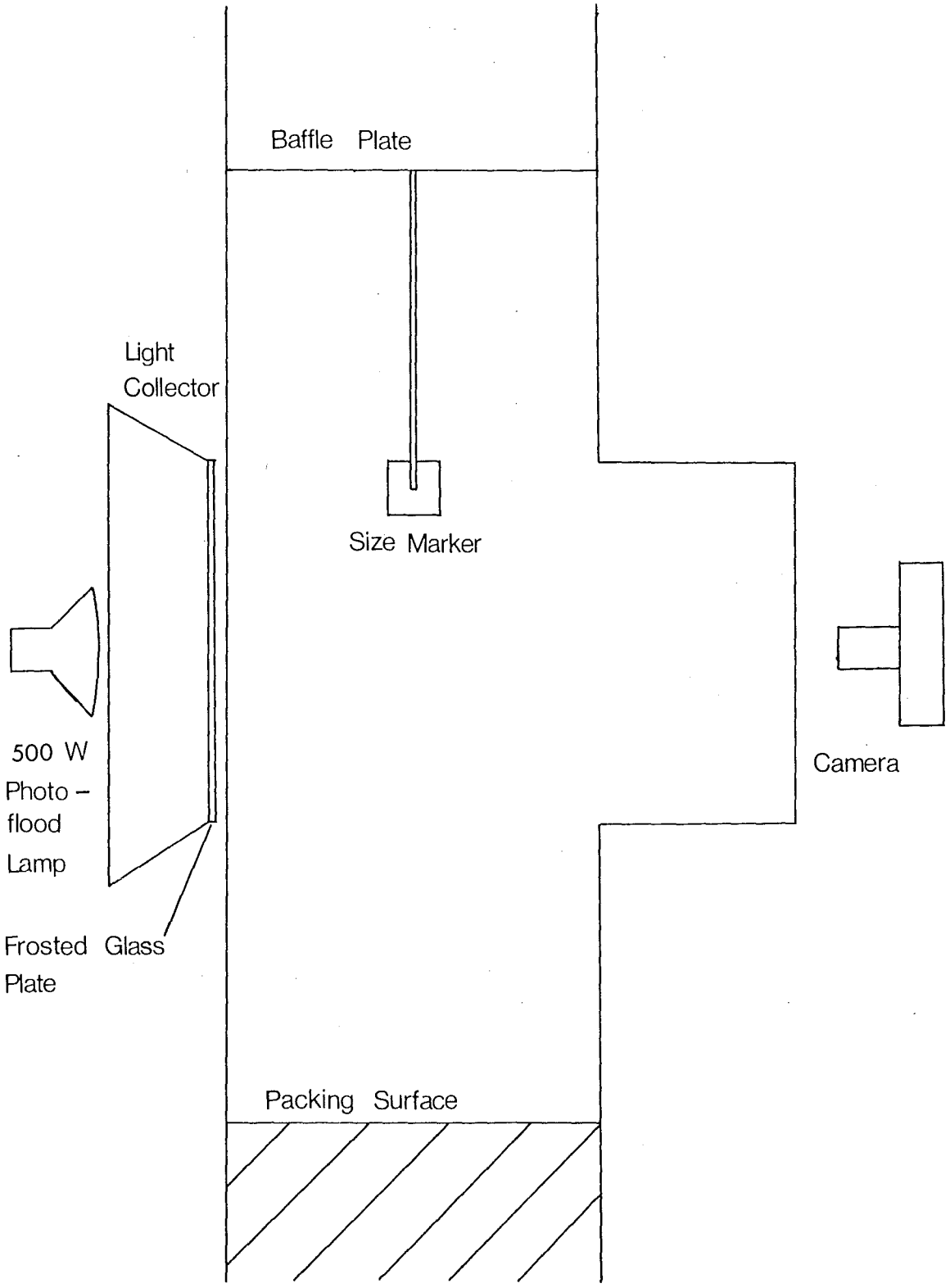

FIGURE 1 – 6 PHOTOGRAPHIC CHAMBER

isolated from the system using PTFE packed stainless steel valves.

Toluene is rated as a Class 3 fire hazard by the American National Fire Protection Association and forms explosive mixtures with air in the volume range 1.4 - 1.6%. Toluene in a confined space can reach these concentrations at ambient temperature and the vapour is heavier than air. Further a TLV of 200ppm is recommended to avoid chronic liver damage. It is thus a material deserving some safety precautions:

Electric motors used were induction motors, or in the case of main pumps were sealed in explosion proof cases.

Electrical switches were of the type suitable for explosive atmospheres according to the N.Z.Standard 379 (1959).

The toluene tanks were kept sealed as much as possible and vapour concentrations were periodically checked using Drager tubes to make sure they remained below 200 ppm.

CHAPTER TWO

EXPERIMENTAL PROCEDURE

Chapter contents.

I COLUMN ASSEMBLY

Before assembly the column sections were cleaned with chromic acid and the packing was rinsed in tap water to remove dust. The packing was then hand sorted to remove broken and chipped rings. When the bottom T section was in place it was half filled with packing. The distributor was then inserted into the section and the space around it filled with packing. The rest of the column was then assembled and half filled with water. Loading of the rest of the packing was done a hand - full at a time through the top T section. Filling the column with water not only avoided damage to the packing elements, but also pre-soaked them ensuring that they would be wet by the continuous phase in later work.

The stainless steel tanks and piping were de - greased with acetone then flushed thoroughly with tap water. Finally several hundred gallons of tap water were circulated through the apparatus before use.

II LIQUIDS USED

The light phase used was industrial toluene supplied by the Shell Oil Company in 200 litre drums. A chromatograph analysis of this showed a minor impurity, (less than $\frac{1}{2}\%$), which is believed to have been benzene. As heavy phase, city tap water, with a pH of 7.4 - 7.8, was used. Industrial acetone supplied by Hempthorne & Prosser Limited in 180 litre drums was used as a solute in mass transfer experiments.

The toluene and water were presaturated before proceeding with experiments. This was done by cycling the liquids through the column approximately ten times.

III SOLUTION PREPARATION

For runs with no mass transfer the feed and solvent were used in the mutually saturated condition with no further preparation.

For mass transfer runs the approximate volume of solute required for the concentration desired was calculated and added to the feed tank. This was then mixed using a $\frac{1}{4}$ HP induction motor with a 7.5 cm six-bladed turbine for fifteen minutes. The concentration was then checked and the procedure repeated if necessary. If water was used as solvent a fresh tank was used for each run. This, then needed to be saturated with toluene, and the mixer was used to blend it in until a layer just formed on the surface of the water. When toluene was used as solvent it was necessary to strip it of all acetone between each run. This was done by cycling it through the column with fresh tap water until the concentration of acetone was less than 0.1%.

IV RUN PROCEDURE

An experimental run consisted of the following steps:

(1) The column was filled with water to the bottom of the settling zone. Water, saturated with toluene only, was used in all cases.

(2) The flowrates were selected and the rotameters adjusted.

(3) The phase interface was positioned by manipulating the U - arm and valves on the heavy phase outlet. The response time of the column for changes in the U - arm varied with flowrates but was usually in excess of five minutes.

(4) The temperature and density of the feed and solvent were measured. For mass transfer runs 100ml samples were taken to measure the concentration of solute and interfacial tension.

(5) The column was left to come to steady state. The column was judged to be at steady state for non-mass transfer runs if the phase interface remained steady for fifteen minutes. This could normally be achieved in thirty to forty minutes. It was necessary to sample the outlet concentrations for mass transfer runs to ensure these had stabilised. The time required for this varied greatly with flowrate,

going from seventy five minutes at the lowest flowrates to thirty minutes at the highest.

(6) Temperature and density of the outlet streams were measured. One hundred millilitre samples were taken on mass transfer runs, both of the outlet streams and from the packing surface.

(7) The droplet size distribution was photographed.

(8) The position of the phase interface was noted and all valves were closed simultaneously.

(9) The free holdup was left to settle out. Ten minutes was found to be sufficient for this.

(10) The holdup was calculated from the time taken for a given flow of heavy phase to displace the interface back to its original position.

In several cases the column was found to flood. The column was taken to be flooded when a layer of toluene droplets appeared beneath the distributor. It was found that when this happened the layer slowly increased in size until toluene was being entrained in the heavy phase outlet.

V PHOTOGRAPHIC PROCEDURE

A series of five or ten photographs was taken for any flowrate. This was selected to give a droplet polulation of about five hundred. Collins and Knudsen, (1970) found that a population of two hundred and fifty gave reproducible size distributions for droplet breakup in pipes. Trials with this equipment showed differences between populations of one hundred and seventy and five hundred, but no significant difference between populations of five hundred and one thousand.

The film was developed in undiluted Microphen for eighteen minutes. The size distributions were measured by projecting the film images, using a standard photographic enlarger, onto graph paper. This technique allowed magnification of 2 - 4 times actual size. Projection

of the marker that appeared in every photograph allowed easy identification of the magnification factor. By covering the graph paper with a sheet of perspex the drops could be crossed out with a Chinagraph pencil as they were measured. The counting strategy was to measure all droplets for which the major and minor axes could be unambiguously determined. This thus excluded only those droplets which were obscured by other droplets, or were too out of focus to be measured.

Typical photographs are shown in Figure 2 - 1.

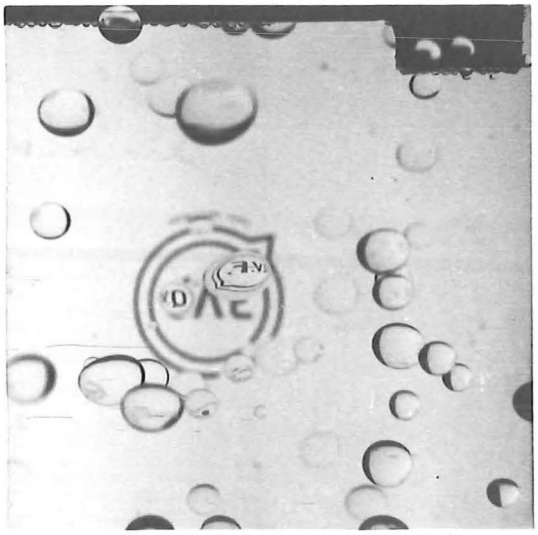

a Pure Phases

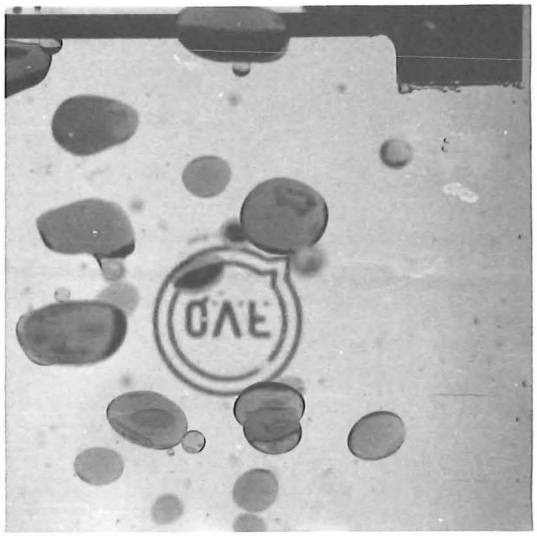

b Mass Transfer

Toluene to Water

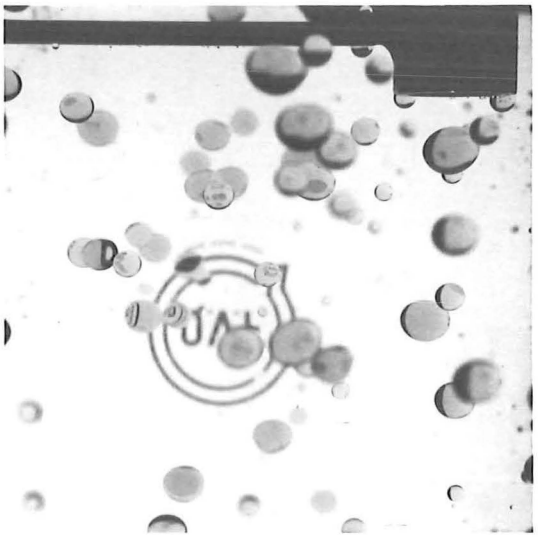

c Mass Transfer

Water to Toluene

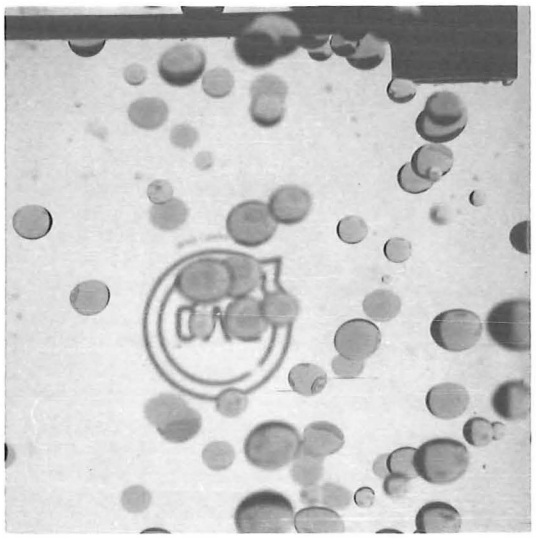

d Saturated Phases

FIGURE 2 – 1 TYPICAL DROPLET PHOTOGRAPHS

SECTION II

HOLDUP IN PACKED COLUMNS

INTRODUCTION

The term holdup in liquid-liquid extraction refers to the volumetric fraction of the free space in the column which is occupied by the dispersed phase. Holdup is thus an important variable in determining the interfacial area between the phases and hence the rate of mass transfer. It is also important in the hydrodynamic design of contactors. When the dispersed phase holdup exceeds a critical value a layer of dispersed phase builds up beneath the distributor and entrainment in the continuous phase outlet occurs - the column is said to be flooded. A knowledge of the holdup behaviour with changes in phase flowrates is thus important in design.

A number of investigations into dispersed phase holdup in packed columns have been reported in the literature: Gayler and Pratt (1951), Gayler, Roberts and Pratt (1953), Wicks and Beckmann (1955), Markas and Beckmann (1957), Johnson and Lavergne (1961), Sitaramayya and Laddha (1961), Watson and McNeese (1973). With the exception of Sitaramayya and Laddha (1961), these investigations have been confined to the behaviour of mutually saturated pure phases. Measurements of holdup during mass transfer (Gayler and Pratt, 1957a), especially transfer out of the dispersed phase, have indicated that significant changes of behaviour may occur under such conditions. Thus it was felt desirable to collect a new set of data which would allow the direct comparison of holdup behaviour for the pure phases and for conditions of mass transfer. Measurements of holdup under conditions of an equilibrium distribution of a solute between the phases enables the effects of mass transfer to be distinguished from those of physical property changes.

The section consists of four chapters. In chapter three a survey of the published literature on holdup in packed columns is presented. Analysis of experimental measurements of holdup in terms

of the literature model (Gayler, and Pratt, 1951, Gayler, Roberts and Pratt, 1953) is presented in chapters four and five for the pure phases and conditions of mass transfer respectively. Finally, chapter six deals with proposed modifications to the literature model.

CHAPTER THREE

LITERATURE SURVEY

Chapter contents.

DISPERSED PHASE HOLDUP

Appel and Elgin, (1937) measured extraction coefficients, $K_w a$, and holdup for the extraction of benzoic acid between toluene and water in spray and packed columns. The similarities between plots of $K_w a$ and holdup against flowrates indicated that the major effects occuring could be attributed to changes in the interfacial area of the phases. Holdup was found to be only slightly dependent on the continuous phase flowrate and, at low flowrates, linearly dependent on the dispersed phase flowrate. Measurement of holdup values was by drainage of the column.

Row, Koffolt and Withrow, (1941) used a 22cm ID packed column to study the toluene - benzoic acid - water system. Thirteen mm unglazed Berl saddles, 13mm unglazed Raschig rings and knitted copper cloth were used as packing materials. Points noted were a sharp increase in holdup just before flooding occured, and, a similarity between the shapes of plots $K_w a$ and holdup against flowrates. Measurement of holdup was done by simultaneously shutting off all flows to and from the column and measuring the volume of continuous phase needed to restore the interface to its steady-state position.

Allerton, Strom and Treybal, (1943) used a 9cm ID column packed with 13mm diameter carbon Raschig rings to measure extraction rates, holdup and capacity in a comparitive study between sieve tray columns and packed columns. The system kerosene - benzoic acid - water was used and holdup was measured by the interface correction method. Results similar to previous studies (Appel and Elgin, 1937, Row, Koffolt, and Withrow, 1941) were found, but, it was noted that the dispersed phase rose through the column as continuous rivulets rather than as droplets.

Gier and Hougen, (1953) used a 15cm ID column packed with 13mm and 10mm unglazed Raschig rings to study concentration gradients in the diethyl ether - adipic acid - water system. Holdup was calculated from

the change in interface position and reported data show a linear dependence on dispersed phase flowrates for a given continuous phase flowrate.

The most extensive attack on the problem has been carried out by Gayler and Pratt, (1951, 1953, 1957a), and Gayler, Roberts and Pratt, (1953). Dispersed phase holdup was measured for five water - organic systems using 7.5cm, 15cm and 30cm ID columns and a wide variety of ceramic Raschig rings and ceramic Berl saddles as packing. The holdup measured by the volume change at the interface was termed the normal holdup. The residual dispersed phase trapped in the packing interstices, termed the permanent holdup, was measured by drainage of the column.

For a wide range of organic solvent - aqueous systems, a characteristic relationship between normal holdup and flowrates was found:

(1) At low dispersed phase flowrate holdup varied linearly with flowrate.

(2) At some critical point the holdup began to increase rapidly. Flooding of the column occured in this region for many systems.

(3) For some systems with high coalescence rates, a further region was found in which the holdup was almost independent of flowrate.

The effect of increasing the continuous phase flowrate was small in the linear region but hastened the transition to rapidly increasing holdup.

Concluding that the permanent holdup played only a small part in the mass transfer processes, Gayler, Roberts and Pratt correlated the normal holdup in the linear and rapidly increasing regions with the equation:

$$V_d + \frac{x}{1-x} V_c = \epsilon \bar{V}_o \, x \, (1-x) \qquad (3\text{-}1)$$

where V_d and V_c are superficial velocities of the dispersed and continuous phases respectively, x is the fractional holdup, ϵ the

fractional voidage of the packing and $\overline{V}_o$ is a characteristic droplet velocity. The authors assume that the characteristic velocity is equal to the time average velocity of a droplet accelerating from rest over an average path length. By fitting a function for path length to experimental data a graphical correlation for $\overline{V}_o$ was presented.

In a later paper by Gayler and Pratt, (1957b) extensive holdup data is given for systems with acetone transferring in both directions between water and four organic solvents. Transfer of acetone from the organic phase to the aqueous was found to result in substantially lower holdups than transfer in the reverse direction. The reason for these differences was attributed to coalescence but no investigation was made into them. Holdup data for the system water - uranyl nitrate - methyl isobutyl ketone in a packed column has also been presented by these authors.

Sitaramayya and Laddha, (1961) found that their data for the extraction of acetone from water in a 5cm ID packed column using three organic solvents was correlated by equation (3-1). Their experimental values of $\epsilon \overline{V}_o$ together with values calculated using the correlation of Gayler, Roberts and Pratt, (1953) were correlated with the equation

$$\overline{V}_o = 0.683 \left[\frac{a}{\epsilon^3} \frac{\rho_c}{\Delta \rho g} \right]^{\frac{1}{2}} \qquad (3\text{-}2)$$

where a is the superficial area of the packing.

Wicks and Beckmann, (1955) found, that for the toluene - water system in 7.5cm, 10cm and 15cm ID columns packed with Raschig rings, a separate line was required for each continuous phase flowrate when using the Gayler, Roberts, Pratt model. Lewis, Jones and Pratt, (1951) noted that for small diameter packings droplet motion was not by free rise but rather resulted from the impaction of following drops. To account for this Wicks and Beckmann defined three types of holdup:

(1) Free holdup - the volume of dispersed phase which rises freely to the interface due to buoyancy forces.

(2) Operational holdup - the volume of dispersed phase which is active in mass transfer.

(3) Total holdup - the total value of dispersed phase within the packing at any time.

The total holdup was correlated using four arbitary parameters

$$X_T = A\ V_d^r + B\ V_d\ V_c^s \qquad (3\text{-}3)$$

The free holdup was measured by the interface volume method. The column was then mechanically pulsed to remove the remainder of the operational holdup. The residual holdup was found by column drainage. The reproducibility of results after repacking was found to be much improved if the packing was settled by blowing it with air.

Markas and Beckmann, (1957) used isotope tagged toluene droplets to study flow characteristics in a 15cm ID column packed with Raschig rings. Two things were found:

(1) The dispersed phase holdup displays a hysteresis effect when the phase flowrates are taken past the loading point. This hysteresis holdup forms part of the permanent holdup and is permanently trapped within the packing.

(2) All the non-hysteresis permanent holdup, i.e. that measured by drainage of the column after the free holdup has settled out, moves slowly through the packing.

Johnson and Lavergne, (1961) obtained data for a 10cm ID column packed with Raschig rings and Interlox saddles. Three aqueous-organic solvent systems were used. The normal or free rising holdup was measured by the interface volume method and the residual or permanent holdup determined by column drainage. Improvements in reproducibility were again noted when air was used to settle the packing after dumping. To correlate the total holdup the approach of Sakiadis and Johnson, (1954) was used, whereby a Bernouilli balance is done over both phases.

The resulting equation was rearranged in the form:

$$A\left[\frac{V_c}{V_d}\right]^{2-n}\left[\frac{x}{1-x}\right]^3 + B = \frac{x^3}{V_d^{2-n}} \qquad (3\text{-}4)$$

where A,B,n are constants for a particular system. In practice it was found necessary to use the equation in the form:

$$A\,\frac{V_c^{\,r}}{V_d^{1.5}}\left[\frac{x}{1-x}\right]^3 + B = \frac{x^3}{V_d^{1.5}} \qquad (3\text{-}5)$$

where r is an adjustable parameter.

Johnson et al (1971) extended the study of packed columns to high density difference systems by using liquid metals countercurrently to water. Holdup was measured by introducing cold water into the column to freeze the metal droplets. The holdup ranged from 15 to 35% for 5mm saddles and from 10 to 25% for 6mm Raschig rings. This was greater than that predicted by correlations (Gayler, Roberts and Pratt, 1953, Sitaramayya and Laddha, 1961),

Watson and McNeese, (1973) and Watson, McNeese et al, (1975) studied the mercury - water system in 2.5cm and 5cm ID columns packed with a variety of materials. Holdup was measured from the volume change at the interface when flows were simultaneously stopped. Correlation of the holdup was done using a slip velocity defined as:

$$\frac{V_d}{x} + \frac{V_c}{1-x} = V_s \qquad (3\text{-}6)$$

Although considerable scatter was found when V_s was plotted against x, the authors claimed it could be considered approximately constant over the range of flowrates used. The characteristic velocity $\overline{V}_o$ defined by Gayler, Roberts and Pratt, (1953) varied through the range in an apparently systematic manner. This is related to V_s by:

$$\overline{V}_o = \frac{V_s}{1-x} \qquad (3\text{-}7)$$

NOMENCLATURE

a - superficial packing area (cm^2/cm^3)

$A, B, r, s,$ - constants in equation (3-3) (-)

g - gravitational acceleration $(cm^2\ s^{-1})$

n - constant in equation (3-4) (-)

V_c - superficial velocity of continuous phase $(cm^3 s^{-1}/cm^2)$

V_d - superficial velocity of dispersed phase $(cm^3 s^{-1}/cm^2)$

$\overline{V}_o$ - characteristic velocity as defined by equation (3-1) $(cm\ s^{-1})$

V_s - slip velocity $= \frac{V_d}{x} + \frac{V_c}{1-x}$ $(cm\ s^{-1})$

x - free rising holdup of dispersed phase (-)

X_T - total holdup of dispersed phase (-)

ϵ - packing void fraction (-)

ρ_c - continuous phase density $(g\ cm^{-3})$

$\Delta\rho$ - phase density difference $(g\ cm^{-3})$

CHAPTER FOUR

PURE PHASE HOLDUP BEHAVIOUR

Chapter contents.

THEORY

The literature survey revealed three analyses of holdup in packed columns: that of Gayler, Roberts and Pratt, (1953) based on the relative slip velocity of the phases, that of Wicks and Beckmann, (1955) based on dimensional analysis, and that of Johnson and Lavergne, (1961) based on a Bernouilli pressure balance over a section of the packing. The model of Gayler, Roberts and Pratt was selected as being the most fundamental and giving the best insight into the physical processes occuring. As such, it would be the easiest to modify to account for any changes in mechanism occuring during mass transfer.

I MODEL DERIVATION

(1) Slip Velocity

The derivation of the model is as follows:

The mean rate of rise of the dispersed phase droplets relative to the column is:

$$\overline{V} = \frac{V_d}{\epsilon x} \qquad (4\text{-}1)$$

where V_d is the dispersed phase superficial velocity, x is the fractional holdup, and ϵ is the packing voidage. The mean rate of rise relative to the continuous phase is thus:

$$\overline{V}_r = \frac{V_d}{\epsilon x} + \frac{V_c}{\epsilon(1-x)} \qquad (4\text{-}2)$$

By analogy with hindered settling of solid suspensions (Steinour, 1944) $\overline{V}_r$ is expressed in terms of a modified Stokes law velocity, where the buoyancy force is proportional to the difference between the density of the mixed phase and the dispersed phase.

Thus:

$$\bar{V}_r = \frac{2 C_o d^2 g(\rho_m - \rho_d)}{36 \mu_c} \phi(1-x) \qquad (4-3)$$

where C_o is a constant to correct for wall drag and

$$\rho_m = x \rho_d + (1-x) \rho_c \qquad (4-4)$$

The factor $\phi(1-x)$ allows for the interferance of drops with each other. Substituting for ρ_m.

$$\bar{V}_r = \frac{2 C_o d^2 g(\rho_c - \rho_d)(1-x)}{36 \mu_c} \phi(1-x) \qquad (4-5)$$

$$= C_o V_s (1-x) \phi(1-x) \qquad (4-6)$$

where V_s is the Stokes law velocity of an isolated sphere.

Eliminating $\bar{V}_r$ between equations (4-2) and (4-6) gives:

$$\frac{V_d}{\epsilon x} + \frac{V_c}{\epsilon(1-x)} = C_o V_s (1-x) \phi(1-x) \qquad (4-7)$$

The hindered settling factor $\phi(1-x)$ was shown to be constant and equal to unity by plotting

$$\frac{V_d}{x(1-x)} + \frac{V_c}{(1-x)^2} \quad \text{against } 1 - x$$

and using the boundary conditions

$$(1-x) \rightarrow 1.0 \text{ as } V_d \rightarrow 0 \qquad (V_c = 0)$$

Thus, rearranging:

$$V_d + \frac{x}{1-x} V_c = \epsilon \bar{V}_o x (1-x) \qquad (4-8)$$

where $\bar{V}_o$ has been substituted for $C_o V_s$. This can be interpreted as the limiting mean velocity of a droplet at zero continuous flowrate and very low dispersed phase flowrate. It is referred to as the characteristic

velocity. Plotting $V_d + \frac{x}{1-x} V_c$ against $x(1-x)$ should, therefore, give straight lines through the origin with slope $\epsilon \bar{V}_o$.

(2) Characteristic Velocity

The passage of a droplet through a packed section of a column can be modelled by assuming that the droplet accelerates from rest to some fraction of its terminal velocity. It is then stopped by collision with a packing element and the process is repeated up the column. The characteristic velocity must be defined in terms of an average path length and average time between collisions.

$$\bar{V}_o = \bar{s} / \bar{t} \qquad (4\text{-}9)$$

If the packing is large enough for the drops to be able to move freely, then $\bar{s}$ should be a function of the packing shape and size, and $\bar{t}$ should be a function of the physical properties of the system and the drop terminal velocity.

Taking a force balance over an accelerating drop:

$$\frac{4}{3}\pi\frac{d^3}{8} C_d \frac{d^2s}{dt^2} = \frac{4}{3}\pi\frac{d^3}{8}\Delta\rho g - C_d \pi \frac{d^2}{4} \frac{\rho_c}{2}\left(\frac{ds}{dt}\right)^2 \qquad (4\text{-}10)$$

If flow is chiefly within the Stokes law region then:

$$C_d = \frac{24}{Re}, \qquad V_s = \frac{d^2 \Delta\rho g}{18\mu_c}$$

Substituting in (4-10), and rearranging:

$$\frac{d^2s}{dt^2} = \frac{\Delta\rho g}{\rho_d}\left[1 - \frac{1}{V_s}\left(\frac{ds}{dt}\right)\right] \qquad (4\text{-}11)$$

Equation (4-11) is an ordinary differential equation and can be integrated using the boundary conditions,

$$s = \frac{ds}{dt} = 0 \quad \text{at} \quad t = 0$$

$$s = \bar{s} \quad \text{at} \quad t = \bar{t}$$

to give:

$$\bar{s} = V_s \bar{t} \left[1 - \frac{\varrho_d V_s}{\Delta\varrho g \bar{t}} \left(1 - \exp\left[- \frac{\Delta\varrho g \bar{t}}{\varrho_d V_s} \right] \right) \right] \qquad (4\text{-}12)$$

Since $\bar{V}_o = \bar{s} / \bar{t}$ and substituting the actual terminal velocity of the drop for the Stokes law V_s:

$$\frac{\bar{V}_o}{V_t} = 1 - \frac{\varrho_d V_t \bar{V}_o}{\Delta\varrho g \bar{s}} \left(1 - \exp\left[- \frac{\Delta\varrho g \bar{s}}{\varrho_d V_t \bar{V}_o} \right] \right) \qquad (4\text{-}13)$$

If V_o is used to mean $\bar{V}_o$ in an infinite diameter column and the substitutions:

$$y = \frac{V_o}{V_t}, \qquad z = \frac{\Delta\varrho g}{\varrho_d V_t^2} \bar{s}$$

are made, then:

$$y = 1 - y/z \left[1 - e^{-z/y} \right] \qquad (4\text{-}14)$$

$\frac{V_o}{V_t}$ is thus expressed as a unique function of the physical properties of the system and the average path length between collisions. To express $\bar{s}$ as a function of the packing size, equation (4-14) was plotted on logarithmic coordinates and was found to be represented in the range:

$$0.2 \leqslant \frac{V_o}{V_t} \leqslant 0.6$$

by the approximation:

$$\frac{V_o}{V_t} \simeq 0.346 \left[\frac{\Delta\varrho g \bar{s}}{\varrho_d V_t V_o} \right]^{0.74} \qquad (4\text{-}15)$$

The mean path length can be represented as:

$$\bar{s} = C d_p^n - d_{vs}^o \qquad (4\text{-}16)$$

where d_p is the packing diameter, and d^o_{vs} is the equilibrium droplet size. Lewis et al, (1951) have used dimensional analysis to represent the equilibrium droplet size in the packed colum as:

$$d^o_{vs} = 0.92 \left[\frac{\sigma}{\Delta \rho g} \right]^{\frac{1}{2}} \qquad (4\text{-}17)$$

Then, combining (4-15),(4-16) and (4-17) allows the parameter n to be determined from all the experimental $\bar{V}_o$ data of Gayler, Roberts and Pratt, and by assuming the $\bar{V}_o$ data for a 30cm diameter column to be equivalent to V_o, the parameter C can be determined giving:

$$\bar{s} = 0.38\, d_p - 0.92 \left[\frac{\sigma}{\Delta \rho g} \right]^{\frac{1}{2}} \qquad (4\text{-}18)$$

To correct the characteristic velocity for the effect of the wall void space a simple exponential factor was used:

$$\frac{\bar{V}_o}{V_o} = 1 - \exp\left(- 0.23\, d_c \right) \qquad (4\text{-}19)$$

Thus:

$$y = \frac{\bar{V}_o}{V_t} \left[1 - \exp\left(- 0.23\, d_c \right) \right] \qquad (4\text{-}20)$$

and

$$z = \frac{\Delta \rho_g}{\rho_d V_t^2} \left[0.38\, d_p - 0.92 \left(\frac{\sigma}{\Delta \rho g} \right)^{\frac{1}{2}} \right] \qquad (4\text{-}21)$$

are the new substitutions for equation (4-14). Equation (4-14), based on a force balance over an accelerating droplet , relates the characteristic velocity $\bar{V}_o$, contained in the parameter y, to the physical properties and packing size in the parameter z. This equation requires an iterative calculation to solve and so has been presented in a graphical form (Gayler, Roberts and Pratt, 1953).

EXPERIMENTAL RESULTS

Holdup data was collected for the column as a function of dispersed and continuous phase flowrates. Data was collected through the linear range and up to the flood point. Figures 4 - 1 and 4 - 2 show the holdup plotted against the dispersed phase superficial flowrate V_d. These figures represent data taken for two different drums of toluene. Comparison of chromatographic analyses of drum (1) toluene revealed that a number of low concentration impurities had been introduced into the toluene during use. This was subsequently traced to a faulty neoprene rubber gasket. Analyses of drum (2) toluene before and after use revealed no detectable impurities. Thus figure 4 - 1 represents the system behaviour under the influence of a surfactant, and figure 4 - 2 shows the behaviour of the pure phases.

Both systems follow the patterns found by other investigators (Appel and Elgin, 1937, Row, Koffolt and Withrow, 1941, Allerton, Strom and Treybal, 1943, Gayler and Pratt, 1951, Gier and Hougen, 1953, Gayler, Roberts and Pratt, 1953, Wicks and Beckmann, 1955, Johnson and Lavergne, 1961). Holdup varies linearly with dispersed phase flowrate until some critical point where the holdup begins to increase rapidly. Flooding of the column takes place in this latter region. The continuous phase flowrate is seen not to effect this pattern but rather to displace the point at which the holdup begins to increase rapidly. The dependence of holdup on continuous phase flowrate does, however, vary between drums (1) and (2). The increase in holdup with a change in V_c is much more pronounced for the pure system. As well, the holdup for $V_c = 0$ is 34.5% higher for the pure system.

The Gayler-Pratt model was tested by plotting $V_d + \frac{x}{1-x} V_c$ against $x(1-x)$. Figures 4 - 3 and 4 - 4 give the results for the surfactant and pure systems respectively. Equation (4-8) is seen to satisfactorily represent the linear holdup region. The points which deviate markedly

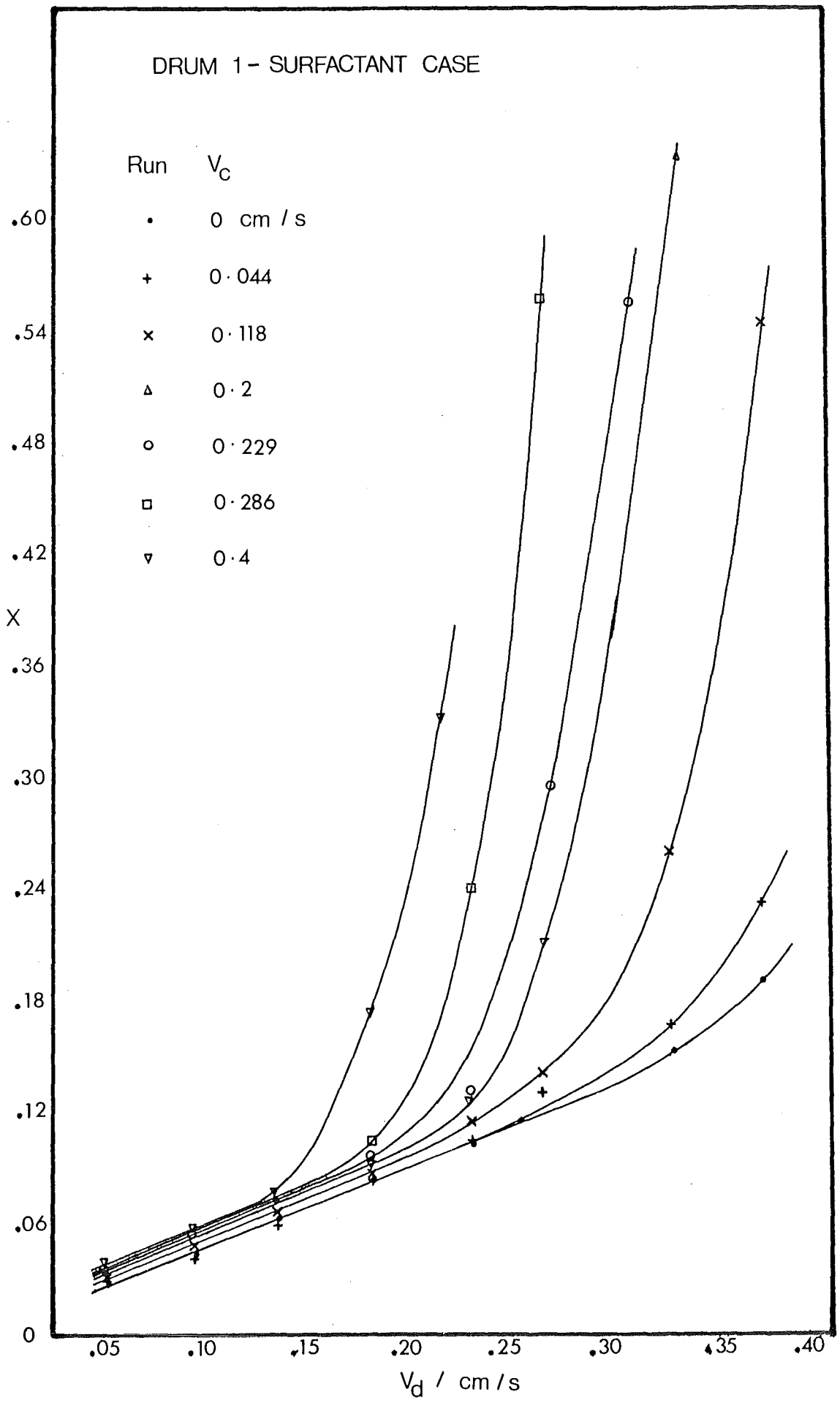

FIGURE 4 - 1 HOLDUP vs FLOWRATES

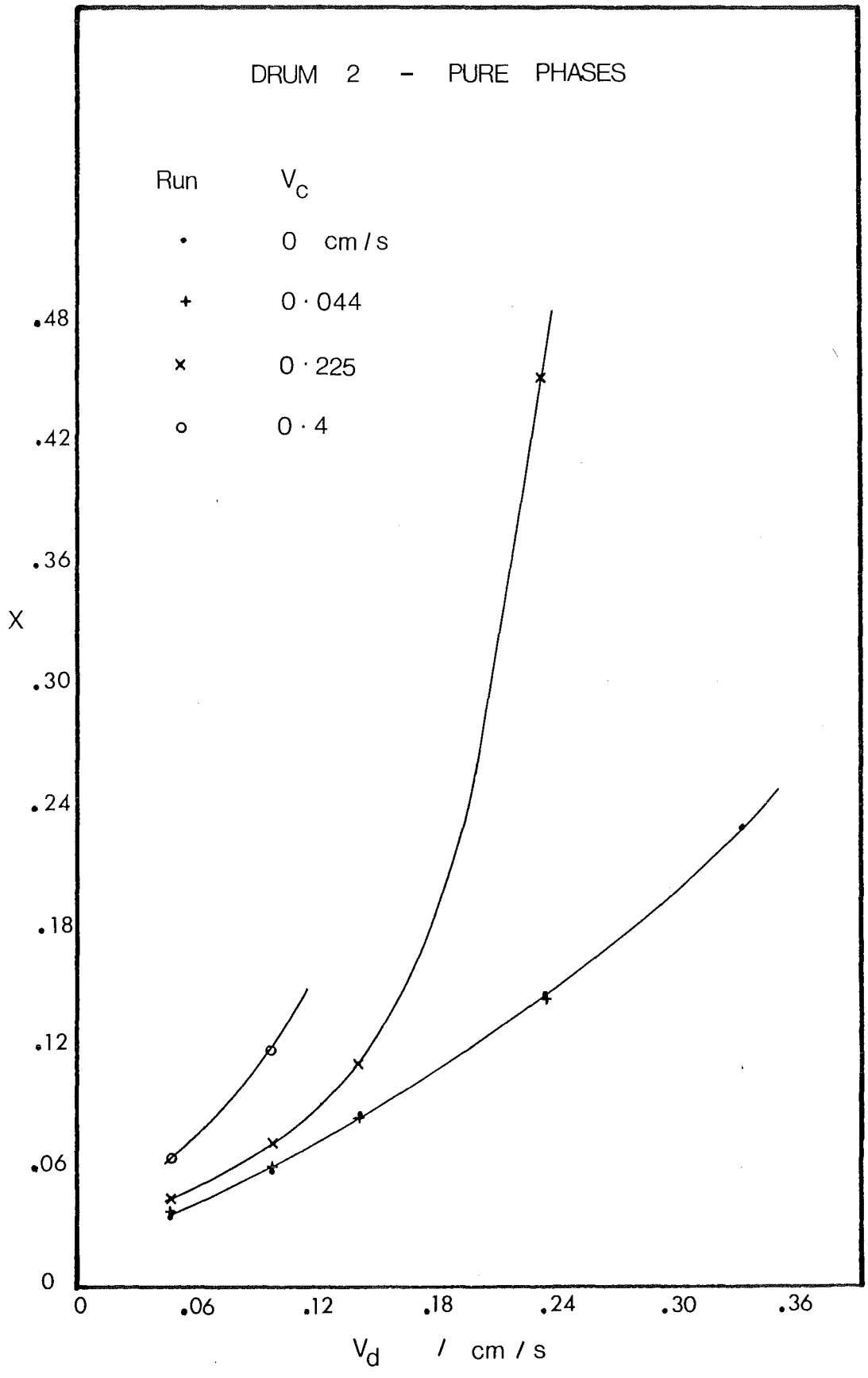

FIGURE 4 - 2 HOLDUP Vs FLOWRATES

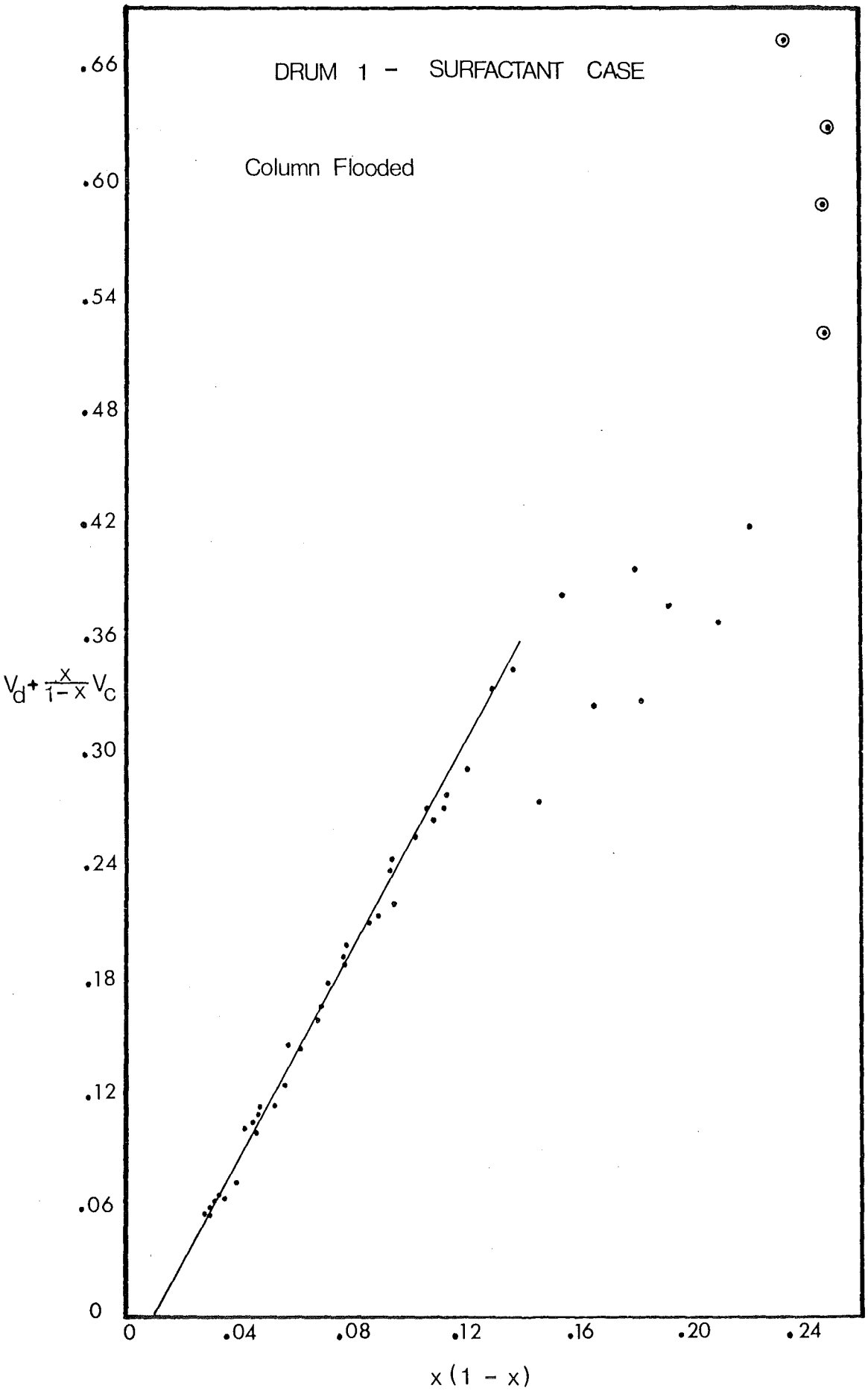

FIGURE 4 - 3 SLIP VELOCITY Vs x(1 - x)

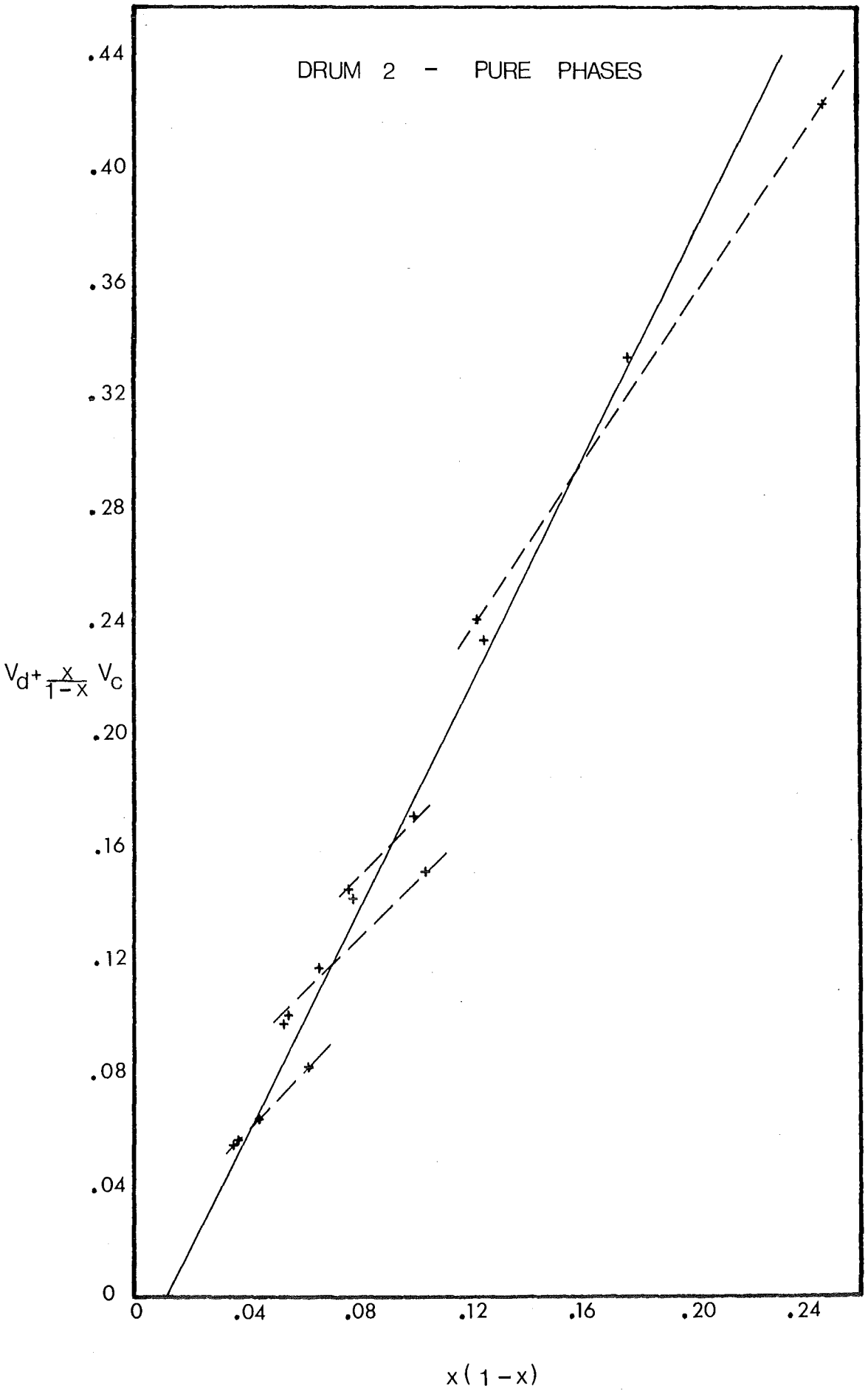

FIGURE 4 - 4 SLIP VELOCITY Vs x (1 - x)

from the straight line representing equation (4-8) all lie in the region of rapidly increasing holdup. For points below flooding this region can be represented approximately by another straight line. This result is contrary to the findings of Gayler, Roberts and Pratt,(1953), who stated that both linear and rapidly increasing holdup regions could be correlated with a single line.

Agreement with equation (4-8), is however, not perfect even in the linear holdup region. Examination of figure 4 - 4 shows that the increase in holdup resulting from an increase in continuous phase flowrate is not totally correlated by the accompanying increase in slip velocity. The result is that the data for each continuous phase flowrate falls on a separate line - a fact noted before by Wicks and Beckmann, (1955). The effect was also present in the surfactant system, but, due to the smaller increase in holdup with continuous phase flowrate, is much reduced. The slope of each line, when data for each continuous flowrate is treated separately, is plotted in figure 4 - 5. The value of $\epsilon\overline{V}_o$ appears to be approximately constant over most of the range for the surfactant system, whereas, for the pure system, there is an apparent trend to lower $\epsilon\overline{V}_o$ values with increasing continuous phase flowrate. However, the number of data points, on which the slopes are based, are statistically too small to justify such a conclusion.

Using the measured physical properties, as given in Appendix I, terminal velocities were calculated for average drop sizes using the Hu-Kintner (1955) correlation. Thus, values of $\overline{V}_o$ could be calculated using equation (4-14). Table 1 compares the predicted values of $\overline{V}_o$ with the averaged experimental values.

TABLE 1.

	$\overline{V}_o$/ cm s^{-1} Experimental	$\overline{V}_o$/ cm s^{-1} Equation (4-14)	Deviation %
Drum (1)	3.05	3.39	+11.1
Drum (2)	2.53	3.27	+29.2

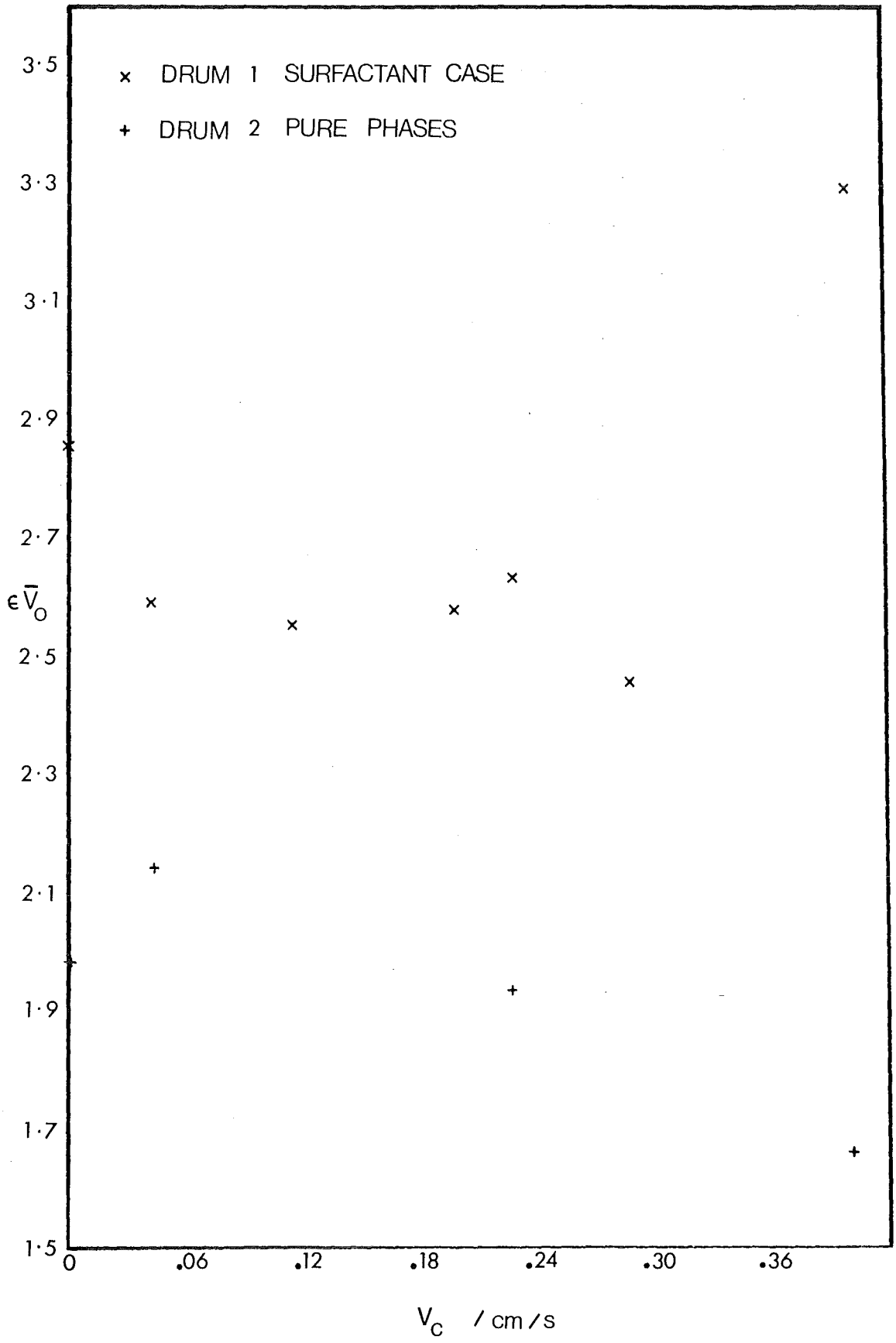

FIGURE 4 - 5 CHARACTERISTIC VELOCITY vs FLOWRATES

Flooding points were determined for four continuous phase flowrates for the surfactant system. Figure 4 - 3 shows that the hollup at flooding is a constant for three out of four flowrates. The fourth point has a higher holdup and is believed to be an error resulting from overshooting the true flood - point. The variation in slip velocity at the flood point confirms the finding of Watson et al, (1975) that the slip velocity at flooding is not neccessarily a constant.

DISCUSSION

The essence of the Gayler, Roberts, Pratt analysis comprises three assumptions:

(1) The behaviour of the system is described by a slip velocity based on the superficial velocities of the phases.

(2) The slip velocity is independent of flowrates, and can be equated to the Stokes law hindered settling velocity of an average droplet moving through the packing.

(3) The average velocity of a droplet in the packing can be modelled as a repeated process of accelerating from rest until it strikes a packing element and so on up the column.

I SLIP VELOCITY CONCEPT

Lapidus and Elgin, (1957) showed that the slip velocity or vectoral velocity difference between the phases was the characterising parameter for vertical-moving fluidised systems, whether the dispersed phase be solid, liquid or gaseous. Experimental support was soon forthcoming for solid-liquid, (Price, Lapidus and Elgin, 1959, Struve, Lapidus and Elgin, 1958), gas-liquid (Bridge, 1962) and liquid-liquid systems, (Beyaert, Lapidus and Elgin, 1961, Weaver, Lapidus and Elgin, 1959). It is now a widely accepted method for the analysis of two phase systems and for liquid-liquid systems has been applied to packed (Gayler, Roberts and Pratt, 1953), spray (Beyaert, Lapidus and Elgin, 1961, Weaver, Lapidus and Elgin, 1959, Dunn, 1963), rotating disc (Strand, Olney and Ackerman, 1962, Misek and Marek, 1970), reciprocating plate (Baird and Lane, 1973) and oscillating baffle columns (Thomas and Weng, 1970).

The concept of universal slip velocity based on superficial phase velocities is, however and idealised one. The critical assumption is that of plug flow between the phases, or, in the case of no continuous

phase flowrate, a stagnant pool. However, studies with bubble columns, (Freedman and Davidson, 1969 and Lockett and Kirkpatrick, 1975), sieve trays, (Beek, 1965), and in fluidisation (Esso Research and Engineering Co., 1967), show that entrainment of the continuous phase by the dispersed phase can cause gross maldistribution of the flow patterns. Freedman and Davidson, (1969) have analysed the so-called Gulf Stream effect, whereby circulation of the continuous phase in a bubble column reduces the effective average vessel holdup. The flow maldistribution was modelled as a tube within a tube with the dispersed phase being channelled into the central tube. Circulation of the continuous phase up the central tube and down the annular space occured due to the differences in hydrostatic head between the annular region and the central tube. Such a model is immediately applicable to a packed column, and may help to explain the processes occuring that cause the splitting of slip velocity function in figure 4 - 4.

A section of packing may be thought of as consisting of a number of regions. Firstly, there exist a number of preferential paths for droplet motion through the packing. Secondly, regions exist where droplet flow is possible, but due to larger numbers of restrictions to negotiate, is less preferable. Thirdly, regions exist where droplets can only enter by back flow. At zero continuous flowrate,flow of the dispersed phase takes place in the preferential channels and over most of the marginal area. Continuous phase recirculation takes place in the marginal areas. When a finite continuous phase flow is superimposed on the column this flow occurs through the marginal areas and effectively reduces the flow area available to the dispersed phase. The actual superficial velocity of the dispersed phase within its channel is thus greater than that given by using the column cross-sectional area.

Such a model also offers an explanation of the two distinct types of behaviour on the holdup-flowrate plots. As the dispersed phase flowrate increases, the flow through the central channels increases

linearly. The maximum possible flowrate through these channels is, however, limited by the rate of droplet rise. Thus, a point is reached where the central channels are saturated and flow is forced into the marginal areas, and holdup increases. When a finite continuous phase flowrate is superimposed on the system the dispersed phase is forced more into the central channels which thus become saturated at a lower dispersed phase flowrate.

II HINDERED SETTLING

Gayler et al assumed that the slip velocity could be equated to the hindered settling velocity of an average droplet in the packing. The hindered settling effect refers to the fact that the slip velocity of a particle moving in a cloud of similar particles differs from that of a single particle in an infinite media. The literature on this subject has been reviewed recently by Barnea and Mizrahi, (1973, 1975) and three factors were given as contributing to the effect. Firstly, the pseudo-hydrostatic effect. The average effective hydrostatic pressure gradient differs from that of the continuous phase alone. Thus, expressions for the driving force should use the effective suspension density ϱ_m rather than the continuous phase density ϱ_c.

$$\varrho_m = \varrho_d \, x + \varrho_c \, (1-x) \qquad (4\text{-}22)$$

Supporting experimental evidence has been provided by Richardson and Meikle (1961). This factor was incorporated by Gayler et al into the expression for the driving force to give:

$$F_B = \frac{\pi}{6} \, d^3 \, \Delta\varrho \, g \, (1-x) \qquad (4\text{-}23)$$

Secondly, Barnea and Mizrahi pointed out that the transfer of momentum between a particle and the continuous phase is hindered by the presence of other particles. This may be modelled by the increase in suspension viscosity which occurs:

$$\frac{\mu_\phi}{\mu_c} = \exp\left[\frac{5x}{3(1-x)}\right] \qquad (4\text{-}24)$$

The applicability of this factor to the packed column is somewhat more doubtful. The droplet size is generally large (5 - 6mm) compared with the size of the channel (packing element ID = 12mm). Motion is thus closer to chain bubbling than to the movement of a cloud of particles. Furthermore, the correction applies to a steady-state flow situation rather than the modelled situation of a droplet accelerating from rest. No allowance for this factor was made by Gayler et al.

Finally, Barnea and Mizrahi pointed out that the dissipation of energy by friction between the continuous phase and the walls of the container causes an additional effect which may be modelled by:

$$\frac{V_{t\phi}}{V_t} = \frac{1}{1 + x^{\frac{1}{3}}} \qquad (4\text{-}25)$$

The coefficients in equations (4-24) and (4-25) were found by fitting data from six different sources (Barnea and Mizrahi, 1973). The applicability of this expression is also effected by the relative size of the droplets and the channel. However, wall drag has a well documented effect on the terminal velocity of single droplets moving inside tubes (Uno and Kintner, 1956, Strom and Kintner, 1958, Harmathy, 1960). The work of Strom and Kintner, (1958) indicates that:

$$V_t = V_{t\infty}\left[1 - \left(\frac{d}{D}\right)^2\right]^{1.43} \qquad (4\text{-}26)$$

where V_t is the droplet terminal velocity in an infinite tank, and d, D are the diameters of the droplet and the tube respectively. Thus, the correction for wall drag may be incorporated into the characteristic velocity. Equation (4-7) can be rearranged in the form:

$$\frac{V_d}{x(1-x)} + \frac{V_c}{(1-x)^2} = \epsilon\, \bar{V}_o\, \phi\, (1-x) \qquad (4\text{-}27)$$

A plot of $\frac{V_d}{x(1-x)} + \frac{V_c}{(1-x)^2}$ versus $(1-x)$ appears in figure 4 - 6. When $V_c = 0$ and $V_d \rightarrow 0$ then $(1-x) \rightarrow 1$, hence:

$$\frac{V_d}{x(1-x)} + \frac{V_c}{(1-x)^2} \rightarrow \epsilon \bar{V}_o \text{ as } (1-x) \rightarrow 1.0$$

The data is not constant over the range. However, the slip velocity is based on the average free holdup and the superficial velocities based on the total column area. It is thus impossible to separate those effects due to hindered settling and those due to flow maldistribution.

III FLOW REGIME

In addition to equating the slip velocity to the hindered settling velocity of an average droplet, Gayler et al assumed that flow occured in the Stokes law regime. Equating drag and buoyancy forces gives:

$$V_{t\infty} = \sqrt{\frac{4}{3} \frac{d \Delta\rho g(1-x)}{\rho_c C_d}} \qquad (4\text{-}28)$$

Droplet terminal velocities in an infinite tank give, for a 5mm diameter droplet, a Reynolds number of 625. This is well into the intermediate region of the Reynolds number - drag coefficient curve and in this region

$$C_d \propto Re^{-\frac{1}{2}} \qquad (4\text{-}29)$$

Thus, substituting in equation (4-28) gives:

$$V_t \propto (1-x)^{\frac{2}{3}} \qquad (4\text{-}30)$$

However, all experimental evidence shows dependence on $(1-x)$, i.e.

$$C_d \propto \frac{1}{Re}$$

which is the Stokes law region. For a single particle in an infinite tank Stokes law is valid for $Re < 2$. For a 5mm diameter droplet this implies:

$$V < 0.04 \text{ cm s}^{-1}$$

For a 5mm diameter toluene droplet inside a 12mm ID packing element

$$V_t = 9.4 \text{ cm s}^{-1}$$

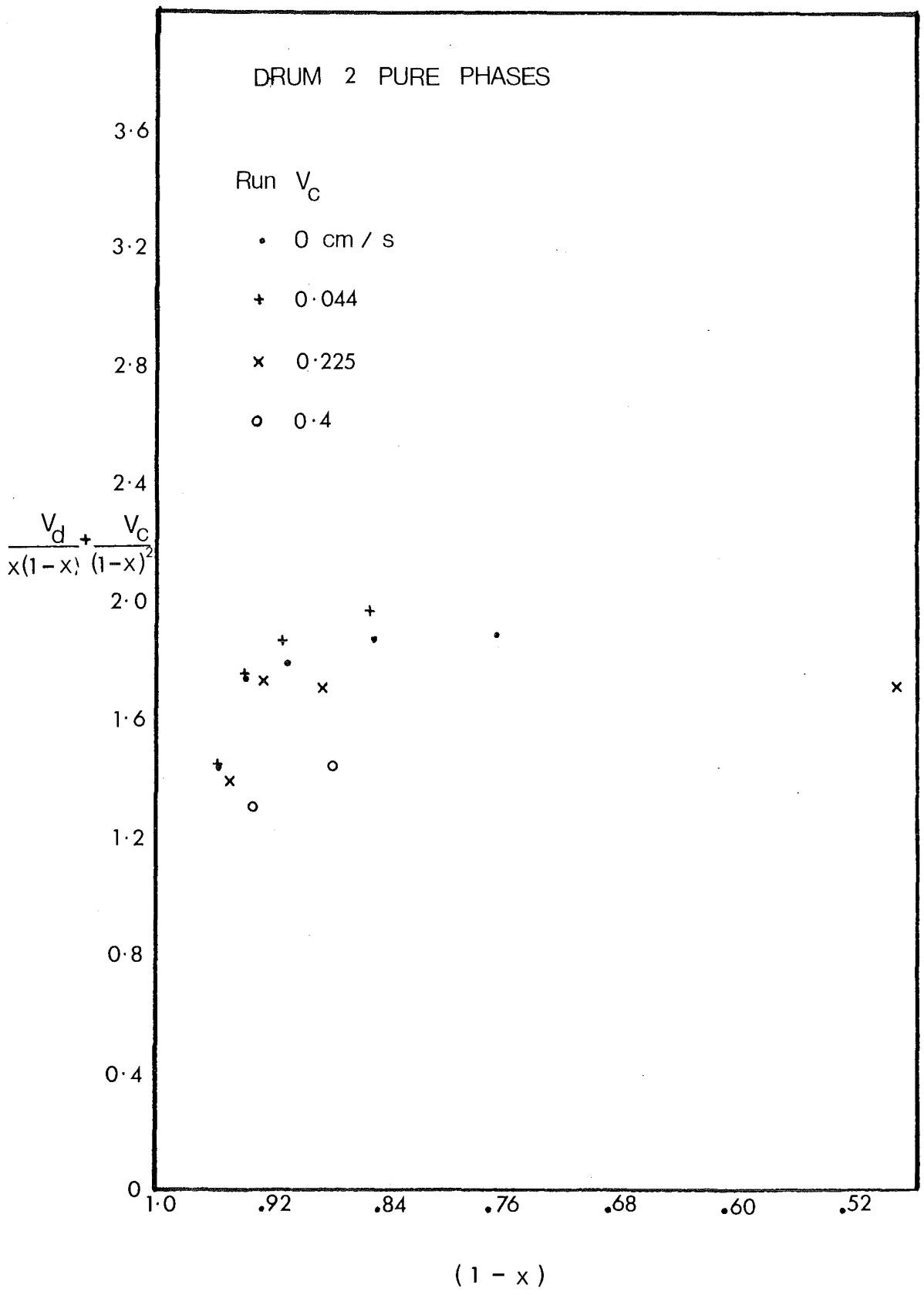

FIGURE 4 - 6 HINDERED SETTLING FACTOR vs (1 - x)

The reasons for this discrepancy are not clear. Zabel et al (1973) have shown that there is a significant decrease in drag on droplets falling in a stream. However, the Reynolds number dependence of the drag coefficient appears to be qualitatively the same as for single droplets. No data are available to show the wall effect under these conditions.

A further consideration is the fact that the motion of the droplet is not all free rise. A proportion of the droplet time is spent passing through restrictions and boucing off obstacles. The measured $\bar{V}_o$ value thus represents the net motion of the droplet.

IV CHARACTERISTIC VELOCITY

The characteristic velocity $\bar{V}_o$ is predicted by modelling the drop motion as a series of accelerations from rest to some fraction of its terminal velocity and ignoring accelerational drag and wall drag.

(1) Accelerational Drag

The drag on an accelerating sphere has been shown to be increased by up to 100% over the steady state value, (Hughes and Gilliland, 1952 Torobin and Gauvin, 1959). The situation in the Stokes law region for a rigid sphere was described by Basset (1888, 1910), as

$$F(t) = \tfrac{1}{2}\frac{\pi d^3}{6}\rho_f\frac{dV}{dt} + 3\rho_f\nu dV + \frac{3}{2}d^2\rho_f\sqrt{\pi\nu}\int_o^{\cdot}\frac{\frac{dV}{d\tau}\,d\tau}{\sqrt{t-\tau}} \qquad (4\text{-}31)$$

where $F(t)$ is the fluid resistance to the motion of the sphere. The first two terms give the added mass and steady state resistances respectively. The last term shows that the drag is dependent on the history of the motion. Results by Mockros and Lai, (1969) showed that the validity of this equation extended well past the Stokes law range. However no data is available on the applicability of this equation to liquid-liquid systems or the effect of wall drag during acceleration. The magnitude of the errors caused by ignoring accelerational drag are illustrated by a calculation. The data of Moorman, (1955) shows that equation (4-31) represents the motion of a 1.27cm diameter rigid sphere until a Reynolds number of 378 is reached. Moorman's data show that at that point the

distance of motion, in terms of droplet diameters traversed is:

$$s/d = 2.46$$

$$s = 2.46 * 1.27 = 3.12 \text{ cm}$$

The time of motion estimated from plotted data is 0.375 sec

$$V = 378 * \frac{0.16}{1.27} = 47.6 \text{ cm s}^{-1}$$

$$\frac{V}{V_t} = 47.6 / 68.5 = 0.695$$

Using the integrated form of equation (4-11) predicts

$$\frac{V}{V_t} = 1 - \exp(-3.29)$$

$$= 1 - 0.036 = 0.964$$

and using equation (4-12) gives

$$s = 25.7 (1 - 0.304 (1 - \exp(-3.29)))$$

$$= 25.7 * 0.707 = 18.2\text{cm}$$

Thus ignoring accelerational drag over the first 0.375 seconds of motion results in a 40% error in the estimated velocity and a 480% error in the estimated distance of motion. This is an extreme example since droplets do not start accelerating from rest after passing through a restriction, and the higher their initial velocity, the less influence of accelerational drag.

(2) Wall Drag

Substitution in Strom and Kintners, (1958), expression for wall drag, (equation (4-26)), shows that for a 5mm diameter droplet in a 12mm diameter tube:

$$\frac{V_t}{V_{t\infty}} = 0.75$$

For d = 6mm

$$\frac{V_t}{V_{t\infty}} = 0.67$$

When the corrected terminal velocities are used in equation (4-14) only small changes in $\overline{V}_o$ result.

TABLE 2

	$\bar{V}_o$/cm s^{-1} Experimental	$\bar{V}_o$/cm s^{-1} Equation (4-14) using $V_{t\infty}$	$\bar{V}_o$/cm s^{-1} Equation (4-14) V_t corrected for wall drag	Deviation/ %
Drum (1)	3.05	3.39	3.27	7.2
Drum (2)	2.53	3.27	3.11	22.9

The reason for this becomes apparent when equation (4-15) is rearranged:

$$\frac{V_o}{V_t} \simeq 0.35 \left[\frac{\Delta\rho g}{\rho_d} \frac{\bar{s}}{V_t V_o} \right]^{0.74} \qquad (4\text{-}32)$$

$$V_o^{1.74} \simeq 0.35 \left[\frac{\Delta\rho g}{\rho_d} \right]^{0.74} (\bar{s})^{0.74} V_t^{0.26} \qquad (4\text{-}33)$$

$$V_o \propto \bar{s}^{0.43} V_t^{0.15} \qquad (4\text{-}34)$$

$\bar{V}_o$ is thus primarily dependent on path length $\bar{s}$.

(3) Path Length

The equation derived for path length was:

$$\bar{s} = 0.38\, dp - 0.92 \left[\frac{\sigma}{\Delta\rho g} \right]^{\frac{1}{2}} \qquad (4\text{-}35)$$

When 16mm diameter rings are used and values for the physical properties of system (2) are substituted:

$$\bar{s} = 0.162 \text{ cm.}$$

This is a very small value when compared to the size of a droplet (5 - 6mm) and the size of a packing element (16mm OD). The path lengths for drops near the column wall were observed to range between 5cm and 30cm. This problem reveals a basic weakness in the Gayler,Roberts,Pratt model. The characteristic velocity $\bar{V}_o$ is found experimentally to be in the range 2 - 5cm s^{-1}, yet the terminal velocity of average drops is in the range 10 - 15cm s^{-1}. If the process is modelled as a droplet accelerating from rest to some fraction of its terminal velocity, then

it is necessary to have a very short path length in order to obtain a low average velocity. Thus $\bar{s}$ is a fitted parameter rather than having a real physical significance. The errors resulting from ignoring accelerated drag have also been absorbed into this parameter.

The problem arises because, as mentioned before, $\bar{V}_o$ is a parameter representing the net effect of two processes. These are the free rise modelled by Gayler et al, and secondly, the passage of the drops through restrictions. This is a much slower process and is controlled by the buoyancy forces required to deform a drop sufficiently to pass through the restrictions, (Wilkinson, Mumford and Jeffreys,1975).

V INFLUENCE OF A SURFACTANT

Table 1 shows that the surfactant system has a higher characteristic velocity than the pure system. The model qualitatively predicts this because the surfactant system has a lower interfacial tension. Thus the predicted drop size is smaller and the path length longer than for the pure system. Opposing this, the increase in drag coefficient caused by the surfactant would tend to decrease V_t slightly. The surfactant system has an average droplet size of 4 - 5mm and an interfacial tension of 27 dyne cm^{-1}. The pure system has an average droplet size of 5 - 6mm and an interfacial tension of 30 dyne cm^{-1}. The terminal velocity of both size ranges are approximately the same, once corrected for wall drag (9.0 - 9.5 cm s^{-1} vs 9.5 - 8.8 cm s^{-1}). However, the effect of the surfactant in increasing the drag coefficient will tend to lower the terminal velocity of those droplets below that of the pure system. Thus, it would seem that the smaller surfactant drops with a lower interfacial tension are better able to negotiate the restrictions in the packing. A cautionary note must be sounded in making this comparison, however. The packing was redumped before measurements were made on system (2). As no special measures were taken to orientate the packing, it is likely that some of the variation in

$\overline{V}_o$ is due to the changes in the packing structure (Wicks and Beckmann, 1955, Johnson and Lavergne, 1961). Gayler and Pratt,(1951) and Gayler et al, (1953) report differences of up to 20% in holdup and 10% in characteristic velocity after repacking the column.

VI MEASUREMENT OF HOLDUP

Examination of the literature shows that two main methods have been used to measure holdup in packed columns. In the drainage method the flows to the column are stopped, the column is drained, and the volume of each phase is measured (Gayler and Pratt, 1951, Wicks and Beckmann, 1955, Johnson and Lavergne, 1961). In the interface volume method, the flows to the column are stopped, the holdup is allowed to settle out, and the volume of continuous phase which must be added to restore the interface to its original position is measured, (Appel and Elgin, 1937, Row, Koffolt and Withrow, 1941, Gier and Hougen, 1953, Wicks and Beckmann, 1955, Johnson and Lavergne, 1961).

The differences between the two methods arise from the fact that some dispersed phase remains trapped within the packing after settling out of the freely moving drops. Wicks and Beckmann, (1955) go further and distinguish between the holdup that can be freed by mechanically pulsing the column, and that which can only be removed by drainage of the column. Markas and Beckmann, ('957), have revealed a hysteresis effect when the column has been operated above the loading point. This hysteresis holdup was shown to be immobile within the packing.

A drop which is firmly trapped within the packing interstices rapidly comes to equilibrium with the continuous phase and then makes no further contribution to the mass transfer processes. Thus, for a column with an established hysteresis holdup, or one that has been operating above the loading point for any length of time, this holdup will make no contribution to the mass transfer. There is no justification

therefore, for including the hysteresis holdup in the value of holdup used for calculating the interfacial area of the dispersed phase.

Markas and Beckmann (1957), used isotope tagged droplets to study the rate of motion of the dispersed phase through a packed column. The column was operated using tagged droplets until steady-state was achieved. The dispersed phase was then switched to untagged droplets and the proportion of tagged droplets as a function of the total holdup (excluding hystersis holdup) at the switchover point was recorded as a function of time. The response function consisted of two linear regions. There was a fast initial replacement of 40% or more of the total holdup in a period of ten minutes. The remainder of the total holdup was then replaced at a constant rate over a period of up to three hours. Increasing the dispersed phase flowrate from 0.035 cm^3s^{-1}/cm^2 to 0.072 cm^3s^{-1}/cm^2 increased the proportion replaced in the first ten minutes to 60% and decreased the total replacement time to about two hours. These findings support earlier arguments about the existance of two distinct zones of flow for the dispersed phase. However, the proportion of tagged toluene displaced in the initial region is in excess of the free rising holdup. Thus, it would seem that either a significant proportion of the dispersed phase in the preferential channels remains trapped during the settling out process, or, there is a considerable interaction between the preferential channels and the other flow regions.

Observations of the behaviour in preferential channels at restrictions near the column wall show that most of the droplets held up at a restriction are cleared when the flows to the column are stopped. Two effects contribute to this. Firstly, there is a mutual momentum effect whereby a drop moving through a restriction tends to draw droplets behind it into the restrictions, (Wilkinson, Mumford and Jeffreys, 1975). Secondly, coalesence between touching drops takes place sooner or later. The increase in buoyancy forces with respect to surface forces means

that such drops are better able to move through restrictions, (Wilkinson,Mumford and Jeffreys, 1975). The proportion of dispersed phase remaining at restrictions near the column wall is estimated at 5 - 30% of the steady-state value with an average value of about 15%. The results of Markas and Beckmann, (1957), showed that the proportion of total holdup displaced in the initial region was up to 4.6 times the free settling holdup. It is thus apparent that considerable interaction between the preferential channels and the secondary regions occurs.

A study by Chartres and Korchinsky, (1975) into unsteady state mass transfer models treated the total mass transfer as the integral sum of the contributions of all droplet sizes. It was found that within any size interval the effect of widely varying residence times was negligible and that the size interval could be characterised by an average residence time. The average droplet residence time will be strongly dependent on the proportion of flow occuring through the preferential channels. Thus the active interfacial area is dependent not only on the free rising holdup, but also on the amount of interaction between the preferential and secondary channels. Use of the free rising holdup at low dispersed phase flowrates could result in errors of 450% in the interfacial area. However the error decreases rapidly as the flowrate is increased.

Only the free rising holdup was determined in this study. However, it is intended as a study of the influence of mass transfer on the column hydrodynamics. Thus if no gross changes in the permanent holdup or in the interaction rate between free rising and permanent holdup occur as a result of mass transfer then a comparative study of the free rising holdup should be valid.

CONCLUSIONS

Tha analysis of dispersed phase holdup in packed columns by Gayler, Roberts and Pratt, (1953) has been critically reviewed. The analysis involved three major assumptions.

The assumption of a slip velocity based on the superficial velocities of the phases, although widely used, is based on the idealised model of noninteractive plug flow for both phases. The effects of maldistribution of flow have been shown to provide a possible explanation for the experimental finding in this and other works, (Wicks and Beckmann, 1955, Markas and Beckmann, 1957), that the slip velocity V_s is not a unique function of holdup. They also provide an insight into the two distinct regimes of holdup found.

Of the three factors contributing to hindered settling the use of the effective suspension density is directly applicable and results in the characteristic velocity being multiplied by the term $(1-x)$. The effect of wall drag can be incorporated in the characteristic velocity. Previous findings that a Stokes law velocity is valid (Gayler, Roberts and Pratt, 1953) were verified. No convincing reasons could be advanced for this. A plot of $\phi(1-x)$ against $1-x$ was found not to be linear over the whole range. However the effects of flow maldistribution and hindered settling could not be separated.

The assumption that the characteristic velocity can be modelled as the average velocity of a drop accelerating to some fraction of its terminal velocity is a gross simplification. The difference in magnitude between the characteristic velocity and the terminal velocity of a droplet means that a small path length must be used in order to get a low average velocity. This parameter is up to two orders of magnitude smaller than experimentally observed values and incorporates the effects of ignoring accelerational and wall drag.

Techniques for the measurement of holdup were reviewed. Evidence of a complex interaction between the free-rising and the permanent holdup (Markas and Beckmann, 1957) means that at low dispersed phase flowrates use of the free-rising holdup may result in a serious under-estimate of the interfacial area active in mass transfer.

NOMENCLATURE

C - constant in equation (4-16) (-)

C_d - drag coefficient (-)

C_o - wall drag correction factor (-)

d - droplet diameter (cm)

d_c - column diameter (cm)

d_p - packing element diameter (cm)

d_{vs}^o - equilibrium droplet diameter defined by equation (4-17) (cm)

D - tube diameter (cm)

e - exponential function (-)

F_B - buoyancy force (dynes)

$F(t)$ - time dependent fluid resistance (dynes)

g - gravitational acceleration (cm s^{-2})

n - constant in equation (4-16) (-)

Re - Reynolds number (-)

s - droplet path length (cm)

$\bar{s}$ - average droplet path length (cm)

t - time of droplet motion (s)

$\bar{t}$ - average time of droplet motion (s)

V - droplet velocity (cm s^{-1})

$\bar{V}$ - mean rate of rise of dispersed phase relative to column ($cm\ s^{-1}$)

V_c, V_d - superficial phase velocities ($cm^3\ s^{-1}/cm^2$)

V_o - characteristic velocity of an infinite diameter column ($cm\ s^{-1}$)

$\bar{V}_o$ - characteristic velocity ($cm\ s^{-1}$)

$\bar{V}_r$ - mean rate of rise of dispersed phase relative to continuous phase ($cm\ s^{-1}$)

x - dispersed phase free holdup (-)

y - parameter defined by equation (4-20) (-)

z - parameter defined as $z = \frac{\Delta\rho g}{\rho_d V_t^2}\ \bar{s}$

ϵ - packing voidage fraction (-)

μ - dynamic viscosity ($g\ cm^{-1}\ s^{-1}$)

π - 3.14159 (-)

ν - kinematic viscosity ($cm^2\ s^{-1}$)

ρ - density ($g\ cm^{-3}$)

ρ_m - mixed phase density = $\rho_d\ x + (1-x)\ \rho_c$ ($g\ cm^{-3}$)

$\Delta\rho$ - phase density difference ($g\ cm^{-3}$)

σ - interfacial tension ($g\ s^{-2}$)

τ - integration parameter in equation (4-25) (s)

ϕ - hindered settling function (-)

Subscripts

c - continuous phase

d - dispersed phase

f - fluid

s - Stokes law

t - terminal

ϕ - suspension

∞ - in an infinite media

CHAPTER FIVE

INFLUENCE OF A THIRD COMPONENT

Chapter contents.

INTRODUCTION

Models of the mass transfer process normally assume it to consist of three simple steps: diffusion from the first liquid to the interface, transfer across the interface, and diffusion from the interface to the second liquid. The interface is assumed to be at equilibrium and to have a constant resistance (often assumed to be negligible). Equilibrium, however, requires that not only concentration and thermal profiles be in equilibrium, but also that the forces acting on the interface be in equilibrium. When only one of these forces, the interfacial tension, is dependent on the transfer process then movement of the interface may occur.

Evidence of such spontaneous interfacial convection was provided as long ago as 1855 by Thomson, when he described the motion of alcohol droplets on a water interface. It was not until Lewis and Pratt, (1953) observed violent agitation of the drop interface during attempts to measure the dynamic interfacial tension in the presence of mass transfer, that the importance of this phenomenon in liquid extraction was appreciated. A review of the early work in this field was done by Scriven and Sternling, (1960), and more recent work has been reviewed by Sawistowski, (1971).

The experiments of Thomson (1855) showed that interfacial convection can effect the rate of mass transfer both by altering the conditions of mass transfer, and thus the transfer coefficient, and also by changing the interfacial area of contact. Experimental evidence of the effects of a non-equilibrium system are common. Johnson and Bliss, (1946) report increased overall transfer coefficients for transfer from the continuous phase to the dispersed phase, and increased coalescence when transfer was in the reverse direction. Gayler and Pratt report increases in droplet size when the phases are unsaturated, (1953 a and b), and

substantial reductions in holdup when transfer of a solute is from the organic dispersed phase to the aqueous phase, (Gayler and Pratt, 1957). An increase of up to 200% in the flooding rate for a rotating disc column was reported, (Thornton and Pratt, 1953).

THEORY

The dependence of interfacial tension on the concentration of all the components in the interface means that the presence of a diffusing component may result in the onset of spontaneous interfacial convection. The factors which govern this are:

(1) The direction of mass transfer.

(2) The sign of the interfacial tension-concentration gradient.

(3) The ratio of molecular diffusivities.

(4) The ratio of kinematic viscosities.

Analyses predicting the conditions under which small interfacial disturbances are amplified have been done for the steady state by Sternling and Scriven (1959), and an unsteady state model has been produced by Marsh, Sleicher and Heideger (1965).

The type of interfacial convection which appears depends upon the hydrodynamic state of the bulk liquid. When the liquids are at rest an ordered pattern of roll cells appears (Sawistowski, 1971). Random disturbances result in localised areas of lower interfacial tension. The Marangoni principle (1871), states that liquids of lower surface tension will spread on liquids of higher surface tension. Thus the localised areas expand bringing adjoining layers into motion parallel to the interface. At some point flow turns back into the fluid normal to the interface. Simultaneously, fresh liquid from the bulk phase is drawn into the site of the original disturbance and a roll cell is formed. See figure 5 - 1.

Under conditions of turbulence or forced convection a slightly different mechanism applies. Eddies of bulk liquid arriving at the interface result in localised changes in the interfacial tension. If the interfacial tension decreases with concentration then the immediate interfacial area will expand. However, the depleted eddy is replaced by lower concentration liquid and the interfacial tension rises again.The flow to

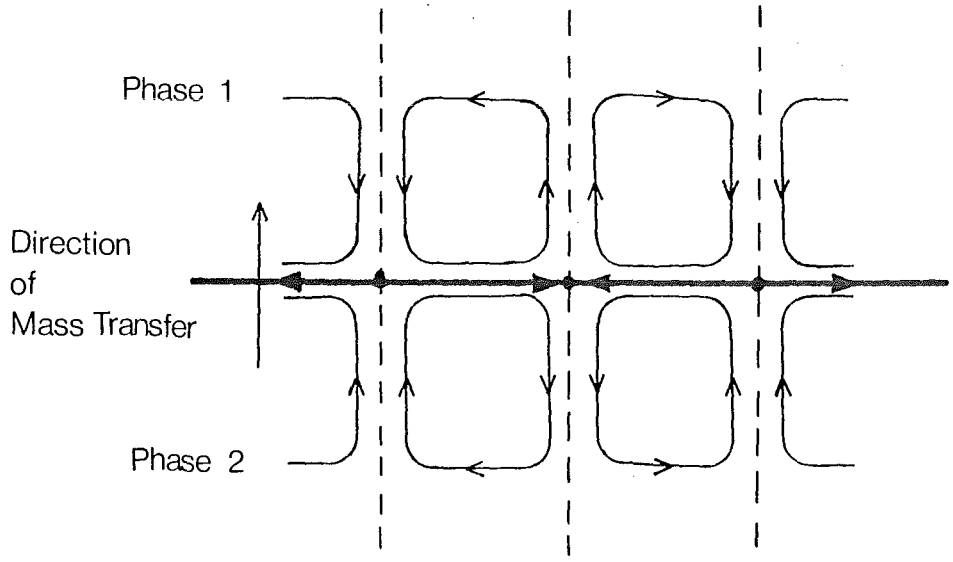

a Formation of Roll Cells

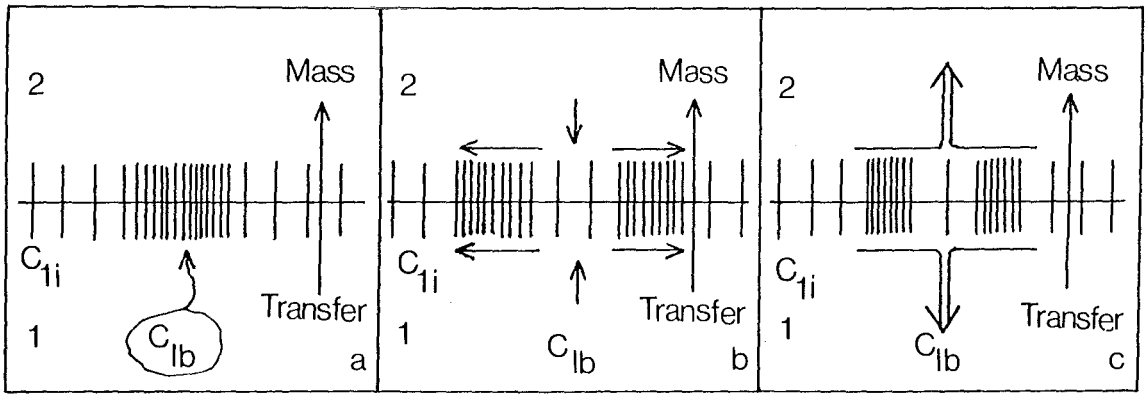

b Eruption Mechanism

FIGURE 5 - 1 INTERFACIAL INSTABILITY MECHANISMS

the centre induced in both phases results in a jet like flow normal to the interface commonly called an erruption. These transient disturbances are possible for either direction of mass transfer, but are far more common when transfer is in the direction which is naturally unstable.

It is important to distinguish the role of interfacial phenomena in enhancing the mass transfer process from its effect on the interfacial area of the phases. Interfacial convection does not directly effect the interfacial area of most practical liquid-liquid systems (Sawistowski, 1971). The changes in shape accompanying movements of the interface do no significantly change the area. Only when the depth of one phase is smaller than the scale of interfacial movements, as, for example, in thin films, is the direct effect of interfacial convection important. The influence of the Marangoni effect, however, is most significant. Collisions between drops may result in coalescence or the drops may bounce apart. In order for coalescence to occur, the colliding drops must remain together long enough for the film of continuous phase between them to drain sufficiently and rupture. Drainage, in the absence of mass transfer occurs by the action of buoyancy forces. Mass transfer into the film will reduce its interfacial tension with respect to the bulk continuous phase. Thus, by the Marangoni principle, drainage of the film will be accelerated and the coalescence rate increased. Transfer out of the film will, by a similar argument retard film drainage and decrease the rate of coalescence.

Interfacial phenomena can strongly influence circulation within the droplet and the transfer of momentum to the continuous phase. Thus, it can be expected that mass transfer will also exert an influence on the hydrodynamic drag coefficient. Sehrt and Linde (1967), present data for the transfer of acetic acid between water and benzaldehyde as dispersed phase. Increases in drag coefficient are found for both directions of transfer, but approach 100% for transfer from benzaldehyde to water, while a maximum increase of 35% is found for

the reverse direction of transfer. Mass transfer from benzaldehyde to water is the naturally unstable direction of transfer, (Sawistowski, 1971). Similar data for the transfer of propionic acid between water and nitrobenzene as dispersed phase have been found by Sawistowski, (1973).

If, as an approximation, the drag coefficient is assumed to be proportional to the pure phase coefficient, i.e.

$$(C_d)_{\text{mass transfer}} = \alpha (C_d)_{\text{pure phases}} \qquad (5\text{-}1)$$

where α is a constant.

Then equation (4-10) becomes:

$$\frac{d^2 s}{dt^2} = \frac{\Delta \rho g}{\rho_d} - \alpha \frac{18 \mu_c}{d^2 \rho_d} \frac{ds}{dt} \qquad (5\text{-}2)$$

Integrating this using the same boundary conditions gives:

$$\bar{s} = \frac{V_s \bar{t}}{\alpha} \left[1 - \frac{\rho_d V_s}{\alpha \Delta \rho g \bar{t}} \left(1 - \exp\left[- \frac{\alpha \Delta \rho g \bar{t}}{\rho_d V_s} \right] \right) \right] \qquad (5\text{-}3)$$

or

$$\alpha y = 1 - \frac{y}{\alpha Z} \left[1 - \exp\left(\frac{-\alpha Z}{y} \right) \right] \qquad (5\text{-}4)$$

Further, since

$$V_t = \sqrt{\frac{4}{3} \frac{d \Delta \rho g}{\rho_d C_d}} \qquad (5\text{-}5)$$

then

$$\frac{(V_t)_{\text{mass transfer}}}{(V_t)_{\text{pure phase}}} = \frac{1}{\sqrt{\alpha}} \qquad (5\text{-}6)$$

EXPERIMENTAL RESULTS

Holdup data was collected for the column under conditions of mass transfer for a limited range of dispersed and continuous flowrates. Three sets of experiments were performed: transfer of a solute from the dispersed phase, transfer to the dispersed phase, and finally, with the solute in equilibrium distribution between the phases. Figures 5 - 2, 5 - 3, and 5 - 4 show the dispersed phase free holdup plotted against the dispersed phase superficial flowrate V_d. In each case the free holdup for the pure phases, for the continuous phase flowrate $V_c = 0$, has been plotted to provide a comparison. Figure 5 - 5 compares data for all three systems plus the pure phases at the lowest common continuous phase flowrate used.

The data for transfer from the dispersed phase to the continuous phase qualitively confirm previous findings, (Gayler and Pratt,1953, and 1957b, Dunn, 1963). Reductions in holdup of 30 - 50% over the pure phases are found. Also the loading region where holdup increased rapidly for the pure phases does not seem to occur, or at least is very much reduced. The data for the lowest continuous phase flowrate V_c = 0.044 $cm^3\ s^{-1}/cm^2$, suggest that the latter is the case, and that rather than the holdup rising sharply until flooding occurs, the system moves into the third regime found by Gayler and Pratt, (1951), where holdup changes only slightly with dispersed phase flowrate. Indeed, when mass transfer occured from the dispersed phase it was found impossible to flood the column using the maximum available flowrates. The increases in holdup occuring when the continuous phase flowrate V_c was increased are somewhat smaller than for the pure phases.

Changes were not as marked for the reverse transfer and saturated phases runs. Both cases however show a decrease in holdup over the pure phases. Holdup for the saturated case lies only 5 - 7% below the pure phase line when V_c = 0.044 $cm^3\ s^{-1}/cm^2$. Variation of

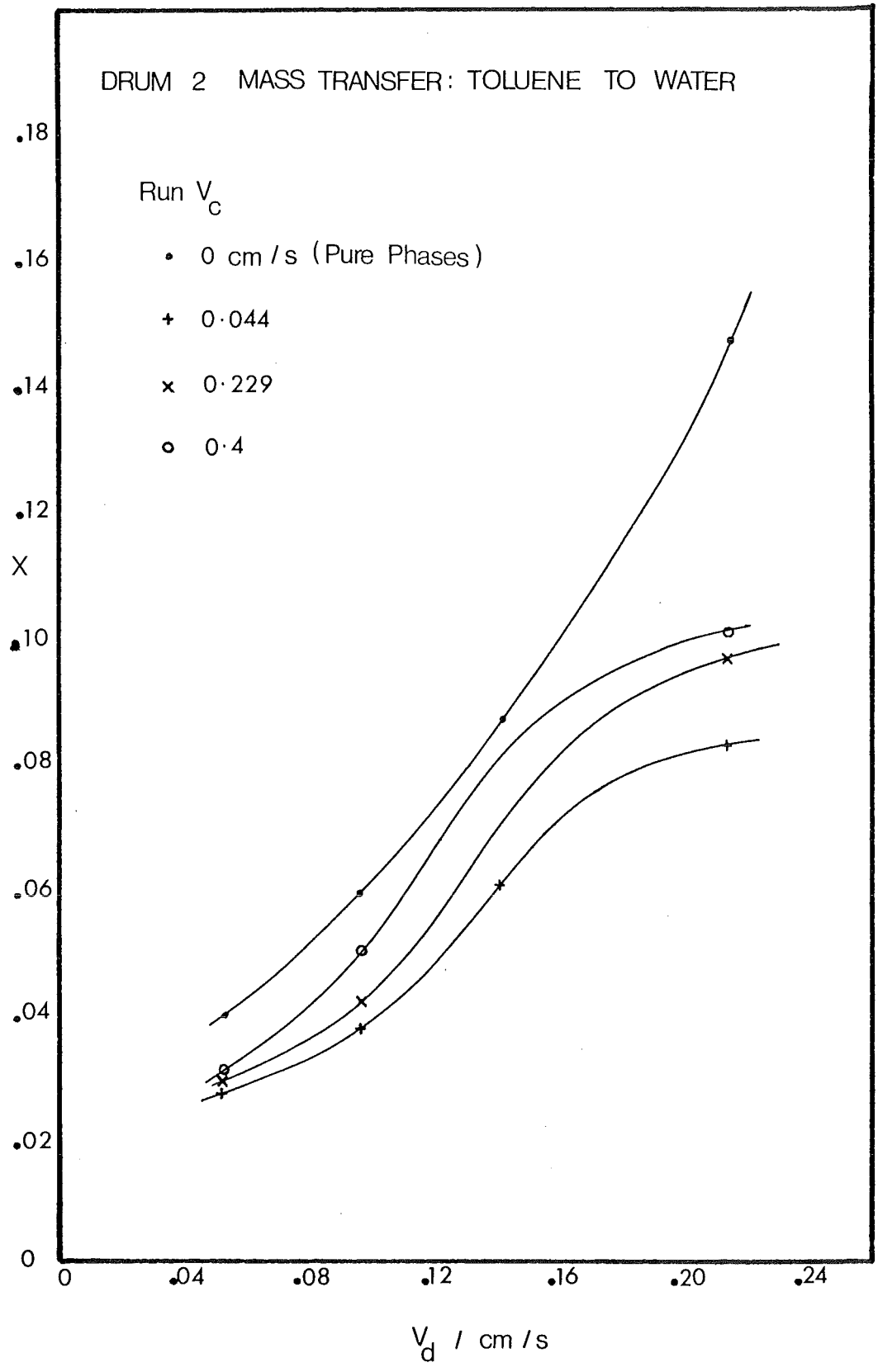

FIGURE 5 – 2 HOLDUP vs FLOWRATES

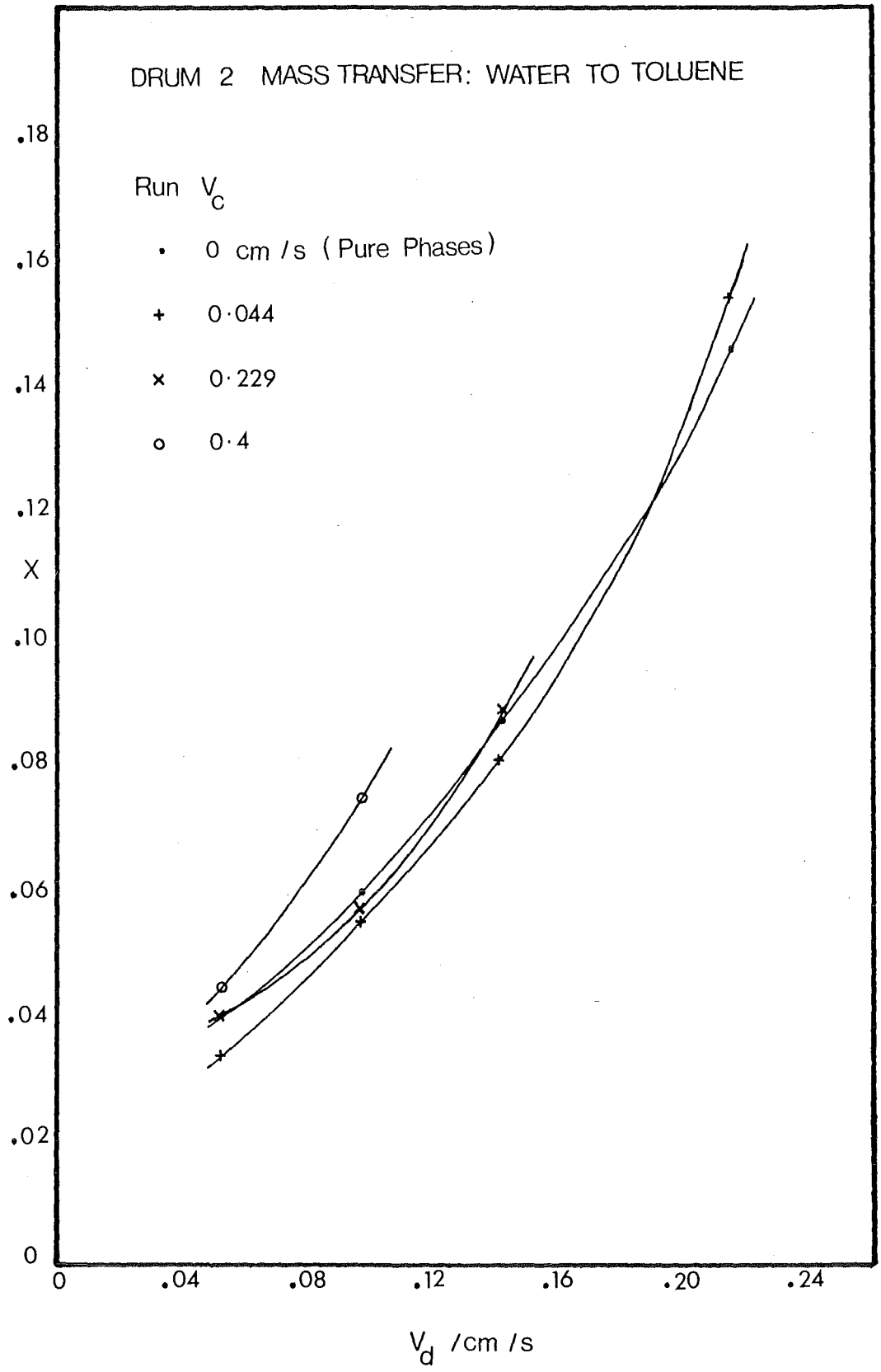

FIGURE 5-3 HOLDUP vs FLOWRATES

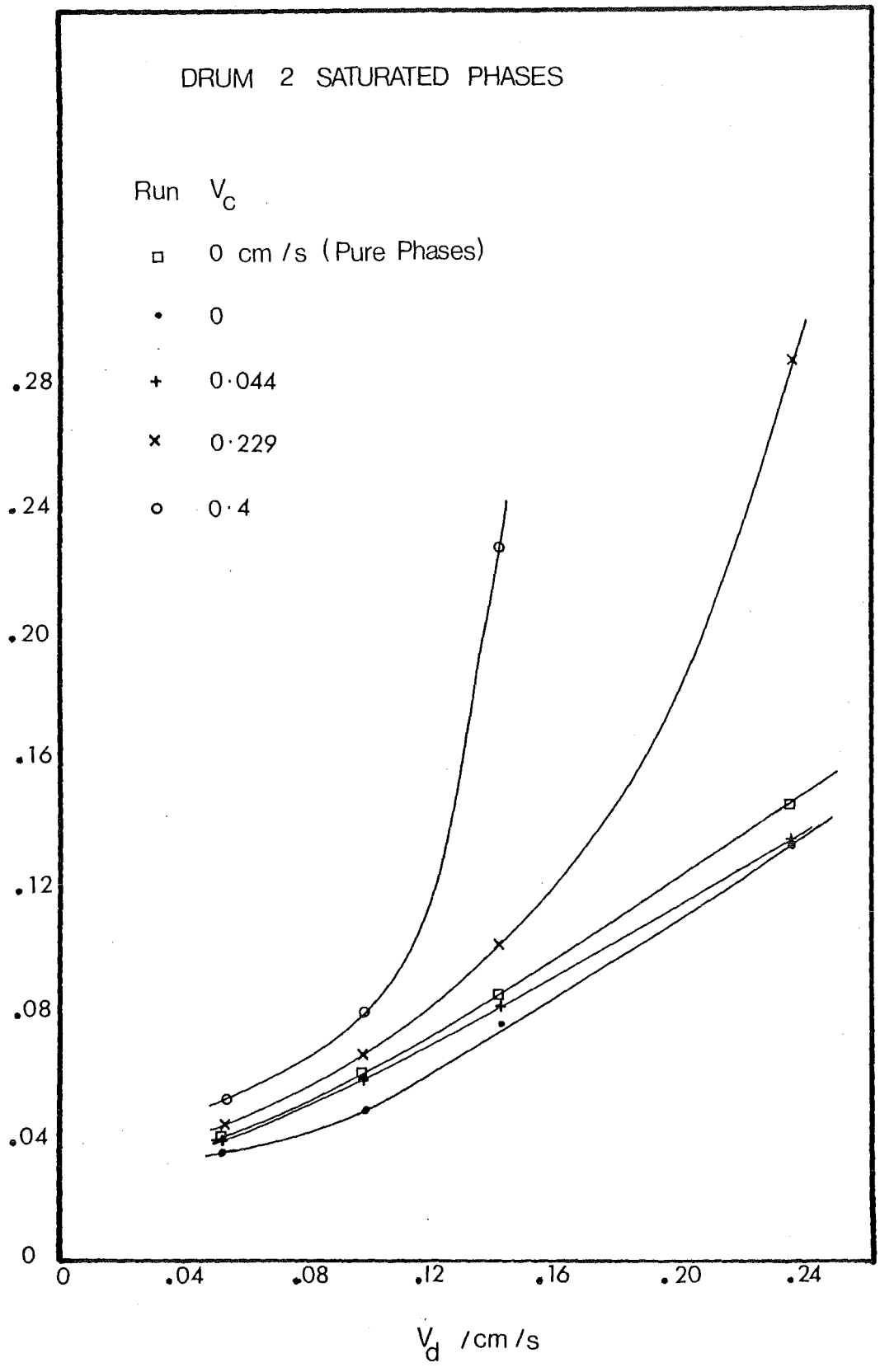

FIGURE 5 - 4 HOLDUP vs FLOWRATES

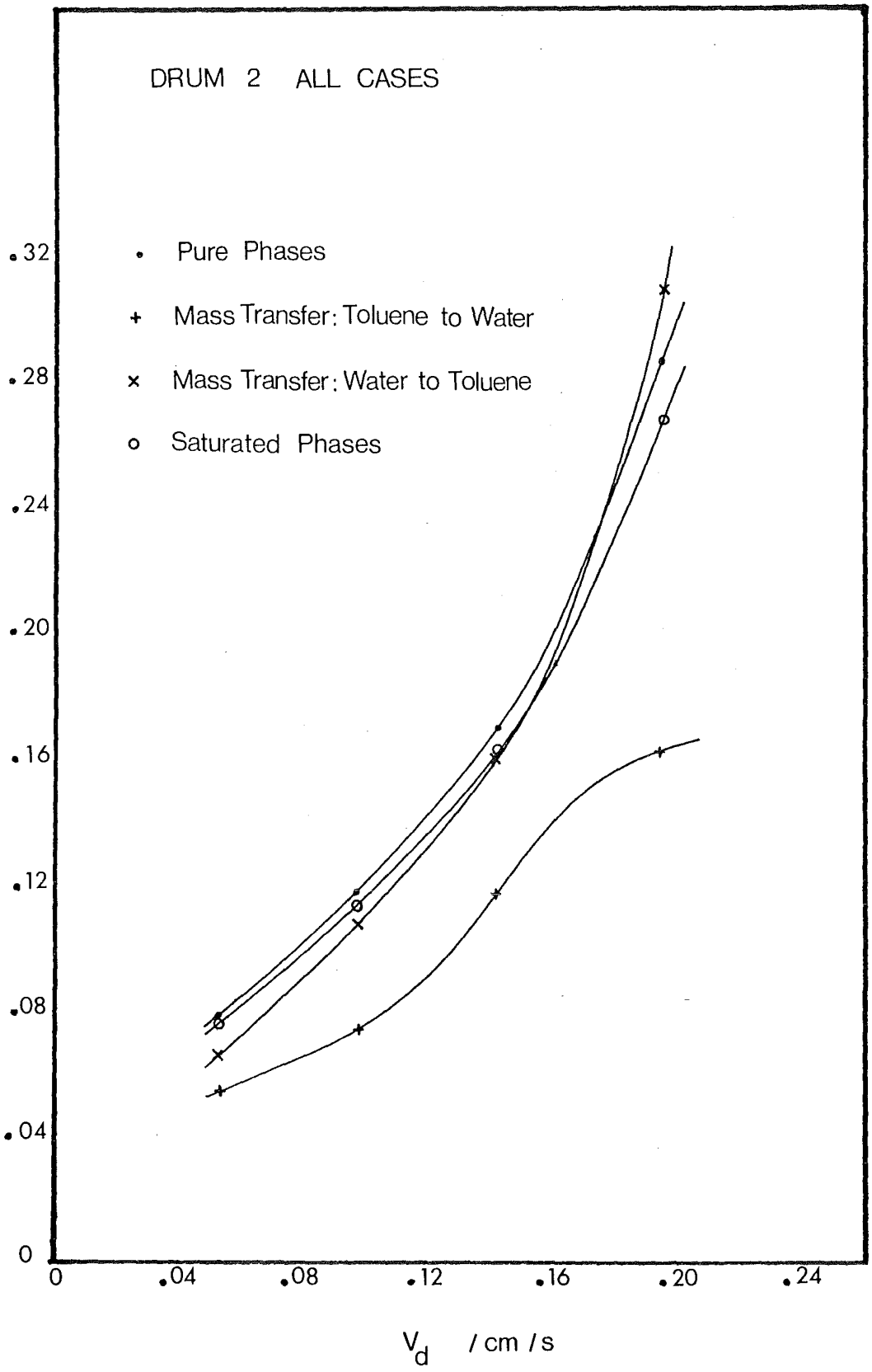

FIGURE 5 – 5 HOLDUP vs FLOWRATES

holdup with increasing continuous phase flowrate is, however, intermediate between the pure phase case and transfer from the dispersed to continuous phases. The overall pattern again seems to consist of a linear region followed by a region of rapidly increasing holdup and the occurance of flooding.

Holdup for the reverse transfer case is initially 17.5% lower than the pure phase case when $V_c = 0$. The rate of increase of holdup with V_d is, however, greater than for the pure phases and at $V_d = 0.234$ $cm^3\ s^{-1}/cm^2$ the holdup is 7% greater than for the pure phases case. Variation of holdup with continuous phase flowrate is slightly less than for the saturated case. A flooding point determined under these conditions was about 10% less than the pure phases value.

Figure 5 - 6 shows a plot of $V_d + \frac{x}{1-x} V_c$ versus $x(1-x)$ for the pure phases and for transfer from the dispersed to the continuous phase. The decreases in holdup for transfer out of the dispersed phases are reflected in a significant increase in the slope of the line, and hence the characteristic velocity $\overline{V}_o$. The small variation in holdup when the continuous phase flowrate was increased is reflected in the fact that practically no splitting of the line occurs. A linear regression analysis shows that the points are as well represented by a single line as by separate lines for each continuous phase flowrate.

Figure 5 - 7 is a plot of $V_d + \frac{x}{1-x} V_c$ versus $x(1-x)$ for the reverse transfer runs and the saturated phases runs. Again points lying in the region of rapidly increasing holdup deviate from the straight line relationship of equation (4-8). Splitting of the lines by variations in the continuous phase flowrates are found in both cases. The degree of splitting is somewhat less than for the pure phases reflecting the smaller increases of holdup with continuous phase flowrate than occur for the pure phases. The data for each continuous phase flowrate can be represented by a separate line. No trend is found in the slope of the lines and averaged values are used.

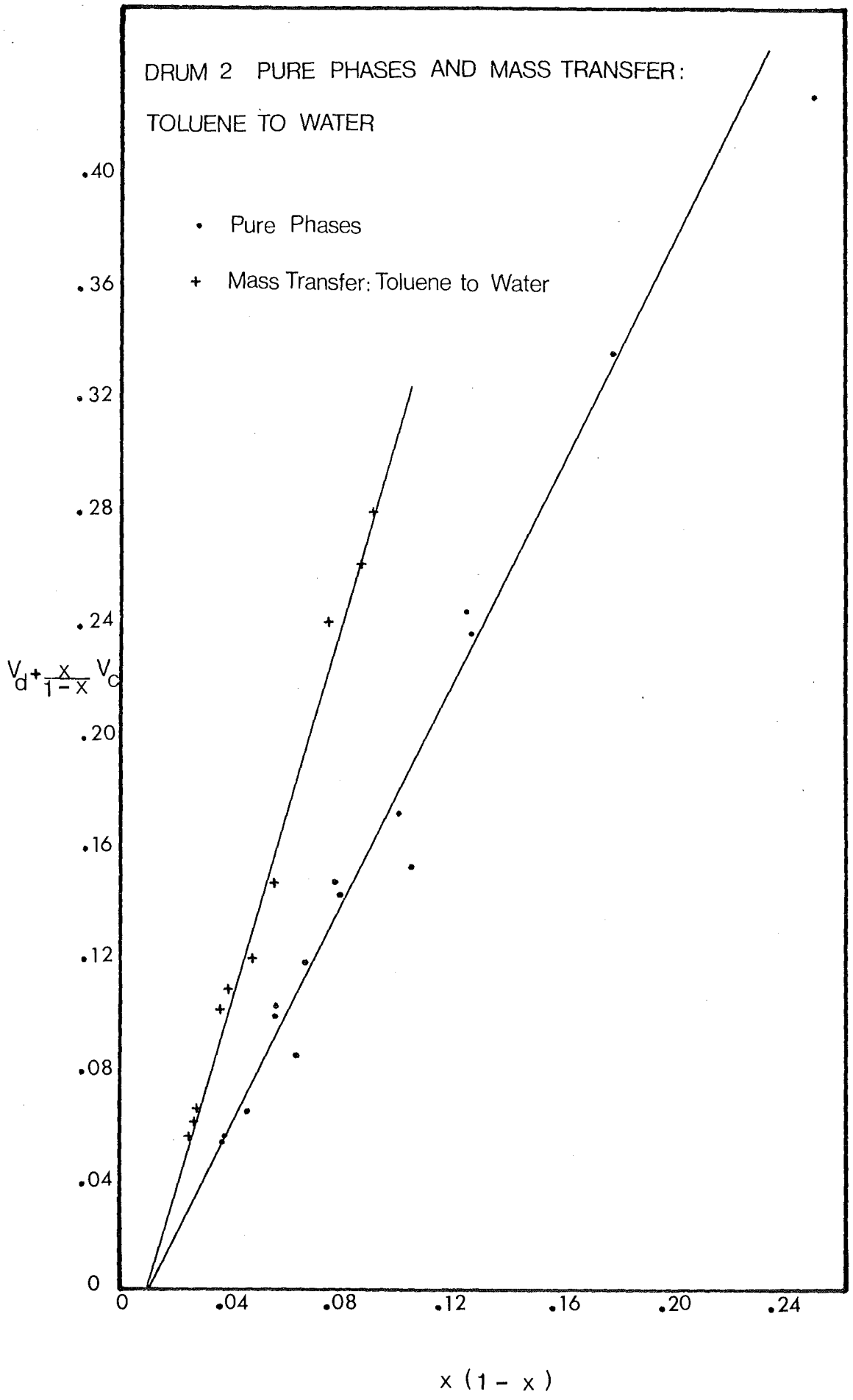

FIGURE 5 - 6 SLIP VELOCITY vs x (1 - x)

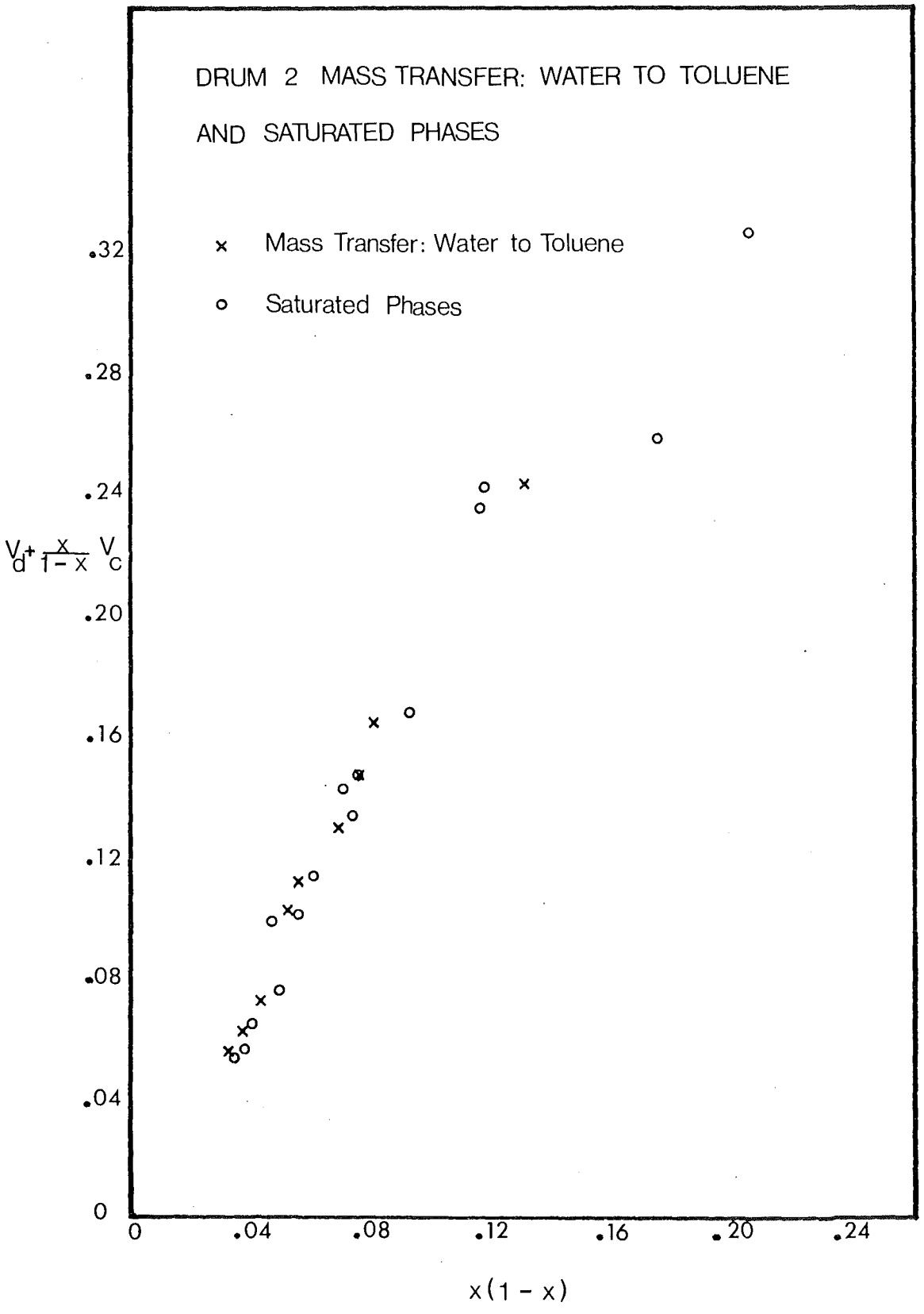

FIGURE 5 - 7 SLIP VELOCITY vs x(1 - x)

The measured physical properties were used to calculate the terminal velocity for drop sizes predicted by equation (4-17), using the Hu - Kintner (1955) correlation. Table 3 gives the experimental values of characteristic velocity $\overline{V}_o$ together with the values predicted by equation (4-14).

TABLE 3

	$\overline{V}_o$/cm s^{-1} Experimental	$\overline{V}_o$/cm s^{-1} Equation (4-14)	Deviation /%
(1) Pure Phases	2.55	3.27	+ 28.2
(2) Transfer out of dispersed phase	4.39	3.40	- 22.5
(3) Transfer into dispersed phase	2.70	3.33	+ 23.2
(4) Saturated phases	2.78	3.48	+ 21.9

DISCUSSION

The Gayler-Roberts-Pratt correlation predicts values of the characteristic velocity $\bar{V}_o$ that are about 4% greater than for the pure phases. Further, the predicted values for $\bar{V}_o$ for transfer of a solute both into and out of the dispersed phase and for saturated phases are nearly identical. The correlation fails to predict the large differences in $\bar{V}_o$ found experimentally for transfer out of the dispersed phase.

I INFLUENCE OF PHYSICAL PROPERTIES

Addition of a solute to the system means changes in the physical properties. Within each set of mass transfer runs small variations in the feed concentration occured. Thus, there was a variation in the physical properties about an average value for each particular system.

(1) Direct Effect

The physical properties appearing in the correlation are the density difference $\Delta\rho$, the dispersed phase density ρ_d, and the interfacial tension σ. The terminal velocity of dispersed phase droplets is also dependent on the continuous phase density ρ_c and viscosity μ_c. Changes in the phase densities ρ_d and ρ_c, and the density difference $\Delta\rho$, are small. The average value for ρ_c changes by 0.02% for the saturated case, 0.12% with a variation of 0.09% for transfer out of the dispersed phase, and 0.35% with a variation of 12% for transfer into the dispersed phase. Similarly the maximum change in the dispersed phase density was 0.35% with a variation of 0.15%. The changes are magnified slightly in the density difference $\Delta\rho$, with the maximum changes of 2% with a variation of $1\frac{1}{2}$%. Viscosities were not measured for all cases, but the points checked indicate a change of about 1% in the continuous phase viscosity μ_c. The physical property

which is very sensitive to the presence of a solute is the interfacial tension. A reduction of 18.9% was found for the saturated phases, while reductions of 15.3% with a variation of 7.5% about the mean for transfer out of the dispersed phase, and 14.6% with a variation of 6.7% for transfer into the dispersed phase were found.

Equation (4-32) showed that the characteristic velocity $\bar{V}_o$ has an equal dependence on the path length $\bar{s}$, and the group $\left[\frac{\Delta\rho g}{\rho_d}\right]$, with a lesser dependence on the droplet terminal velocity. Thus changes of 3% in $\left[\frac{\Delta\rho g}{\rho_d}\right]$ correspond to a change of 1.3% in V_o.

(2) Path Length

The path length was expressed as:

$$\bar{s} = 0.38\ dp - 0.92\left[\frac{\sigma}{\Delta\rho g}\right]^{0.5} \qquad (5\text{-}7)$$

The group $0.92\left[\frac{\sigma}{\Delta\rho g}\right]^{0.5}$ represents the maximum stable drop size under the influence of gravitational and buoyancy forces, (Gayler and Pratt, 1951). The group predicts a decrease in the drop size in the column in all cases since the interfacial tension has decreased. The predicted value of drop diameter is close in magnitude to the first term 0.38 dp. Thus changes of 15% in σ and 3% in $\Delta\rho$ are magnified to 25% changes in $\bar{s}$ and then an 11% increase in $\bar{V}_o$.

The correlation is thus very sensitive to the predicted drop diameter. Table 4 compares the predicted values using the equation:

$$d = 0.92\left[\frac{\sigma}{\Delta\rho g}\right]^{0.5} \qquad (5\text{-}8)$$

with the actual behaviour found.

TABLE 4

	dequil/mm Equation (5-8)	d 32 /mm Experimental	d 43 /mm Experimental
(1) Pure phases	4.5	5.5	6.0
(2) Transfer into dispersed phase	4.2	5.3	5.8
(3) Saturated phases	4.0	5.0	5.5
(4) Transfer out of dispersed phase	4.1	7.5	9.0

The model thus fails on two counts:

(1) A decrease in drop size is predicted in all cases with a decrease in interfacial tension. This is true when the droplet size in the packing is determined by breakup criteria alone. However, the presence of a diffusing solute can mean that the drop size present is an equilibrium size determined by the rates of breakup and coalescence.

(2) An increase in the characteristic velocity $\overline{V}_o$ is linked with a decrease in drop size. This is qualitatively correct for the first three cases but fails badly when transfer is out of the dispersed phase.

(3) Terminal Velocity

Equation (4-32) also shows a dependence of $\overline{V}_o$ on the droplet terminal velocity. Substitution of the new physical properties in the Hu - Kintner (1955) correlation shows a decrease in V_t of 4.7% for the mass transfer cases and a 6.2% decrease in V_t for the saturated case. These correspond to 0.7% and 0.9% decreases in $\overline{V}_o$. The calculated changes in V_t are for an equivalent pure liquid and thus do not account for any changes occuring as a result of interfacial convection.

II INTERFACIAL CONVECTION

(1) Direction of Instability

Sehrt and Linde, (1967) found increases in the drag coefficient of up to 100% when transfer of a solute was occuring in the direction of natural instability. The main factors governing which direction of

transfer is naturally unstable are the ratio of molecular diffusivities r^2, the ratio of kinematic viscoties ν^2, and the sign of the interfacial tension gradient , (Sawistowski, 1971). The Wilke - Chang, (1955), correlation was used to calculate values of the diffusion coefficient for acetone in both phases. Denoting the continuous phase as phase 1 and the dispersed phase as phase 2:

$$r^2 = \frac{D_1}{D_2} = \frac{1.154 * 10^{-5}}{2.65 * 10^{-5}} = 0.43$$

$$\nu^2 = \frac{\nu_1}{\nu_2} = \frac{0.99}{0.594} * \frac{0.87}{0.999} = 1.45$$

The interfacial tension gradient is negative for this system. Thus with:

$$r^2 < 1 \quad \nu^2 > 1 \quad \frac{d\sigma}{dc} < 0$$

the Sternling - Scriven model of hydrodynamic instability predicts stationary instability for transfer in the direction continuous to dispersed, (Sawistowski, 1971).

(2) Effect on Characteristic Velocity

The values of characteristic velocity predicted using equation (4-14) are recalculated using equation (5-4), assuming a 100% increase in the drag coefficient for transfer from the continuous phase to the dispersed phase and a 35% increase for transfer in the reverse direction. The droplet terminal velocities are corrected for the increased drag coefficient using equation (5-6) and for wall drag using equation (4-25). Table 5 gives the results.

TABLE 5

	$\overline{V}_o$/cm s^{-1} Experimental	$\overline{V}_o$/cm s^{-1} Equation (4-14)	$\overline{V}_o$/cm s^{-1} Equation (5-6) plus wall drag
(1) Pure phases	2.53	3.27	3.11
(2) Transfer out of dispersed phase	4.39	3.40	2.85
(3) Transfer into dispersed phase	2.70	3.33	2.54
(4) Saturated Phase	2.78	3.48	3.38

The changes in $\overline{V}_o$ when wall drag alone is taken into account are relatively small as the pure phases and saturated phase values show (equation (5-4) with $\alpha = 1$). Increasing the drag coefficient, however, has a greater effect. The 100% increase in drag coefficient has reduced $\overline{V}_o$ for transfer into the dispersed phase by 29.7%, while the reduction in C_d for reverse transfer has reduced $\overline{V}_o$ by 16.8%. If the data for case (2), transfer out of the dispersed phase, are overlooked, then equation (4-14) qualitatively predicts the trends better than equation (5-4), i.e. there is no evidence that increases in the drag coefficient caused by interfacial convection are significant.

III COMPARISON WITH OTHER DATA

Values of the characteristic velocity $\overline{V}_o$ under conditions of mass transfer have been published by Gayler and Pratt (1957b). Figure 5 - 8 compares data of Gayler and Pratt for transfer in both directions and data from this work in all four cases. It can be seen that three out of four cases together with data from Gayler and Pratt (1957b), for transfer into the dispersed phase qualitatively follow the function derived by Gayler, Roberts and Pratt. Deviation from the line is consistently low. This may result from the fact that Gayler, Roberts and Pratt used the drag coefficient for solid spheres to calculate the droplet terminal velocities, whereas the Hu - Kintner (1955) correlation has been used in this instance. The points for transfer out of the droplets all lie well above the function. This highlights the failure of the correlation when Marangoni induced coalescence is a significant factor in the column.

IV PHYSICAL BEHAVIOUR

Figure 5 - 2 reveals an important difference in behaviour between transfer from the dispersed phase and the other three systems. That is

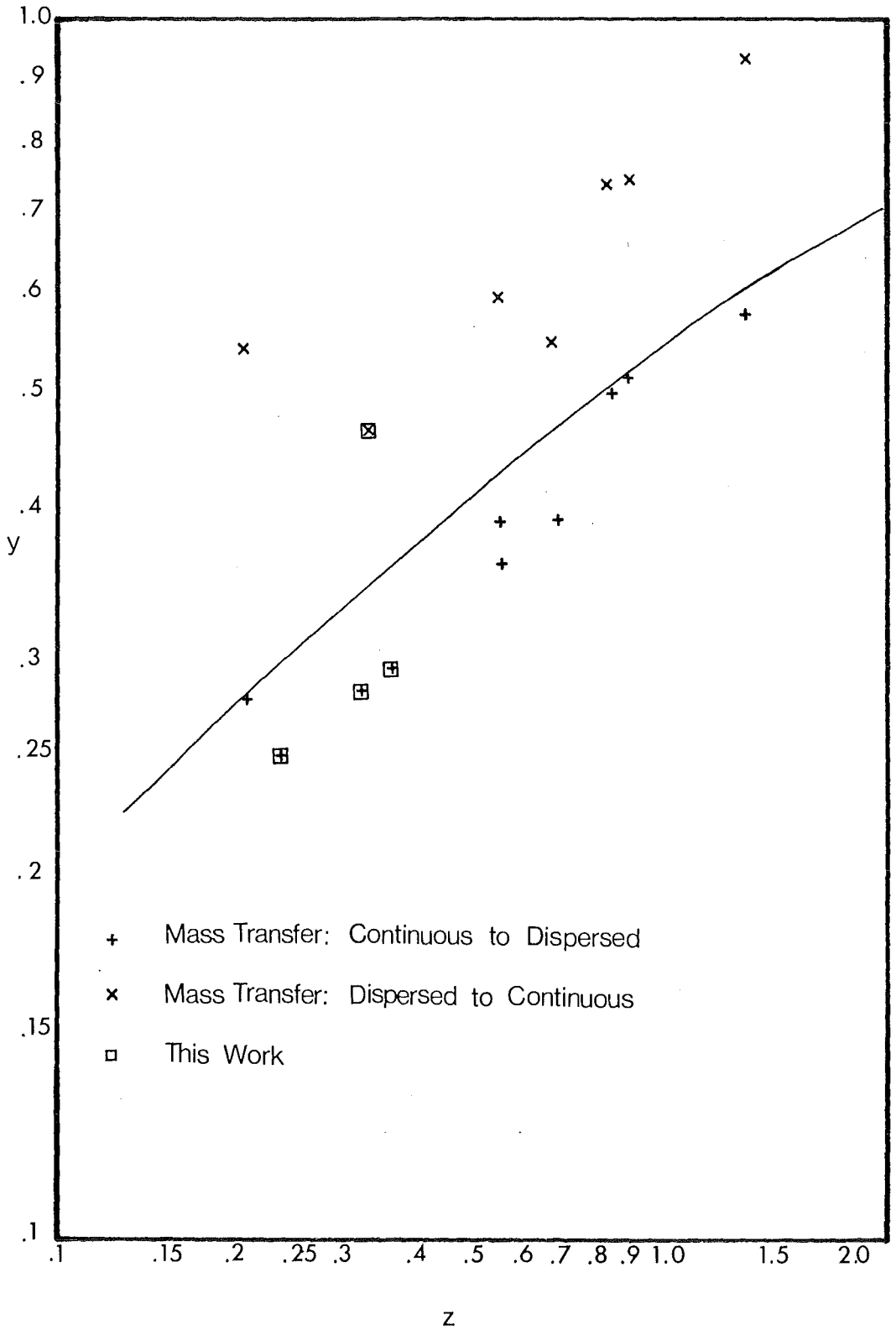

FIGURE 5 - 8 COMPARISON OF MASS TRANSFER DATA AND CORRELATION

the suppression of the loading zone and a subsequent increase in capacity. The increase in drop size observed experimentally implies that a substantial amount of coalescence is occuring. If the behaviour at a restriction for the pure phases is pictured as a string of drops passing one at a time through the restriction then the delay time will be proportional to the velocity of the string and its length. If, however, the drop string coalesces to a single drop, then the delay time will be considerably reduced. Thus the characteristic velocity will be increased. Also the point at which the central channels become saturated will occur at substantially higher flowrates. Furthermore, the flow through the secondary areas will also be in the form of coalescing and redispersing strings. Wilkinson et al (1975), has shown that the ratio of buoyant to surface tension forces is the parameter which controls whether or not a drop will pass through a restriction. Since this ratio increases with increasing drop volume, flow will be easier for the coalesced strings.

V PERMANENT HOLDUP

In the previous chapter it was pointed out that comparison of free rising holdup would be valid if no gross changes in the interaction between permanent and free holdups were caused by mass transfer. Three out of the four systems examined display very similar behaviour. The holdups, characteristic velocities and drop size changes seem to be adequately correlated by the changes in physical properties occuring. It would seem likely, then, that no significant changes in the interaction rate between the permanent and free rising holdups have occured. In the case of transfer out of the droplet, substantial amounts of coalescence are induced. The increase in characteristic velocity shows that the larger droplets are better able to move through restrictions. Thus, one would expect the permanent holdup to be smaller,

and the proportion of dispersed phase left in the preferential channels to be smaller than in the pure phases case. The free rising holdup will be a larger proportion of the total holdup than in the pure phases case. Thus, although the interaction rate will have changed, the conclusions reached will not be effected since the actual effect will be greater than that indicated by the free rising holdup.

CONCLUSIONS

The behaviour of the saturated phases and the case of transfer into the dispersed phase was qualitatively very similar to the pure phase case. Two distinct regions were found in plots of holdup against flowrate. The characteristic velocity increased by 6.7% and 9.9% over the pure phases for the case of transfer into the dispersed phases and saturated phases respectively. Transfer out of the dispersed phase brought reductions in holdup of 30 - 50%. An extended linear regime was found and an increase in characteristic velocity of 73.5%.

The Gayler, Roberts, Pratt correlation for the characteristic velocity qualitatively follows the trend found for transfer into the dispersed phase and the saturated phase with predicted increases in $\overline{V}_o$ of 1.8 and 6.4% respectively. However, an increase of only 4% is predicted for transfer out of the dispersed phase. Changes in the group $\frac{\Delta\rho_g}{\rho_d}$ contribute a maximum 1.3% change in $\overline{V}_o$, while changes in the path length contribute to an increase of up to 11% in $\overline{V}_o$.

The model predicts a decrease in droplet size with a decrease in interfacial tension in all cases. Also, an increase in the characteristic velocity is linked with a decrease in drop size. Marangoni induced coalescence when transfer is out of the dispersed phase means that the first is not necessarily true, and experimental evidence shows that an increase in droplet diameter can be accompanied by an increase in $\overline{V}_o$.

Changes in the physical properties, primarily interfacial tension, resulted in predicted decreases of up to 6.2% in the droplet terminal velocity using the Hu - Kintner (1955) correlation. This resulted in maximum decreases in $\overline{V}_o$ of 0.9%. Convective instability was found to be predicted for the direction of transfer continuous to dispersed. The effect of an increased drag coefficient was found to have a large effect on the predicted values of $\overline{V}_o$. The predicted effects were

not,however, supported by the experimental evidence.

Similarities between the behaviour of the pure phases, the saturated phases, and the case of transfer into the dispersed phase suggest that little change in the interaction rate between the free rising and permanent holdups has occured as a result of mass transfer. Comparison of the free rising holdups is thus valid. Changes in the interaction rate for transfer out of the dispersed phase mean that the actual effect on the active holdup will be greater than that inferred from the behaviour of the free rising holdup.

NOMENCLATURE

c - solute concentration (mole l^{-1})

C_d - drag coefficient (-)

d - droplet diameter (cm)

d_{mn} - weighted droplet diameter = $\sum_{i=0}^{\infty} n_i d_i^m / \sum_{i=0}^{\infty} n_i d_i^n$ (cm)

d_p - packing element diameter (cm)

D - molecular diffusivity ($cm^2\ s^{-1}$)

e^2 - ratio of kinematic viscosities (-)

g - gravitational acceleration ($cm\ s^{-2}$)

n_i - number of droplets diameter i (-)

r^2 - ratio of molecular diffusivities (-)

s - droplet path length (cm)

$\bar{s}$ - average droplet path length (cm)

t - time of droplet travel (s)

$\bar{t}$ - average time of droplet travel (s)

V - droplet velocity ($cm\ s^{-1}$)

V_c, V_d - superficial phase velocities ($cm^3\ s^{-1}/cm^2$)

$\bar{V}_o$ - characteristic velocity ($cm\ s^{-1}$)

x - dispersed phase free holdup (-)

y - parameter defined by equation (4-20) (-)

z - parameter defined by equation (4-21) (-)

α - constant used in equation (5-1) (-)

μ - dynamic viscosity ($g\ cm^{-1}\ s^{-1}$)

ν - kinematic viscosity ($cm^2\ s^{-1}$)

ρ - density ($g\ cm^{-3}$)

$\Delta\rho$ - phase density difference ($g\ cm^{-3}$)

σ - interfacial tension ($g\ s^{-2}$)

Subscripts

c - continuous

d - dispersed

s - Stokes law

t - terminal

CHAPTER SIX

REVISED MODEL FOR CHARACTERISTIC VELOCITY

Chapter contents.

INTRODUCTION

In chapter four the Gayler - Roberts - Pratt, (1953) model for the characteristic velocity was shown to be an inadequate approximation to actual behaviour, even under the conditions for which it was derived. This was because it treated droplet motion as a continuous sequence of acceleration steps and neglected the fact that regions of free rise are separated by restrictions through which the droplets must pass. Furthermore, in chapter five it was shown that the model fails when mass transfer induced coalescence occurs. Experimental values of the characteristic velocity $\overline{V}_o$ measured under such conditions were found to lie on a separate line parallel to the function derived by Gayler, Roberts and Pratt for the pure phases.

The parameter used by Gayler et al to fit their model to the experimental data was the droplet path length $\overline{s}$. Thus, the simplest approach would be to redefine the path length when transfer out of the dispersed phase is occuring. This has the advantage that it makes only a small change to an existing and established design method. This approach however, gives no information about the basic processes occuring, and hence the limitations of the design method. Thus, it was felt desirable to develop an improved model of droplet flow which reflected more closely the actual behaviour observed.

Such a model would need to contain the following features:

1) The net velocity of a droplet results from both free rise and delays at restrictions.
2) The characteristic velocity represents the average flowrate of a wide range of droplet sizes with different residence times in the column.

Thus it would be better to take the contribution of each droplet size rather than to try to represent the distribution by a mean diameter.

MODEL

The droplet motion is modelled as a continuous sequence of steps in which a region of free rise is followed by passage through a restriction. Thus, the free rise occurs over a distance $\bar{s}$ in an average time $\bar{t}$. A queue of droplets of length h forms beneath the restriction and the droplet progresses through the queue in a time t_o.

If $\bar{V}_i$ is the average velocity of a droplet of diameter i, then:

$$\bar{V}_i = \frac{\bar{s} + h}{\bar{t}_i + t_o} \tag{6-1}$$

As a first approximation the free rise model of Gayler et al may be used to relate the free rise distance $\bar{s}$ and the average time $\bar{t}_i$. Thus:

$$\bar{s} = V_t \bar{t}_i \left[1 - \frac{\rho_d V_t}{\Delta\rho g \bar{t}_i} \left(1 - \exp\left[\frac{-\Delta\rho g \bar{t}_i}{\rho_d V_t} \right] \right) \right] \tag{6-2}$$

To obtain expressions for the queue length h and delay time t_o, an energy balance is made over the queue.

$$\Delta PE + \Delta KE - \Delta SE = \Sigma F \tag{6-3}$$

where PE is potential energy, KE is kinetic energy, SE is surface energy and ΣF is viscous losses. If it is assumed that the queue moves at a constant velocity and remains a constant length, then:

$$\Delta KE = 0$$

and

$$\frac{\pi}{6} h d^3 \Delta\rho g = \sigma\Delta A + \Sigma F \tag{6-4}$$

where $\sigma\Delta A$ is the work done deforming a droplet within the restriction.

If the standard orifice equation is used to predict the viscous losses:

$$\Sigma F = V \Delta P$$

$$= V \frac{\varrho_d \left[\frac{d^4}{d_o^4} - 1 \right] u^2}{2 (C)^2} \qquad (6\text{-}5)$$

where u is the queue velocity, V is the droplet volume, d_o is the restriction diameter and C is the orifice coefficient. If the value of C is taken as 0.67 as suggested by Treybal (1963) for sieve plates, then:

$$h = \frac{\sigma \Delta A}{\Delta \varrho \, g V} + \frac{\varrho_d \left[d^4 / d_o^4 - 1 \right] u^2}{2(.67)^2 \Delta \varrho \, g} \qquad (6\text{-}6)$$

If the restriction is occupied by a single droplet at any one time then the droplet shape within the restriction may be modelled as two truncated spheres - see figure 6 - 1.

Conservation of volume gives:

$$d^3 = 2d_t^3 + \sqrt{d_t^2 - d_o^2} \left[\frac{d_o^2}{2} - d_t^2 \right] \qquad (6\text{-}7)$$

where d is the original droplet diameter, d_t is the diameter of the truncated sphere and d_o is the restriction diameter.

The increase in surface area is given by:

$$\Delta A = 2\pi d_t^2 - \pi d_t (d_t - \sqrt{d_t^2 - d_o^2}) - \pi d^2 \qquad (6\text{-}8)$$

$$= \pi d_t^2 + \pi d_t \sqrt{d_t^2 - d_o^2} - \pi d^2 \qquad (6\text{-}9)$$

Equation (6-7) cannot be rearranged to give an explicit equation for d_t in terms of d and d_o. However, knowing d and d_o, the numerical solution

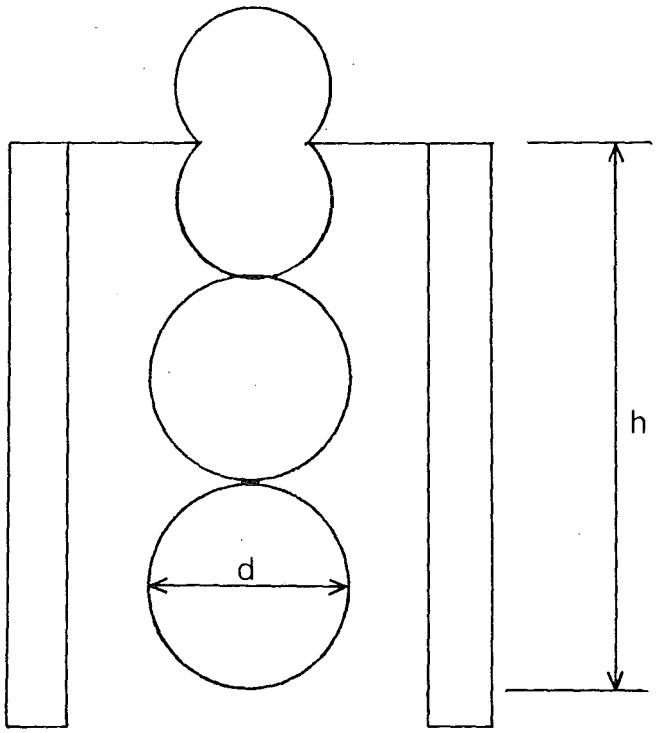

a Queue Structure

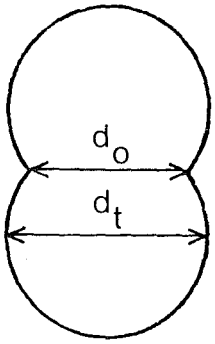

b Droplet Deformation

FIGURE 6 – 1 MODEL OF RESTRICTION BEHAVIOUR

to equation (6-7) can be obtained and thus the increase in area from equation (6-9). However in chapter eight it is shown that droplet breakup occurs throughout much of the packed height. Thus it was felt better to replace the increase in surface area resulting from deformation with the increase in surface area caused by the droplet breaking into two equal daughter droplets. This means that the first term in equation (6-6) is effectively independent of the restriction diameter. Thus conservation of volume gives:

$$d^3 = 2d_p^3 \tag{6-10}$$

where d_p is the diameter of the daughter droplet formed. The increase in surface area is then given by:

$$\Delta A = 2\pi d_p^2 - \pi d^2 \tag{6-11}$$

$$= \pi d^2 (2^{\frac{1}{3}} - 1) \tag{6-12}$$

$$= 0.26\ \pi\ d^2 \tag{6-13}$$

Thus, the queue length h is a function of the mean droplet diameter, the restriction diameter d_o, and the queue velocity u. Since u is a constant

$$h = u\ t_o \tag{6-14}$$

and

$$\overline{V}_i = \frac{\overline{s}_i + h}{\overline{t}_i + h/u} \tag{6-15}$$

For any packing size it can be assumed that the distance travelled in one cycle of free rise followed by movement through a restriction is

constant, i.e.

$$\bar{s} + h = K \qquad (6\text{-}16)$$

$$= f(D_p)$$

where D_p is the packing size. Thus:

$$\bar{V}_i = \frac{K}{\bar{t}_i + h/u} \qquad (6\text{-}17)$$

The free rise time $\bar{t}_i$ will vary with droplet diameter. Thus the overall characteristic velocity $\bar{V}_o$ must be related to the individual $\bar{V}_i$. If $H(d)$ represents the normalised droplet volumetric distribution, then following Misek (1967):

$$\bar{V}_o = \int_o^\infty \bar{V}_i \, H(d) \, \partial d \qquad (6\text{-}18)$$

The queue velocity u may be related to the superficial dispersed phase flowrate in a similar manner. Taking a mass balance over a cross-section of the column gives:

$$\frac{\pi}{4} d_c^2 V_d = N_1 \int_o^\infty \frac{\pi}{4} d^2 V_t \, H(d) \, \partial d + N_2 \int_o^\infty \frac{\pi}{4} d^2 u \, H(d) \, \partial d \qquad (6\text{-}19)$$

$$d_c^2 V_d = N_1 \int_o^\infty d^2 V_t \, H(d) \, \partial d + N_2 \, u \int_o^\infty d^2 \, H(d) \, \partial d \qquad (6\text{-}20)$$

$$u = \frac{d_c^2 V_d - N_1 \int_o^\infty d^2 V_t H(d) \, \partial d}{N_2 \int_o^\infty d^2 H(d) \, \partial d} \qquad (6\text{-}21)$$

where d_c is the column diameter, N_1 is the number of channels occupied by droplets moving at their terminal velocity V_t, and N_2 is the number of channels occupied by queues.

RESULTS AND DISCUSSION

The characteristic velocity $\overline{V}_o$ represents the integral volumetric flow of all droplet diameters. Experimental volume distribution data is available for discrete droplet sizes (Appendix IV). Thus, the integral of equation (6-18) may be represented as a summation over the range of droplet sizes.

I FREE RISE BEHAVIOUR

(1) Characteristic Velocity

The effects of changing to a size distribution model rather than using an average droplet diameter can be seen by calculating the characteristic velocity for the case when free rise only is occuring. For this case the queue length and thus the delay time at a restriction are zero, i.e.

$$h = t_o = 0$$

and the free rise path length $\overline{s}$ will be equal to the cycle path length K. Thus:

$$\overline{V}_i = \frac{K}{\overline{t}_i} \qquad (6\text{-}22)$$

and

$$\overline{V}_o = \int_o^{\infty} \frac{K}{\overline{t}_i} H(d)\, \partial d \qquad (6\text{-}23)$$

The volumetric distribution H(d) may be represented by the experimental volume distribution for a low dispersed phase flowrate after 140cm of packing. If the Hu-Kintner correlation is used to calculate terminal velocities, which are then correlated for the wall effect using equation

(4-22), then an assumed value of 5cm for the path length K results in the following values for equation (6-23) when values of $\bar{t}_i$ found by numerically solving equation (6-2) are substituted.

TABLE 6

	$\bar{V}_o$/cm s^{-1} Experimental	$\bar{V}_o$/cm s^{-1} Equation (6-23)
(1) Pure phases	2.53	6.82
(2) Transfer out of dispersed phase	4.39	3.91
(3) Transfer into dispersed phase	2.70	6.86
(4) Saturated phases	2.78	7.28

(2) Physical Significance

Table 6 shows that the predicted values for three of the four systems based on free rise are well above the experimental characteristic velocities. Thus, the basic problem of the Gayler, Roberts and Pratt model of having a characteristic velocity much smaller than the droplet terminal velocity is still reflected in the size distributed model. The exception however, is when transfer out of the dispersed phase occurs, and the net velocity is close to the experimental value. This fact tends to reinforce arguments about the differences in the mechanism of droplet flow which occurs when coalescence of the dispersed phase is taking place. Thus, when the pure phases are dispersed, there is relatively little coalescence, and the type of flow occuring is representative of the saturated phases case and when transfer into the dispersed phase is occuring.

At low flowrates most of the dispersed phase occupies the preferential channels. The net motion of the droplet consists of two successive stages. In the first, free rise occurs until the droplet

comes to a restriction. Unless the passage through the restriction occurs at a velocity greater than the droplet terminal velocity a queue of droplets will form below the restriction. Once the droplet has passed through the queue and restriction it then enters another region of free rise. If coalescence occurs beneath the restriction then the situation changes slightly. The whole coalesced mass will pass through the restriction at once, probably breaking up again as it leaves (see chapter eight). The situation is thus similar to slug flow, and the net velocity of the droplets will not be greatly different in either the free rise regions or through restrictions.

II RESTRICTION BEHAVIOUR

(1) Queue Velocity

The regions of droplet free rise have been modelled as being separated by restrictions at which queues form. The full form of equation (6-18) is:

$$\overline{V}_o = \int_o^\infty \overline{V}_i \, H(d) \, \partial d$$

and substituting equation (6-1) for $\overline{V}_i$ gives:

$$\overline{V}_o = \int_o^\infty \frac{s + h}{\overline{t}_i + t_o} \, H(d) \, \partial d \qquad (6\text{-}24)$$

The queue length is given by equation (6-6):

$$h = \frac{d\Delta_A}{\Delta \varrho g V} + \frac{\varrho_d \left[d^4/d_o^4 - 1 \right] u^2}{2(.67)^2 \Delta \varrho g}$$

Equation (6-6) shows that for any droplet size, the queue length is dependent upon two variables - the restriction diameter d_o, and the queue velocity u. When these are specified the queue length h and delay time t_o are determined for any given mean droplet size (Equations (6-6)

and (6-14)). Furthermore, the free rise path length $\bar{s}$ is also determined (equation (6-16)), for any given cycle path length K. Estimates of the queue velocity u were made by numerically solving equations (6-24) and (6-6) using a search technique to best fit the experimental characteristic velocities. Figure 6 - 2 shows the queue velocities calculated in this manner as a function of the cycle path length K, and the restriction diameter d_o, for the pure phases system.

As might be expected the primary dependence is on the cycle path length and thus the droplet free rise path length. Obviously the greater the region with a high average velocity, the greater must be the delay at restrictions in order to obtain the desired net velocity. The much smaller dependence on restriction diameter results from the way in which the model of behaviour at restrictions has been formulated. The head which forms at the restriction consists of two components - a distortion, or surface area term and a viscous term. The increase in surface area is much greater than the viscous losses, and so predominates in the equation. The assumption that this term is independent of the restriction diameter will be dealt with later. The viscous term is dependent on the groups:

$$u^2 \quad , \quad \left(\frac{d}{d_o}\right)^4 - 1$$

Thus, the effect of restriction diameter will be greatest at short free rise path lengths, and thus highest queue velocities. Secondly, the viscous term will increase as the ratio of droplet diameter to restriction diameter increases. Thus, the pure phase case which has the largest mean diameter shows the strongest dependence on restriction diameter.

The fact that the estimated queue velocities are nearly identical for the three cases (excluding transfer out of the dispersed phase) suggest that for systems with low coalescence rates the changes in

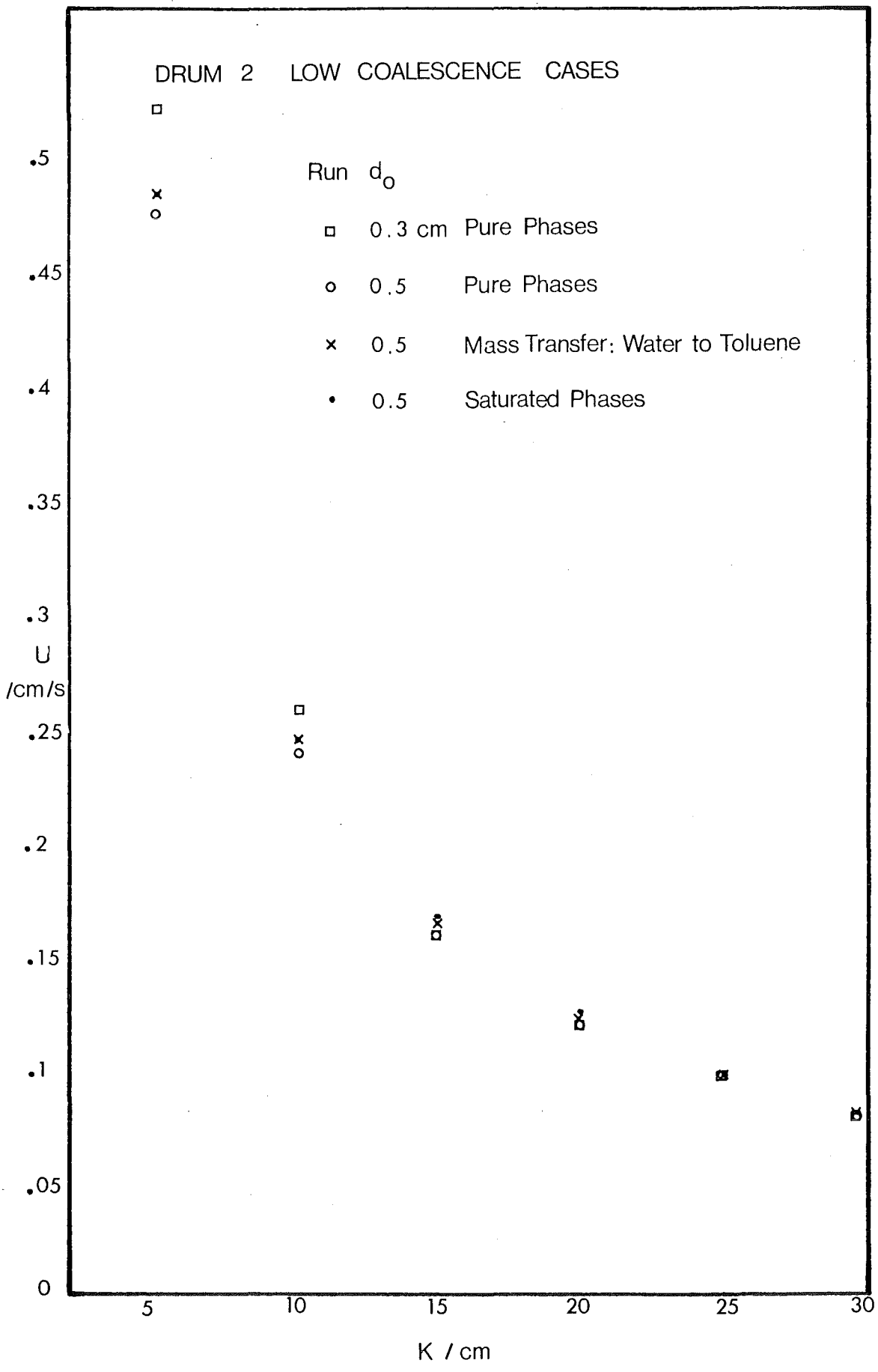

FIGURE 6 – 2 QUEUE VELOCITY vs CYCLE PATH LENGTH

characteristic velocity can in fact be correlated with the changes in free rise behaviour between the systems. This in turn can be correlated with the changes in droplet size distribution between the systems. When transfer out of the dispersed phase is occuring there is rapid coalescence of all droplets collecting beneath a restriction. The coalesced mass then moves rapidly through the restriction. Thus the concept of queue formation is not applicable to this case.

(2) Influence of Packing Height

These queue velocities are based on the droplet size distribution at the top of the packing. However, it is later shown that the final distribution is not established until at least 80cm of packing has been traversed (chapter eight). Thus the integrated free rise velocity is shown as a function of packing height for the surfactant system in figure 6 - 3. The importance of the droplet size distribution is revealed by the changes in free rise behaviour as a function of height. The initial distribution is large and the estimated free rise velocity is within 4% of the experimental characteristic velocity. The droplet size distribution breaks down as the packing height increases. However, after 10cm of packing the integral free rise velocity is still only 40% greater than the experimental $\overline{V}_o$ value. The integral free rise velocity continues to increase until after 45cm it has reached: $\overline{V}_o$ = 6.15 cm s^{-1}. It could be argued that the characteristic velocity is set by the lowest free rise velocity at any point in the column. However, this occured only two centimetres from the distributor, and it is likely that the velocity of the droplets at this point is still determined by the distributor exit velocity rather than by the terminal velocity under the action of buoyancy and drag forces. This influence should have been dissipated after 10cm of packing though. Thus it would seem reasonable to assume that the characteristic velocity is strongly influenced by the largest droplet size distribution which is moving

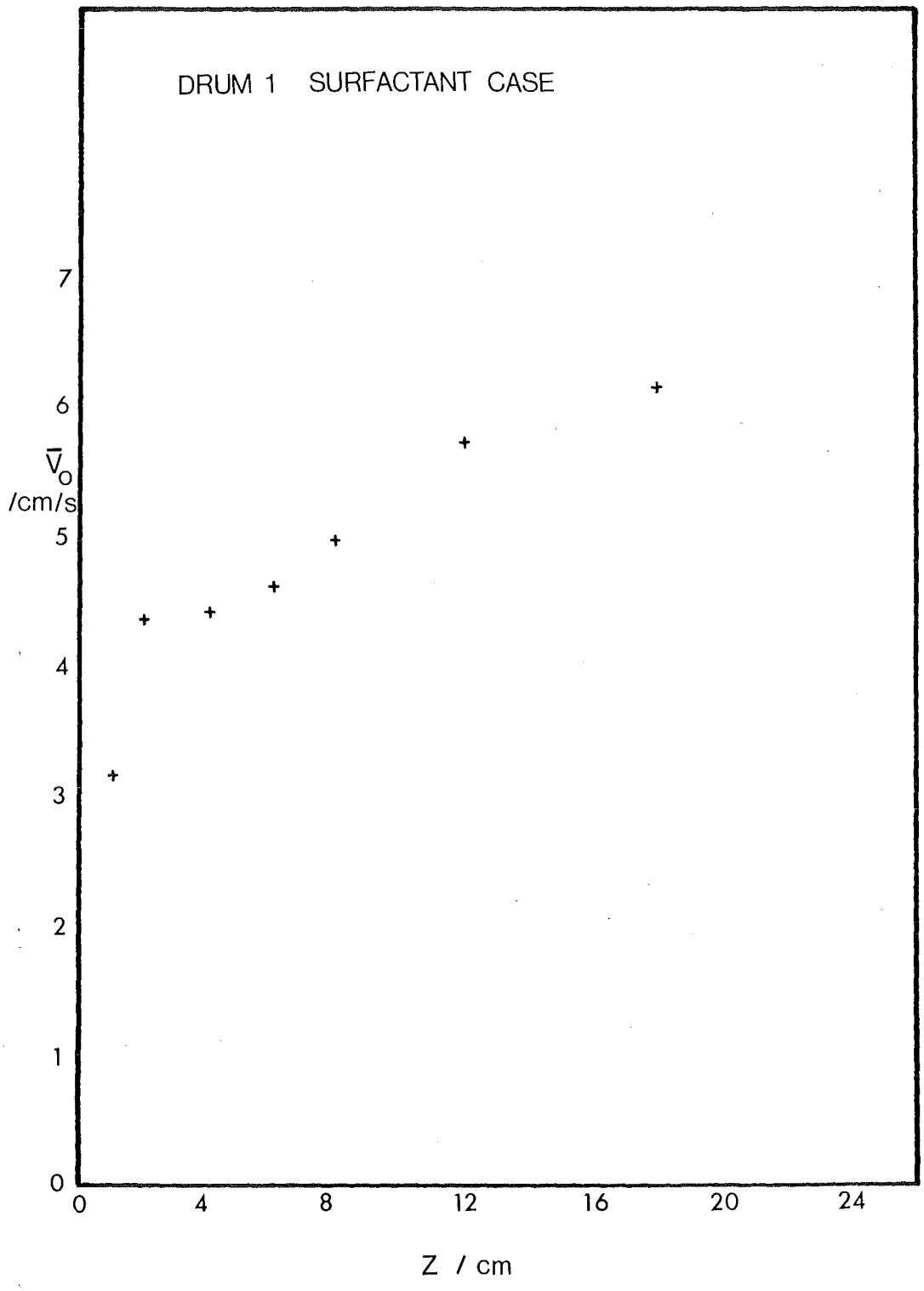

FIGURE 6 – 3 INTEGRAL FREE RISE VELOCITY vs PACKING HEIGHT

under the action of buoyancy forces in the column.

(a) Physical Corroboration. This is further backed up by the behaviour of the column as flooding was approached. Flooding did not occur uniformly over the column, but rather was initiated at specific points, usually 10 - 15cm above the distributor. The droplet density in this region would increase noticeably above that further up the column. The bottom edge of this layer would then move slowly downwards until entrainment in the heavy phase outlet occured.

Markas and Beckmann (1957) have measured total holdup values as a function of packing height for a 15cm ID column using radiometric methods. Unfortunately their measurements begin after 40cm of packing, but show little variation over the remainder of the packed height, apart from an increase in the last few centrimetres which was attributed to recirculation. Calculation of the integral free rise velocity for the present case shows that after 45cm of packing it has reached 90% of the value at the top of the packing. Thus, little change would be expected in the characteristic velocity and thus holdup over the range of packing heights examined by Markas and Beckmann.

(3) Influence of Dispersed Phase Flowrate

Changing the dispersed phase flowrates changes not only the flowrate through a restriction but also the droplet size distribution and thus the free rise characteristics. The most extensive data on size distributions as a function of flowrates are those for the surfactant case. In figure 6 - 4 the integral free rise velocity for a zero continuous phase flowrate is plotted against the superficial dispersed phase velocity. The complex behaviour found reflects the involved manner in which the droplet size distributions depend upon the phase flowrates (chapter eight).

However, when equations (6-6) and (6-24) are solved to find the queue velocities necessary to fit the experimental characteristic

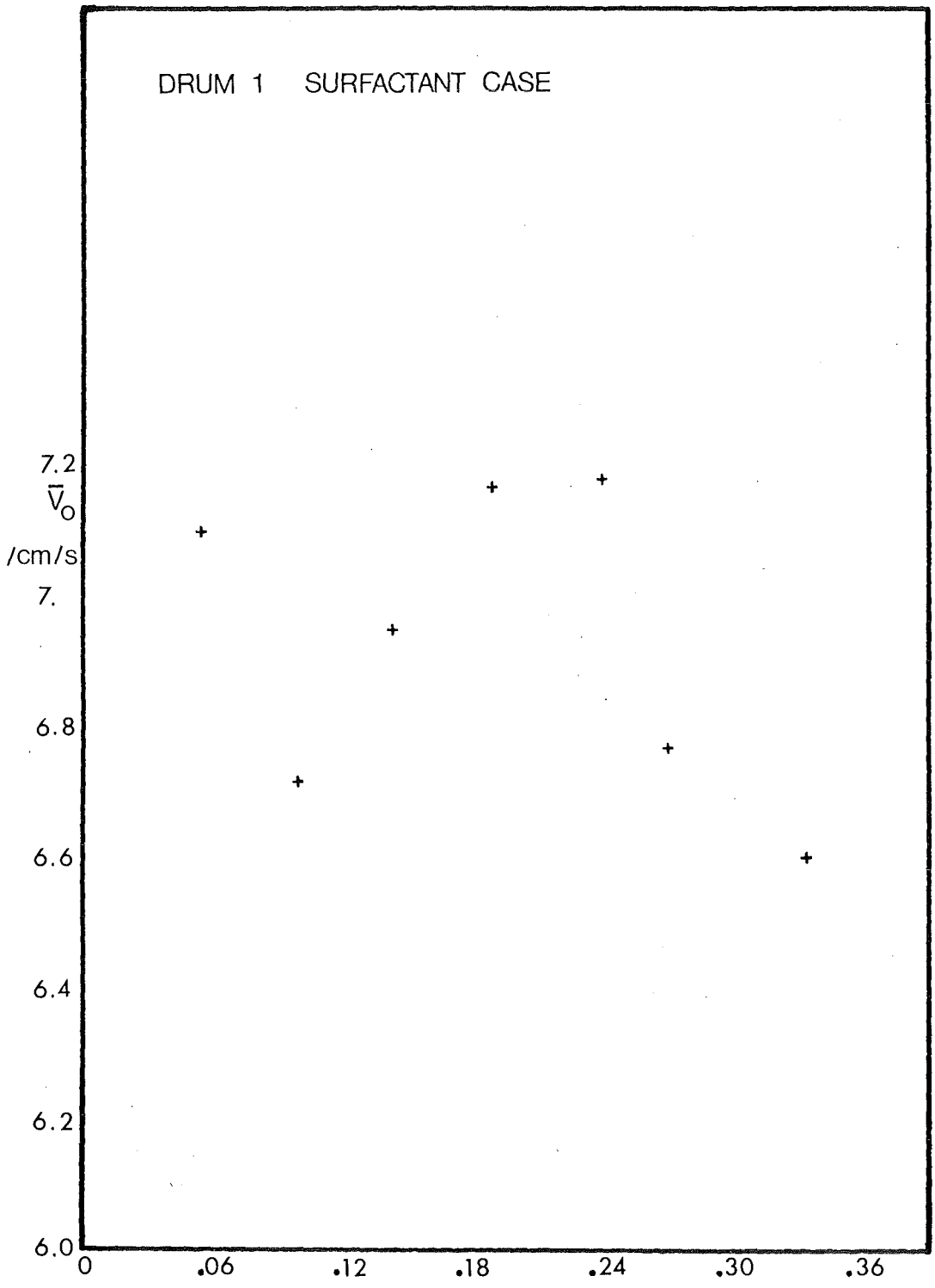

FIGURE 6 – 4 INTEGRAL FREE RISE VELOCITY vs DISPERSED PHASE FLOWRATES

velocity a reasonably linear dependence on dispersed phase flowrate is found as shown in figure 6 - 5. Agreement is best when a relatively small restriction diameter (0.3cm) is used. If the dependence on dispersed phase flowrate is taken as simple first order, then linear regression gives,

$$u = 0.534\ V_d + 0.631 \qquad (6\text{-}25)$$

This equation is based upon the droplet size distributions obtained for the surfactant system using a cycle path length K of 5cm.

(a) Influence of Packing Height. The variation in free rise velocity with height reveals a problem in relating the queue velocity to the dispersed phase flowrate. A much smaller delay time is needed for the distribution at 10cm packed height than is needed for the distribution at the top of the column. Thus a queue velocity of 0.7 cm s^{-1} at the top of the column increases to 1.7 - 2.5cm s^{-1} at 10cm packed height. In order for the fitting of the queue velocity as a function of the dispersed phase flowrate, using the droplet size distributions at the top of the packing, to be valid, it is necessary that the relationship between the distribution at 10cm packed height and at 140cm packed height does not alter with dispersed phase flowrate. It is also necessary for the number of channels occupied by the dispersed phase to remain constant if a linear dependence on dispersed phase flowrate is to be obtained. This seems a reasonable assumption for behaviour in the linear holdup regime.

(4) Approximations in the Model

(a) Queue Structure. A second effect adds to the uncertainty in evaluating the queue velocity. The droplet behaviour at restrictions has been modelled as a line of droplets one behind the other, directly beneath the restriction. In practice however the droplets tend to form a layer beneath the restriction. Furthermore, one of the characteristics

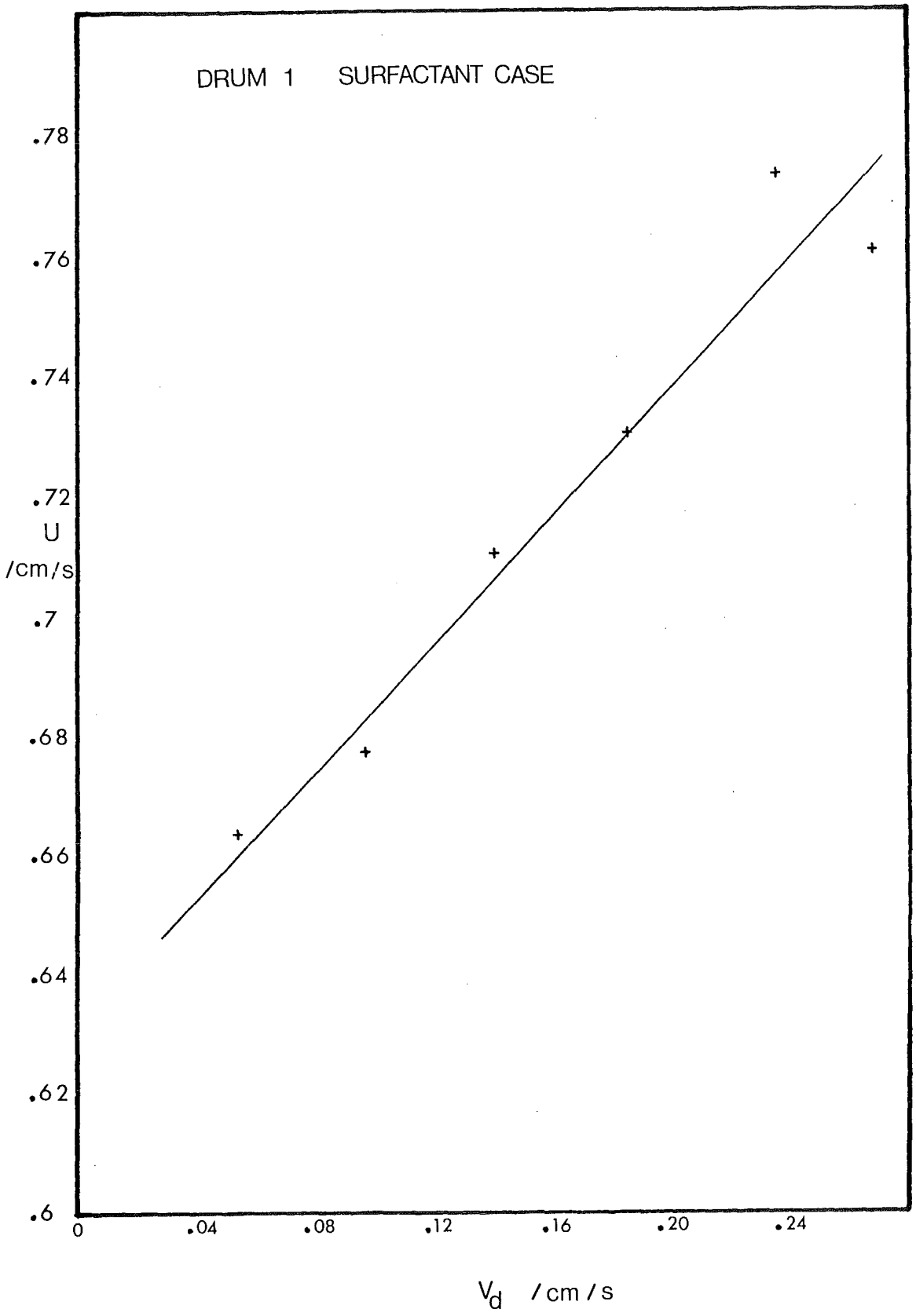

FIGURE 6 – 5 QUEUE VELOCITY vs
DISPERSED PHASE FLOWRATE

of the droplet behaviour is that they tend to pass through the restrictions more than one at a time (figures 7 - 2 to 7 - 5). These factors mean that the delay time at a restriction is greater than would be indicated by ecuation (6-17). If the situation can be represented as in figure 6 - 6 then:

$$h_e \frac{\pi}{4} d_i^2 = t_o \frac{\pi}{4} d_o^2 u \qquad (6\text{-}26)$$

Thus

$$t_o u = \left(\frac{d_i}{d_o}\right)^2 h_e \qquad (6\text{-}27)$$

where d_i is the equivalent cylindrical diameter of the space beneath the restriction, and h_e is the depth of the droplet layer. The buoyancy head will now provide the increases in surface area and the viscous losses for all droplets occupying the restriction at anytime. Thus:

$$h_e = \sum_{j=1}^{j=n} \frac{\sigma \Delta A}{\Delta \varrho g V} + \frac{\varrho_d \left[1 - d_o^4/d_i^4\right] u^2}{2(.67)^2 \Delta \varrho g} \qquad (6\text{-}28)$$

and

$$t_o u = \left(\frac{d_i}{d_o}\right)^2 \left[\sum_{j=1}^{j=n} \frac{\sigma \Delta A}{\Delta \varrho g V} + \frac{\varrho_d \left[1 - d_o^4/d_i^4\right] u^2}{2(.67)^2 \Delta \varrho g} \right] \qquad (6\text{-}29)$$

where n is the number of droplets occupying the restriction. If d_i = 0.6cm and d_o = 0.3cm then the delay time will be four times greater than that predicted by the simple queue model for a given queue velocity. The the buoyancy head required will be reduced in the ratio $\left(\frac{d_o}{d_i}\right)^2$.

The increase in surface area when two or more droplets occupy the nozzle is very much greater than for a single droplet. As the increase in surface area is the major factor in determining the buoyancy head required, this will tend to counteract the effect of having a droplet layer rather than a single line. Multiple occupation

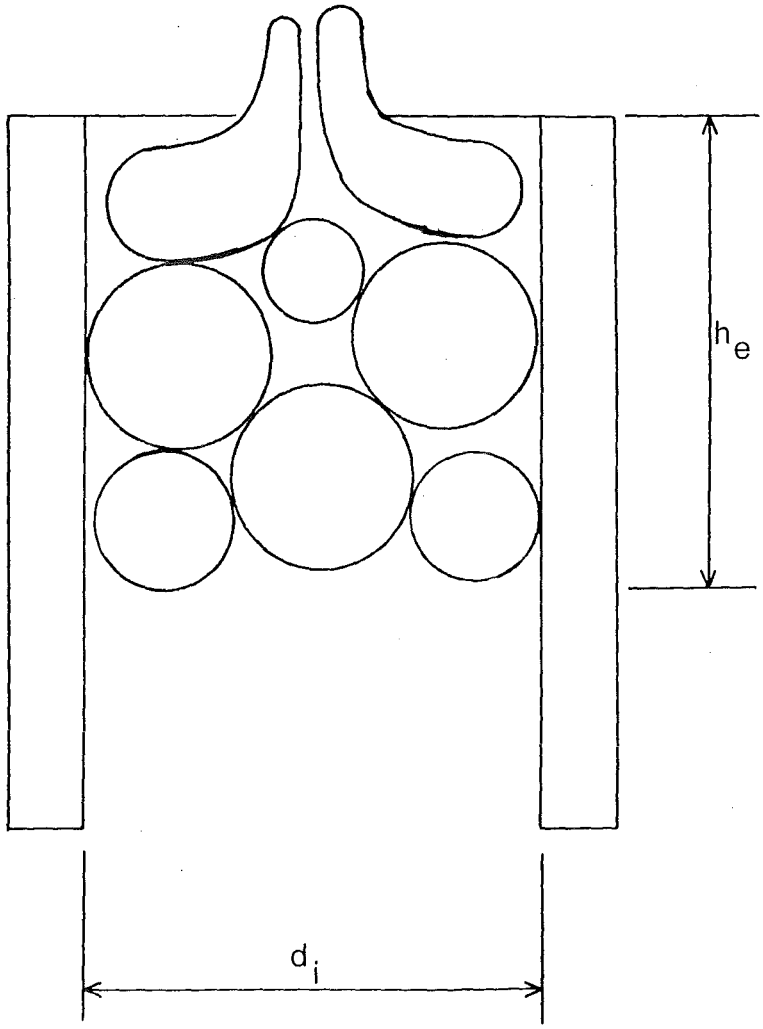

FIGURE 6 – 6 ACTUAL QUEUE STRUCTURE

of the restriction also provides a further reason for dissociating the increase in surface area with the actual restriction diameter. Thus, if two droplets symmetrically occupy a 0.6cm restriction, the increase in surface area will be comparable to both droplets occupying 0.3cm diameter restrictions simultaneously. Whether or not the increase in surface area is adequately represented by the increase when the droplet breaks into two equal spheres is open to question. Figures 7 - 2 to 7 - 5 show that in many instances the droplets are deformed into long jets with surface areas much greater than that of two spheres. Furthermore the number of droplets occupying the restriction and thus the tendency to form long jets increases as the dispersed phase flowrate increases. However, it would seem that the characteristic velocity is set by the behaviour in the first 30cm of packing. In this region the droplet size is relatively large and the tendency for multiple occupation of restrictions should be less then that for distributions near the top of the packing.

(b) Terminal Velocity. The predicted value of $\overline{V}_o$ in Table 6 when transfer is out of the dispersed phase is actually smaller than the experimental value. This reflects a problem in being able to estimate the velocity of large droplets in tubes. The Strom-Kintner equation (1958) can be used to correct the terminal velocity of a droplet moving in an infinite tank for the effect of the droplet to tube diameter ratio β ($= \frac{d}{D}$, where d is the droplet diameter). The upper limit for the validity of this equation however, is $\beta = 0.65$. The equations of Harmathy (1960), enable the prediction of the tube velocity for the range:

$$0 \leqslant \beta \leqslant 1.3$$

However the lower limit of validity of these equations is:

$$Re \geqslant 500$$

Figure 6 - 7 shows the velocity distribution predicted by Harmathy's equation. The Reynolds numbers all lie below the lower limit of validity for the equation. Ho and Leal (1975), and Charles and Mason (1963) have shown that the velocity of large droplets inside tubes becomes independent of the droplet volume once the diameter ratio exceeds 0.9. Table 7 compares the effect of using various constant velocities to describe the motion of the larger diameter droplets.

TABLE 7

Large Diameter Velocity/ cm s^{-1}	$\bar{V}_o$/cm s^{-1} Equation (6-23)	$(\bar{V}_o)$ Experimental
1.0	3.73	4.39 cm s^{-1}
2.0	3.91	
3.0	4.48	

The estimation of the correct velocity is also made more difficult by the interaction between the droplets. Ho and Leal have shown that for droplets moving in creeping flow inside a 1cm diameter tube two regimes of continuous phase flow exist. A recirculating core centred on the tube axis, with a diameter equal to that of the deformed drop is found between adjacent droplets. This core moves at the same velocity as the droplet. Outside this central core a thin shell moves backwards with respect to the droplet. It is thus apparent that processes happening to one droplet will be readily transmitted to other droplets in the same channel. An analytic description of this behaviour is available only for the creeping flow case.

(c) Orifice Equation. The standard orifice equation has been used to try to account for the acceleration of the droplet into the restriction and the viscous pressure drop. The equation is being used in a similar manner to the way in which Treybal uses it for sieve tray design (Treybal, 1963). Possible differences will arise from the fact

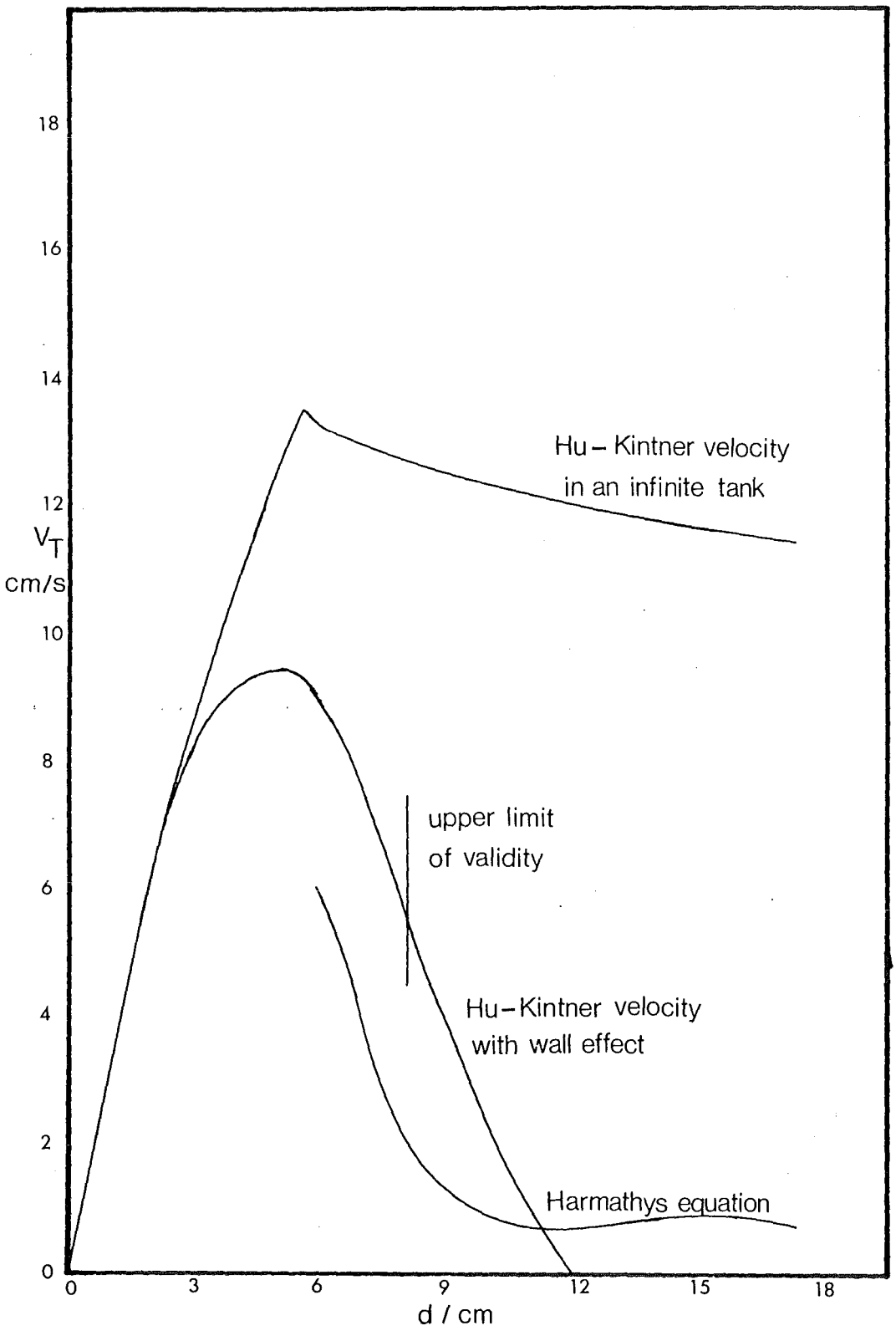

FIGURE 6 – 7 DROPLET TERMINAL VELOCITY EQUATIONS

that discrete droplets occupy the restriction rather than a continuous stream. The velocity profile within discrete droplets is unlikely to be the same as that within a jet forming from a continuous pool. Thus, the coefficient of 0.67 recommended by Treybal may not be the best value for this case. However, any discrepancies will be absorbed into the major parameter, the queue velocity. Other possible errors include the effect of ignoring accelerational drag, changes in the chamber diameter during free rise, droplets bumping into the wall during free rise, interaction between droplets during free rise, uncertainty about the correct path length and the effects of mutiple occupation of the restriction.

(5) Significance of Dependence upon Flowrates

The characteristic velocity has been shown to depend both upon the droplet size distribution and upon the queue velocity (or delay time). The latter has been shown to increase linearly with dispersed phase flowrate. However, in chapter four it was shown that the effect of a continuous phase flowrate superimposed upon the system was to cause a higher flowrate through the preferential channels for a given total dispersed phase flowrate. Thus the effect of the continuous phase flowrate is to displace the slip velocity function while retaining the same dependence upon the dispersed phase flowrate. This dependence of $\overline{V}_o$ upon the flowrates V_d and V_c gives some basis to the empirical equations used by Wicks and Beckmann (1955) and Markas and Beckmann (1957).

(6) Dependence on Packing Structure

It has been pointed out before that a number of different flow regimes exist in a packed column. The free - rise restriction regime proposed applies mainly to the preferential channels. The amount of free rise is much reduced in the secondary flow regions and the flowrate into these channels and thus the queue velocity governs the

net rate of motion in them. Thus the results of Markas and Beckmann (1957) show a decreased replacement time for flow through the secondary regions upon an increase in the dispersed phase flowrate. The extent to which the characteristic velocity is a weighted mean of the flow through both regions depends upon the rate of interchange between them. However, if as proposed, the characteristic velocity is governed largely by the free rise behaviour in the first few centimetres of packing the degree of interchange established should be relatively small.

III APPLICATION OF THE MODEL

Taking all the points raised into account it is proposed that, as a first approximation, the characteristic velocity may be determined as follows:

(1) For systems with low rates of coalescence, the net velocity can be determined using equation (6-24):

$$\overline{V}_o = \int_o^\infty \frac{\overline{s} + h}{\overline{t}_i + t_o} H(d)\, \partial\, d$$

The queue length h may be determined using equations (6-6) and (6-25):

$$h = \frac{\sigma \Delta_A}{\Delta \rho g V} + \frac{\rho_d \left[d/d_o{}^4 - 1 \right] u^2}{2(.67)^2\, \Delta \rho\, g}$$

and

$$u = 0.534\, V_d + 0.631$$

The free rise path length $\overline{s}$ may be obtained from equation (6-16) as:

$$\overline{s} = 5 - h$$

The free rise time $\overline{t}_i$ may be obtained by numerical solution of equation

(6-2):

$$\bar{s} = V_t \bar{t}_i \left[1 - \frac{\rho_d V_t}{\Delta\rho g \bar{t}_i} \left(1 - \exp\left[-\frac{\Delta\rho g \bar{t}_i}{\rho_d V_t} \right] \right) \right]$$

The delay time t_o may be obtained from equation (6-14):

$$t_o = h/u$$

The volume distribution H(d) used should be the largest distribution which is moving under the action of buoyancy and drag forces only. Thus a numerical integration over the range of droplet diameters can be performed to obtain the characteristic velocity.

(2) For systems with high coalescence rates, the effect of restrictions may be neglected and the characteristic velocity determined using equations (6-22) and (6-23):

$$\bar{V}_i = \frac{5}{\bar{t}_i}$$

$$\bar{V}_o = \int_o^\infty \frac{5}{\bar{t}_i} H(d) \partial d$$

Holdup may then be established using the standard slip velocity equation (equation (4-8)).

$$V_d + \frac{x}{1-x} V_c = \epsilon \bar{V}_o x(1-x)$$

This model is based upon results obtained for the toluene - acetone - water system. Further experimental evidence covering other systems and different packing types must be obtained before this model can be established as a design correlation. More precise estimates of the droplet path length would also be desirable. The improvement in the prediction of $\bar{V}_o$ using this method is shown in Table 8.

TABLE 8

	$\bar{V}_o$/cm/s Exp.	$\bar{V}_o$ Eqtn.(4-14)	Deviation / %	$\bar{V}_o$ Eqtn(6-24)	Deviation / %
(1) Pure Phases	2.53	3.27	+29.2	2.88	+13.8
(2) Transfer out of Dispersed Phase	4.39	3.20	-22.5	3.91	-10.9
(3) Transfer into Dispersed Phase	2.70	3.33	+25.2	3.01	+11.1
(4) Saturated Phases	2.78	3.48	+21.9	3.13	+12.8

CONCLUSIONS

A new model for the characteristic velocity relating holdup to slip velocity in packed columns has been proposed. This model takes into account the fact that the net droplet motion consists of two components. These are free rise and motion through restrictions. A previous model was based upon free rise only (Gayler, Roberts and Pratt, 1953). A second important difference between the Gayler - Roberts - Pratt model is the way in which the droplet size distributions are handled. The characteristic velocity is treated as the integral sum of the contributions from all droplet sizes rather than using a mean diameter as previously.

Comparison of the integral free rise velocity for the different cases confirms the difference in flow mechanism when transfer of a solute occurs out of the dispersed phase. For the pure phase and saturated phases, and when transfer into the dispersed phase was occuring, the integral free rise velocities, based on the droplet size distributions at the packing surface, are approximately 250% greater than the experimental characteristic velocity. However, when transfer out of the dispersed phase occurs the integral free rise velocity is close to the experimental value within the uncertainty in estimating the terminal velocity of large droplets. Thus, it would seem that the motion of large droplets represents a type of slug flow while that of smaller droplets is governed both by their terminal velocity, and by their behaviour at restrictions.

Basing models on the droplet size distribution at the top of the column does have some dangers however. The droplet size distribution varies up the column as the initially large distribution breaks down to an equilibrium size. Thus, the integral free rise velocity of distributions in the first 30cm of packing are only 40% greater than the experimental characteristic velocity and it seems

very likely that the behaviour in this region determines the overall value of $\overline{V}_o$ for the column.

Droplet behaviour at restrictions has been modelled as a queue of droplets passing one at a time through the restriction. The buoyancy head represented by the queue provides the increase in surface area caused by droplet deformation and an orifice type pressure drop. The delay time at the restriction is then determined by the length of the queue and the queue velocity. The increase in surface area at the restriction has been taken as that occuring when the droplet breaks in two. Since this term predominates over the orifice pressure drop, the queue velocity is determined primarily by the amount of free rise occuring rather than by the restriction diameter. A linear dependence of queue velocity on dispersed phase flowrate was found. Possible defficiencies in the model result from the fact that droplets tend to form a layer beneath a restriction rather than a queue one beneath another. Secondly, multiple occupation of the nozzle by two or more droplets may cause errors in the surface area term.

The dependence of queue velocity on the dispersed phase flowrate means that the characteristic velocity is a function of both the dispersed and continuous phase superficial flowrates. This may account for the splitting of the slip velocity function with changes in the continuous phase flowrate.

NOMENCLATURE

ΔA - increase in surface area (cm^2)

C - orifice coefficient (-)

d - droplet diameter (cm)

d_c - column diameter (cm)

d_i - equivalent cylindrical diameter of region beneath a restriction (cm)

d_o - restriction diameter (cm)

d_p - diameter of droplet formed by breakup at a restriction (cm)

d_t - diameter of truncated sphere (cm)

D - tube diameter (cm)

D_p - packing diameter (cm)

f - function (-)

ΣF - pressure drop due to flow through a restriction (dyne cm^{-2})

g - gravitational acceleration (cm s^{-2})

h - queue length (cm)

h_e - depth of droplet layer (cm)

H(d) - droplet volumetric distribution (-)

i - index for droplet diameter (-)

j - index for number of droplets occupying a restriction (-)

K - cycle path length (cm)

KE - kinetic energy (erg)

n - number of droplets occupying a restriction (-)

N - number of channels occupied by dispersed phase (-)

ΔP - pressure drop (dyne cm^{-2})

PE - potential energy (erg)

Re - Reynolds number (-)

$\bar{s}$ - free rise path length (cm)

SE - surface energy (erg)

$\bar{t}$ - time of free rise (s)

t_o - delay time at a restriction (s)

u - queue velocity (cm s^{-1})

V - droplet volume (cm^3)

V_c, V_d - superficial phase flowrates ($cm^3\ s^{-1}/cm^2$)

$\bar{V}_i$ - net velocity of droplet diameter i (cm s^{-1})

$\bar{V}_o$ - characteristic velocity (cm s^{-1})

V_t - terminal velocity (cm s^{-1})

β - ratio of droplet diameter to tube diameter (-)

ϱ - density (g cm^{-3})

$\Delta\varrho$ - phase density difference (g cm^{-3})

σ - interfacial tension (dyne cm^{-1})

Subscripts

c - continuous phase

d - dispersed phase

i - of diameter i

SECTION III

DROPLET SIZE DISTRIBUTIONS

INTRODUCTION

The droplet diameter together with the dispersed phase holdup determine the interfacial area between the phases and hence the rate of mass transfer in a liquid-liquid contactor. If the droplet diameter is uniform, or can be represented by a mean value, then the interfacial area per unit volume is given by:

$$a = \frac{6 \epsilon x}{d}$$

where x is the dispersed phase holdup, ϵ the packing voidage fraction, and d the mean droplet diameter.

A characteristic feature of many pieces of extraction equipment is the wide range of droplet sizes that are generated. Unfortunately the mass transfer processes do not change linearly with droplet volume. This fact has caused the practice of using a mean diameter to fall into some disrepute and more sophisticated models of mass transfer based on the integral contribution of all droplet sizes are now appearing, (Chartres and Korchinsky, 1975, Gal-or and Hoelscher, 1966). These models use empirical functions to represent the droplet distribution.

The size distribution of a dispersion is determined by the equilibrium which exists between the breakup of droplets and their rate of coalescence. An extensive literature exists on both these subjects. Relatively little information exists on droplet distributions in packed columns however, and it was felt desirable to collect a set of data that would shed some light on the basic mechanisms controlling the size distribution. Secondly, the influence of a third component on the distributions required investigation.

The section consists of three chapters. The considerable literature on droplet breakup, coalescence, and satellite droplet formation is reviewed in chapter seven together with some recent work

on perforated plate columns that has direct applicability to packed column behaviour. The experimental data obtained in this study is presented in chapter eight. The applicability of breakup mechanisms in the literature is discussed and models of behaviour proposed. Finally, in chapter nine a computer simulation is used to test the hypotheses about droplet behaviour developed in chapter eight.

CHAPTER SEVEN

LITERATURE SURVEY

Chapter contents.

SATELLITE DROPLET FORMATION

I PARTIAL COALESCENCE

II NOZZLE FORMATION

III FORMATION DURING INSTABILITY BREAKUP

SIEVE PLATE PHENOMENA

I SINGLE PLATE BEHAVIOUR

II MULTI-PLATE BEHAVIOUR

III MODELLING

NOMENCLATURE

DROPLET BREAKUP

The breakup of large droplets until a stable size is reached is one of the fundamental processes occuring in liquid-liquid contactors. This breakup may proceed by a variety of mechanisms depending on the type of contactor and the flow conditions prevailing. A broad division may be made between the breakup which occurs as a result of the external field acting on the droplet, and that which results from interaction between the droplet and the contactor walls, packing elements or nozzles. The action of the external liquid field on the droplet may result in breakup as a result of viscous shear or turbulent pressure fluctuations. Interactive breakup may occur as a result of impactions on packing elements or as a result of the droplet passing through the restrictions between adjacent packing elements.

BREAKUP IN A TURBULENT LIQUID FIELD

(1) Dimensional Analysis

The important variables controlling breakup of a droplet depend to some extent on the flow field containing it. However, in nearly all cases the ratio of the inertial forces tending to disrupt the drop, to the interfacial tension forces tending to maintain it, is one major criterion for deformation and breakup. This is expressed in dimensionless terms by the Weber number.

Hinze (1955), has analysed the stresses affecting a droplet in a free liquid field. The order of magnitude stresses are:

External stress τ / unit area

Interfacial tension $\frac{\sigma}{d}$ / unit area

Viscous stress $\frac{\mu_d}{d}\sqrt{\frac{\tau}{\rho_d}}$ / unit area

where d is the spherical droplet diameter.

Dimensional analysis yields three possible dimensionless group:

$$\frac{\tau_d}{\sigma}\ ,\quad \frac{\mu_d}{\sigma}\sqrt{\frac{\tau}{\rho_d}}\ ,\quad \frac{\tau_d}{\mu_d}\sqrt{\frac{\rho_d}{\tau}}$$

The first group corresponds to the Weber number

$$We = \frac{\tau_d}{\sigma} \qquad (7\text{-}1)$$

Eliminating τ between the remaining possible groups gives

$$\frac{\mu_d}{\sqrt{\rho_d \sigma_d}} = Y_i \qquad (7\text{-}2)$$

where Y_i is a viscosity group.

For conditions at droplet breakup these were arranged as:

$$We_{crit} = J\ (1 + \phi(Y_i)\ ) \qquad (7\text{-}3)$$

where ϕ is an arbitary function.

Good experimental support was found when this equation was applied to the breakup of liquid droplets in an air stream.

(2) Laminar Shear

Taylor (1932, 1934), considered the deformation and breakup of droplets in a viscous flow field. The presence of the drop disturbs the flowfield and generates a stress system which can be resolved into tangential and normal stresses at the drop interface. The tangential stress is assumed continuous, however the normal stress is discontinuous due to the curvature of the interface. For small deviations from sphericity the pressure difference is given by:

$$\Delta P_G = -4\,\gamma\,\mu_c \left\{\frac{19p + 16}{16p + 16}\right\} \cos(2\phi') \qquad (7\text{-}4)$$

where $p = \frac{\mu_d}{\mu_c}$, ϕ' is a polar angle, and γ is the shear rate. Hence the curvature of the interface changes so that:

$$\Delta P = \Delta P_G + \frac{2\sigma}{a} \qquad (7\text{-}5)$$

where a is the droplet radius and $\frac{2\sigma}{a}$ is the Laplace capilliary pressure for a curved interface. For small deformations this is satisfied when the

equator of the drop assumes an ellipsoidal form given by:

$$r(\phi'') = a(1 - D\cos(2\phi'')) \qquad (7\text{-}6)$$

where $\phi'' = \phi' + \frac{\pi}{4}$ and the deformation is given by:

$$D = \frac{\gamma a \mu_c}{\sigma}\left[\frac{19p + 16}{16p + 16}\right] \qquad (7\text{-}7)$$

Taking $\tau = \mu_c \gamma$ we have:

$$\text{Deformation} = f\left(We, \frac{\mu_1}{\mu_c}\right) \qquad (7\text{-}8)$$

Taylors results, confirmed and extended by Rumscheidt and Mason (1961), show that the deformation equation holds even for relatively large deformations. Taram and Bellinger (1968), have plotted the critical value of $We\left[\frac{19p + 16}{16p + 16}\right]$ at droplet breakup against p and found a universal plot. This plot goes through a minimum between p = 0.1 and p = 1, and increases to infinity at critical upper and lower limits of p.

It was pointed out by Taylor that when a droplet was deformed in a hyperbolic shear field it was drawn out into a long thread which was stable while it was extending but disintegrated when the flow field stopped. The problem of the stability of an extending viscous thread was treated theoretically by Tomotika (1935, 1936). A general equation was derived relating the growth rate of a disturbance to physical properties, jet diameter, and disturbance wave-length. For Taylor's case it was shown that the wave length of the dominant distubance increases to infinity as p tends to zero and as p becomes large. Particular solutions to Tomotika's equation correspond to many published equations - the equation for the breakup of a gas jet in a low viscosity liquid derived by Rayleigh (1892), the equation for a low viscosity liquid jet in a low viscosity liquid derived by Christiansen (1957), the equation for a high viscosity jet in a gas derived by Weber (1931). The applicability of each of these particular solutions has been reviewed by Scheele and Meister (1967) and a generalised graphical solution presented.

(3) Dynamic Pressure

A droplet will only be drawn out into a long thread if the viscous flowfield containing it is much larger than the droplet i.e. the viscous flow region must exist as a stable shear field for sufficiently long for the droplet to be deformed. The viscous nature of a flow field decreases as the Reynolds number increases and a point is reached where viscous dissipation is confined to flow within small eddies. At this point a more likely source of droplet disruption becomes the dynamic pressure changes caused by fluctuations in eddy velocity over the length of the droplet. Following Hinze:

$$We_{crit} = \frac{\rho_c \bar{V}^2 d_{max}}{\sigma} \tag{7-9}$$

where d_{max} is the maximum stable drop size. If it assumed that droplet breakup is caused by velocity fluctuations in eddies with a wave length less than or equal to the drop diameter, then, since the kinetic energy of an eddy increases with wave length, the critical wave length will be

$$\lambda = d_{max} \tag{7-10}$$

For isotropic turbulence:

$$V_\lambda = C (\epsilon \lambda)^{\frac{1}{3}} \tag{7-11}$$

where V_λ is the eddy velocity and ϵ is the energy input per unit mass. Hence

$$\bar{V}^2 = C_1 (\epsilon d_{max})^{\frac{2}{3}} \tag{7-12}$$

Since viscous effects will be very small for turbulent flow we can assume

$$V_i << 1$$

Then

$$\frac{\rho_c d_{max}}{\sigma} C_1 (\epsilon d_{max})^{\frac{2}{3}} = \text{const.} \tag{7-13}$$

or

$$d_{max} \left[\frac{\rho_c}{\sigma}\right]^{3/5} \epsilon^{2/5} = \text{const.} \tag{7-14}$$

(a) Agitated Vessels. To obtain an expression for the energy input per unit volume Rushton et al (1950), assumed that for a stirred tank at high Reynolds numbers:

$$\epsilon = C N^2 D_I^3 \tag{7-15}$$

where D_I is the impellor diameter.

Hence

$$d_{max} \left(\frac{\rho_c}{\sigma}\right)^{3/5} N^{4/5} D_I^{6/5} = C \tag{7-16}$$

Using d_{32}, the Sauter mean diameter, instead of d_{max}, this equation has been used successfully by Vermeulen et al (1955), Shinnar (1961), Chen and Middleman (1967) and Sprow (1967), to correlate stirred tank studies where droplet breakup predominates over coalescence.

(b) Pipe Flow. The equation derived by Hinze was derived independently by Kolmogorov (1949), from the theory of homogenous isotropic turbulence, in order to explain the data of Baranayev et al (1949), on the droplet distribution of immiscible liquids in turbulent pipe flow.

For that case

$$d_{max} \simeq \left(\frac{\sigma}{k_f \rho_c V^2}\right)^{3/5} \lambda_o^{2/5}$$

$$= C D^{2/5} \left(\frac{\sigma}{\rho_c}\right)^{3/5} V^{-6/5} \tag{7-17}$$

where k_f is a drag coefficient. As an alternative mechanism it was pointed out that in the region of the tube wall the variations in velocity may be much greater than in the main stream flow. Assuming a logarithmic velocity profile to hold:

$$\Delta P \simeq \rho_c V^2 \left[\left(\ln\left[\frac{y + d}{d_o}\right] \right)^2 - \left(\ln\left[\frac{y}{d_o}\right] \right)^2 \right] \tag{7-18}$$

Equating this to the drop capilliary forces gives

$$d_{max} \sim \frac{1}{V}\left(\frac{\sigma}{\rho_c}\right)^{0.5} \sqrt{\frac{V}{\ln (y/d_o)}} \qquad (7\text{-}19)$$

Thus, the first mechanism gives:

$$d_{max} \sim \frac{\sigma^{0.6}}{V^{1.2}} \qquad (7\text{-}20)$$

and the second gives:

$$d_{max} \sim \frac{\sigma^{0.5}}{V} \qquad (7\text{-}21)$$

The data of Karamayev et al (1949) indicate that:

$$d_{av} \sim \frac{\sigma^{0.5 - 0.6}}{V} \qquad (7\text{-}22)$$

In complete contrast to this, the data of Sleicher (1962), Paul and Sleicher (1965) and Collins and Knudsen (1970), for turbulent pipe flow indicates:

$$d_{max} \sim \frac{\sigma^{1.5}}{V^{2.5}} \qquad (7\text{-}23)$$

They obtained, by dimensional analysis:

$$We\sqrt{\frac{V\mu_c}{\sigma}} = C\left[1 + \phi\left(\frac{V\mu_d}{\sigma}\right)\right] \qquad (7\text{-}24)$$

Rearrangement of this reveals that:

$$We = C_1\left(\frac{\mu_d}{\mu_c} V_i\right)^{\frac{1}{3}}\left[1 + \phi\left(\frac{V\mu_d}{\sigma}\right)\right]^{\frac{2}{3}} \qquad (7\text{-}25)$$

$$= f\left(\frac{\mu_d}{\mu_c}, V_i\right) \qquad (7\text{-}26)$$

(c) Packed Columns. In a study of turbulent cocurrent flow in a packed column Duffy and Kadlec (1975), found:

$$d_{32} = C\, f(x)\, \epsilon^{-2/5}\left(\frac{d\rho}{\theta}\right)^{-1/5} \qquad (7\text{-}27)$$

where dp is the packing diameter, f(x) is a phase fraction function, and θ is the residence time of a droplet. The group $\frac{dp}{\theta}$ can be interpreted as the number of expansion-contraction cycles experienced by a droplet travelling through the bed.

II INTERACTIVE BREAKUP

The literature surveyed so far, with the exception of Duffy and Kadlec (1975), has dealt with the stability of a droplet under the action of an external flow field. In many practical pieces of extraction equipment the dispersed phase is subject to additional disturbances as a result of interaction of the droplets with solid walls, packing elements or nozzles.

(1) Packed Columns

(a) Physical Behaviour. Lewis, Jones and Pratt (1951), and Gayler and Pratt (1953), investigated droplet behaviour in a 5 cm ID column packed with a range of Raschig rings and Berl saddles. For seven organic-water systems it was found that, as long as the packing size was above a critical value, the outlet Sauter mean droplet diameter was independent of the inlet droplet size distribution and the size and type of packing material. When the packing size was below the critical value the mean droplet diameter increased above the inlet value. This finding was in disagreement with Morello and Beckmann (1950), who found that the use of small packings for the toluene - diethylamine - water system in 4.5 cm ID columns prevented coalescence. The results of Lewis, Jones and Pratt (1951), also indicated that the rate of breakdown to equilibrium size of an initially larger distribution was very much faster than the rate of growth of an initially smaller than equilibrium size distribution.

(b) Dimensional Analysis. Dimensional analysis of the physical properties by Lewis et al led to:

$$\frac{d_{32}\Delta\rho\sigma}{\mu_c^2} = 1.67\left[\frac{\Delta\rho\sigma^3}{\mu_c^4 g}\right]^{0.475} \qquad (7\text{-}28)$$

Or, approximating 0.475 by 0.5,

$$\frac{d_{32}^2\Delta\rho g}{\sigma} = 1.25 \qquad (7\text{-}29)$$

Gayler and Pratt (1953a) extended the analysis to account for the effect of the flowrates. A characteristic drop diameter d_{32}^o was defined, this being the mean drop diameter at zero continuous phase flowrate and very low dispersed phase flowrate. Then,

$$d_{32} = d_{32}^o\left(\frac{\overline{V}_o}{V_R}\right) \qquad (7\text{-}30)$$

where V_R is the mean droplet velocity relative to the packing. Using

$$V_R = \frac{V_d}{\epsilon x} \qquad (7\text{-}31)$$

and substituting equation (7-29) for d_{32}^o gives:

$$d_{32} = 0.92\left(\frac{\sigma}{\Delta\rho g}\right)^{0.5}\left(\frac{\overline{V}_o \epsilon x}{V_d}\right) \qquad (7\text{-}32)$$

(c) Mass transfer. The effect of unsaturation of the phases and of the presence of a solute was also investigated by Gayler and Pratt (1953a). Both unsaturation of the phases and transfer of a solute out of the dispersed phase were found to cause increases in the mean droplet diameter leaving the column. Transfer of the solute into the dispersed phase, or an equilibrium distribution of the solute caused no changes in behaviour from that of the pure saturated phases. Similar observations on the effects of mass transfer out of the dispersed phase on the mean droplet diameter have been reported for spray (Dunn, 1963, Johnson and Bliss, 1946), rotary annular (Thornton and Pratt, 1953), rotating disc (Misek and Marek, 1970, Logsdail, Thornton and Pratt, 1957), and

pulsed plate columns (Logsdail and Thornton, 1957, Thornton, 1957).

(d) Impaction Mechanism. Ramshaw and Thornton (1967), analysed the breakup process for a droplet impacting on the thin baffle. When a energy balance is done over a droplet which breaks into two daughter droplets:

$$E_{K1} + E_p - E_S = E_{K2} \qquad (7\text{-}33)$$

where E_K is the kinetic energy, E_p is the potential energy, and E_S is surface energy. At the critical droplet size the parent droplet has just sufficient kinetic energy to supply the increase in surface energy caused by the breakup. Thus $E_{K2} = 0$ and the following equation is obtained:

$$\frac{\pi}{12} d_{crit}^2 \sigma \left[\left(\frac{d_{crit} V_t^2 \rho_d}{\sigma} \right) + 1.80 \left(\frac{d_{crit}^2 \Delta\rho g}{\sigma} \right) - 3.12 \right] = 0 \qquad (7\text{-}34)$$

Reasonable experimental agreement with equation (7-34) was found for droplets impacting on a 0.1mm thick baffle.

The rate of approach to the equilibrium drop size of a larger than equilibrium inlet distribution was also studied by Ramshaw and Thornton (1967) using the toluene-water system in a 7.5cm ID column packed with 19mm Raschig rings. The rate of approach to equilibrium was found to be approximately exponential with height. Mass transfer into the dispersed phase did not effect the existence of a critical droplet size and accelerated the exponential rate of breakdown towards it. Transfer out of the dispersed phase caused coalescence of the droplets and no analysis was attempted.

(2) Nozzle Breakup

(a) Continuous Phase. The formation of droplets from an orifice or nozzle has been treated by Harkins and Brown (1919), Hayworth and Treybal (1950), Null and Johnson (1958), Rao et al (1966) and Scheele and Meister (1968). Scheele and Meister use a two stage model whereby

the drop volume consists of the static volume when the buoyancy and kinetic forces just balance the interfacial tension forces, together with the volume of liquid which flows into the drop during the necking down process. The equation presented was:

$$V_F = H\left[\frac{\pi\sigma D_N}{g\Delta\rho} + \frac{20\mu Q D_N}{D_F^2 g\Delta\rho} - \frac{4\rho_d Q U_N}{3 g\Delta\rho} + 4.5\left(\frac{Q^2 D_N^2 \rho_d \sigma}{(g\Delta\rho)^2}\right)^{\frac{1}{3}}\right] \quad (7\text{-}35)$$

where H is the Harkins-Brown correction factor for the amount of liquid left on the nozzle tip after the drop has broken off. Meister and Scheele (1969 a and b) have also presented an analysis, based on Rayleighs instability theory, of drop formation from cylindrical jets.

(b) Discrete Droplets. The work of Odell (1975), has shown that when the liquid beneath the nozzle consists of discrete drops rather than a continuous pool, the spectrum of drop sizes formed is very much wider and there is a large increase in the number of satellite drops formed. Ooi (1977), using an all glass cell and nozzle has collected photographic evidence that a number of mechanisms are operative in such a case. At low flowrates a Scheele-Meister force balance mechanism predominates. As the flowrate increases competition for the nozzle area becomes apparent. A forming Scheele-Meister drop occupies most of the area. The rest of the nozzle is occupied by a drop so highly deformed that it forms a jet, and breakup of this is by an instability mechanism. At high flowrates all drops form jets with as many as four separate drops occupying a single 6mm diameter nozzle. This work is considered in more detail later in the chapter.

DROPLET COALESCENCE

The coalescence rate between droplets in a liquid-liquid extractor depends upon the collision rate between the droplets and the proportion of these collisions which result in coalescence. The rate of collisions between droplets is determined by the hydrodynamics in and geometry of the contactor. The effectiveness of the collisions is determined by the hydrodynamics in the contactor and the mechanism of coalescence.

I COALESCENCE MODELS

(1) Plane Interface

A large volume of research has been published on single drop studies at plane interfaces. The controlling parameter appears to be the rate at which the film of continuous phase between the drop and bulk phase drains sufficiently for rupture to occur. Mathematical models of the drainage process have been developed by Bashforth and Adams (1883), Gillespie and Rideal (1956), Charles and Mason (1960), Princen and Mason (1965), and Hartland (1969). Correlations of the coalescence time based on dimensional analysis have been produced by Jeffreys and Hawksley (1965), Jeffreys and Lawson (1971), and Smith and Davies (1970).

(2) Inter Droplet

The amount of research into inter-drop coalescence is much more limited. Mathematical models of the process have been developed by McAvoy and Kintner (1965), MacKay and Mason (1963), Princen (1963) and Maraschino and Treybal (1971). A detailed survey of this and other work on coalescence is available by Jeffreys and Davies (1969).

Groothius and Zuiderweg (1960), have used pairs of drops to demonstrate the influence of mass transfer on coalescence. Transfer out

of the droplet enhanced the coalescence rate, while transfer in the reverse direction reduced or suppressed coalescence. The findings of these workers have been confirmed by other workers studying single drops at flat interfaces, (MacKay and Mason, 1963, Jeffreys and Lawson, 1965, Davers and Ewanchyna, 1957 and Thiessen, 1963).

II COALESCENCE IN PACKED COLUMNS

Jeffreys and Davies (1969), studied the coalescence of primary dispersions in packings. The behaviour found is dependent on the wetting behaviour of the packing. If the packing is wet by the dispersed phase, then droplet/interface coalescence predominates. If it is wet by the continuous phase then coalescence is inter-droplet.

Thomas and Rumford (1971), investigated the use of knitted mesh packed beds for the coalescence of primary dispersions. The behaviour of packings wet by the continuous phase was similar to that of conventional packings. For voidage greater than 95% breakdown of the droplets by Thorntons mechanism (impaction breakup) was found to occur. Lower voidage packings resulted in the growth of droplets by coalescence. Coalescence of the droplets into a surface film on the packing occured when the packing was wet by the dispersed phase. This was followed by drainage of the film through the packing. At low flowrates and packing voidages greater than 95% the droplets leaving the packing were formed by a force balance mechanism. At higher flowrates, or lower voidage packings jetting occured with breakup due to Rayleigh instabilities.

Wilkinson et al (1975), in a study of packed bed coalescers, have analysed the parameters controlling the passage of droplets through spherical packings. By equating the droplet buoyancy forces with the change in Laplacian capilliary pressure for the deformed drop:

$$\frac{h \Delta \rho_g}{2\sigma} = \frac{1}{R_1} - \frac{1}{R_2} \qquad (7\text{-}36)$$

where R is a radius of curvature. Geometric arguments were used to relate the radii of curvature to the packing diameter and separation. Thus the resultant force on a drop can be obtained as a function of the packing size and the group $\left(\frac{\Delta\rho_g}{2\sigma}\right)$. It was shown that a range of droplet sizes exist for which the buoyancy forces are insufficient to provide the increase in surface energy needed to pass through a restriction. Such drops collect beneath the restriction until sufficient coalescence has occured for the buoyancy forces to provide the required increase in surface energy.

SATELLITE DROPLET FORMATION

The existence of a large number of fine droplets ($< 1\frac{1}{2}$mm) is a characteristic feature of the drop size distribution for packed columns. Under some circumstances it is the entrainment of these fine droplets which governs the limiting flows in the column. Three sources for the formation of satellite droplets have been reported in the literature: partial coalescence, nozzle formation and instability breakup.

I PARTIAL COALESCENCE

Wark and Cox (1935), were the first to notice that coalescence need not be a single step. A drop may coalesce partially, producing a second smaller drop which can coalesce producing an even smaller drop and so on. The phenomenon has been analysed by Charles and Mason (1960), for the case of a drop at a flat interface. Upon rupture of the continuous phase film, the coalescing drop is deflated by the excess internal pressure resulting from the curvature of the interface. A cylindrical column forms, the radius of which decreases until its circumference is less than its height, and a Rayleigh disturbance can grow. The formation of a secondary drop then depends upon the relative rates of drainage and necking down.

McKay and Mason (1963), investigated partial coalescence in inter-droplet coalescence. The pressure difference between the drops:

$$\Delta P = \frac{4\sigma}{a_1}\left(1 - \frac{1}{\beta}\right) \qquad (7\text{-}37)$$

becomes small as the drop diameter ratio $\beta \left(= \frac{a_2}{a_1} > 1\right)$ approaches unity. Thus the rate of drainage decreases. As β approaches unity the decrease in surface area upon coalescence increases to a maximum. This means that the forming drop tends to resume a spherical shape and the base of the

draining drop is conical rather than cylindrical, so reducing the effective height of the cylinder. This becomes more pronounced as ΔP decreases and a situation is reached where drainage is completed before the breakup conditions are reached. This occured at $\beta = 3.5$.

Jeffreys and Lawson (1965), have shown that a second mechanism exists, whereby mixing of the coalescing drop with the bulk phase occurs, and the secondary drop is ejected from the coalescence region with some violence. No analytic description of the process has been developed.

Hanson and Brown (1967), equated the viscous dissipation within the cylinder formed by the coalescing droplet, to the work of compression on the cylinder to develop an expression for the drainage time. They also demonstrated that the mode of coalescence depended on the depth to which the coalescing drop submerged in the interface. Simple drainage was operative when the depth of penetration was less than 0.20 d and violent coalescence for depths of penetration greater than 0.26 d.

II NOZZLE FORMATION

Hauser et al (1936) used a high speed motion camera to study droplet formation. They found that during the necking down process a stem formed between the drop and the liquid on the nozzle tip. The stem breaks off close to the drop and then detaches from the liquid on the tip. It may then break up into one or more satellite drops by an instability mechanism.

Edgerton et al (1937), used the formation of satellite drops to explain the peculiar shape of the Harkins-Brown (1919) correction curve for the determination of surface tension by the drop weight method. The proportion of liquid left on the tip increases with tip diameter, until satellite formation occurs. It then decreases to a minimum and then, as the tip diameter increases further, begins to increase again as the

amount of liquid left on the tip becomes the controlling factor once more.

III FORMATION DURING INSTABILITY BREAKUP

The linearised stability theories (Rayleigh, 1879, Weber, 1931, Tomotika, 1935) for the breakup of a cylindrical thread predict the formation of a series of uniform regularly spaced droplets. Goren (1964), and Mikami et al (1975), have shown that when the growing disturbances become large the linearisation of the stability theories is no longer valid. Goren assumed that the surface area of the thread is a minimum at all times within the constraints of the problem. This leads to a predicted shape for the thread of successive protruberences joined by cylindrical links. The growth of unstable disturbances within these cylindrical links may then lead to the formation of satellite droplets. Mikami et al confirmed this finding and pointed out that breakup of the thread under extensional flow does not occur simultaneously over the thread. The spacing of the principal drops varies and the connecting filiaments do not give the same number of droplets.

Meister and Scheele (1969), investigated the effect of mass transfer on jet length. For the transfer of acetone between benzene jets and water both directions of transfer were found to result in longer jets. Sawistowski (1973), has suggested that a quasi-equilibrium state is formed causing differences in solute concentration between the necks and protruberences. Thus the differences in interfacial tension caused would result in flow into or out of the necking region.

Berkholder and Berg (1974), have extended the analysis of Sternling and Scriven to the case of laminar jet flow. The characteristic equation derived has been solved numerically for particular cases. Qualitative agreement with the results of Meister and Scheele was found.

SIEVE PLATE PHENOMENA

A continuing investigation into the behaviour of perforated plate liquid-liquid extraction columns has been carried out in this department over a number of years. The projects of Odell (1975), and of Ooi (1977), the latter being currently in progress, have highlighted the differences between dispersing a continuous pool of liquid through a nozzle or orifice, and redispersing an uncoalesced dispersion. The results of these investigations seem particularly relevant to packed column behaviour and will be reviewed here.

The former used a rectangular perspex column with four plates. The plates were made of brass and had 6mm ID nozzles for dispersed phase flow and downcomers for continuous phase flow. The droplet size distribution above the bottom three plates could be photographed. However, the use of brass plates meant that much of the detail about the basic breakup mechanisms was hidden inside the nozzles. To overcome this problem Ooi is using a breakup cell of all-glass construction. A 4.75mm ID nozzle generates a primary dispersion. This is then redispersed through a single 3.18mm or 4.76mm diameter nozzle or orifice.

I SINGLE PLATE BEHAVIOUR

Figures 7 - 1 to 7 - 4 show the type of behaviour found using the different diameters of nozzle or orifice. The 4.76mm orifice appears in figure 7 - 1. At low flowrates droplet breakup is evidently by a force type balance mechanism with a single droplet occupying the entire nozzle area. There is however some variation in drop size. Figure 7 - 2(a) shows that this is probably due to the residual volume remaining after one or more droplets of the force balance size have broken away from the parent drop. No satellite droplets are produced in spite of the formation of a long neck as a droplet breaks away from the parent.

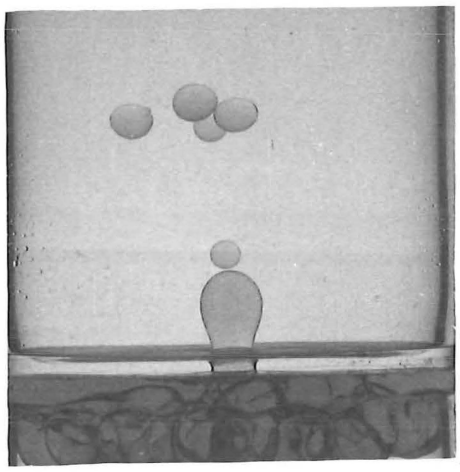

a V_d = 11·4 cm / s

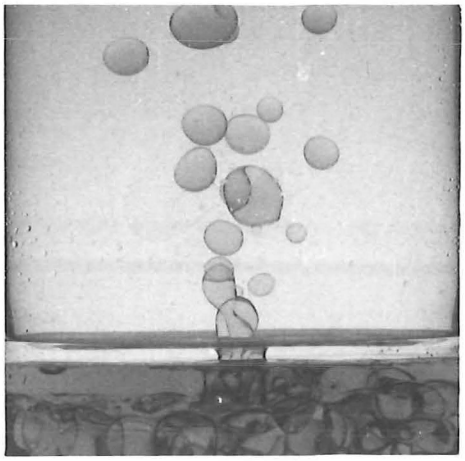

b V_d = 21·6 cm / s

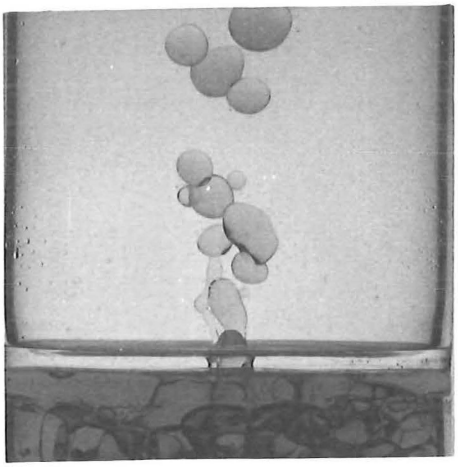

c V_d = 25·0 cm / s

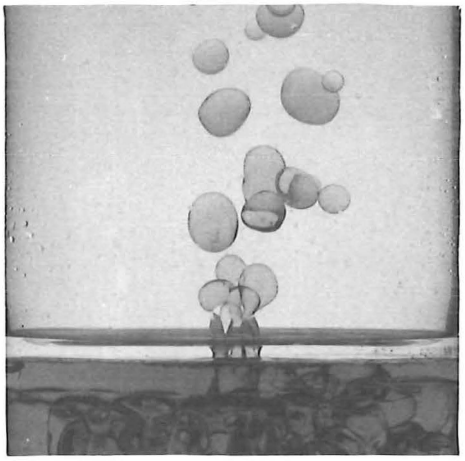

d V_d = 32·0 cm / s

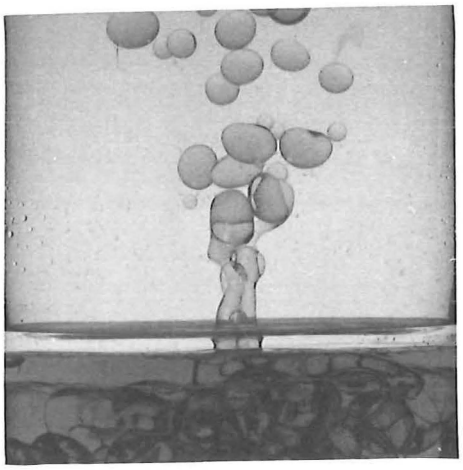

e V_d = 33·7 cm / s

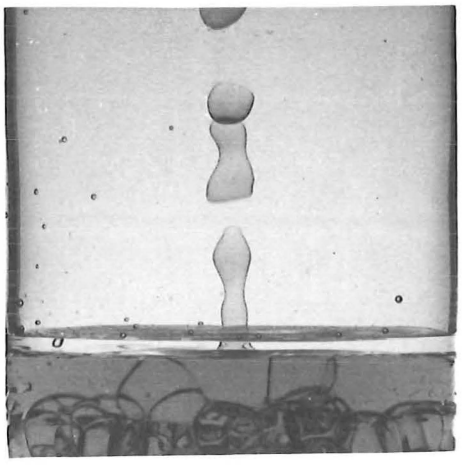

f V_d = 32·0 cm / s

FIGURE 7 – 1 DROPLET BREAKUP AT A 4·76mm ORIFICE

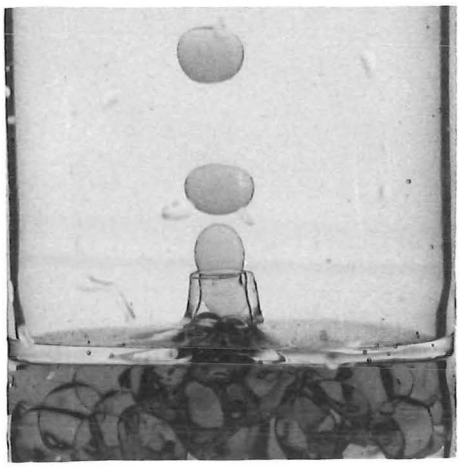

a V_d = 13·2 cm / s

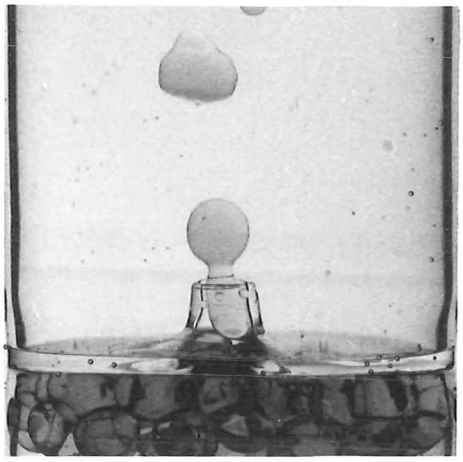

b V_d = 20·9 cm / s

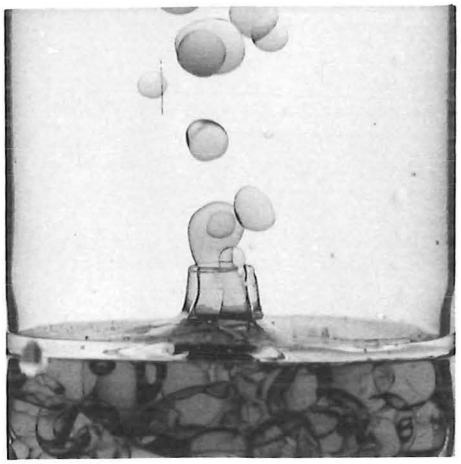

c V_d = 24·9 cm / s

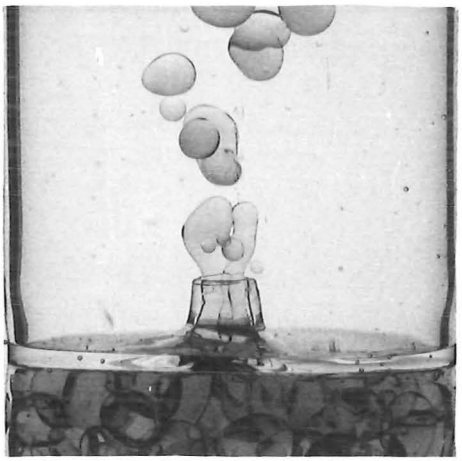

d V_d = 32·4 cm / s

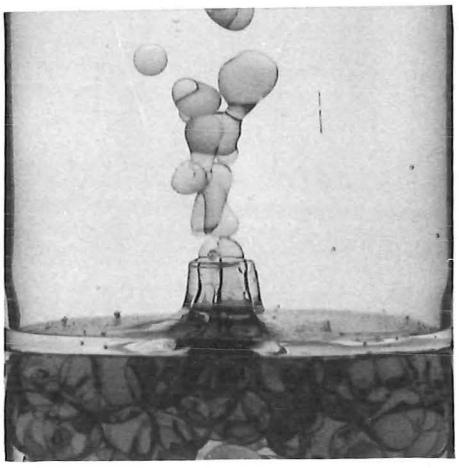

e V_d = 35·3 cm / s

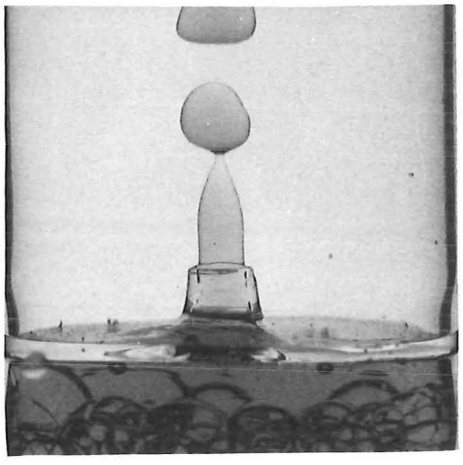

f V_d = 24·9 cm / s

FIGURE 7 – 2 DROPLET BREAKUP AT A 4·76mm NOZZLE

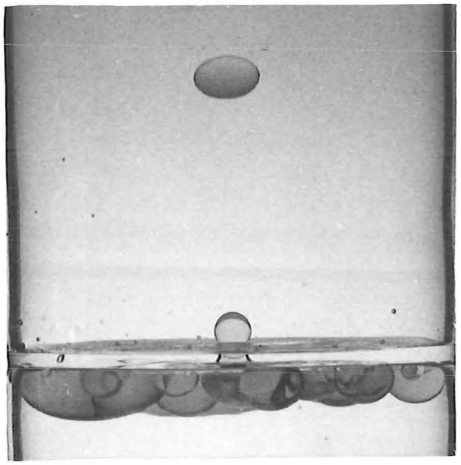

a V_d = 1·0 cm/s

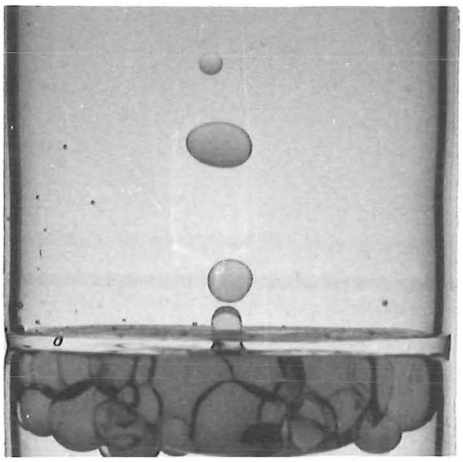

b V_d = 8·0 cm/s

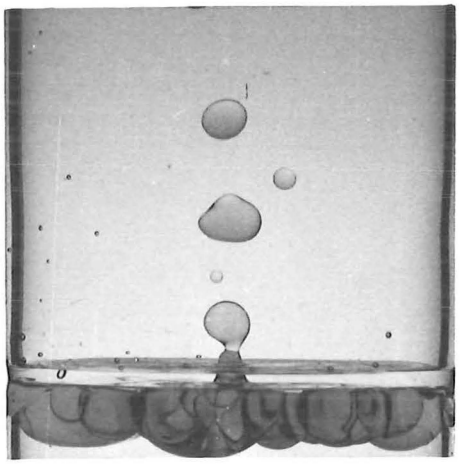

c V_d = 13·9 cm/s

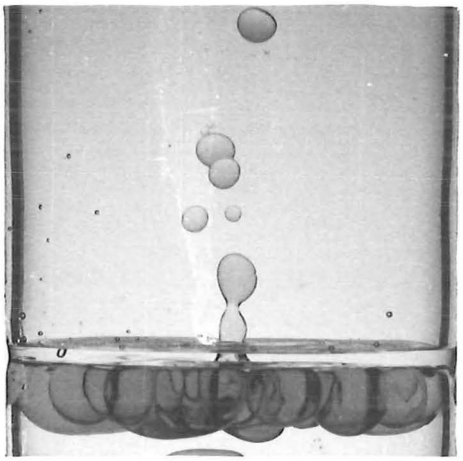

d V_d = 13·9 cm/s

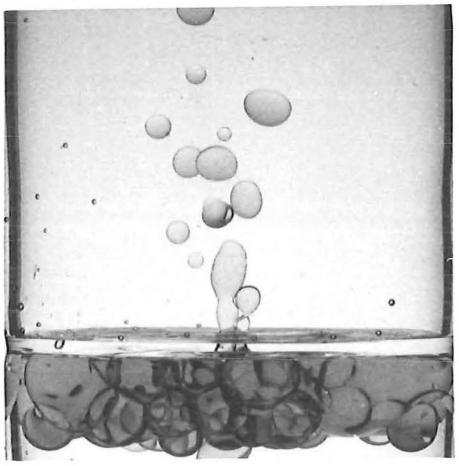

e V_d = 24·8 cm/s

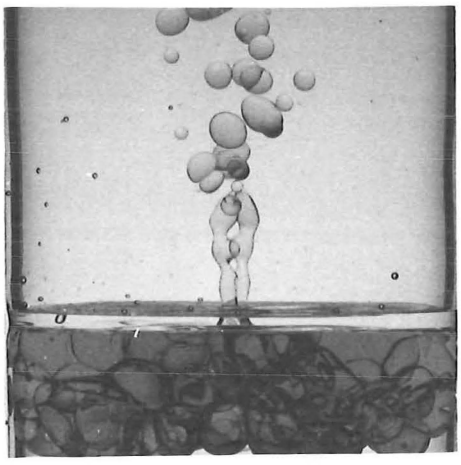

f V_d = 32·0 cm/s

FIGURE 7 – 3 DROPLET BREAKUP AT A 3·18mm ORIFICE

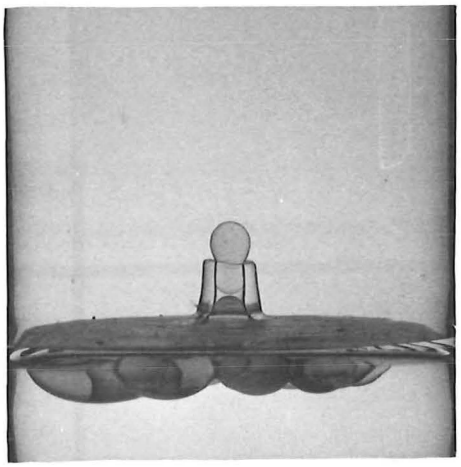

a V_d = 0·7 cm / s

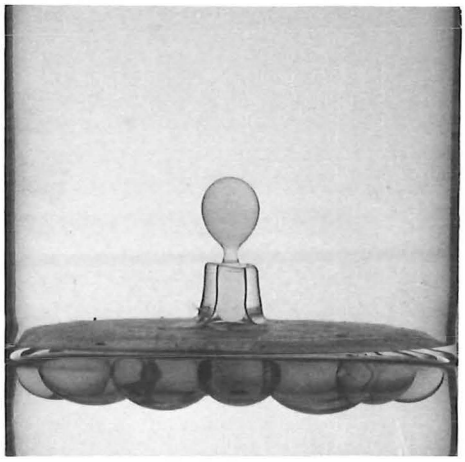

b V_d = 7·9 cm / s

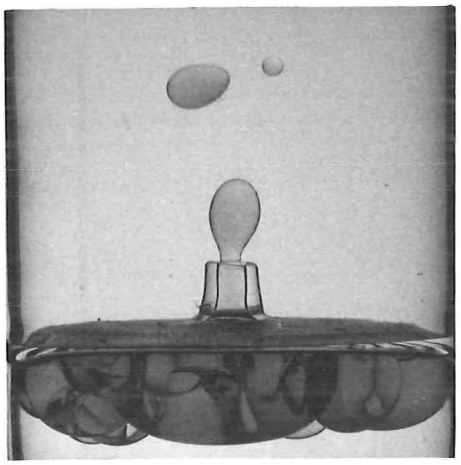

c V_d = 15·8 cm / s

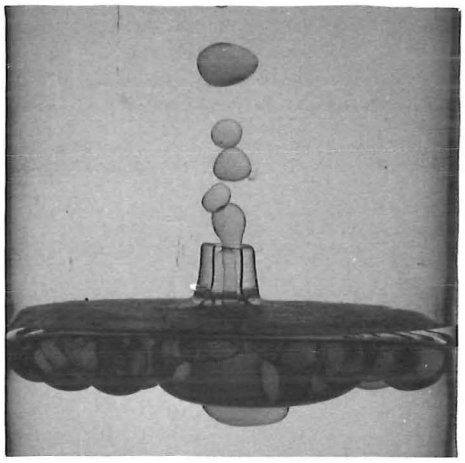

d V_d = 20·1 cm / s

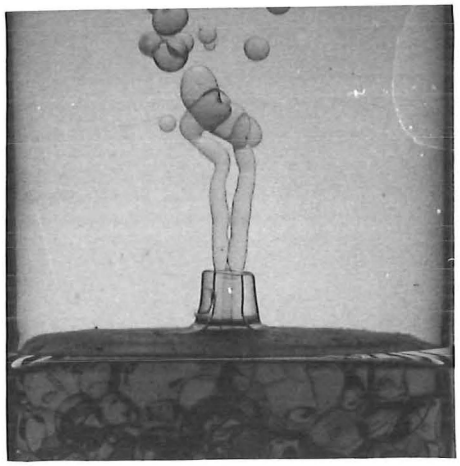

e V_d = 39·5 cm / s

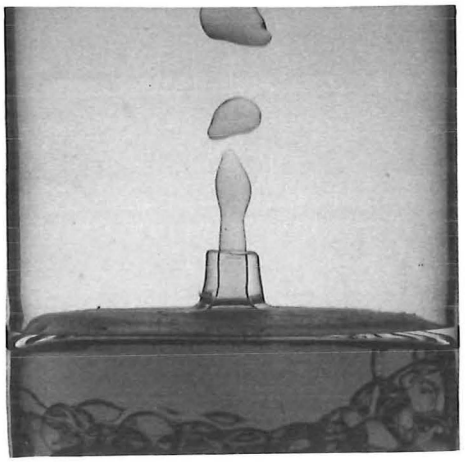

f V_d = 39·5 cm / s

FIGURE 7 - 4 DROPLET BREAKUP AT A 3·18mm NOZZLE

Comparison with figures 7 - 2 to 7 - 4 shows that this mechanism occurs in all cases at low flowrates.

Differences from the case of a coalesced pool become more apparent as the flowrate is increased. Competition for the nozzle space between adjacent drops is evident. If one drop occupies most of the nozzle area then a situation such as in figure 7 - 1(c) occurs. The drop occupying most of the area breaks up by a force balance mechanism as before. The other drop, however, is squeezed out into a thin thread and breakup occurs from the end of the thread. This results in a wide range of drop sizes. Some variation in drop sizes is apparent even when there is only a single drop in the nozzle. Figure 7 - 4(d) shows that the parent drop need not occupy the whole nozzle area even when it is the only drop there.

Multiple occupation of the nozzle becomes more important as the flowrate increases. A transition region exists where jetting and force balance breakup both occur. Jetting replaces the force balance mechanism entirely after this transition region - figure 7 - 4(e). In general, however, two to four separate streams occupy the nozzle at any one time. A wide range of droplet sizes is formed under such conditions and satellite formation is frequent. As a comparison figures 7 - 1(f) and 7 - 2(f) show the behaviour found when jetting occurs from a coalesced layer.

II MULTI-PLATE BEHAVIOUR

Odell was able to measure the changes in size distribution which occured when a distribution was redispersed through two further plates. Two systems were studied - a pure phase kerosene - water system, and a system with mass transfer of methyl ethyl ketone out of the dispersed phase.

Figures 7 - 5 and 7 - 6 show the pure phase behaviour for nozzle

PURE PHASES NOZZLE VELOCITY = 5.2 cm/s

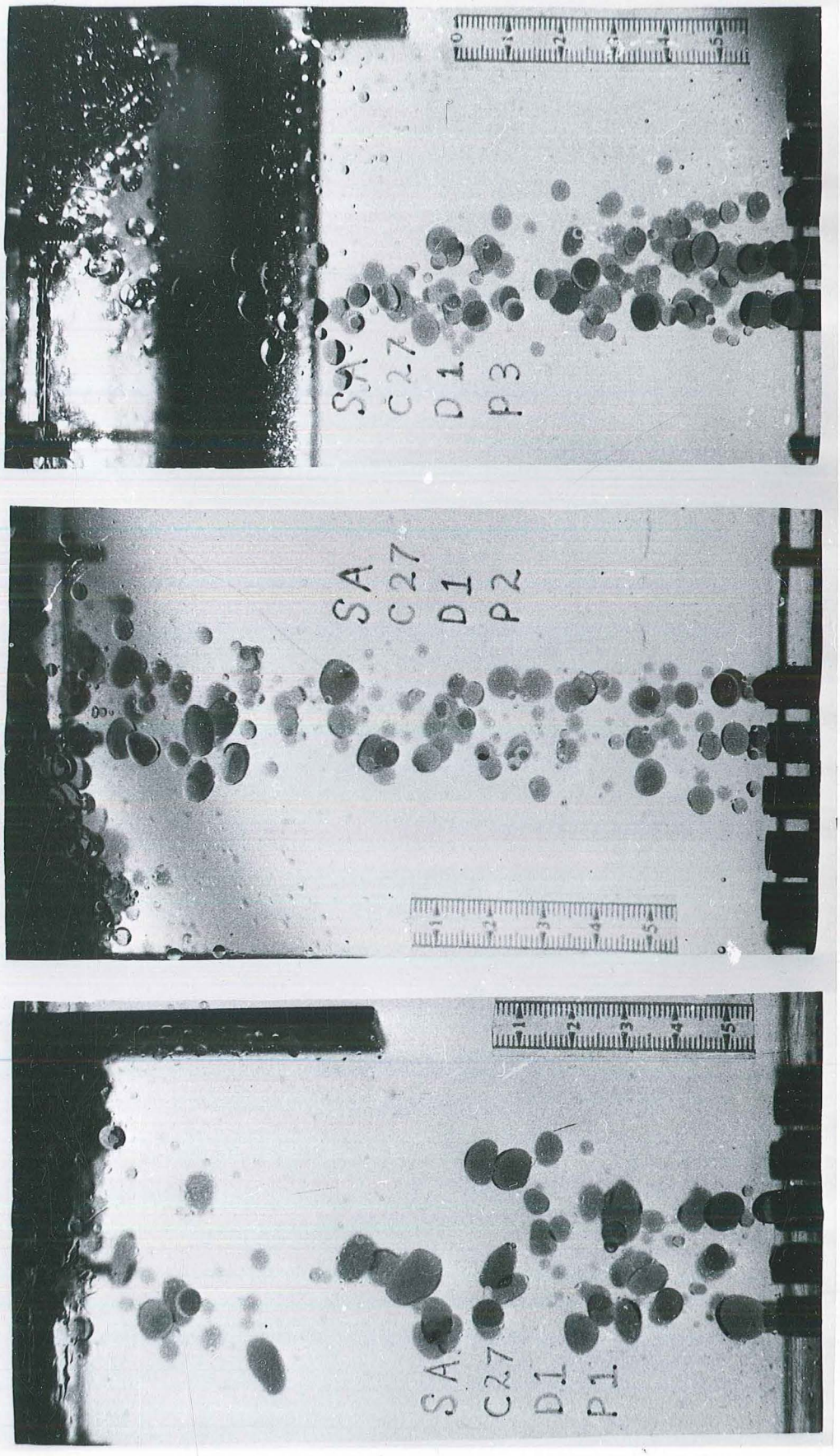

FIGURE 7 - 5 DROPLET BREAKUP AT SIEVE PLATES

PURE PHASES NOZZLE VELOCITY = 27.4 cm/s

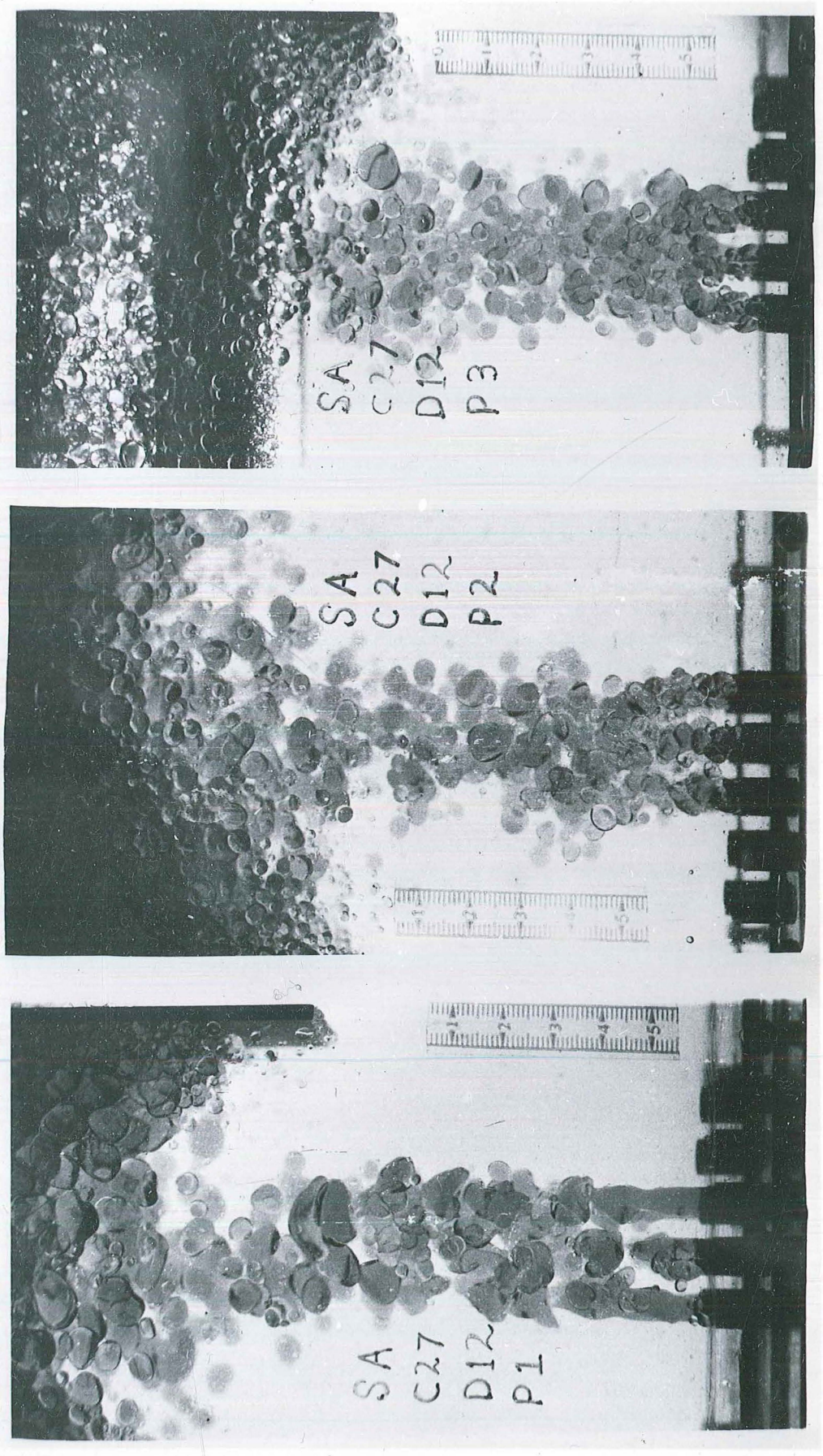

FIGURE 7-6 DROPLET BREAKUP AT SIEVE PLATES

velocities of 5.2cm s^{-1} and 27.4cm s^{-1} respectively. A relatively large input distribution is found on plate one and this breaks down over the next two plates. A fairly wide distribution of drop sizes is found. At the higher flowrate jetting is occuring on the bottom plate. It is apparent, however, that little if any coalescence has occured beneath plates two and three.

Figure 7 - 7 and 7 - 8 show the behaviour of the system when solute transfer is out of the dispersed phase. Radical differences in behaviour are immediately obvious. Significant coalescence is now occuring and the layers beneath each plate are now much closer to being a single pool. Single streams can be seen emerging from the nozzles, rather than discrete droplets, and breakup occurs at the ends of the streams.

The difference in behaviour of the two systems is reflected in the droplet size distributions shown in figure 7 - 9. The pure phases have an initially broad distribution with a shallow peak at about 5mm. After the second plate there is some growth of the 2 - 5mm droplets at the expense of the larger diameter droplets. A further decrease in the number of larger diameter droplets occurs at the next plate and a definite peak has emerged centred on 4mm.

The mass transfer system also has a broad initial distribution with a maximum droplet size close to that of the pure phases. The peak is almost flat between 6 - 9mm. After the second plate the peak is much sharper, mainly at the expense of a decrease in the number of larger droplets, but it is still centred in approximately the same place. The distribution after plate three has broadened somewhat and represents a situation intermediate between the first and second plates.

A computer program was developed to predict the drop size distribution on plates two and three for the pure phase case, using the plate one distribution as a starting point. The probability of breakup for droplets larger than a critical diameter was arbitarily set at 80%

MASS TRANSFER KEROSENE TO WATER

NOZZLE VELOCITY = 5.2 cm/s

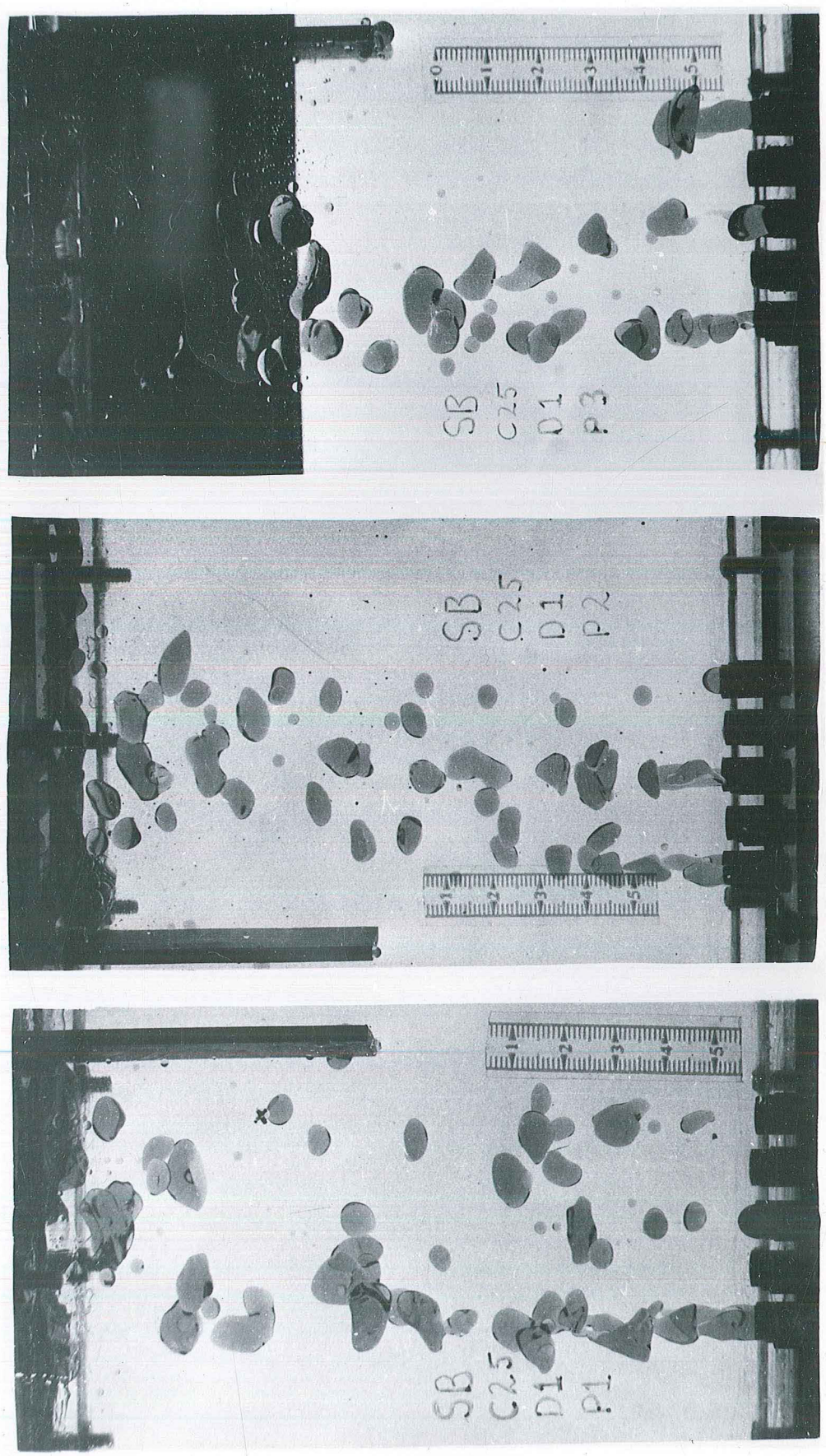

FIGURE 7 - 7 DROPLET BREAKUP AT SIEVE PLATES

MASS TRANSFER KEROSENE TO WATER

NOZZLE VELOCITY = 27.4 cm/s

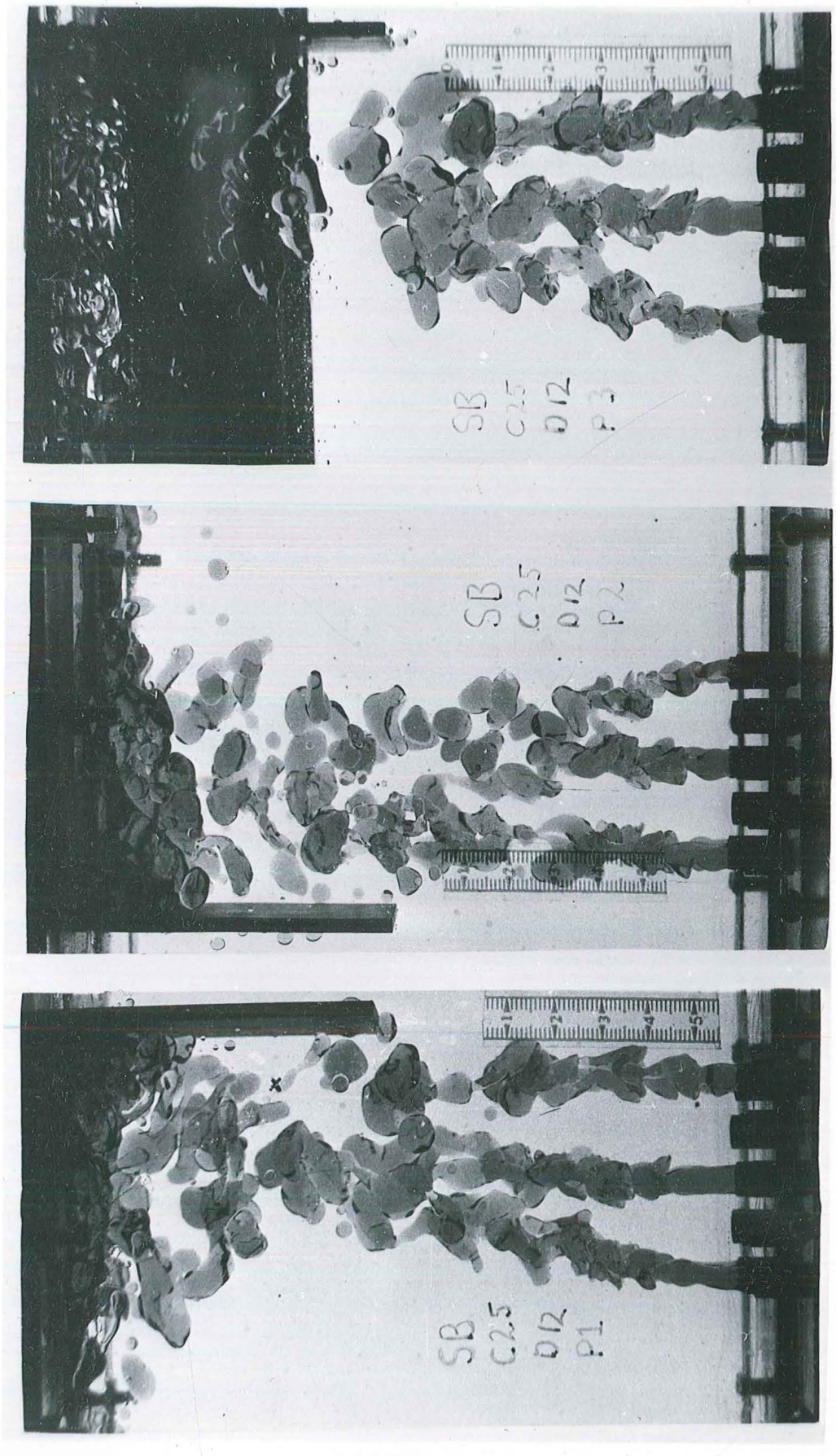

FIGURE 7 – 8 DROPLET BREAKUP AT SIEVE PLATES

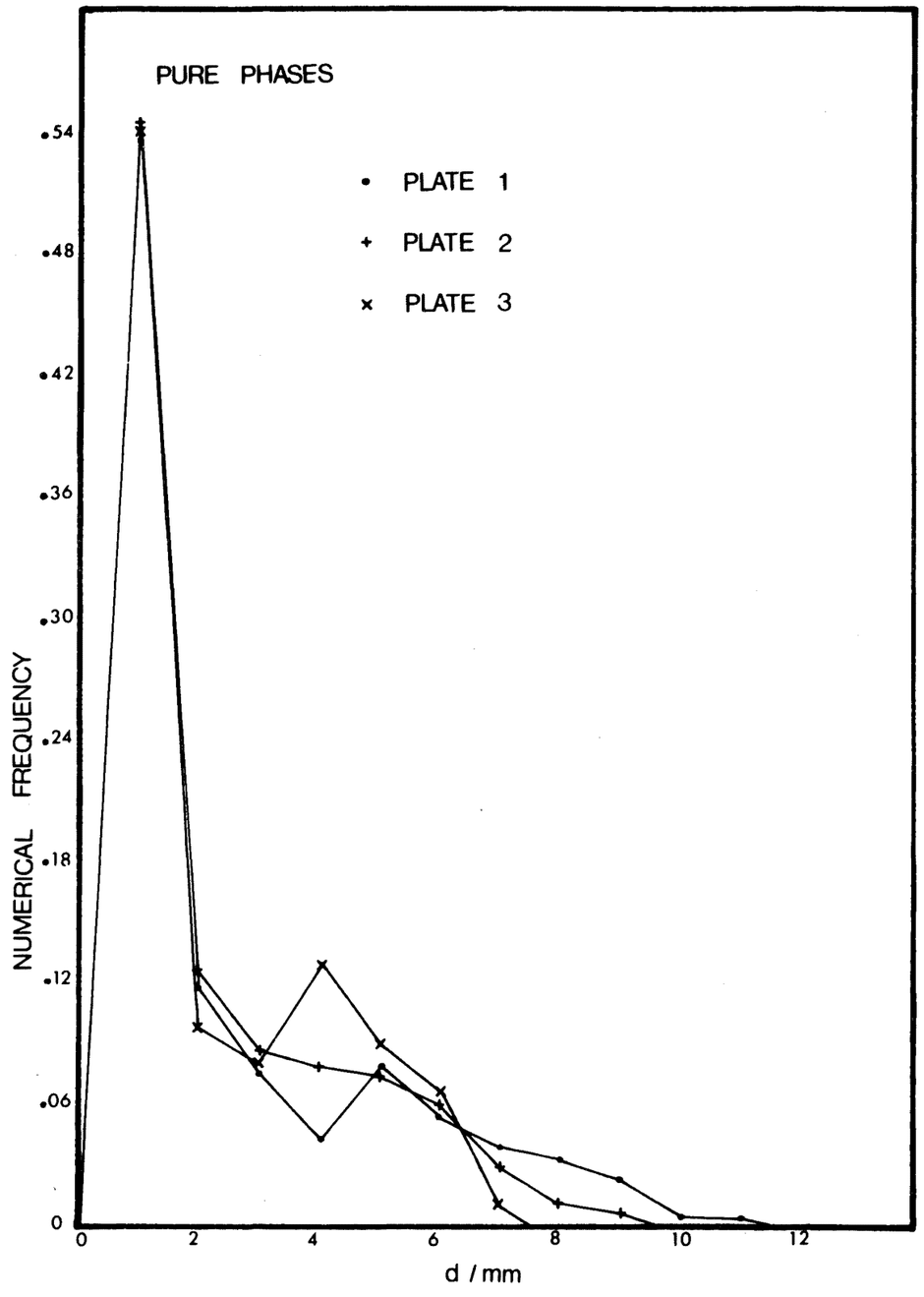

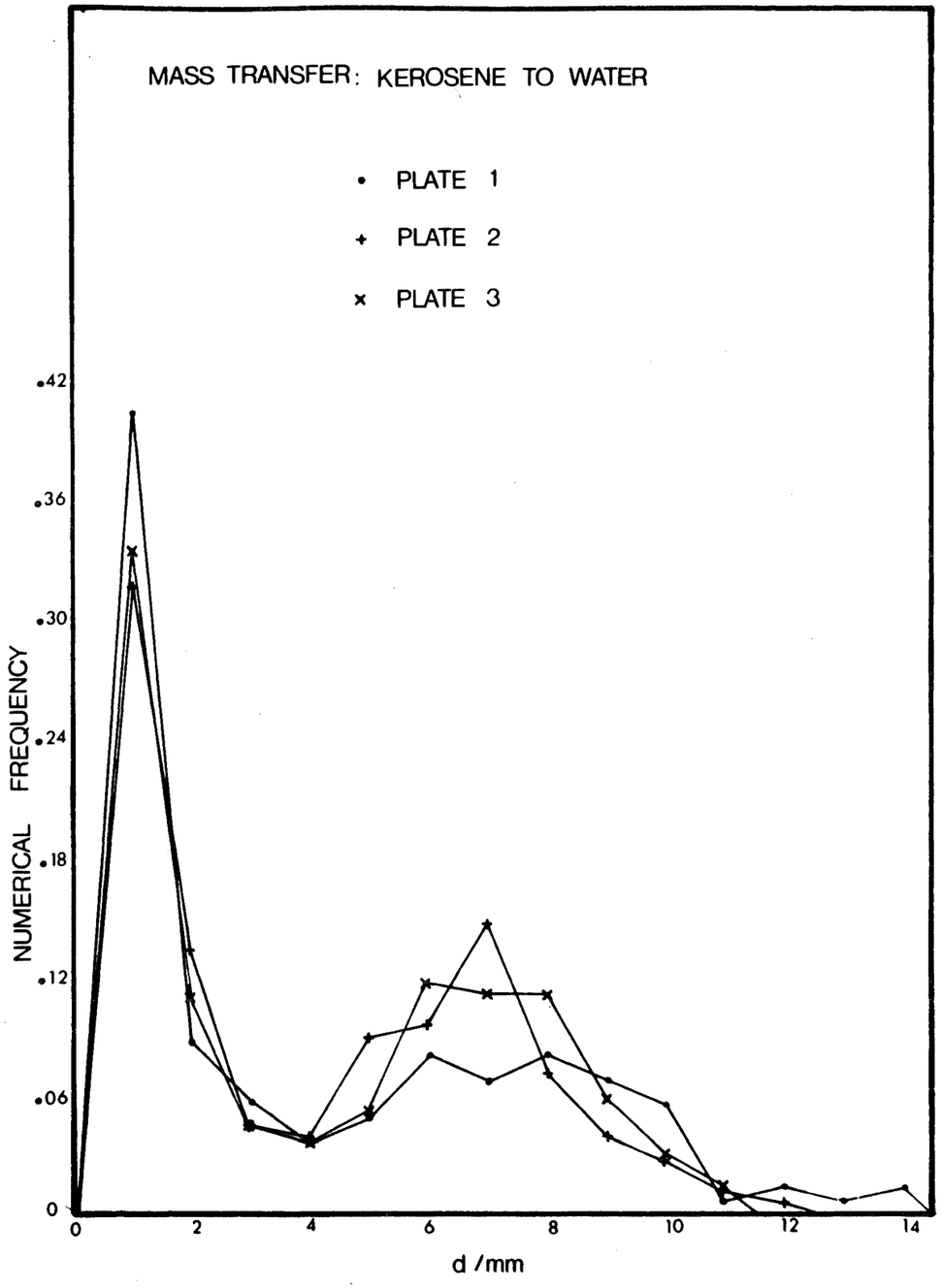

FIGURE 7 - 9 DROPLET SIZE DISTRIBUTIONS

This critical diameter was initially taken as the Scheele-Meister drop size, but was later changed to the nozzle diameter. The total volume of droplets predicted to be unstable was calculated. This volume was then redistributed over a range of drop sizes using an arbitary set of probability coefficients chosen to best fit the data. While a good experimental fit could be obtained in this way it was highly empirical and in order to get exact agreement with experiment a different set of coefficients was needed for each plate.

III MODELLING

Analyses of droplet formation at nozzles or orifices have, in general, been based on a balance of the forces acting on the forming drop, (Hayworth and Treybal, 1950, Null and Johnson, 1958, Rao et al, 1966, and Scheele and Meister, 1968). The complexity of the forces acting have meant that it has been necessary to treat formation as a two stage process. In the first stage the volume of the drops for which the forces acting are just balanced, is calculated. This volume is then corrected in the second stage for the flow into the drop during the time of necking down.

Thus, the Scheele-Meister (1968), model for drop formation at low velocities gives for the first stage:

$$F_B = V_{FS} \Delta \varrho g = F_I + F_D - F_K \qquad (7\text{-}38)$$

where V is the droplet volume and for the final droplet volume

$$V_F = H \, (V_{FS} + V_{FN}) \qquad (7\text{-}39)$$

where H is the Harkins-Brown (1919) factor. This model was extended by Heertjes et al (1971), so that flow into the drop during necking can be predicted without use of the Harkins-Brown factor. Thus:

$$V_F = H \, V_{FS} + Q_N \, t_{rl} \qquad (7\text{-}40)$$

where t_{rl} is the time of release after equilibration of forces.

These analyses are developed for the dispersion of a continuous stream of liquid flowing with a parabolic velocity profile through a wetted nozzle. The assumption of a parabolic velocity profile is reflected in the kinetic energy term:

$$F_K = \frac{4}{3} \rho_d Q U_N \qquad (7\text{-}41)$$

For a flat velocity profile the $\frac{4}{3}$ factor would be replaced by 1.0. The kinetic energy term is generally small compared with the interfacial tension and necking terms so this correction will also be small. More serious, however, is the effect on the necking term; whether the empirical term of Scheele and Meister, or the unsteady state model of Heertjes et al is used. The flowrate through the nozzle is determined partly by the volume of the parent droplet and partly by the complex interaction between the parent droplet and the other members of the dispersion below the nozzle. The interactive effect may serve either to enhance or retard the flow of an individual droplet. Figure 7 - 4(d) shows an example where flow through a nozzle is apparently retarded by other droplets with the effect that the parent drop elongates and occupies only a portion of the nozzle area. Equally questionable is the use of the Harkins-Brown factor to determine the fraction of the ideal drop which leaves the nozzle. This factor was determined for the production of droplets formed on wetted tips and is unlikely to apply to the breakup of discrete droplets in a nonwetting nozzle.

Partial and multiple occupation of the nozzle also result in some doubt as to the correct diameter to use. Graham and Chan, (1974), have defined a factor f, which is the fractional occupation of the nozzle. This can be incorporated into the equations to give the correct area of breakup. The fractional occupation of the nozzle fluctuates at any given flowrate giving rise to a distribution of drop sizes. There

is also a decrease in fractional occupation as the flowrate increases - figures 7 - 3(d) and 7 - 3(e).

Application of the Scheele-Meister equation to the redispersion of a dispersion is thus accompanied by some diffuculties. An alternative approach is that of Izard (1972). The profile of the forming drop is calculated using the pressure balance technique of Bashforth and Adams (1883). A vertical force balance is then done through the droplet to find the point at which the droplet will break away from the nozzle. This avoids use of the Harkins-Brown factor and an explicit necking term. The problem of interaction between droplets and mutiple occupation will, however, remain.

NOMENCLATURE

a - radius of droplet (cm)

C, C_1 - constants (-)

d - droplet diameter (cm)

d^o - droplet diameter at substantially zero flowrates (cm)

d_c - column diameter (cm)

D - droplet deformation defined by equation (7-7) (-)

D_F - droplet diameter defined by equation (7-35) (cm)

D_I - impellor diameter (cm)

D_N - nozzle diameter (cm)

e - packing voidage fraction (-)

E - droplet energy (erg)

f - function (-)

F - force acting on a droplet (dyne)

g - gravitational acceleration (cm s^{-2})

h - differential head on droplet giving buoyancy force (cm)

H - Harkins-Brown correction factor (-)

k_f - internal drag coefficient (-)

N - impellor rotational velocity (rad s^{-1})

p - viscosity ratio $= \frac{\mu_d}{\mu_c}$ (-)

ΔP - pressure difference (dyne cm^{-2})

Q - volumetric flowrate ($cm^3\ s^{-1}$)

Q_N - volumetric flowrate into a droplet during necking ($cm^3\ s^{-1}$)

$r(\phi'')$ - geometric function for droplet equator - equation (7-6) (-)

R - radius of curvature (cm)

t_{rl} - time of release of a droplet from the start of the necking down (s)

V - bulk average velocity ($cm\ s^{-1}$)

$\overline{V}^2$ - average value of square of difference in turbulent velocity ($cm^2\ s^{-2}$)

V_λ - eddy velocity ($cm\ s^{-1}$)

V_d - dispersed phase superficial velocity ($cm^3\ s^{-1}/cm^2$)

V_t - droplet terminal velocity ($cm\ s^{-1}$)

$\overline{V}_o$ - characteristic velocity defined by equation (4-8) ($cm\ s^{-1}$)

V_R - mean droplet velocity relative to packing ($cm\ s^{-1}$)

V_F - droplet volume (cm^3)

V_i - viscosity number = $\dfrac{\mu_d}{\sqrt{\rho_d \sigma d}}$ (-)

We - Weber number = $\dfrac{\tau d}{\sigma}$ (-)

x - dispersed phase holdup (-)

β - droplet diameter ratio (-)

γ - shear rate (s^{-1})

δ_o - boundary layer thickness (cm)

ϵ - energy input per unit mass ($cm^2\ s^{-3}$)

ϑ - droplet residence time (s)

λ - wave length (cm)

λ_o - micro scale of turbulence (cm)

μ - dynamic viscosity ($g\ cm^{-1}\ s^{-1}$)

π - 3.14159 (-)

ϱ - density ($g\ cm^{-3}$)

$\Delta\varrho$ - phase density difference ($g\ cm^{-3}$)

σ - interfacial tension ($dyne\ cm^{-1}$)

τ - shear stress ($dyne\ cm^{-2}$)

ϕ - arbitary function (-)

$\phi'\phi''$ - polar angles (rad)

Subscripts

32 - Sauter mean

c - continuous phase

d - dispersed phase

D - drag

F - final

FN - necking

FS - static

CHAPTER EIGHT

EXPERIMENTAL DROPLET DISTRIBUTION BEHAVIOUR

Chapter Contents.

INTRODUCTION

The historical technique for handling droplet size distributions has been to use a mean diameter suitably weighted to account for the greater surface area of larger diameter droplets. These are generally of the form:

$$d_{pq} = \sum_{i=0}^{\infty} n_i d_i^p \Big/ \sum_{i=0}^{\infty} n_i d_i^q \qquad (8\text{-}1)$$

The most commonly used values of p and q are:

$$p = 3 \quad q = 2$$

This mean, d_{32} is known as the Sauter mean diameter and physically corresponds to the ratio of volume to surface area. Misek and Marek, (1970), have recently advocated the use of d_{43} for the analysis of an asymmetric rotating disc column (RDC).

More sophisticated mass transfer models require a distribution function and the applicability of functions suggested in the literature (Brodkey, 1967) is reviewed.

A more fundamental approach involves investigation of the mechanisms controlling the droplet sizes. The literature revealed four basic types of process which could lead to droplet breakup. These were

(1) Laminar or turbulent shear (Taylor, 1932 and 1934, Rumscheidt and Mason, 1961, Karam and Bellinger, 1968).

(2) Dynamic pressure fluctuation (Sleicher, 1962, Paul and Sleicher, 1965, Collins and Knudsen, 1970).

(3) Impaction (Ramshaw and Thornton, 1967).

(4) Nozzle breakup or jetting (Harkins and Brown, 1919, Hayworth and Treybal, 1950, Null and Johnson, 1958, Rao et al, 1966, Scheele and Meister, 1968, Meister and Scheele, 1969a and b).

The applicability of these mechanisms is reviewed in light of the experimental data found.

As found in section II, mass transfer can have a two-fold effect. Firstly, changes in physical properties can alter important variables such as the maximum stable drop size. Secondly, coalescence can be drastically effected by motion induced by mass transfer in the continuous phase film separating colliding droplets. The negative interfacial tension-concentration gradient of most aqueous-organic systems means that coalescence may be enhanced by the Marangoni effect when transfer is out of the dispersed phase (Sawistowski, 1971). Other factors such as the onset of interfacial turbulence may overide this effect. Thus the droplet size distribution when coalescence is enhanced will be determined not solely by breakup criteria, but by the equilibrium established between breakup and coalescence.

DISTRIBUTION BEHAVIOUR

I PURE PHASES

Droplet size distribution data was collected for the column as a function of the flowrates V_c and V_d. The range of flowrates used covered the linear holdup regime and the loading region up to the flood-point. As well, data was collected on the changes in the droplet size distribution as a function of the packing height for the surfactant system. The most extensive data is again for the surfactant system and unless noted otherwise distributions shown are for this system at a packing height of 140cm.

(1) General Characteristics

Figures 8 - 1 and 8 - 2 show the numerical frequency distribution at zero continuous phase flowrate and a low dispersed phase flowrate, for the surfactant case and the pure phase respectively. In each case the phases are mutually saturated to eliminate mass transfer. Both distributions are found to be bimodal as had been found before (Lewis, Jones and Pratt, 1951, Ramshaw and Thornton, 1967). There is one main peak accompanied by a lesser peak of satellite drops with diameters less than 2mm. The satellite peak for the pure phase case is noticeably smaller than for the surfactant, with 17% of the total drops compared with 25% in the latter case. The main peak for the pure phase case occurs in the diameter range 4 - 6mm which is slightly higher than for the surfactant case, 3 - 5mm. Another feature of both distributions is the significant tailing of the curves at longer diameters. Thus, the curves extend to d = 11mm for the pure phases case and to d = 10mm for the surfactant case. The importance of these tails becomes apparent when the volume distributions are plotted as in figures 8 - 3 and 8 - 4. The contribution of the satellite droplets to the total volume is negligible and the secondary peak disappears when the volume distribution is plotted.

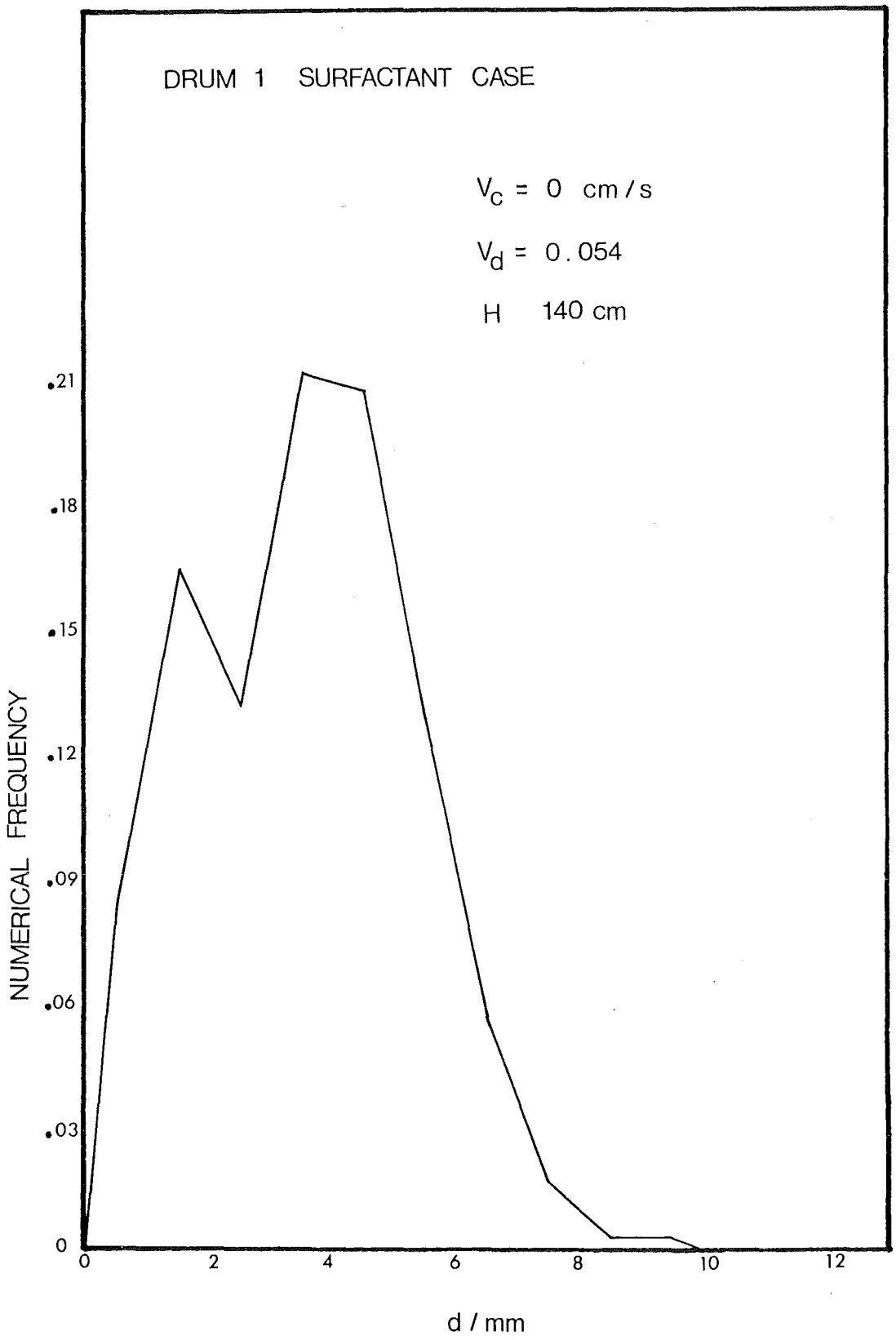

FIGURE 8 - 1 DROPLET SIZE DISTRIBUTION

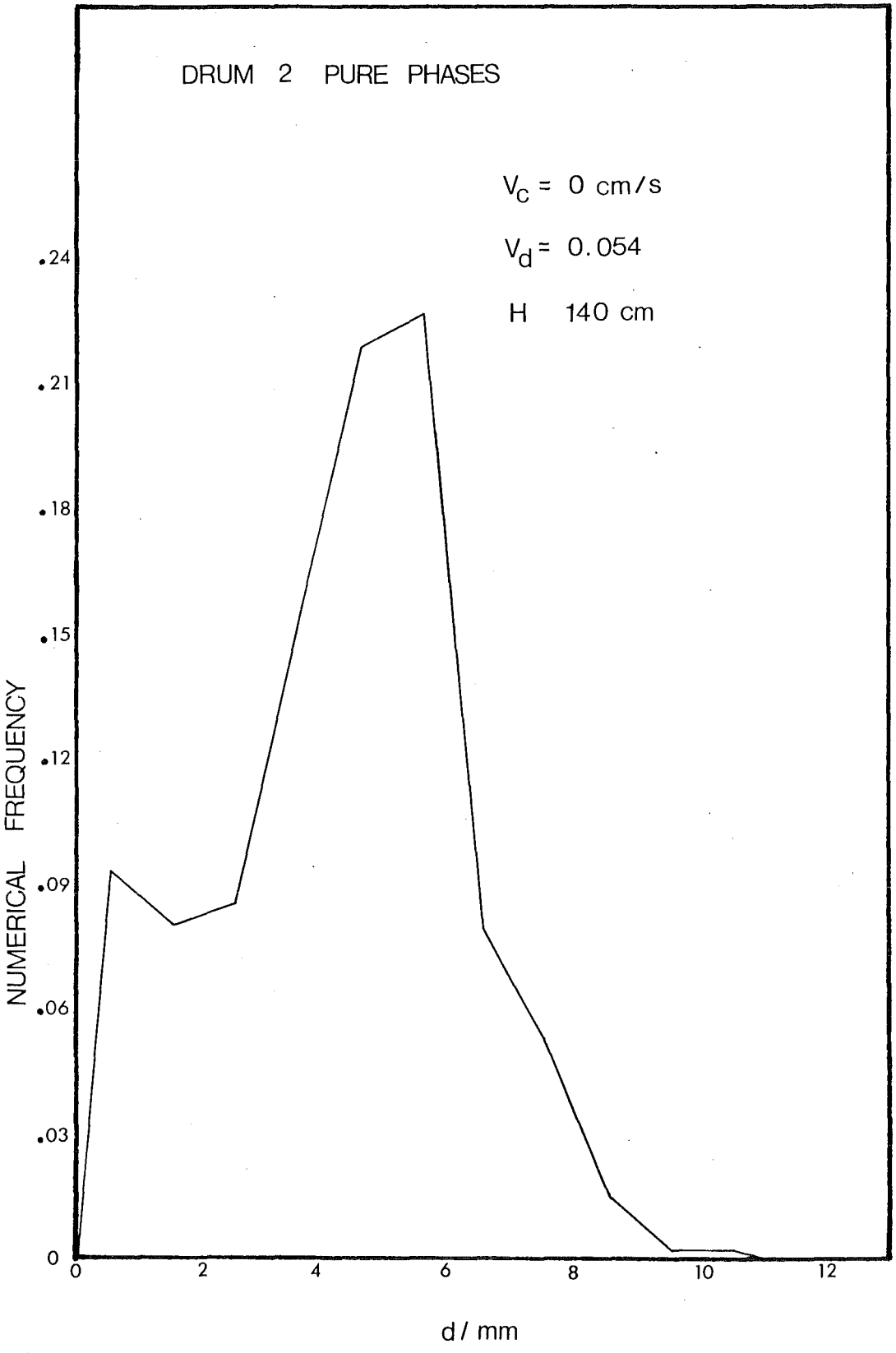

FIGURE 8 – 2 DROPLET SIZE DISTRIBUTION

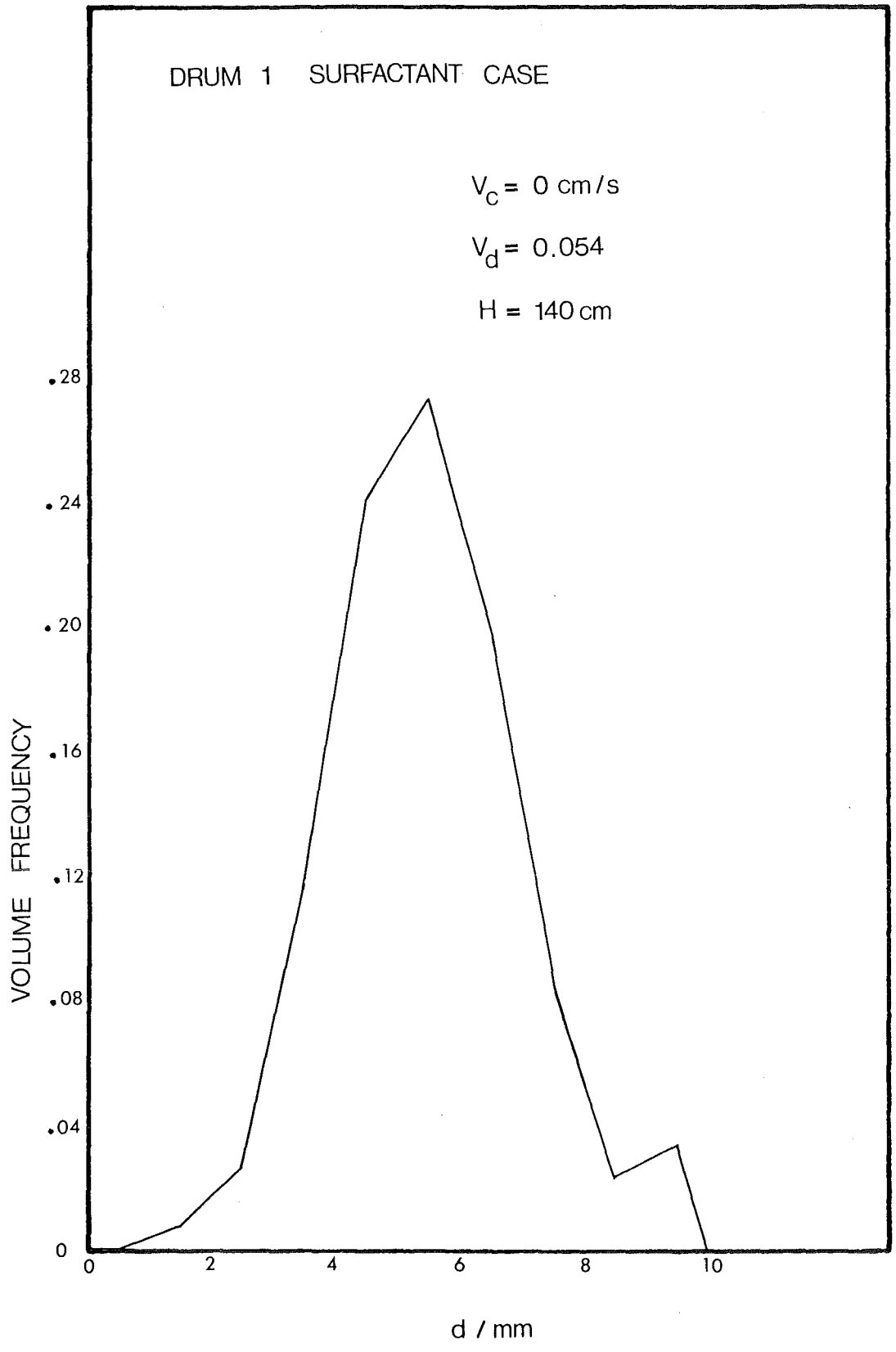

FIGURE 8 – 3 DROPLET VOLUME DISTRIBUTION

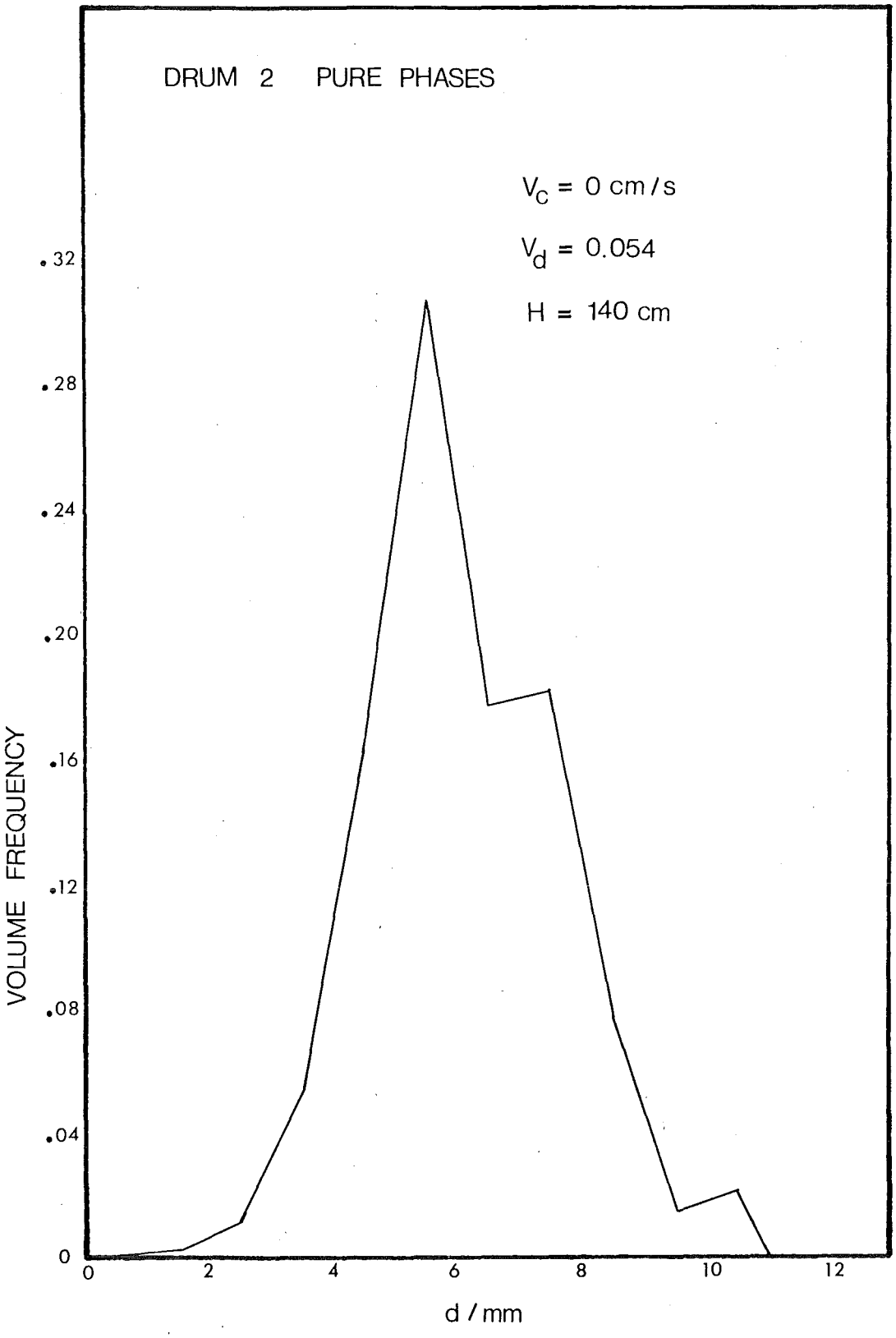

FIGURE 8 – 4 DROPLET VOLUME DISTRIBUTION

(2) Effect of Dispersed Phase Flowrate

Figures 8 - 5 and 8 - 6 show the influence of flowrates on mean diameters by plotting d_{32} and d_{43} against the dispersed phase flowrate V_d for the surfactant case. It can be seen that increasing the dispersed phase flowrate causes the mean diameter to go through a minimum. The effect of the continuous phase flowrate is, in general, to increase the mean diameter for a constant dispersed phase flowrate, and to reduce the dispersed phase flowrate at which the minimum diameter occurs. The value of d_{43} is 9 - 16% greater than the value of d_{32}.

The use of mean diameters, however, gives little information about the droplet size distribution. Figure 8 - 7 shows the influence of dispersed phase flowrate on the numerical frequency distribution of the surfactant case. Two effects are apparent. Firstly the proportion of satellite droplets increases with respect to the main peak. Secondly, the main peak occurs at smaller diameters as the flowrate increases, until, at the highest flowrate, a unimodal fuction is obtained. The changes in flowrate have little effect on the large diameter tail.

(3) Effect of Continuous Phase Flowrate

Figure 8 - 8 shows the same sequence of figure 8 - 7 but with a high continuous phase flowrate. The distribution at low dispersed phase flowrate is qualitatively similar to the zero continuous phase flowrate case. As the dispersed phase flowrate increases the proportion of satellite droplets increases and the region between the peaks begins to decrease. However the main peak tends to broaden so that at the highest dispersed phase flowrate the frequency in the range 2 - 6mm is nearly constant. The continuous phase flowrate also tends to spread the large diameter tail. Thus, droplets up to 14mm in diameter are found at the highest dispersed phase flowrate.

(4) Effect of Packing Height

Figure 8 - 9 shows the changes in the droplet size distribution as a function of the packing height. As noted in chapter one the

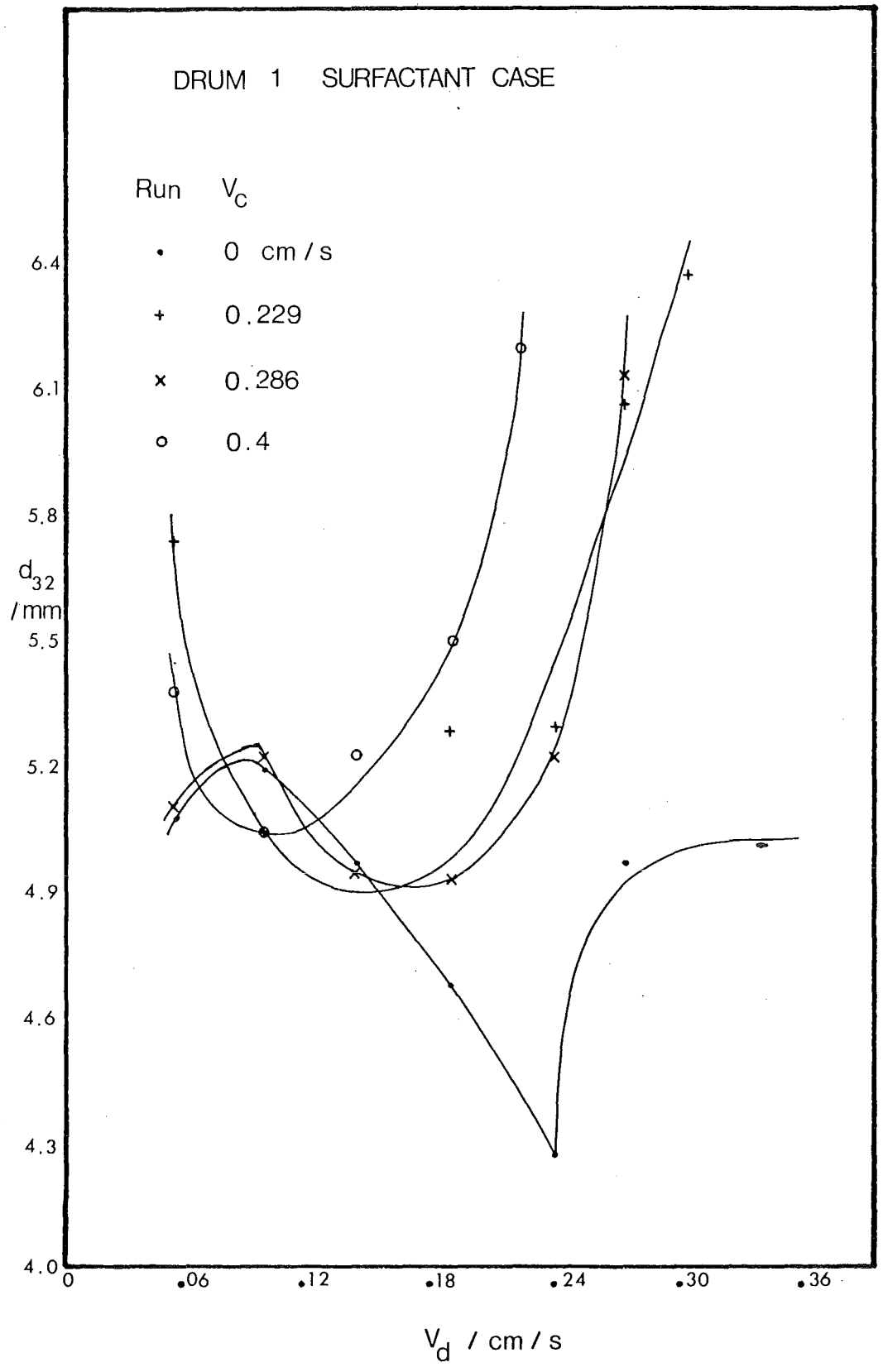

FIGURE 8 – 5 SAUTER MEAN DIAMETER vs FLOWRATES

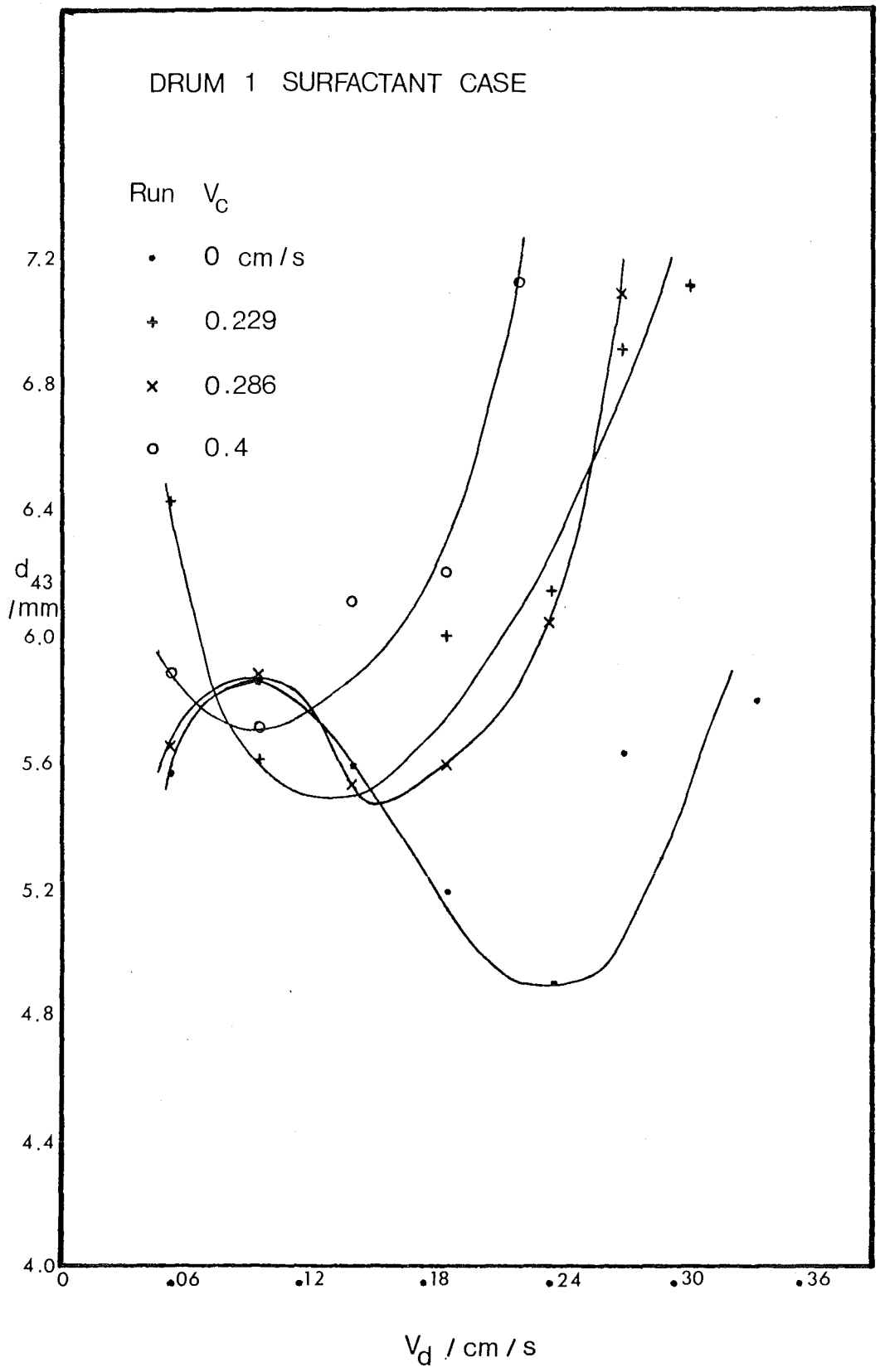

FIGURE 8-6 d_{43} vs FLOWRATES

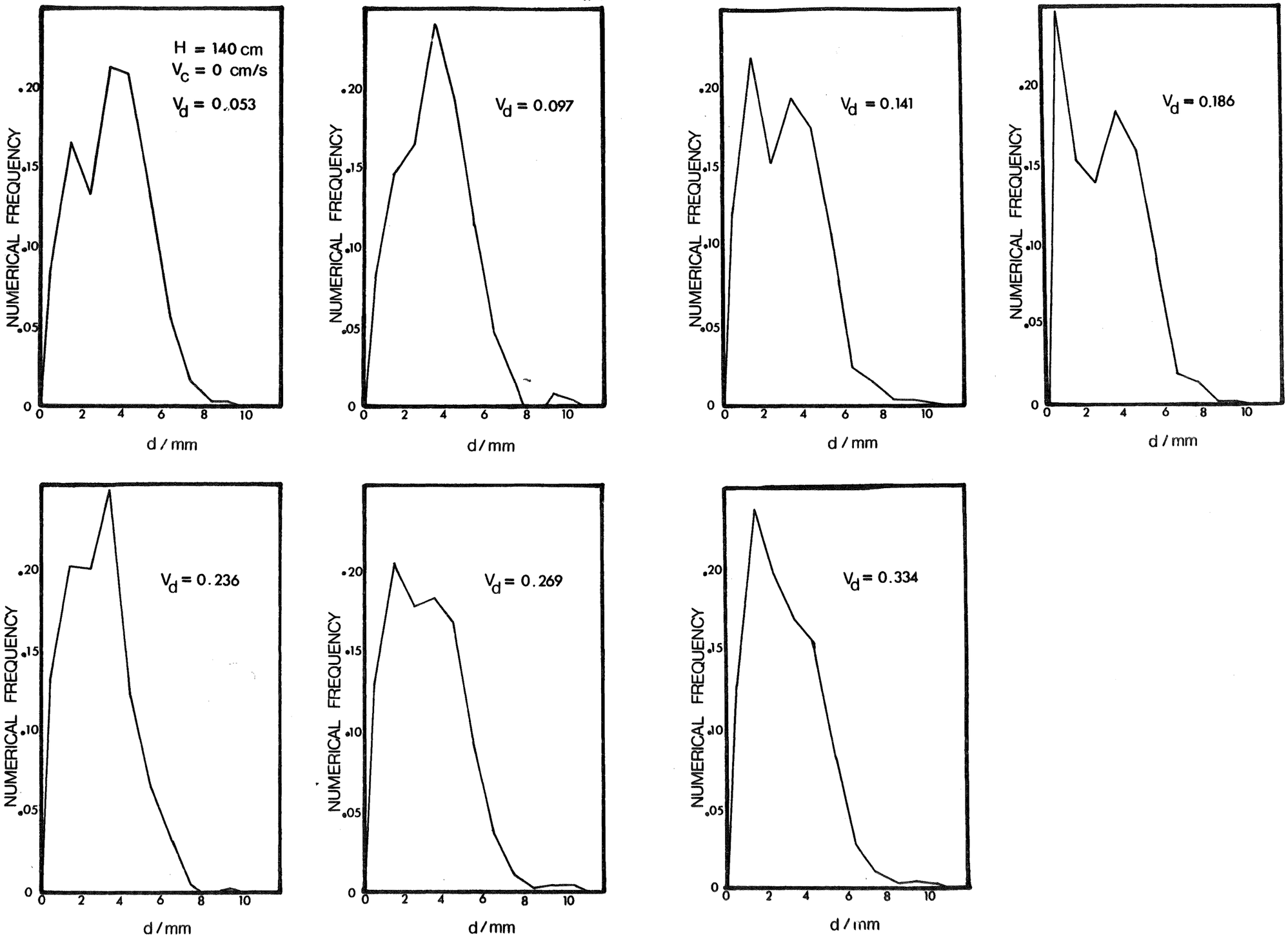

FIGURE 8 – 7 DROPLET SIZE DISTRIBUTIONS vs DISPERSED PHASE FLOWRATE FOR SURFACTANT CASE

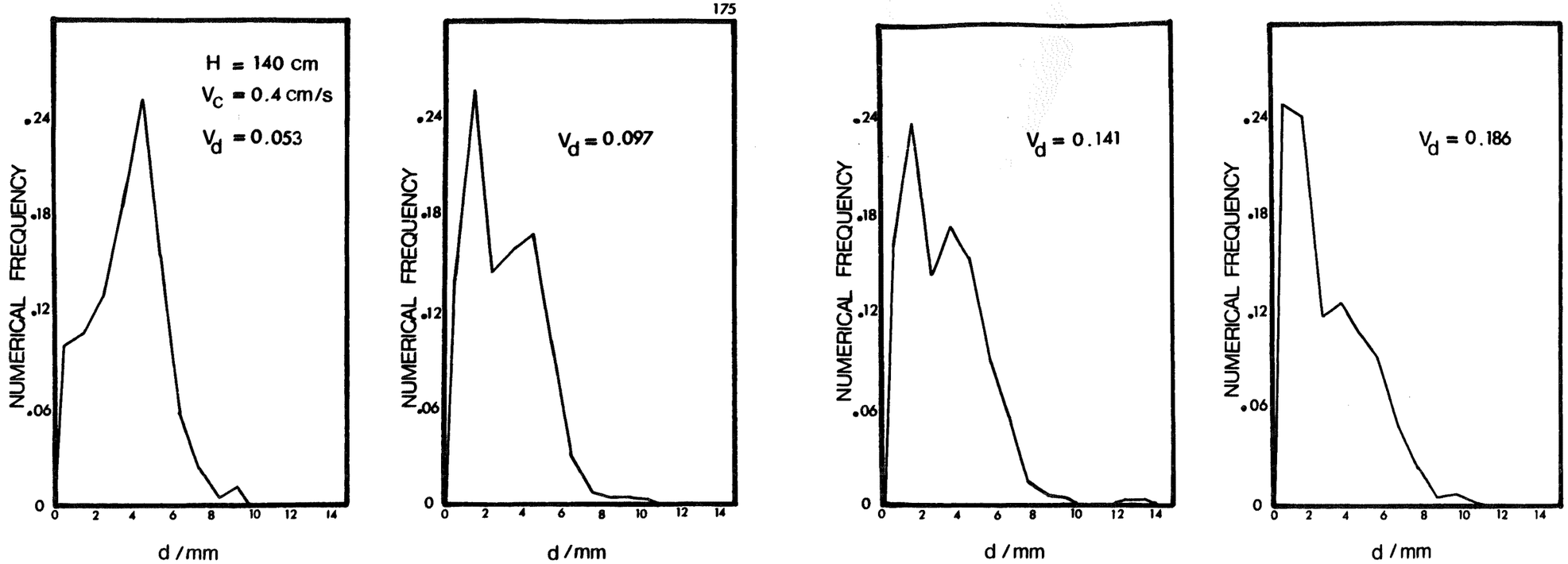

FIGURE 8 – 8 DROPLET SIZE DISTRIBUTIONS vs DISPERSED PHASE FLOWRATE FOR SURFACTANT CASE

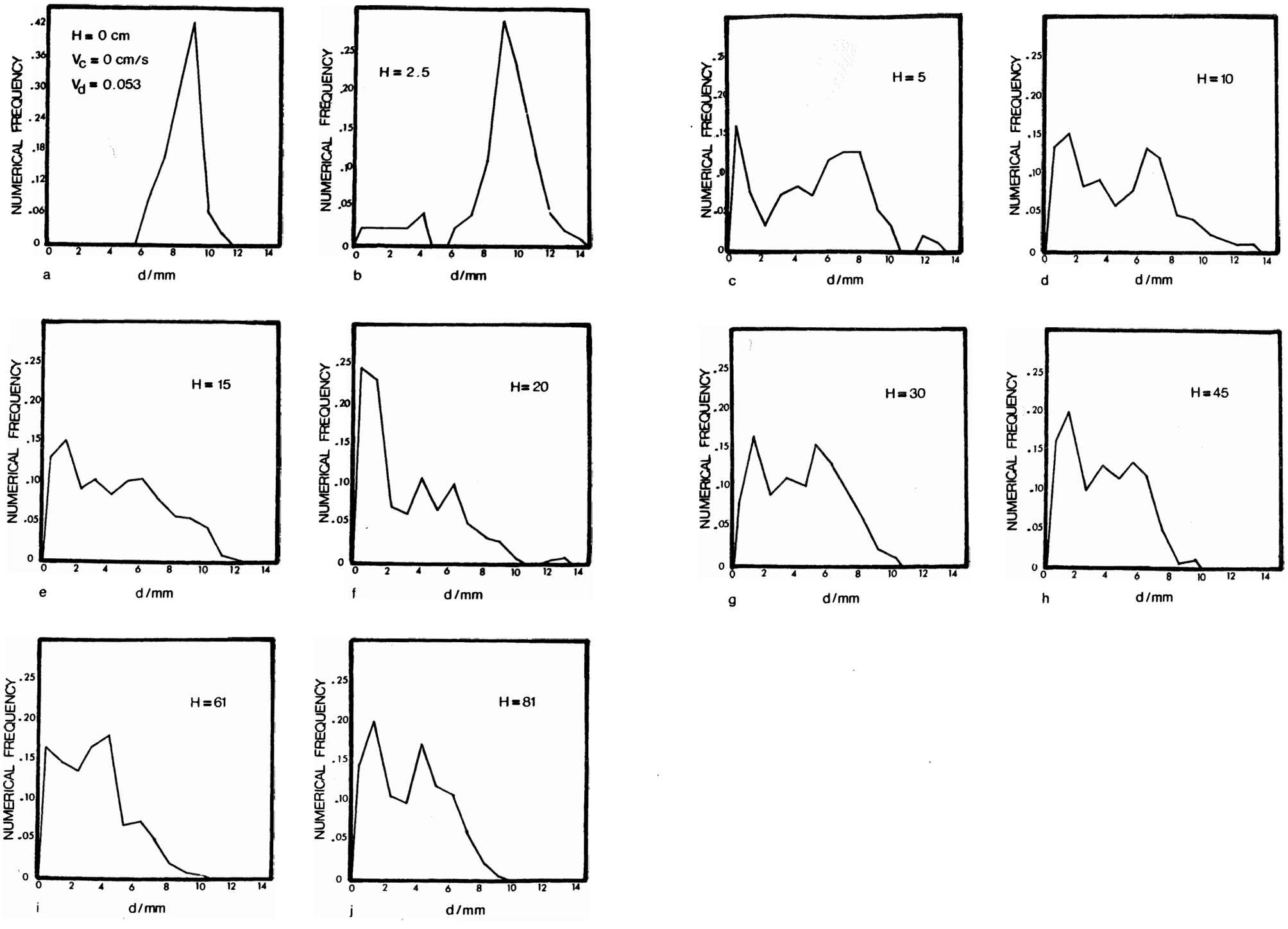

FIGURE 8-9 DROPLET SIZE DISTRIBUTIONS vs PACKING HEIGHT FOR SURFACTANT CASE

distributor mentioned by Gayler and Pratt gives a uniform initial distribution. The distribution obtained with no packing over the nozzles as shown in figure 8 - 9(a) shows this to be the case. A 2.5cm layer of packing is seen to broaden the distribution and a small number of satellite drops appears, as shown in figure 8 - 9(b). The frequency distribution is now approximately normal, with a mean of about 10mm. Addition of another 2.5cm of packing results in considerable changes to the distribution. The main peak is now broadened and covers the range 6 - 9mm. A secondary peak centred on 4.5mm has appeared and a substantial satellite peak is present as shown in figure 8 - 9(c). The distributions obtained with 10cm of packing, 8 - 9(d), and 15cm of packing, 8 - 9(e), show this trend continuing. The main peak is centred on 7mm for 10cm packing and on 6mm for 15cm packing. The secondary peak continues to grow in size whereas the peak of satellite droplets seems to comprise a relatively constant proportion of the total drops counted. Although the main peak for 10cm of packing is centred on 7mm the droplets from 8mm onwards comprise 60% of the total volume. This continues to breakup and at a packing height of 20cm is much reduced. The two main peaks are still present with the original secondary peak now slightly the larger of the two. The satellite peak at this point is larger than either of the other two. The larger diameter tail still extends up to 14mm. After 30cm of packing this tail has been cut back to 10mm, figure 8 - 9(g). After 45cm of packing two peaks still exist but are beginning to merge, figure 8 - 9(h). After 60cm of packing considerable growth of the smaller diameter peak has occured at the expense of the larger diameter peak, figure 8 - 9(i). After 80cm of packing the larger diameter peak has almost completely been assimilated. Comparison with figure 8 - 1 for 140cm of packing shows that the breakup process is still not compete after 80cm, however.

II INFLUENCE OF A THIRD COMPONENT

Droplet size distribution data was collected for the column under conditions of mass transfer for a limited range of continuous and dispersed phase flowrates. The flowrates covered were a high, medium and low continuous phase flowrates and two low dispersed phase flowrates. Three sets of runs were carried out: mass transfer out of the dispersed phase, mass transfer into the dispersed phase, and an equilibrium distribution of solute.

(1) General Characteristics

Figure 8 - 10 shows the size distributions found for the pure phase system and the three solute-added cases. As was found with holdup the behaviour of the saturated phases, and the case of mass transfer into the dispersed phase, are qualitatively similar to that of the pure phase system. The saturated phases have a slightly broader main peak in the range 3 - 6mm as opposed to 4 - 6mm for the pure phases. Although a separate satellite peak does not exist the proportion of droplets in this region is similar to the pure phases case. The higher diameter tail is not as pronounced as before.

Transfer into the dispersed phase results in a main peak centred on 4 - 5mm. The interesting feature that is apparent in this case, is, that the satellite droplets have almost completely disappeared, and the distribution is only slightly different from log-normal. The high diameter tail is similar to that found in the pure phases case.

Transfer out of the dispersed phase results in completely different behaviour as was found with holdup in chapter five. The most evident feature is the large increase in the satellite peak which now comprises 70% of the total drops counted. Secondly, the remaining droplets form a broad distribution that extends up to 16mm. Within this broad distribution there are fairly broad peaks in the 4 - 6mm region and around 8mm.

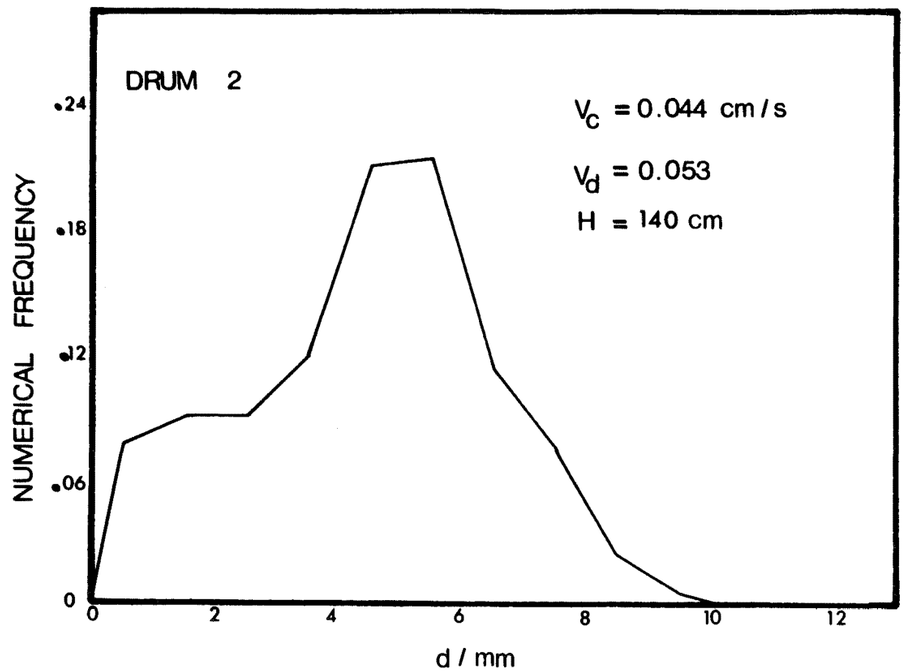

a Pure Phases

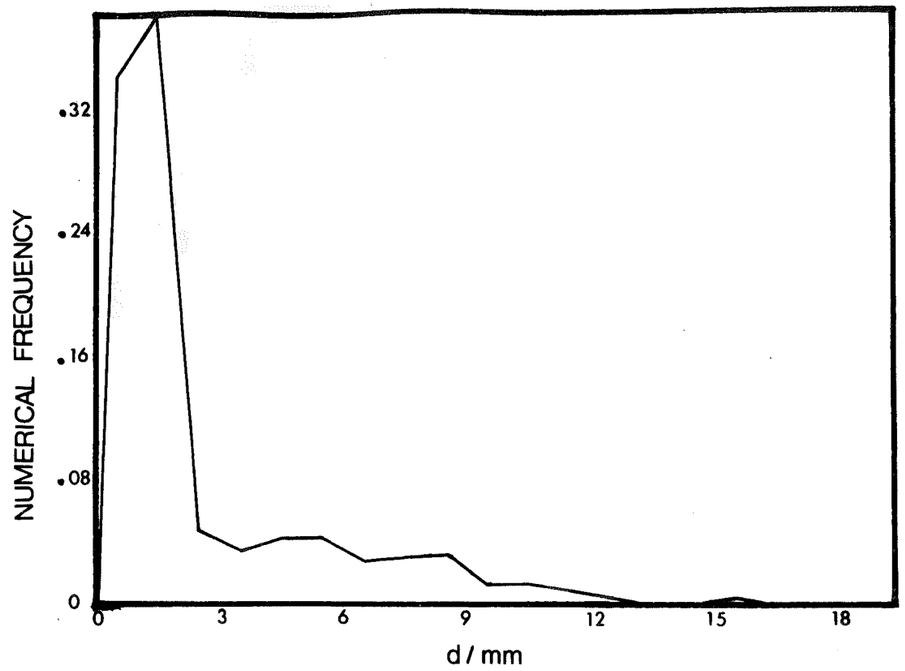

b Mass Transfer Toluene to Water

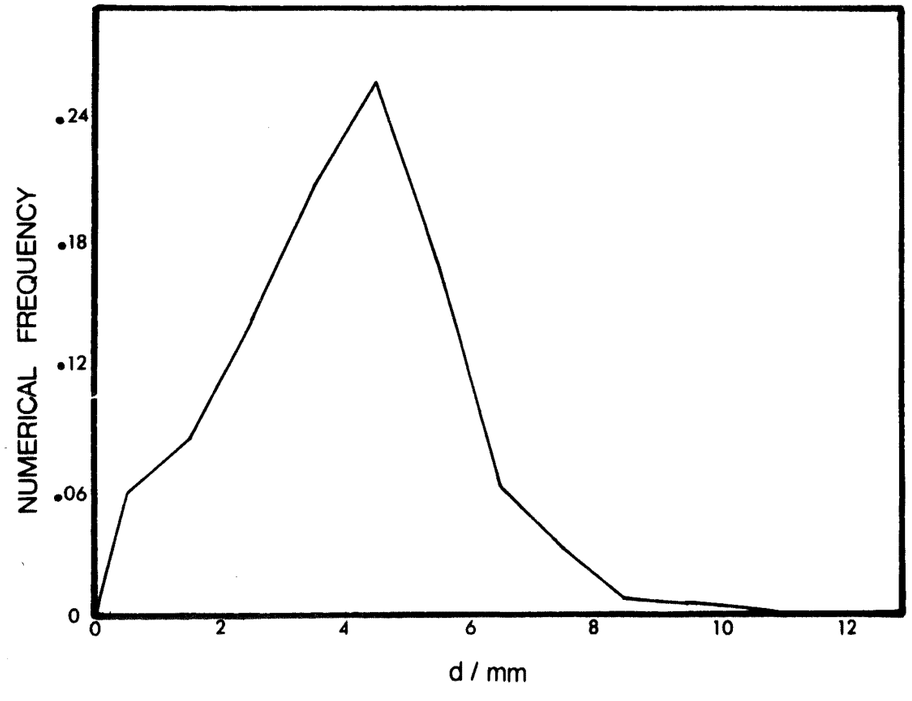

c Mass Transfer Water to Toluene

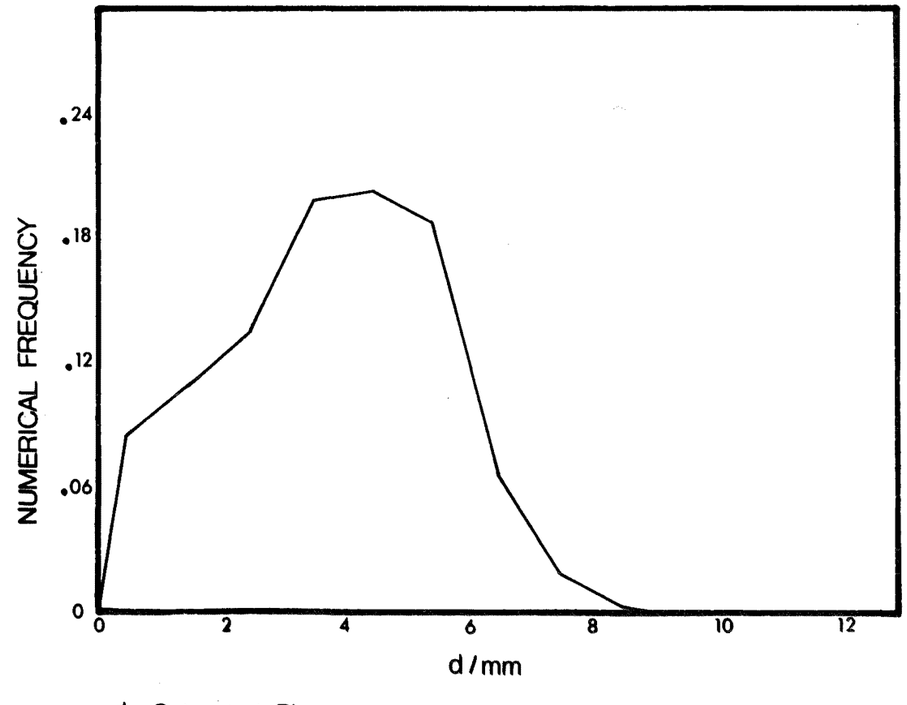

d Saturated Phases

FIGURE 8 - 10 INFLUENCE OF A THIRD COMPONENT ON THE DROPLET SIZE DISTRIBUTION

(2) Effect of Continuous Phase Flowrate

The effect of a high continuous phase flowrate is shown in figure 8 - 11. As with the surfactant case the distributions are broadened. The pure phases case shows two separate peaks as were found with reduced packing heights. The proportion of satellite drops has also increased. Similarly the saturated phases peak has broadened and now has a high diameter tail extending up to 13mm. Here also the satellite droplets have increased and now form a separate peak. The proportion of satellite drops in the case of mass transfer out of the dispersed phase has increased slightly to 73%. The number of drops with a diameter greater than 10mm has also increased slightly.

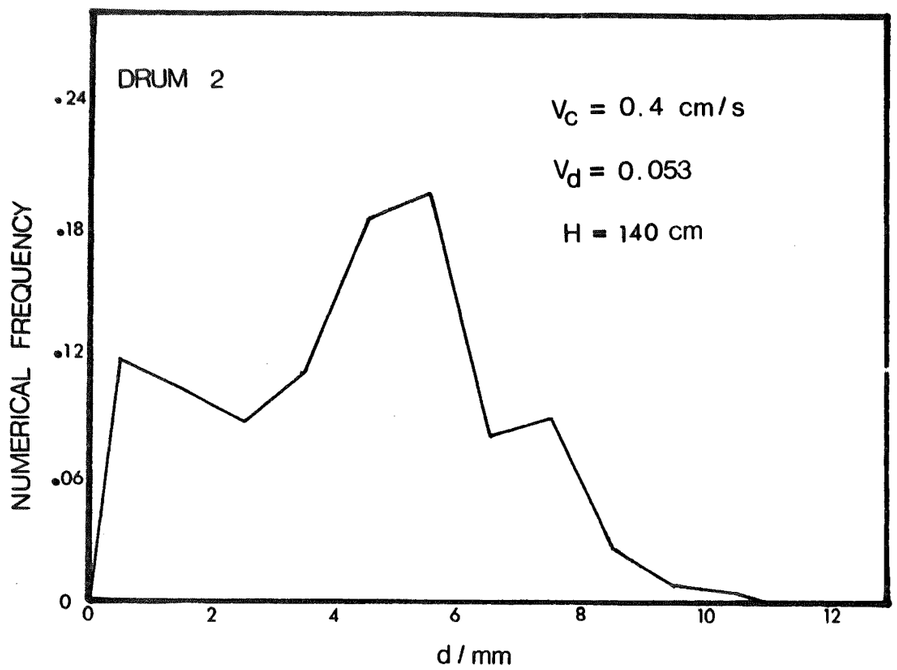

a Pure Phases

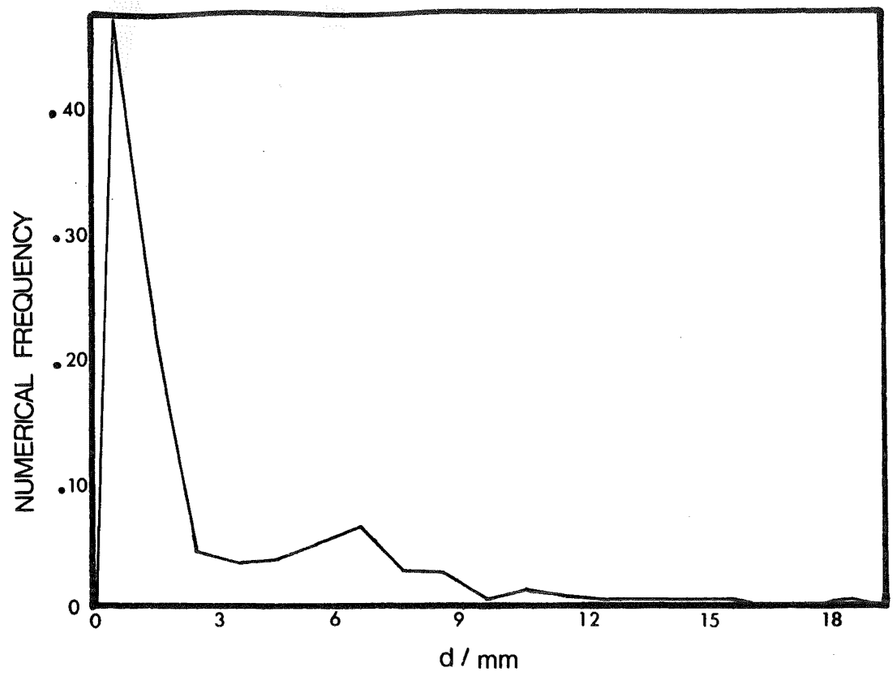

b Mass Transfer Toluene to Water

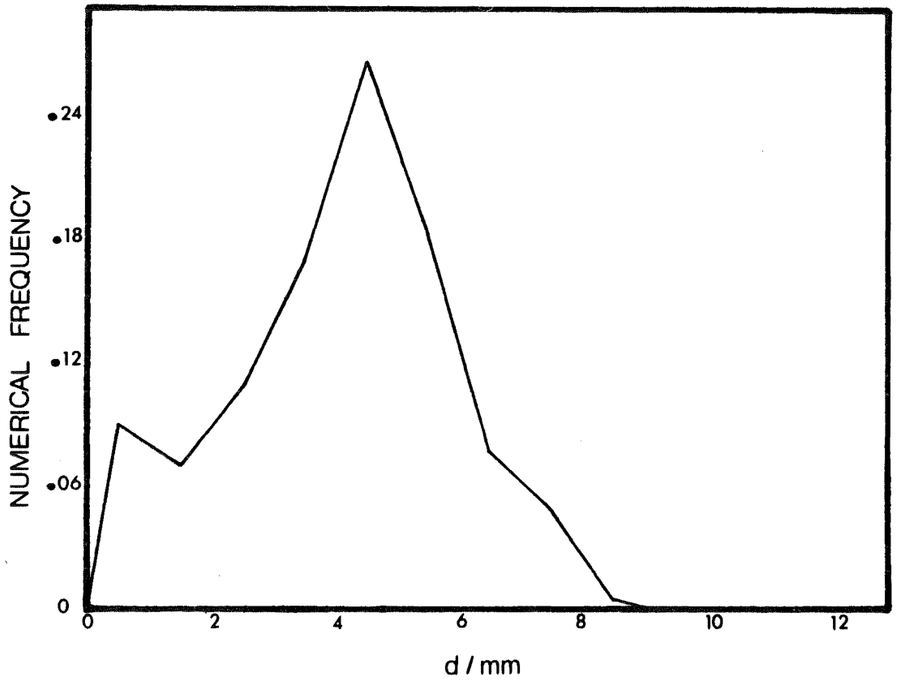

c Mass Transfer Water to Toluene

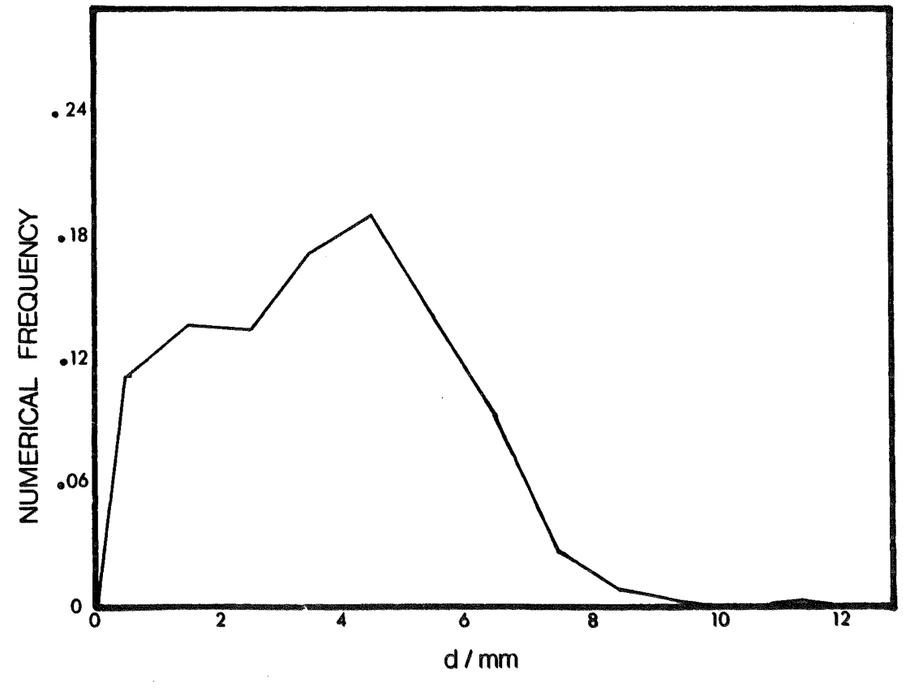

d Saturated Phases

FIGURE 8 – 11 INFLUENCE OF A THIRD COMPONENT ON THE DROPLET SIZE DISTRIBUTION

DISCUSSION

I USE OF MEAN DIAMETERS

Two investigations in the literature have dealt specifically with droplet behaviour in packed columns. Lewis, Jones and Pratt, (1951), produced a model in which the Sauter mean diameter, (d_{32}), was related to an equilibrium diameter and the ratio of the characteristic velocity and the mean dispersed phase velocity. Thus:

$$d_{32} = d_{32}^{o} \left(\frac{\overline{V}_o \, \epsilon x}{V_d} \right) \qquad (8\text{-}2)$$

The equilibrium diameter d_{32}^{o} was the mean diameter at substantially zero flowrates. Dimensional analysis of the physical properties led to the expression

$$d_{32}^{o} = 0.92 \left(\frac{\sigma}{\Delta \rho g} \right)^{0.5} \qquad (8\text{-}3)$$

Ramshaw and Thornton, (1967), used an energy balance over a droplet colliding with a thin baffle to show that this equilibrium diameter corresponded to the critical drop size at which a parent drop had just sufficient kinetic energy to supply the increases in surface energy needed for breakup.

(1) Comparison with Experiment

Figure 8 - 12 compares the experimental values of d_{32} with those predicted using equation (8-2). Agreement with the equation is not good. At the lowest continuous phase flowrate considered the experimental d_{32} values for three of the four systems - pure and saturated phases and transfer into the dispersed phase, are smaller than predicted values. Agreement is generally within 15% however. The exception is when solute transfer is out of the dispersed phase. In this case the experimental mean diameter is 36% greater than that predicted as a

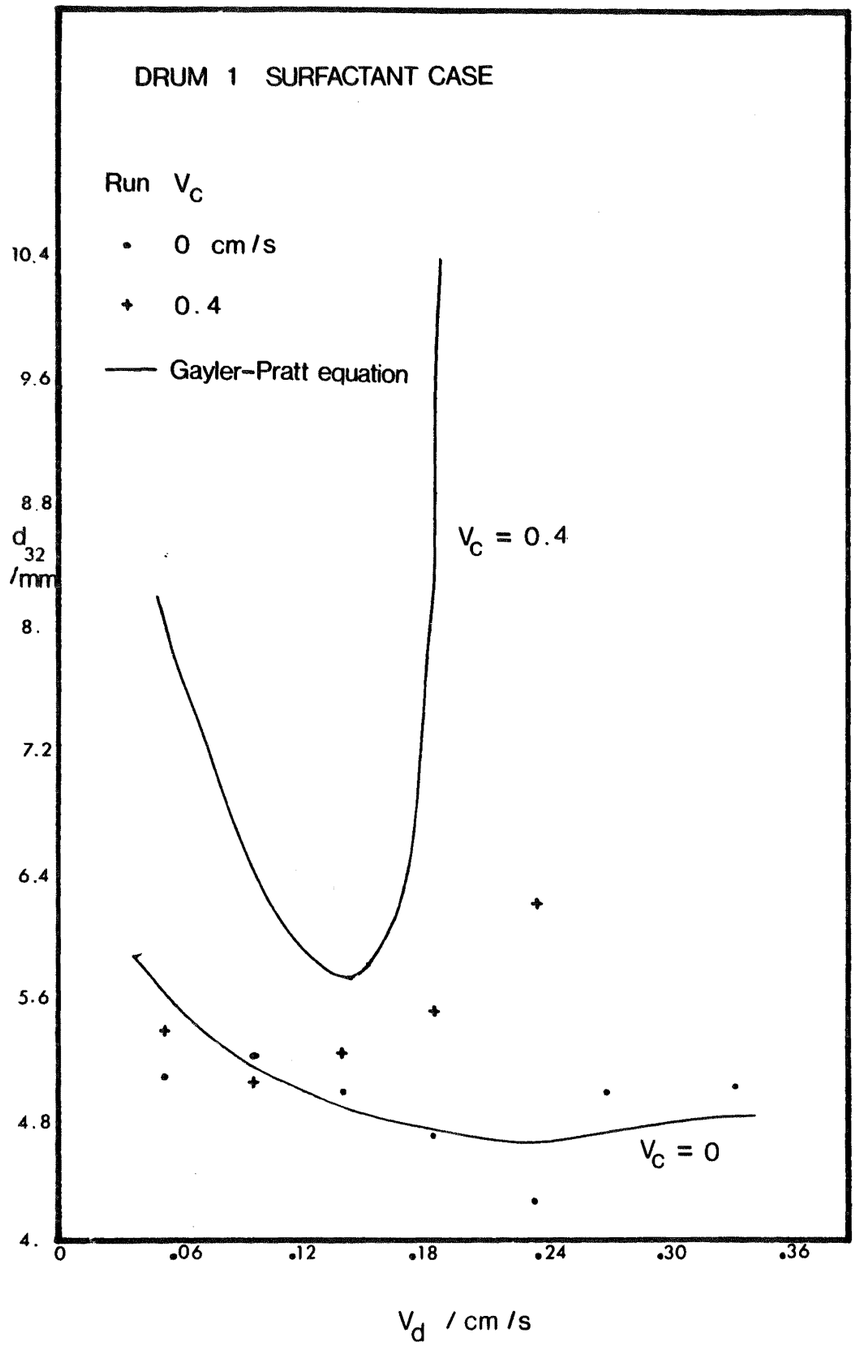

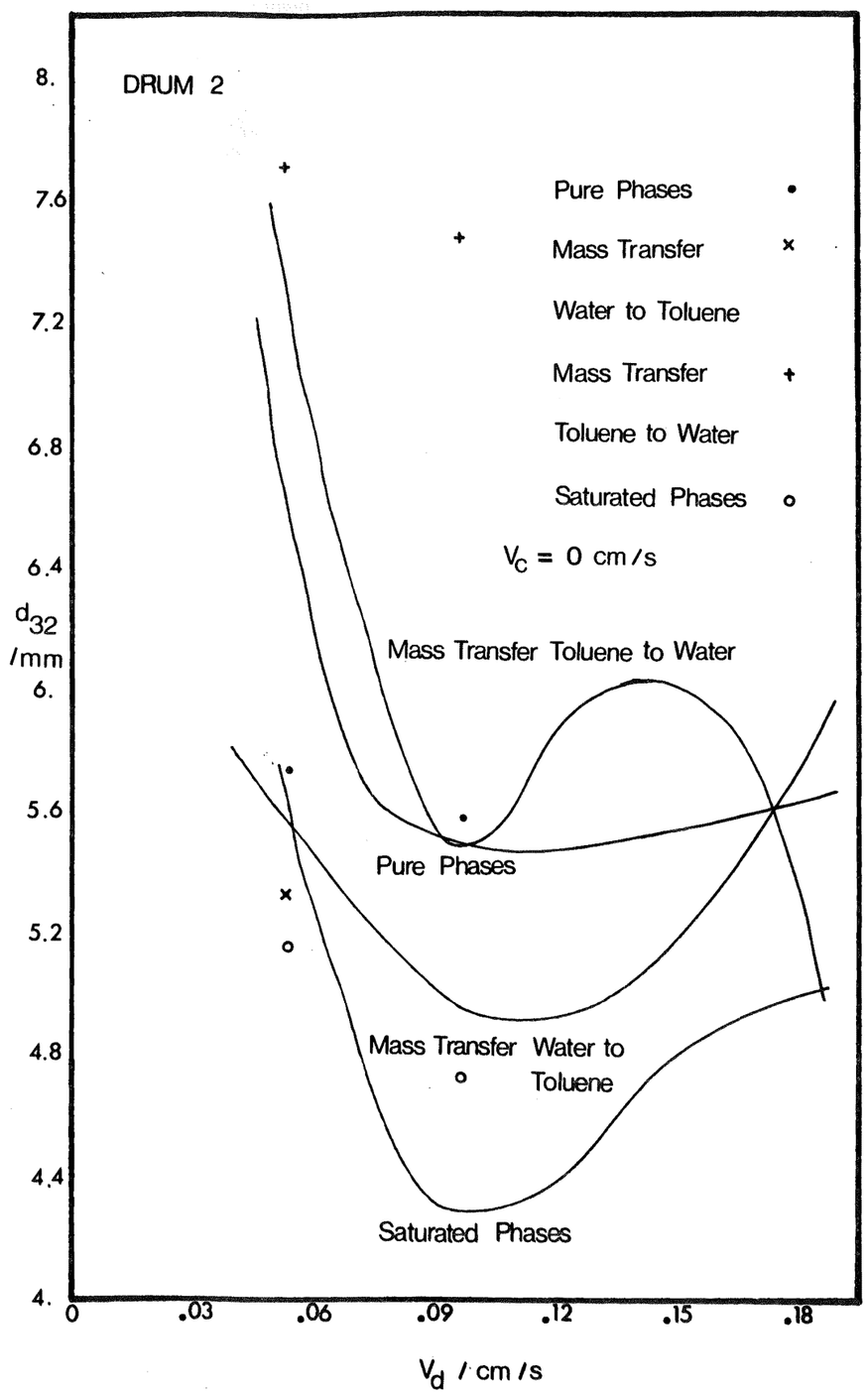

FIGURE 8 – 12 COMPARISON OF GAYLER-PRATT EQUATION WITH EXPERIMENTAL DATA

result of the enhancement of the coalescence rate by the Marangoni effect. Furthermore, the equation (8-2) predicts a stronger dependence of d_{32} on the mean dispersal phase velocity, $\frac{\epsilon x}{V_d}$, at low flowrates than is found experimentally. The most significant failure of the model is its inability to handle changes in the continuous phase flowrate. Increases of up to 77% are predicted for the maximum continuous phase flowrate used. The increases in the experimental mean do not, however, support this prediction. This results from the fact that the variation in holdup with continuous phase flowrate is considerably greater than the changes in mean diameter which occur. The model of Lewis et al, (1951), and Gayler and Pratt, (1953a) thus fails on two counts:

(a) The group $\overline{V}_o \frac{\epsilon x}{V_d}$ does not adequately account for the influence of flowrates on the mean diameter.

(b) No account is taken of the influence of mass transfer on the coalescence rate.

(2) Equilibrium Diameter

The expression for the equilibrium diameter derived by Lewis et al (1951), has also been criticised (Davies, Jeffreys and Azfal, 1972). A simple force balance over a slowly forming droplet at a nozzle predicts a dependence of diameter on the group $\frac{\sigma}{\Delta \rho g}$ to the power of one third. The experimental dependence was found to be:

$$d_{32}^{o} \sim \left[\frac{\sigma}{\Delta \rho g}\right]^{0.5} \qquad (8\text{-}4)$$

Davies et al (1972), fail to appreciate, however, the significance of the group $\left[\frac{\sigma}{\Delta \rho g}\right]^{0.5}$. Lamb (1945), has pointed out that when a heavier liquid is placed on top of a lighter liquid there will be a stability only for disturbances with wave-lengths less than the critical wave-length, where:

$$\lambda_c = 2\pi \sqrt{\frac{\sigma}{\Delta \rho g}} \qquad (8\text{-}5)$$

Verification of this equation can be seen from the behaviour of a pool of light phase liquid below a nozzle into a chamber of heavy phase liquid, Christiansen and Hixson, (1957). When the nozzle diameter is less than the critical wavelength no movement of the light phase occurs. When the nozzle diameter is greater than the critical wavelength spontaneous droplet formation occurs. Thus, the group $\left(\frac{\sigma}{\Delta\rho g}\right)^{0.5}$ is a characteristic property of the system, and Lewis et al, (1951) have simply defined their mean diameter as a fraction of the critical wavelength for the system.

II USE OF DROPLET SIZE DISTRIBUTIONS

The technique of characterising the droplet distribution by a mean diameter has recently been critisized. Olney, (1964), has shown that calculation of the average transfer rate in an RDC based on an average drop diameter can be significantly different than that found by summing over a number of size intervals. Misek and Marek, (1970), have developed a size distributed model for an asymmetric RDC and used d_{43} when a mean diameter was necessary. Unsteady state mass transfer models based on size distributions have been developed by Gal-Or and Hoelscher, (1966), using the distribution function of Bayens, (1968), and by Chartres and Korchinsky, (1975), using the upper limit function of Mugele and Evans, (1951). The success of these more sophisticated models depends upon how well the droplet size distribution can be represented.

(1) Empirical Distribution Functions

Mugele and Evans, (1951), have reviewed the application of the Rosin Rammler, Nukiyama-Tanasawa, and log-probability distribution equations for representing the size distribution of liquid sprays. A modification of the log probability equation known as the upper limit equation was found the most satisfactory. More recently Bayens, (1968), has applied a type of normalised gamma distribution function to

liquid-liquid and gas-liquid systems. Figure 8 - 13 compares the application of these equations to the present data. Mugele and Evans showed that the Nukiyama-Tanasawa equation gave grossly unreasonable results for conditions other than those for which it was designed, and it has not been included.

The Rosin-Rammler equation is used in figure 8 - 13(a). The pronounced large diameter tail for the pure phases and when transfer is into the dispersed phase results in distinct "S" curves. The saturated phases case does not have the large diameter tail and a much better line is obtained. The very large satellite peak obtained for mass transfer out of the dispersed phase completely distorts the first half of the line.

In figure 8 - 13(b) the logarithmic-normal is shown to give a straight line relationship over 90% of the range for three of the systems but has appreciable curvature when transfer is out of the dispersed phase.

The upper limit equation also fails to cover the whole volume range as shown in figure 8 - 13(c). Three of the systems can be represented by a straight line over 95% of the volume range, but once again there is some curvature when mass transfer is out of the dispersed phase.

The function of Bayens, based on a single parameter fails entirely and needs a change of an order of magnitude in the parameter to handle the size range found in this equipment.

Thus, none of the empirical functions used is successful in representing the size distributions over the whole range of diameters. The logarithmic-normal distribution however, gives a reasonable fit to the larger diameter droplets, which are the most important in the mass transfer processes, for three of four systems. None of the equations examined are particularly satisfactory when transfer is out of the dispersed phase.

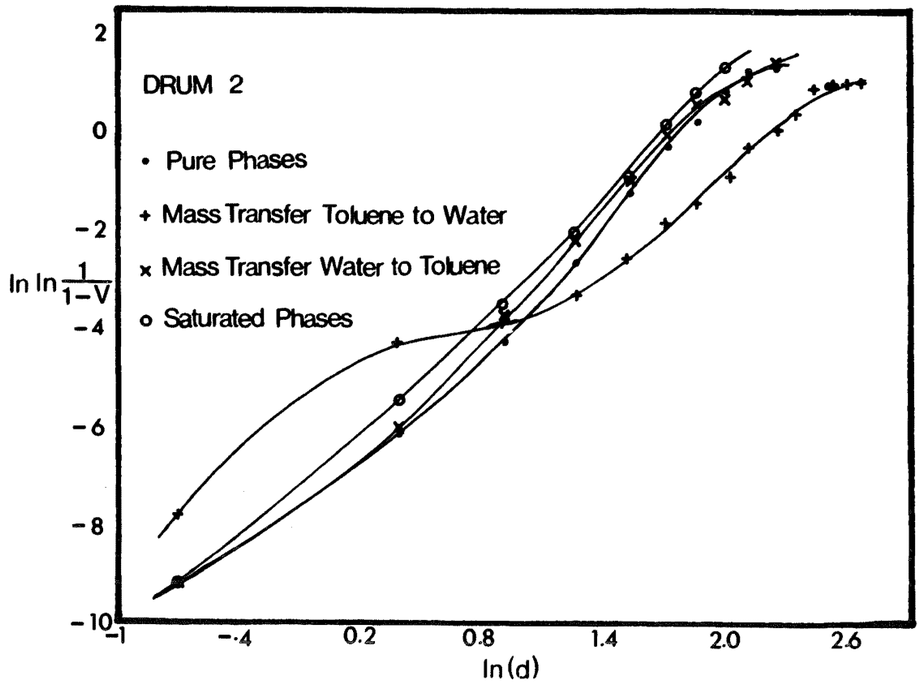

a Rosin Rammler Equation

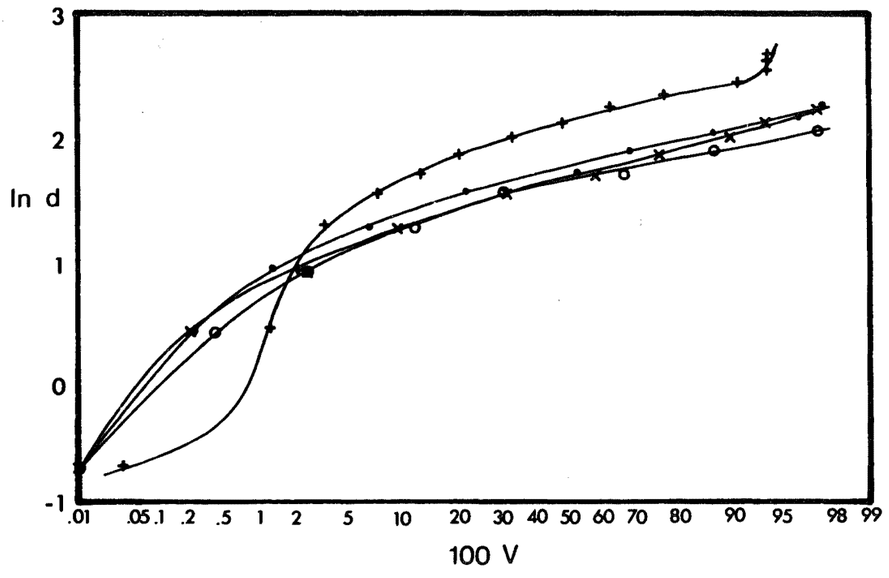

b Logarithmic Probability Equation

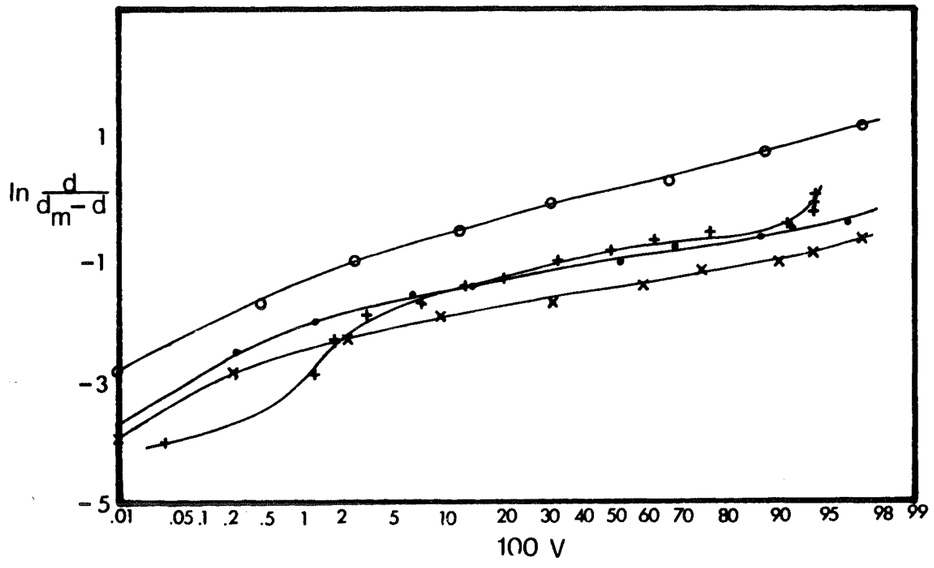

b Upper Limit Equation

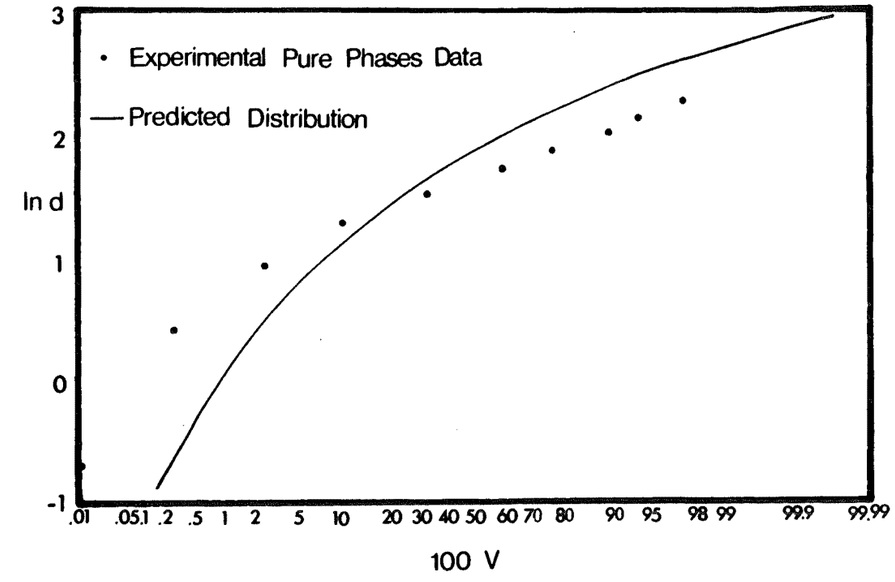

d Bayens Function

FIGURE 8 – 13 EMPERICAL SIZE DISTRIBUTION EQUATIONS

III BREAKUP MECHANISMS

Figure 8 - 9(a) showed that the distributor by itself gives a narrow range of diameters with a mean close to 9mm. The first layer of packing over the nozzles serves merely to modify the distributor action rather than to result in breakup. This presumably occurs by increasing the drag on forming droplets, and increasing the incidence of twinning. Thus figure 8 - 9(b) shows a much broader peak centred about 10mm with larger diameter droplets extending up to 14.1mm. The distribution after 2.5cm of packing can be considered as the input distribution to the column. Breakup does occur in the next 2.5cm of packing however. The main peak now occurs in the range 6.5 - 8.5mm and a secondary peak in the range 3.5 - 5.5mm has appeared. The applicability of various of the breakup mechanisms in the literature can be considered in terms of the changes in distribution found.

(1) Impaction

The impaction mechanism of Ramshaw and Thornton, (1967), assumes a droplet will break into two daughter droplets if its kinetic energy plus the potential energy liberated exceeds the increases in surface energy caused by the breakup. The equation governing the critical drop size is:

$$\frac{\pi d_{crit}^2 \sigma'}{12}\left[We_{crit} + 1.8\ Bo - 3.12\right] = 0 \qquad (8\text{-}6)$$

Thus

$$We_{crit} = 3.12 - 1.8\ Bo \qquad (8\text{-}7)$$

$$\frac{d_{crit} V_t^2 \rho_d}{\sigma'} = 3.12 - 1.8 \frac{\Delta\rho g}{\sigma'} d_{crit}^2 \qquad (8\text{-}8)$$

For any drop size the necessary velocity for instability is

$$V_t = \sqrt{\frac{3.12\,\sigma}{d_{crit}\,\rho_d} - \frac{1.8\Delta\rho g}{\rho_d}\,d_{crit}} \qquad (8\text{-}9)$$

Figure 8 - 14 compares the necessary velocity for instability with the Hu-Kintner terminal velocity in an infinite tank and corrected for wall effect assuming the tube diameter to be the internal packing and using equation (4-22). Thus for droplets travelling at their terminal velocity in a 12mm diameter tube the stable diameter is predicted as 4.9mm. For diameters greater than 4 9mm the critical velocity decreases below the terminal velocity until at d = 6.5mm the model predicts instability due to buoyancy forces alone.

(a) Physical Model

It is important to note that the model applies to thin baffles. Ramshaw and Thornton found a 4.5% increase in the critical diameter upon changing from a 0.1mm baffle to a 1.1mm thick baffle. This results from an approximation in their model. It is assumed that breakup of a droplet will occur if sufficient net energy is available but neglects the manner in which breakup occurs. The photographs of Ramshaw and Thornton show the formation of a dumbell type structure with the two lobes of the droplet connected by a sheet of liquid. Breakup of the droplet occurs when this sheet of liquid has been drawn out sufficiently thinly for a Taylor instability to grow. Furthermore, the model neglects part of the droplets available energy. When the droplet is moving at its terminal velocity part of the gravitational work done is dissipated as drag. When the droplet impacts on a baffle its velocity drops below the terminal velocity, hence the drag force decreases, and the net buoyancy force increases. Thus the model is an approximation to the actual process whereby it is necessary to distort the droplet sufficiently for a thin film to be formed which can rupture by a Taylor instability. The thicker the baffle, the greater the increase in surface energy before a

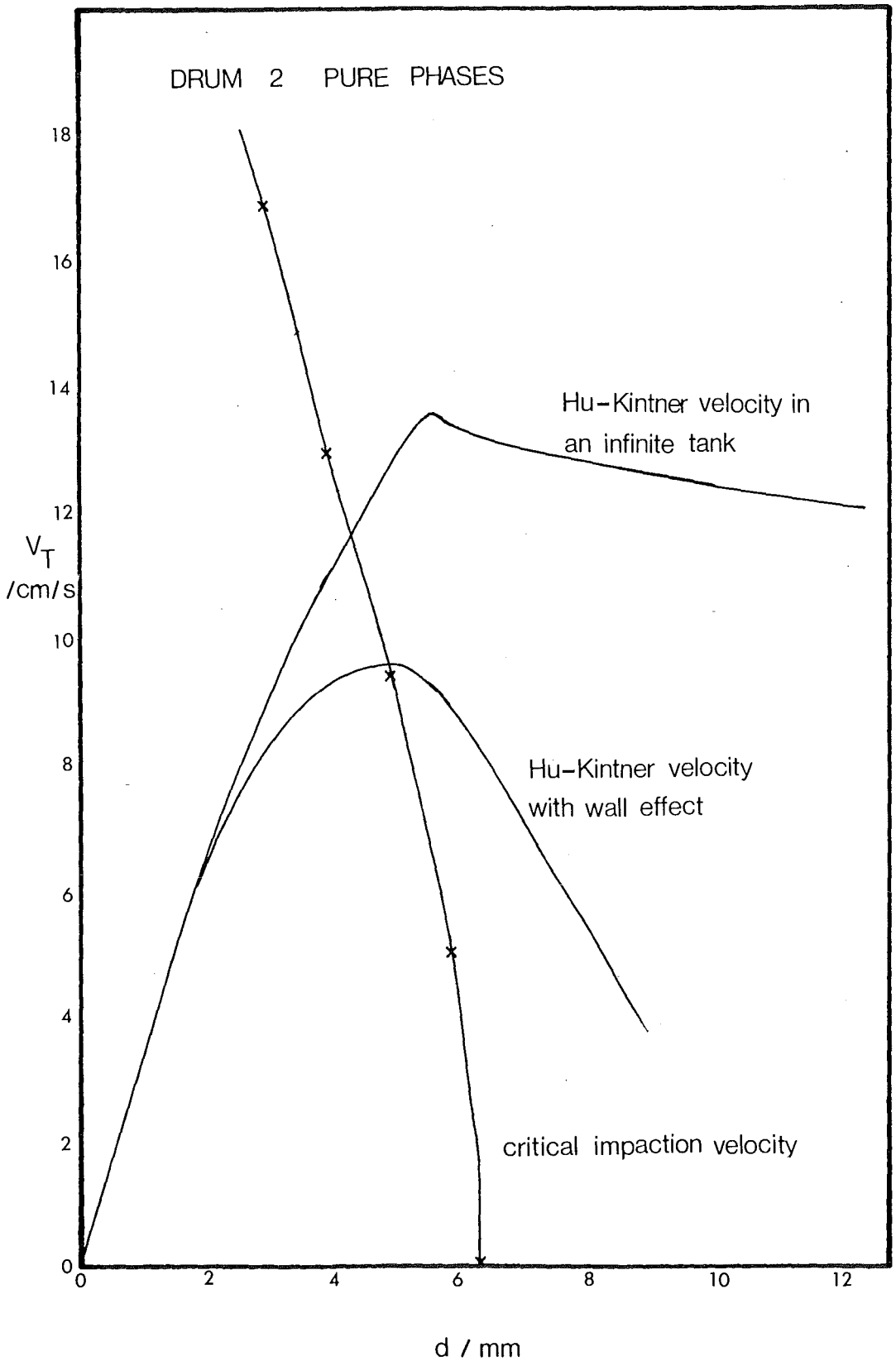

FIGURE 8 - 14 RAMSHAW-THORNTON INSTABILITY EQUATION

sufficiently thin film is formed. Thus, in the limiting case, when droplets were impacting on a thin plate, breakup generally did not occur.

(b) Application to Actual Behaviour

Breakup of a parent droplet into two equal daughter droplets will only occur when the parent droplet strikes the baffle exactly symmetrically. This will obviously be the exception rather than the rule in a randomly packed column. It would seem reasonable then, to expect some distribution in the volume ratio of the daughter droplets. Thus, for a 10mm droplet a range of daughter droplets distributed about

$$d = \sqrt[3]{\frac{10 \cdot 10 \cdot 10}{2}}$$

$$\simeq 8\text{mm}$$

would be expected. Figure 8 - 9(c) shows a distribution of droplets in the range 6.5 - 8.5mm for the main peak which would seem to support this mechanism. The secondary peak in the range 3.5 - 5.5mm is not predicted by this mechanism, however. Secondary breakdown of 8mm droplets would result in drops of approximately 6.3mm diameter. This suggests that the secondary peak corresponds to another breakup mechanism, or represents satellite droplets formed during impaction breakup. There is no evidence to support the latter hypothesis. The photographs of Ramshaw and Thornton show no satellite formation. Similarly movie films of droplet behaviour taken in this study show breakup by impaction to result in only two droplets.

The behaviour found as the packing height increases also supports this mechanism. With 10cm of packing the main peak lies in the range 6 - 7.5mm, whilst breakup of the 8mm drops would result in 6.3mm diameter products. The rate of breakdown decreases as the critical diameter is approached and after 15cm of packing the main peak is in the range 5 - 7mm.

(2) Restriction Processes

Impactions on leading edges of packing elements are not the only type of interaction between the droplets and the packing. The droplets must also pass through restrictions between packing elements. This leads to the suggestion that some droplet breakup may be caused by processes similar to those occuring at nozzles or on sieve plates.

(a) Force Balance Breakup. A review in chapter seven of some recent work in this field showed that dispersing a dispersion through a nozzle or sieve plate can give quite a different result to dispersing a continuous phase. Ooi's (1977), photographs of a single nozzle showed that a force balance mechanism of the Scheele-Meister (1968), type was still operative at low flowrates, but, that as the flowrate increased multiple occupation of the nozzle became more and more important.

Figure 8 - 15 shows the predicted drop size using the unaltered Scheele-Meister equation for drop formation at low velocities. The work of Wilkinson et al (1975), suggests that a minimum nozzle diameter of approximately 2.5mm is reasonable for this system. Thus, for droplet breakup by a force balance mechanism the minimum product size would appear to be 0.645mm irrespective of packing height. This will be a slight overestimate since there is likely to be some modification to the necking term in the Scheele-Meister equation. Another look at figure 8 - 9(c) shows that the main peak extends from 6.5mm up to 8.5mm. This is somewhat broader at the bottom end than would be expected if the impaction mechanism alone were operative. Thus it would seem that, in the first layers of packing,at least, breakup by a force balance mechanism, similar to behaviour at nozzles, is occuring simultaneously with the impaction mechanism.

The existence of a force balance mechanism suggests a possible source of the secondary droplets. If a droplet is being redispersed as a number of Scheele-Meister droplets then a point will be reached where the residual volume is smaller than the volume of a Scheele-Meister drop.

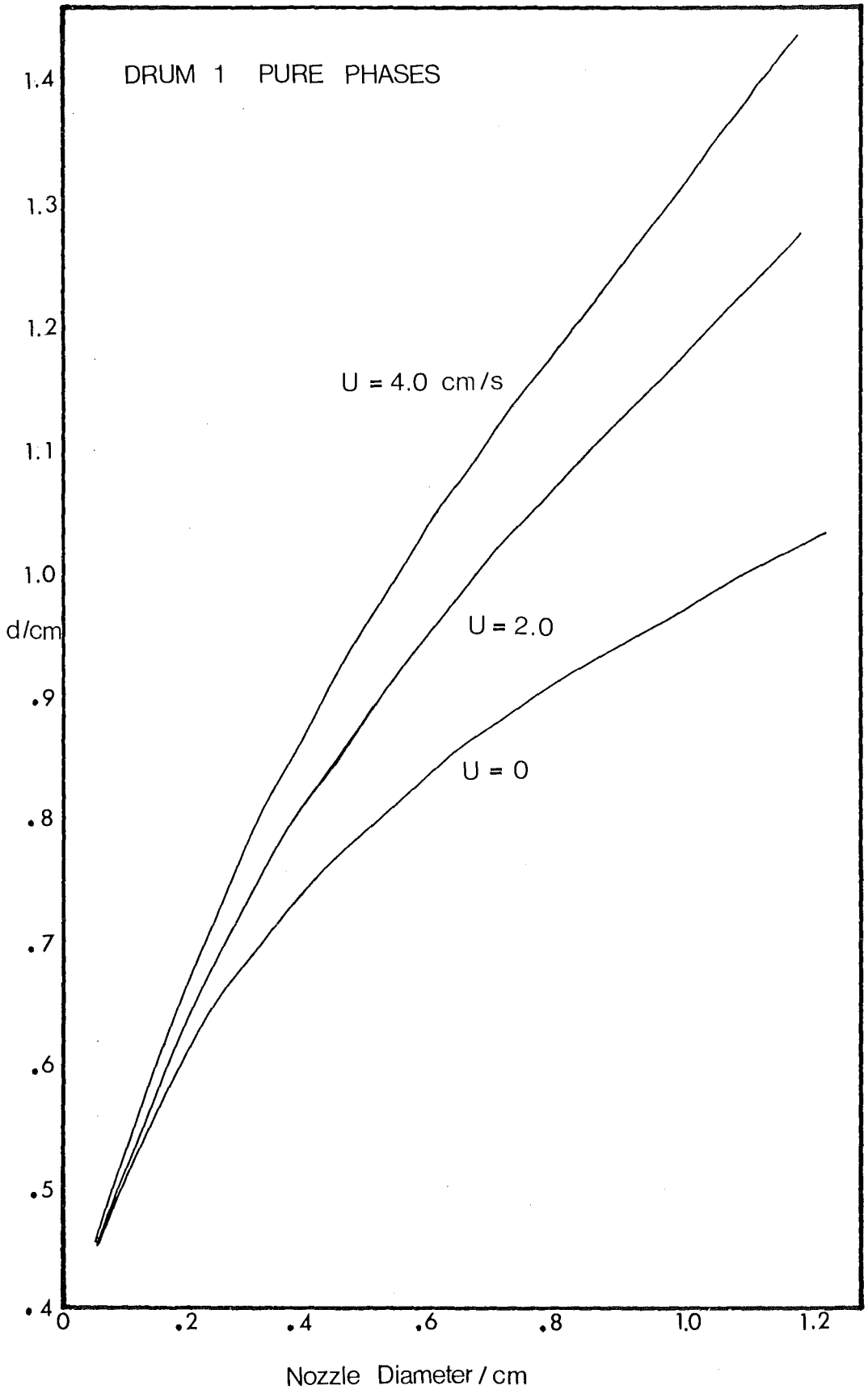

FIGURE 8-15 SCHEELE-MEISTER EQUATION

Thus, the right combination of parent droplets and restriction diameter could yield a secondary peak in the right range. There are two arguments against this, however. The first is the continued growth of the secondary peak as packing height increases, although it is unlikely that any significant breakup by a force balance mechanism occurs after the first 10cm of packing as unrealistically small restriction diameters would be required. The second argument against this hypothesis is the number of secondary drops which are formed. Since only a proportion of the input droplets will breakdown by the force balance mechanism, and two daughter droplets will be formed for every secondary droplet formed, it would be expected that the number of secondary droplets would be less than half the number of main peak droplets. However, after 5cm of packing the secondary peak is about two thirds the size of the main peak.

(b) Jet Formation. A more likely source of these droplets is the jet breakup of highly deformed parent droplets. One of the features of the photographs of Ooi (1977), is the multiple occupation of the nozzle by a number of separate drops. At lower flowrates this tended to take the form of one main droplet occupying most of the nozzle area, while another drop became distorted into a thin thread which broke up by a Rayleigh instability mechansim. For the toluene-water system, the graphical solution to the Tomotika equation of Meister and Scheele, (1967), gives:

$$(ka)_{max} = 0.67$$

where k is the wave-number of a disturbance, and a is the jet radius. Now

$$ka = \frac{2\pi}{\lambda_c} a \qquad (8\text{-}10)$$

Hence

$$\lambda_c = \frac{2\pi}{0.67} a$$

$$= 9.39a$$

If the cylinder volume is converted to an equivalent spherical volume

$$\frac{\pi}{6} d^3 = \pi a^2 \lambda_c \qquad (8\text{-}11)$$

$$= 9.39\pi a^3$$

$$d = 3.84\ a \qquad (8\text{-}12)$$

Thus

if $d_{jet} = 2mm$ $\qquad d = 3.8mm$

$d_{jet} = 3mm$ $\qquad d = 5.8mm$

Breakup of a parent droplet in this manner would result in a far greater number of product droplets than would the residual volume process.

(3) Dynamic Pressure

The literature survey revealed that, in many situations, the critical droplet size is determined by the fluctuations in dynamic pressure across the droplet. For turbulent pipe flow Sleichers, (1962, 1965), equation gives:

$$We\sqrt{\frac{\mu_c V}{\sigma}} = 38\left[1 + 0.7\left(\frac{\mu_d V}{\sigma}\right)^{0.7}\right] \qquad (8\text{-}13)$$

Substitution of the relevant physical properties into this and taking the velocity of the droplet terminal velocity equation gives:

$$d = 21.85cm$$

Thus, the mechanism can be fairly safely neglected.

IV PHYSICAL FLOW MODEL

The behaviour of the droplet size distributions with height also lends some weight to arguments advanced in chapter four about the flow structure of a packed bed. It was argued that preferential channels existed in which the dispersed phase met with minimum resistance to flow. There also existed secondary channels in which the resistance to flow was higher and the amount of free rise was much reduced. The size distributions show an initially rapid breakdown of larger diameter droplets followed by a relatively long section of packing in which a tail of these larger droplets persist. The reduction in free rise in the secondary regions reduces the influence of the impaction mechanism, while the increased number of restrictions mean that the droplets must, of necessity, be larger in order to progress, (Wilkinson et al, 1975). Thus, it is proposed that the larger diameter tail found on most distributions represents flow through the secondary areas. It should be noted that large droplets in the secondary regions do breakup as the packing height increases, although the rate is very much less than in the preferential channels. This is very likely to be dependent upon the rate of interchange between the preferential channels and the secondary flow ares. Alternatively it might be argued that the large diameter tail is due to coalescence within the preferential channels. However, coalescence is likely to be inhibited when mass transfer into the dispersed phase occurs. Yet the droplet distribution under these conditions still shows a large diameter tail.

V SATELLITE DROPLETS

Whilst the satellite droplets form a small proportion of the dispersed phase volume, and make a correspondingly small contribution to the mass transfer process, their presence in the column can lead to problems with the entrainment. The literature survey showed that such

droplets can be formed both during coalescence and breakup.

(1) Partial Coalescence

MacKay and Mason (1963), showed that the diameter ratio of coalescing droplets must exceed 3.5 for partial coalescence to occur. Hanson and Brown (1967), noted that the minimum drop size for mechanism II partial coalescence, (Jeffreys and Lawson, 1965), exceeded 6.5mm for medium range interfacial tension systems. Thus, any partial coalescence will occur by the simple drainage mechanism of Charles and Mason (1960). Hanson and Brown have further shown that the diameter ratio of the satellite drop to the parent drop was not dependent on the parent drop but remained at about 0.29. Thus, a 14mm drop would produce partial coalescence with a drop of diameter:

$$d < \frac{14}{3.5} \text{ mm}$$

$$< 4.0 \text{ mm}$$

The satellite produced would be of diameter:

$$d_{sat} < 4.0 * 0.29 \text{ mm}$$

$$< 1.16 \text{ mm}$$

It would be expected then that the majority of droplets formed in this manner would lie in the diameter range 0 - 1.0mm. However, figure 8 - 9 shows that significant numbers of drops in the 1.0 - 2.0mm range are formed. An even stronger argument against this mechanism is the number of satellite droplets which are formed. The number of satellite droplets formed at the nozzle is small (figure 8 - 9(b)). However, after 2.5cm of packing a significant number have been formed in spite of the lack of small drops to coalesce. Furthermore, the proportion stays roughly constant although the number of larger drops decreases with packing height.

(2) Formation at Restrictions

Hauser et al, (1936), showed the origin of satellite drops produced during drop formation at wetted tips, to be a stem formed between the detaching drop and the liquid remaining on the nozzle. The stem length was longest when drop formation was most rapid and also increased with decreases in interfacial tension. Edgerton et al, (1937), showed that this satellite formation resulted in the maximum in the Harkins-Brown, (1919) correction factor curve. The curve is however unlikely to apply to the breakup of an already dispersed phase, as it is based on a constant wetted area of formation. The perimeter of a non-wetting drop is free to change during the breakup process. This could result in the easier formation of a stem and more satellite formation than would be expected from the curves of Harkins and Brown, (1919).

(3) Formation during Instability Breakup

The analysis of Goren, (1964), has shown that non-linearity of instability breakup can lead to the formation of satellite droplets. For a cylinder to form a satellite droplet, instability theory implies:

$$d = 1.92\, d_{jet}$$

Thus

$$d_{jet} = 0.52\text{mm} \quad \text{for} \quad d = 1\text{mm}$$

$$d_{jet} = 1.04\text{mm} \quad \text{for} \quad d = 2\text{mm}$$

This means that droplets of the right size would be formed from cylindrical linkages of 25 - 33% the diameter of the original thread.

Satellite droplets are known to be produced during droplet formation at nozzles, (Meister and Scheele, 1968, Hauser et al, 1936, Edgerton, Hauser and Tucker, 1937), and during instability breakup (Goren, 1964, Bondarenko, 1961). Ramshaw and Thornton, (1967) make no mention of satellite production in their study of the impaction

mechanism, although the baffles used were no greater than 1mm in thickness. Similarly, no evidence was found in this study for satellite production by this mechanism. Thus, on the evidence considered so far satellite formation would seem to be a breakup phenomena rather than a coalescence phenomena. Furthermore, force balance and wave instability mechanisms would seem to be the most likely sources.

VI INFLUENCE OF FLOWRATES

Detailed data on the variation in size distribution with phase flowrates is available only for the surfactant systems. However, the similarities of the surfactant and pure phase distributions at low flowrates suggest that reasonable inferences can be made about the other systems from the behaviour of the surfactant system.

(1) Dispersed Phase Flowrate

Increasing the dispersed phase flowrate was found to increase the number of satellite drops and to shift the main peak towards smaller diameters (figure 8 - 7). In chapter six a model of droplet motion was proposed whereby regions of free rise are separated by restrictions. The flowrate through the restrictions increased with superficial velocity of the dispersed phase. So too did the buoyancy head beneath the restriction. This model provides as explanation for the changes in droplet size distribution which occur with changes in the dispersed phase flowrate. As the net head beneath the restriction increases there will be a gradual transition from breakup by a force balance mechanism to breakup from a jet, as shown by Ooi, (1977). Thus, droplets with a diameter less then the Ramshaw-Thornton equilibrium diameter can be produced. Since jet breakup has also been suggested as a source of satellite droplets this would serve also to explain the increases in the satellite peak.

The flow model proposed envisages the loading zone of holdup

occuring when saturation of the central channels forces flow into the secondary regions. The size distributions for flowrates above the loading zone do indeed show a higher proportion of larger drops. The various mean diameters which have been suggested are sensitive to the proportion of these larger drops. Thus, as the dispersed phase flowrate increases, jetting tends to reduce the main peak and hence the mean diameter. However, as the flowrate increases the proportion of flow through the secondary channels increases and the large diameter tail increases. The net effect is that the mean diameter goes through a minimum with dispersed phase flowrate.

(2) Continuous Phase Flowrate

The effect of increasing the continuous phase flowrate is to reduce the flow area available to the dispersed phase. Thus, as the dispersed phase flowrate increases the flow through the secondary areas increases. However, the reduced area means higher velocities and more breakup. The merging of medium sized droplets produced in this way with the preferential channel droplets means that there is a net broadening of the main peak (figure 8 - 8).

VII INFLUENCE OF A THIRD COMPONENT

The presence of a third component distributed between the phases can effect the droplet size distribution in three ways. Firstly, the input distribution may change due to the effect of the mass transfer processes on droplet formation. Secondly, the physical properties are altered, and thus the equilibrium droplet size. Thirdly, a transferring solute will, by virtue of the Marangoni effect, enhance or suppress coalescence.

(1) Effect of Physical Properties

The change in physical properties occuring were analysed in

chapter five. Reductions in interfacial tension of 18.9%, 15.3% and 14.6% were found for the saturated phases, transfer out of the dispersed phase and transfer into the dispersed phase respectively. Equation (8-3) gives the equilibrium droplet diameter as

$$d^{o} = 0.92\left[\frac{\sigma}{\Delta\rho g}\right]^{0.5} \qquad (8\text{-}14)$$

The value density difference varies from a 2% increase for the saturated system to a 0.3% decrease for transfer into the dispersed phase. Thus decreases of 10.5%, 9%, and 7.2% in the equilibrium diameter are predicted for the saturated, transfer out and transfer in systems respectively. Comparison of these predictions with figure 8 - 10 show reasonable agreement for the saturated phases and transfer into the dispersed phase cases. If the position of the main peak is taken as indicative of the stable drop size, then for the pure phases this occurs in the range 4.5 - 5.5mm. Thus, a 10% reduction would be 4 - 5mm. The main peak for the saturated phases is slightly broader than the pure phase peak extending from 3.5 - 5.5mm. The main peak for the transfer into the dispersed phase occurs in the region 4 - 5mm. Transfer out of the dispersed phase, however,completely changes the behaviour found. Since increasing the solute concentration results in a lowering of the interfacial tension, enhancement of coalescence occurs when transfer is out of the dispersed phase. Thus, the single dominant peak is replaced with a broad distribution containing two or more apparent peaks.

(2) Satellite Droplets

The other dominant feature of the distributions is the change which occurs in the satellite peak. Thus the pure and saturated phases have comparable numbers of 0 - 2mm droplets, while the transfer into the dispersed phase case has a reduced number and the transfer out case has a very much enhanced satellite peak. This would seem to favour the argument that the satellite droplets are a result of partial coalescence,

although earlier evidence suggested that this was unlikely. This is not necessarily the case, however. The larger the droplet, the easier it is to distort it (Wilkinson, Mumford and Jeffreys, 1975). Thus it will be much easier to form jets or long stems from larger drops than it will from smaller drops. Coalescence would therefore act indirectly to increase the satellite population by maintaining the number of large drops. The behaviour of the distribution with height (figure 8 - 9) lend some support to this idea. Not only is the formation of satellite droplets enhanced by coalescence but, the enhancement of coalescence caused by the Marangoni effect is much reduced for these small droplets. Small droplets with diameters less than 2mm act essentially as rigid spheres and mass transfer is by the slow process of diffusion. Above 2mm in diameter circulation occurs within the droplet and the mass transfer is greatly enhanced (Heertjes, de Nie and de Vrie, 1971). Thus, the rate of coalescence of satellite droplets does not increase to the same extent as for larger droplets. The small increase in the number of satellite drops when transfer is into the dispersed phase argues that some coalescence is occuring in the pure phase case but at a slow enough rate for breakup criteria to dominate and determine the shape of the distribution.

(3) Effect of Mass Transfer on Breakup

One effect not yet considered is the influence of mass transfer on the actual breakup process. Bayens and Lawrence (1968), report that mass transfer from a jet caused the formation of abnormally large drops directly, and not as a result of coalescence. Similarly Meister and Scheele (1969), reported increases in jet length for mass transfer in either direction. The linear stability analysis of Berkholder and Berg (1974), produces a very complex characteristic equation relating the growth rate of a disturbance to a number of dimensionless groups. The most important of these appear to be the

Marangoni number Ma, the Suratman number Su, and the surface elasticity number E_1.

To evaluate the Marangoni number the interfacial concentration is required, as well as the concentration gradient:

$$(C_o)_a = C_{id} / (1 + m (D_c/D_d)^{\frac{1}{2}}) \qquad (8\text{-}15)$$

for transfer out of the jet, and:

$$(C_o)_a = C_{ic} / (m + (D_d/D_c)^{\frac{1}{2}}) \qquad (8\text{-}16)$$

for transfer into the jet.

The maximum concentration gradient, as calculated from penetration theory (Higbie, 1935), is given by:

$$\left(\frac{dC}{dr}\right)_a = - \frac{C_{id}}{\sqrt{\pi D_d t}} \frac{m (D_c/D_d)^{\frac{1}{2}}}{1 + m (D_d/D_c)^{\frac{1}{2}}} \qquad (8\text{-}17)$$

for transfer out of the jet, and

$$\left(\frac{dC}{dr}\right)_a = \frac{C_{ic}}{\sqrt{\pi D_c t}} \frac{(D_d/D_c)^{\frac{1}{2}}/m}{1 + (D_d/D_c)^{\frac{1}{2}}/m} \qquad (8\text{-}18)$$

for transfer into the jet. The minimum gradient will be given by:

$$\left(\frac{dC}{dr}\right)_a = \frac{(C_o)_a - C_i}{a} \qquad (8\text{-}19)$$

Values of diffusivities were calculated from the Wilke-Chang correlation in chapter five. A value of the distribution coefficient m can be obtained from Gayler and Pratt (1957a). The interfacial tension gradient is obtained as: (Appendix I)

$$\frac{d\sigma'}{dC} = - \frac{\sigma'^2}{1.5} \qquad (8\text{-}20)$$

$$= -434$$

Using $C_i = 3.95 * 10^{-4}$ moles/cm^3 for transfer out of the dispersed phase then gives:

$$\left(\frac{dC}{dr}\right)_{min} = \frac{C_i(.218 - 1)}{a}$$

$$= - 6.18 * 10^{-3}$$

$$\left(\frac{dC}{dr}\right)_{max} = \frac{- C_i}{\sqrt{\pi * 1.165*10^{-5} * .2}} * \frac{.7\left(\frac{1.134*10^{-5}}{2.65*10^{-5}}\right)^{\frac{1}{2}}}{1+0.7*\left(\frac{2.65*10^{-5}}{1.134*10^{-5}}\right)^{\frac{1}{2}}}$$

$$= - 3.225*10^{-2}$$

Then

$$(Ma)_{min} = \frac{\left(\frac{d\sigma}{dC}\right)\left(\frac{dC}{dr}\right)_{min} a^2}{\mu_d D_d} \qquad (8\text{-}21)$$

$$= 4.09*10^6$$

$$(Ma)_{max} = \frac{\left(\frac{d\sigma}{dC}\right)\left(\frac{dC}{dr}\right)_{max} a^2}{\mu_d D_d} \qquad (8\text{-}22)$$

$$= 2.2*10^7$$

The Suratman number is given by:

$$Su = \frac{\sigma_o \rho a}{\mu_d^2} \qquad (8\text{-}23)$$

$$= 3.09*10^4$$

These results, when compared with the graphs of Berkholder and Berg, (1974), suggest that transfer out of the dispersed phase could have a weakly destabilising effect on droplet breakup, especially by instability processes.

For transfer into the jet:

$$(Ma)_{min} = 4.15 * 10^{6}$$

$$(Ma)'_{max} = 9.61 * 10^{7}$$

Transfer in this direction could thus be expected to have a slightly stronger stabilising effect.

VIII INFLUENCE OF WETTING BEHAVIOUR

Studies with single orifices, (Haynes, Himmelblau and Schechter, 1968), and perforated plate columns, (Garner, Ellis and Hill, 1956), have shown that the wetting characteristics of the nozzle and dispersed phase are most important in determining the drop size formed. Thomas and Mumford, (1971), have shown that when the packing material in a column is wet by the dispersed phase the input droplets coalesce into a film on the packing elements, film drainage through the column occurs, and droplets detach from the bed by a drip-point or jetting mechanism. Davies et al, (1972), have suggested that the droplet size distributions found by Lewis et al, (1951), and Gayler and Pratt, (1953a), were determined not by breakup criteria within the packing, but by hydrodynamic and wetting conditions at the outlet. No evidence was found to support this view in this study. Isolated regions where wetting of the column wall occured were found. These invariably occured when a droplet stream was passing through a narrow restriction between a packing element and the column wall. The droplets coalesced into a film, and then broke up from the edge of the film once past the restriction. The dispersed phase was not observed to form a surface film on the packing, but rather remained as discrete droplets. Furthermore no breakup or jetting was observed at the outlet surface. The fact that the packing elements were soaked in continuous phase before any dispersed phase touched them undoubtedly contributed to

this behaviour, (Thomas and Mumford, 1971).

IX OTHER FACTORS

(1) Circulation

Finally, the techniques for measuring the droplet size distribution should be considered. A T-section was used at the top of the packing as a photography chamber. A baffle plate at the top of this chamber deflected the continuous phase jet from the inlet. This however set up a circulation pattern within the photography chamber which tended to entrain some of the small droplets (< 1mm). Thus, the numbers of these droplets measured is probably an overestimate of the numbers within the packing. There will, however, be a similar tendency for some circulation of these fine droplets within the packing and this would reduce the error somewhat.

(2) Diffraction

Diffraction through a curved glass section was eliminated by use of the T-section. There was, however, a tendency for some small drops to adhere to the back of the section. These could be found by comparison of successive photographs, but it was found easier to alter the depth of field so that such drops appeared out of focus and could easily been seen.

(3) Coalescence Above the Packing

The measuring technique relies on the assumption that no significant coalescence occurs in the four inches of free rise before the drops are photographed. Observation of the pure phase system showed that although collisions between drops did occur, very few of these collisions resulted in coalescence. This might have been expected to be somewhat worse of an assumption when transfer of a solute out of the dispersed phase occured and coalescence was much enhanced. However, the

greater number of large diameter droplets under such conditions meant that the total number of droplets, and thus droplet collisions, was very much reduced. Thus, it seems reasonable to assume that the measured distributions are a realistic picture of what is happening in the packing.

(4) Influence of Distributor

Some trouble was taken to ensure that the droplet size distribution at the bottom of the column was as uniform as possible. It is worth considering the influence of the distributor, and thus the inlet size distribution on the final distribution. As noted by Lewis et al (1951), the breakdown of larger than equilibrium droplets occurs much more readily than the growth of smaller than equilibrium droplets. Thus, provided that the breakup processes are relatively complete within a given height of packing the tendency of a distributor to produce larger droplets should have little effect on the output distribution. The critical assumption, of course, is that the breakup processes are relatively complete, and the larger the input distribution, the longer this will take. The production of small diameter droplets at the distributor can be reflected in the output distribution, as such droplets have a relatively low coalescence rate within the column, even under conditions of mass transfer out of the dispersed phase. Thus figure 8 - 16 compares the output distributions for the Lewis et al distributor and the distributor appearing in figure 1 - 4(a). The main peak is hardly altered but the satellite peak has increased significantly.

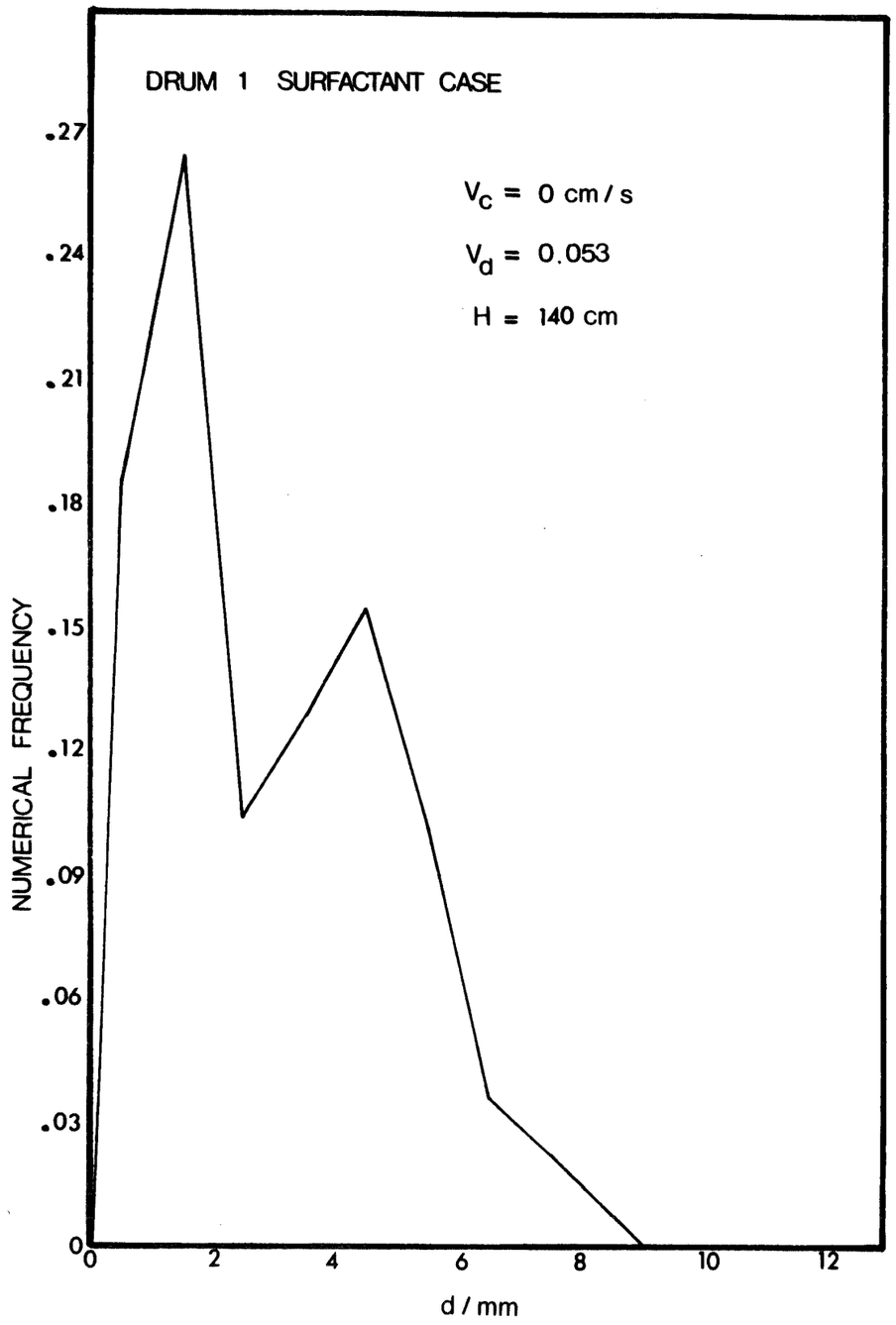

a Distributor 1 – A

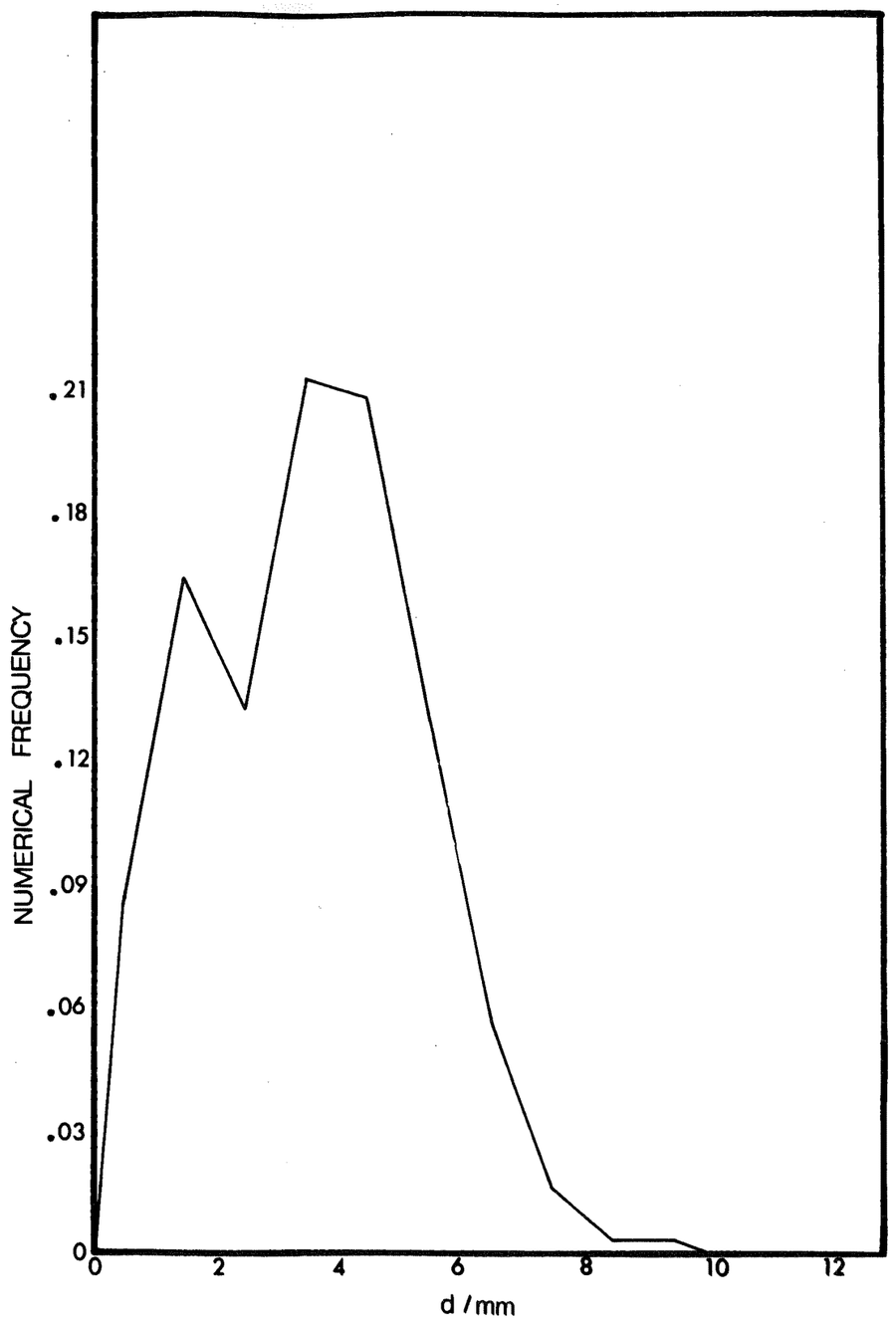

b Distributor 2

FIGURE 8 – 16 EFFECT OF DISTRIBUTOR ON THE DROPLET SIZE DISTRIBUTION

CONCLUSIONS

The technique of calculating the interfacial area in a liquid-liquid contactor based on the use of a mean diameter has been shown to be fraught with considerable dangers. Not only are standard methods (Lewis, Jones and Pratt, 1951, Gayler and Pratt, 1953a), for calculating a mean diameter inadequate, but the size distribution within the column varies considerably with position, as has been found before (Ramshaw and Thornton, 1967).

The droplet size distribution within the column is determined by the equilibrium which exists between coalescence and a number of competing breakup processes. The dependence on flowrates of the various breakup mechanisms differs. Thus, the mean diameters were found to go through a minimum as the dispersed phase flowrate was increased as first one mechanism was controlling, and then another. This behaviour is considerably more complex than the simple dependence on $\frac{x}{V_d}$ predicted by the Gayler - Pratt (1953a) model. The complexity of the behaviour also meant that none of the four empirical distribution functions tested were entirely satisfactory although some functions were successful over 90% or more of the range.

The impaction mechanism of Ramshaw and Thornton, (1967) although an approximation, provides a good description of the breakup of large droplets. It is thus important in determining changes in the relatively large input distribution as a function of packed height. A force balance mechanism of the Scheele - Meister, (1968) type was not found to be a significant factor in the breakup of large droplets. However, the multiple occupation of restrictions within the packing results in droplets being distorted into long jets with subsequent breakup by an instability mechanism. The formation of satellite droplets was also linked with this mode of breakup, with partial coalescence being considered an unlikely source. The large numbers of satellite droplets

formed when mass transfer out of the dispersed phase was occuring was associated with the greater number of large diameter droplets and the lesser enhancement of coalescence for rigid droplets. Dynamic pressure differences over the droplets as a result of turbulent eddying were discounted as a cause of droplet breakup.

The behaviour of the distributions with changes in flowrates further verifies the physical flow models proposed in chapters four and six. As the dispersed phase flowrate increases the restriction head increases and the amount of jet breakup with associated satellite formation increases. As the flowrate is increased still further the amount of dispersed phase forced into the secondary flow channels increases. The flow conditions in these secondary areas favour the passage of larger droplets and this results in the significant tailing seen in most distributions.

The changes in physical properties which occured when a third component was present were found to give a reasonable explanation of the relatively small changes in behaviour for the saturated phases and the case when transfer was into the dispersed phase. Transfer out of the dispersed phase however, resulted in enhancement of the droplet coalescence rate by virtue of the Marangoni effect. The droplet distribution was thus determined by the equilibrium between breakup and coalescence existing rather than by breakup criteria alone. The resulting distribution was significantly different from that in the other cases examined. The linear stability model of Berkholder and Berg, (1974) indicated that transfer out of the dispersed phase could have a slight enhancing effect upon the formation of satellite droplets.

NOMENCLATURE

a - jet radius (cm)

Bo - Bond number = $\frac{\Delta \rho_g d^2}{\sigma}$ (-)

C_i - initial solute concentration (mole cm^{-3})

C_o - undisturbed solute concentration (mole cm^{-3})

d - droplet diameter (cm)

d^o - equilibrium droplet diameter defined by equation (8-3) (cm)

d_{crit} - critical droplet diameter defined by equation (8-6) (cm)

d_{jet} - jet diameter (cm)

D - solute diffusivity ($cm^2\ s^{-1}$)

E_l - surface elasticity number = $\frac{\left(\frac{d\sigma}{dc}\right)^2 (C_o)_a}{R\ T\ \mu\ D}$ (-)

g - gravitational acceleration ($cm\ s^{-2}$)

k - disturbance wave number (cm^{-1})

m - distribution coefficient (-)

Ma - Marrangoni number = $\frac{\left(\frac{d\sigma}{dc}\right)\left(\frac{dc}{dr}\right) a^2}{\mu\ D}$ (-)

n_i - number of droplets of size d_i (-)

p, q - order of mean diameter (-)

r - radial coordinate (-)

R - gas constant ($J\ K^{-1} mole^{-1}$)

Su - Suratman number = $\frac{\sigma_o \rho a}{\mu^2}$ (-)

t - time (s)

T - absolute temperature (K)

V - bulk velocity ($cm\ s^{-1}$)

V_d - dispersed phase superficial velocity ($cm^3\ s^{-1}/cm^2$)

$\overline{V}_o$ - characteristic velocity ($cm\ s^{-1}$)

V_t - droplet terminal velocity ($cm\ s^{-1}$)

We - Weber number = $\frac{d\ V_t^2 \rho_d}{\sigma}$ (-)

x - dispersed phase holdup (-)

ϵ - packing voidage fraction (-)

λ_c - wave length of fastest growing disturbance (cm)

μ - dynamic viscosity ($g\ cm^{-1}\ s^{-1}$)

π - 3.14159 (-)

ρ - density ($g\ cm^{-3}$)

$\Delta\rho$ - phase density difference ($g\ cm^{-3}$)

σ - interfacial tension ($dyne\ cm^{-1}$)

Subscripts

32 - Sauter mean

a - at the surface

c - continuous phase

d - dispersed phase

o - undisturbed

CHAPTER NINE

COMPUTER SIMULATION

Chapter Contents.

INTRODUCTION

Consideration of the experimental droplet size distributions found in this study, together with data relating to droplet behaviour at orifices (Ooi, 1977), has lead to hypotheses about droplet behaviour in a packed column. In order to test these hypotheses more fully a simulation model has been developed.

Models simulating the behaviour of the dispersed phase for agitated vessels have been reported in the literature. Curl (1963), used a population balance approach to model the mixing in dispersed phase agitated tanks. A simple model which assumed uniform drop sizes and a uniform probabilty of coalescence, was used. Coalescence was followed immediately by breakup into two equal sized drops. Bayens and Lawrence (1969), extended this by using a trivariate distribution function. The application of population balance techniques to non - steady state populations led Valentas, Bilous and Amundson (1966), and Valentas and Amundson (1966, 1968), to an integro - differential equation capable of being applied to any dispersed phase system. The model takes no account of the hydrodynamics of the system and is limited in practical application by the complexity of the integral differential equations. To overcome the limitations of simple systems imposed by the use of such equations Spielman and Levenspiel (1965), turned to the use of Monte Carlo techniques. Kattan and Adler (1967) and Rao and Dunn (1970), have used Monte Carlo techniques in the simulation of droplet coalescence and breakup in dispersed phase tubular reactors.

More directly relevant is the work of Collins and Knudsen (1970), and Ward and Knudsen (1967), in modelling droplet size distributions in turbulent pipe flow. A stochastic model was developed based on the concept of a minimum stable drop size and a maximum drop size above which breakage occured. Zeitlin and Tavlarides (1972) have

used a stochastic model to simulate droplet size distributions in agitated vessels. The model assumes that two zones exist in the vessel - one where breakup predominates, and one where coalescence predominates. A recent series of papers by Ramkrishna et al (1973, 1974, 1976), have treated population balance as an integral function of time.

Thus, both analytic and stochastic representations of the system are possible. However, solutions to analytic models generally assume the simplest form of droplet breakup. The more realistic the models of droplet behaviour, the more complex becomes the analytic treatment. The simplicity of the Monte Carlo technique combined with its flexibility make it the obvious approach for simulating droplet distributions in packed columns.

It is necessary to combine the fundamental concepts of droplet breakup and coalescence with a description of the flow field within the contactor, and the droplet hydrodynamics, in order to obtain a general model of the system. This simulation seeks to establish the validity of proposed mechanisms which control the droplet size distribution, and as such does not consider the influence of flowrates. The factors considered, then, are the variation in size distribution with packing height, and the influence of a solute on the size distribution.

MODEL

Breakdown of a normal distribution of droplets has been shown to occur in three parts; the formation of a main peak, a secondary peak, and a satellite peak. The changes in the main peak have been attributed to Ramshaw and Thornton's impaction model (1967). The secondary peak has been attributed to the jet breakup of highly distorted droplets which result from multiple occupation of restrictions within the packing. Lastly, the satellite droplets have been regarded as a by-product both of jet breakup and force balance breakup.

The energy balance derived by Ramshaw and Thornton applies to the division of a parent droplet into two equal daughter droplets. This will occur only when the droplet impacts exactly symmetrically upon an obstacle. In other cases there will be a distribution of volume between the two daughter droplets which depends upon the displacement of the droplet centreline from the restriction. If this is considered random, then as a first approximation, the ratio of the daughter droplet volumes will be uniformly distributed. Thus:

$$V_1/V_2 = x \qquad (9\text{-}1)$$

where $0 \leqslant x \leqslant 1$.

Conservation of volume leads to

$$V_1 = \frac{x}{1+x} V \qquad (9\text{-}2)$$

$$V_2 = \frac{1}{1+x} V \qquad (9\text{-}3)$$

where V is the parent droplet volume. If a satellite droplet is formed it can be considered to reduce the volume of the two daughter droplets symmetrically. Thus V would be replaced by $V - V_{sat}$, where V_{sat} is the satellite volume.

The second possible mechanism considered as a cause of the changes in the main peak was breakup by a force balance mechanism at restrictions within the packing. The Scheele - Meister equation (1968) for force balance breakup at nozzles is:

$$V_1 = H\left[\frac{\pi\sigma D}{g\Delta\rho} + \frac{20\mu Q D}{d_1^2 g\Delta\rho} - \frac{4\rho_d Q U_N}{3 g\Delta\rho} + 4.5\left(\frac{Q^2 D \rho_d \sigma}{(g\Delta\rho)^2}\right)^{\frac{1}{3}}\right] \quad (9\text{-}4)$$

Neglecting the drag term, which is negligible for systems with a viscosity of less than 10 cp, and assuming the Harkins - Brown factor to be equal to 1.0 results in:

$$V_1 = A_{SM} D + D^2 (C_{SM} U^{\frac{2}{3}} - B_{SM} U^2) \quad (9\text{-}5)$$

The parameters A_{SM}, B_{SM}, C_{SM} are functions of the physical properties and are tabulated in Appendix I for the various systems. The nozzle diameter used is necessarily somewhat arbitary. Wilkinson et al (1975) have shown that the size of a droplet which is able to move through a restriction under the action of buoyancy forces must increase as the restriction diameter decreases. Below a restriction diameter of 0.3cm the volume required begins to increase sharply and at about 0.25cm a volume of about 2 cm^3 is required. This corresponds to a droplet diameter of approximately 1.3cm which is close to the largest droplet size found for all systems except the coalescence case. Thus, a restriction diameter of 0.25cm could be regarded as the minimum diameter through which the droplets were able to pass. The upper limit is obviously the internal diameter of a packing element. The distribution is unlikely to be uniform across that range and a maximum diameter can be defined below which there is a uniform distribution. Thus

$$D = 0.25 + x (D_{max} - 0.25) \quad (9\text{-}6)$$

The nozzle velocity can be obtained by the methods in chapter six.

Force balance breakup is however, not the only mode of breakup at restrictions. The distortion of droplets into long threads or jets results in secondary droplet formation by an instability mechanism. Instability theory for jet breakup leads to the expression (chapter eight):

$$d = 1.92 \; D_{jet} \tag{9-7}$$

Thus, if the jet diameter D_{jet}, could be related to the restriction diameter, the parent droplet volume, and the size of other droplets occupying the nozzle, it would be possible to predict the size of secondary droplets using equation (9-7). The dependence on parent drop volume results from the non-linear relationship of surface and buoyancy forces to droplet diameter. The former increases as the square of diameter, while the latter increases as the cube of diameter. Thus, large droplets are easier to deform than smaller ones. To relate the jet diameter explicitly to the restriction diameter the parent droplet volume, and the occupation of the restriction would require the use of three parameters. Furthermore the effects of restriction diameter and occupation are to some extent self-cancelling. The secondary droplet will thus be modelled as a function of the parent droplet only:

$$V_{sec} = A_{sec} \; V \; x \tag{9-8}$$

where A is an arbitary parameter obtained by best-fitting the experimental distributions.

The number of secondary droplets formed in this manner varies. Some drops form none, while others can form two or three. In this model the number of secondary droplets is fixed at one per parent droplet. The residual volume is then subject to a force balance process and may break into two or more daughter droplets. This can be modelled by the adaption of the Scheele - Meister process described earlier.

The volumetric fraction of the satellite droplets is small ($< .05\%$). Their formation thus does not effect the breakup mechanisms mentioned. They can be linked with either jet breakup or with force balance breakup, and the size predicted by:

$$V_{sat} = B_{sat} V x \qquad (9\text{-}9)$$

where B_{sat} is an arbitary parameter used to fit the experimental distributions. In chapter eight it was proposed that satellite formation was associated with large droplets. Thus it is necessary to define a minimum diameter d_{min} below which droplet breakup does not result in satellite formation.

Mechanisms for the various breakup processes have now been proposed. In order to simulate the column however, it is also necessary to predict the rate at which breakup occurs. Breakup by impaction is governed by the critical Weber number. If the actual droplet Weber number sufficiently exceeds the critical value then breakup occurs whether the impaction point is on the droplet centreline or not. As the critical Weber number is approached however, the degree of offset becomes important and not all collisions result in breakup. To account for this increasing instability with droplet size a quadratic breakup probability is proposed. Thus:

$$P = q (d - d_{crit})^2 \qquad (9\text{-}10)$$

where P is the probability of breakup, q is an arbitary parameter, and d_{crit} is the equilibrium droplet size.

A second variable which influences the rate of breakup is the distance between collisions or droplet path length. This is dependent on the droplet size, increasing as droplet size decreases. Thus, there is an increase in path length up the column. This is adjusted in discrete steps up the column rather than linking it explicitly to

droplet diameter.

Breakup at a restriction is dependent upon the restriction diameter and the velocity through the restriction. For a given flowrate the breakup rate will thus be dependent on the restriction diameter and the droplet path length. Thus, no additional assumptions are needed governing the rate of breakup at restrictions within the packing.

The droplet size distribution is not solely determined by breakup processes but rather by the equilibrium which exists between breakup and coalescence. Two modes of coalescence are possible. Firstly coalescence can occur between droplets during free rise. Secondly coalescence between droplets beneath a restriction can occur. The former is an inefficient process as there is frequently insufficient time for the intervening film of continuous phase to drain before the droplets bounce apart. The contact time between droplets beneath a restriction is, however, of the order of seconds and the coalescence rate will be correspondingly higher. Thus, free rise coalescence will be neglected in this model. A constant probability of coalescence is assumed for all droplet diameters except in the case of mass transfer out of the dispersed phase. The enhancement of coalescence which occurs in this case is a result of the Marangoni effect. However, droplets with a diameter less than 2mm tend to act as rigid spheres, rather than having the circulating interfaces of the larger droplets (Heertjes and de Nie, 1971). Mass transfer within these smaller droplets is thus by a diffusion mechanism which is very much slower than the circulation process. This means that the enhancement of coalescence resulting from mass transfer out of the dispersed phase could be considerably less for these small droplets.

The rate of change of the droplet size distribution being simulated is related to real time by superimposing a model of the droplet motion on the processes occuring. Two distinct types of flow exist. Firstly, the free rise of the droplets, and secondly, the

movement through restrictions, as dealt with in chapter six. The free rise velocity can be calculated using equation (4-12) and the integrated form of equation (4-11):

$$\bar{s} = V_t \bar{t} \left[1 - \frac{\varrho_d V_t}{\Delta \varrho_g \bar{t}} \left(1 - \exp\left[\frac{-\Delta \varrho_g \bar{t}}{\varrho_d V_t} \right] \right) \right] \qquad (9\text{-}11)$$

$$V_r = V_t \left(1 - \exp\left[\frac{-\Delta \varrho_g \bar{t}}{\varrho_d V_t} \right] \right) \qquad (9\text{-}12)$$

The model of restriction motion developed in chapter six envisages the same delay for all droplets at a restriction. Thus the simulation uses a constant distance of motion and delay time for all droplets and for all restrictions in the column. This is an approximation since the droplet distributions decrease in size up the column and as shown in chapter six the queue velocity is dependent upon the increase in droplet surface area and thus the droplet diameter. However, the simulation still provides the correct relationship for droplet movement relative to one another which is important in the evolution of the distributions.

It has been pointed out in earlier chapters that the packing structure has a distinct influence upon the rate of droplet breakdown. Thus, most breakdown occurs in the preferential channels where both free rise and restriction motion are important. In the secondary channels the amount of free rise is much reduced and there is a corresponding decrease in the breakup rate. The simulation attempts to model this effect by the creation of two zones of flow. In one the droplets are subject to the normal breakup and coalescence functions. In the other the droplets simply bypass these functions and rejoin the main distribution at the end of one cycle of free rise plus restriction motion. Switching between the normal and bypassing zones is done on the basis of a random selection comprising of a given fraction of the total distribution at the beginning of a cycle.

The model proposed has been assembled into a computer program. The flow chart for this program appears in figure 9 - 1.

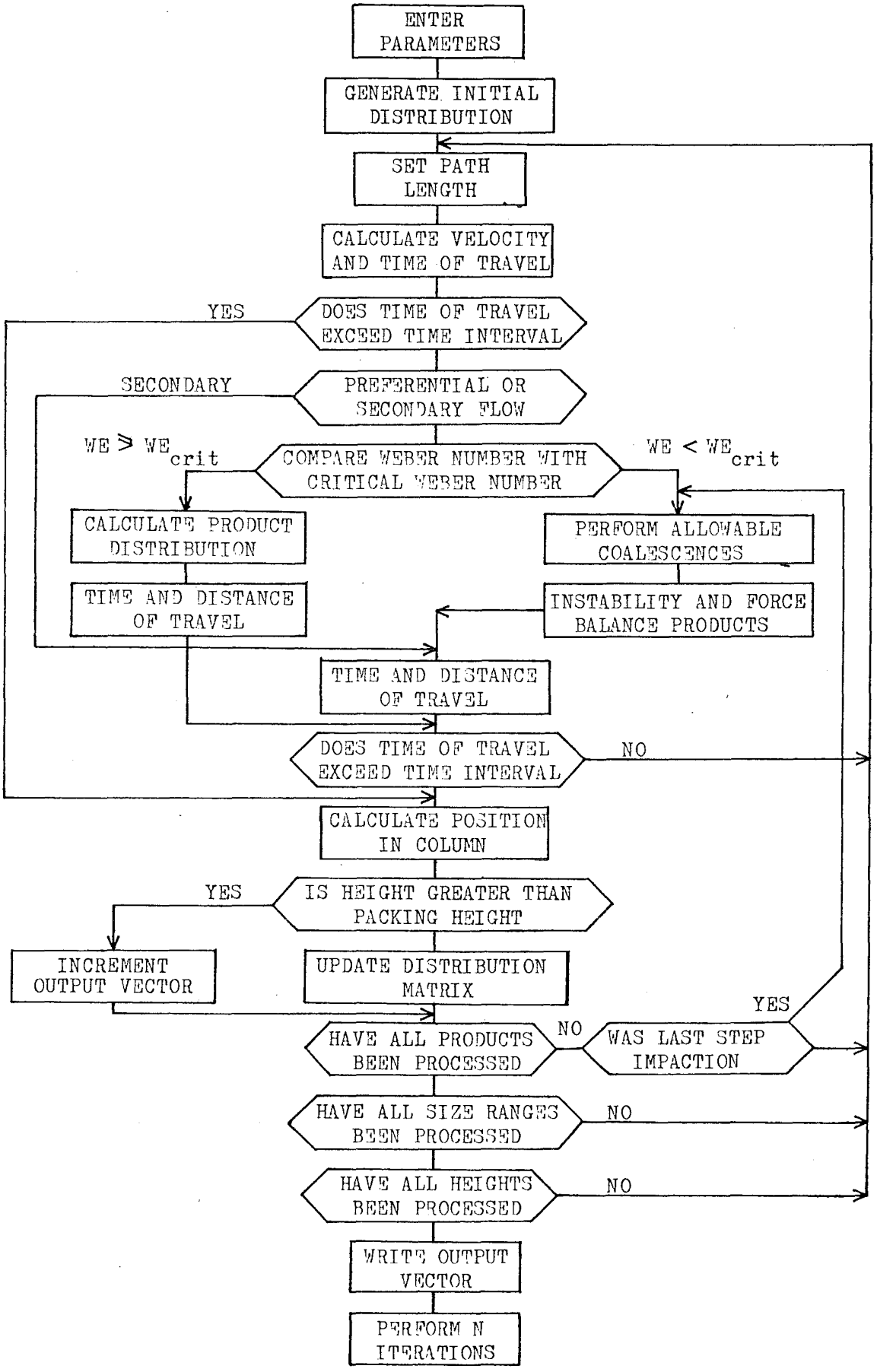

FIGURE 9 – 1 SIMULATION FLOWSHEET

SIMULATION RESULTS AND DISCUSSION

The major factors considered in the simulation were the relative importance of impaction and restriction breakup, and the influence of coalescence on the distributions. Lesser factors considered are the effects of bypassing and the effects of changes in the physical properties.

I IMPACTION

(1) General Features

(a) Main Peak. The initial droplet distribution for the simulation is taken as the distribution found after 2.5cm of packing - figure 8 - 9(b). This is approximated as a normal distribution with a mean of 10mm and a standard deviation of 1.3mm. The simulated breakdown of this distribution when impaction only was occuring is shown in figure 9 - 2. A distinct peak is retained as the droplets slowly breakdown by breaking approximately in two. The breakdown of droplets larger than 9mm occurs fairly rapidly with the main peak appearing in the range 7 - 9mm after 3 cm. After 28cm the main peak lies in the range 5 - 7mm and the droplets greater than 9mm have been reduced to a small tail. The experimental distributions which appeared in figure 8 - 9 are reproduced here as figure 9 - 3. It can be seen that the behaviour of the main peak is very similar to the simulated impaction breakdown.

(b) Uniform Product Distribution. One assumption made about impaction breakup was that the volumes of the pair of products formed were uniformly distributed. Comparison of figure 9 - 3 with the simulations shows that the assumption results in a slightly broader peak than is found experimentally. Thus it might be possible to represent the volume division slightly better by assuming some other distribution about a mean ratio of 1.0 - the normal distribution with a

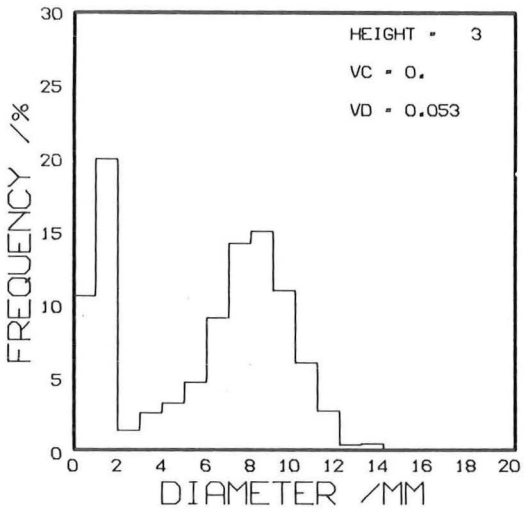

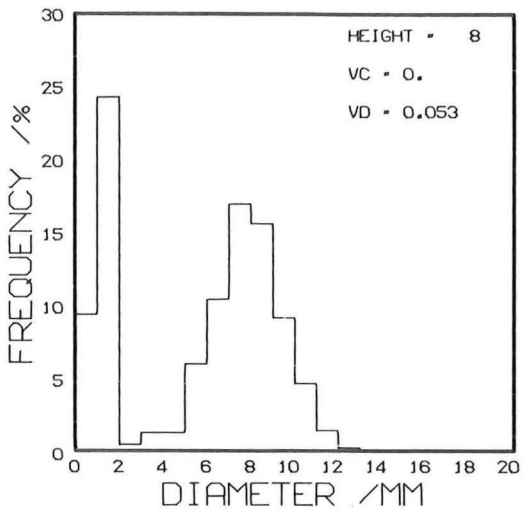

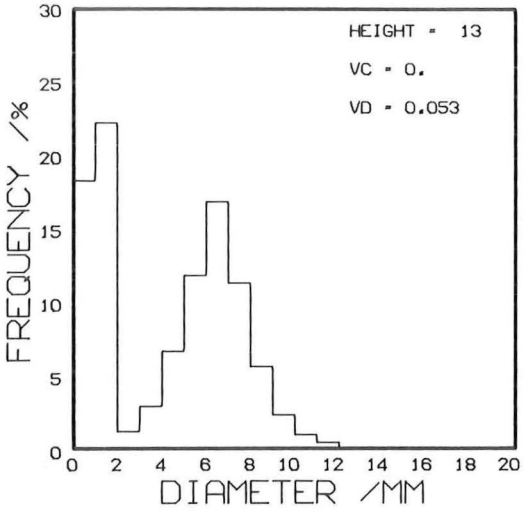

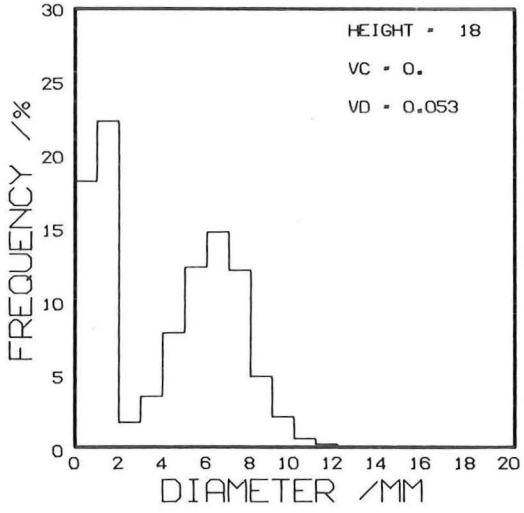

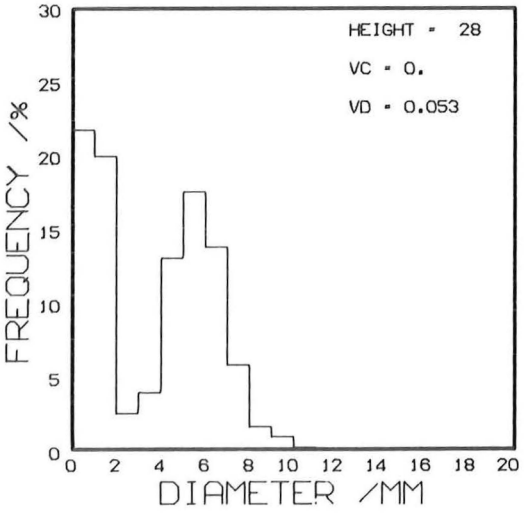

ASSUMPTIONS

Impaction Only

Quadratic Breakup

Probability

40% Bypass

FIGURE 9 – 2 SIMULATED SIZE DISTRIBUTION

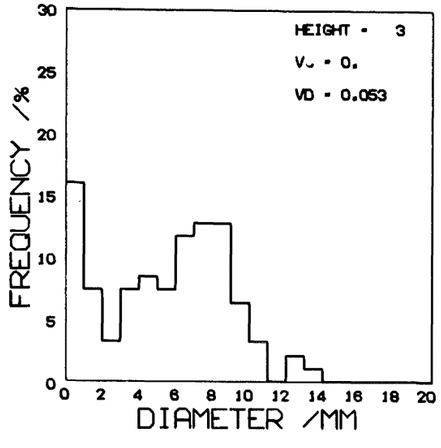

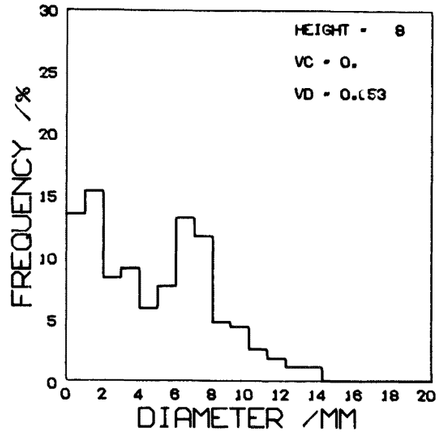

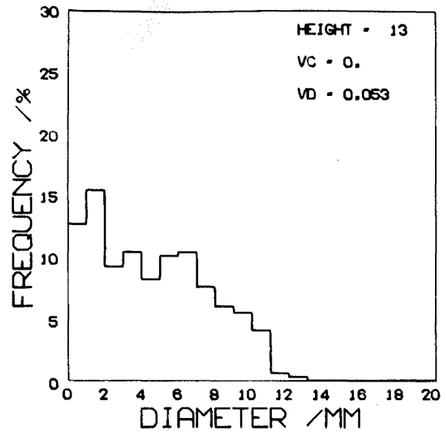

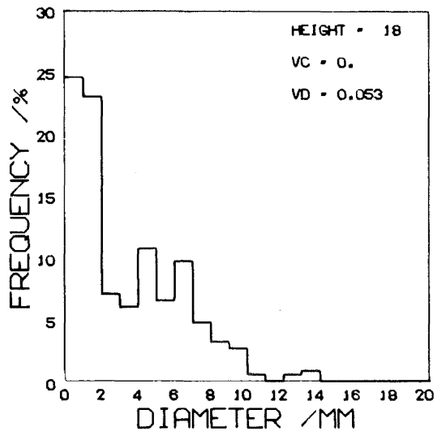

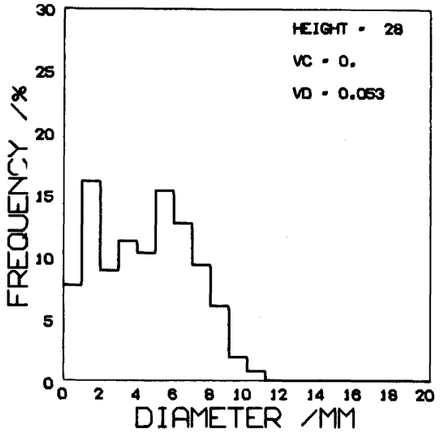

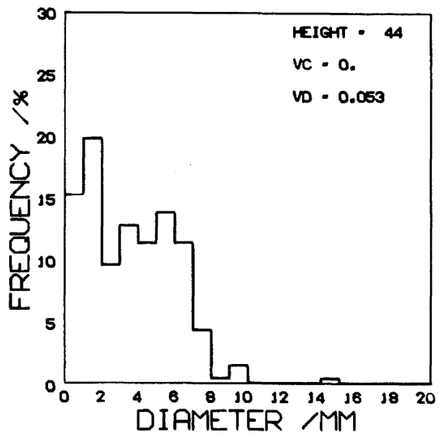

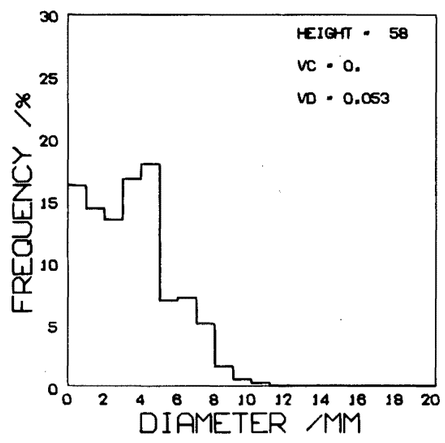

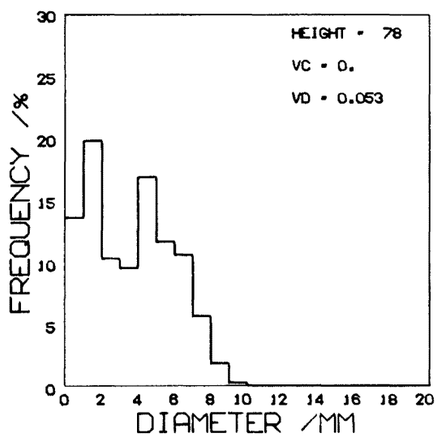

FIGURE 9 - 3 EXPERIMENTAL DROPLET SIZE DISTRIBUTION vs PACKING HEIGHT

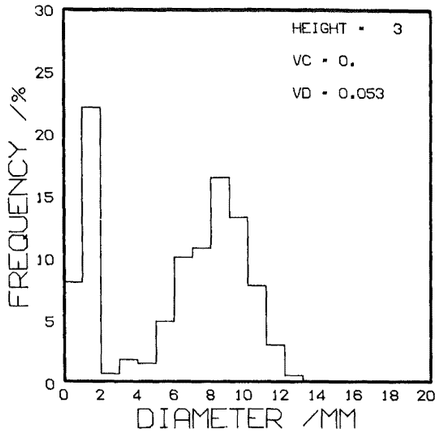

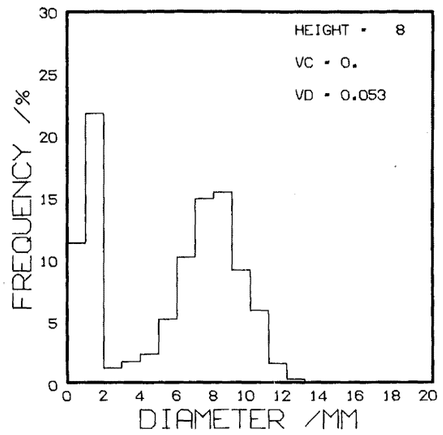

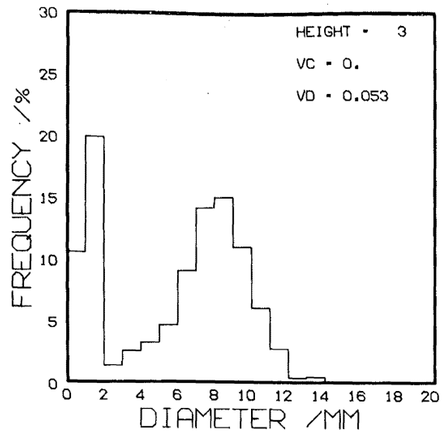

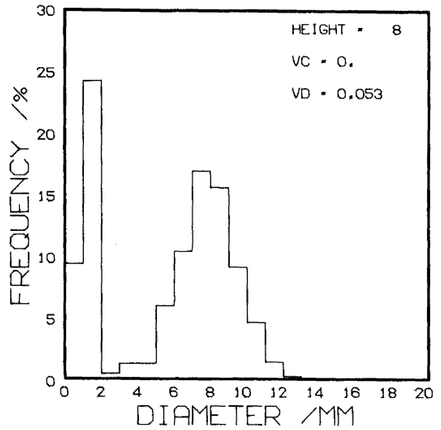

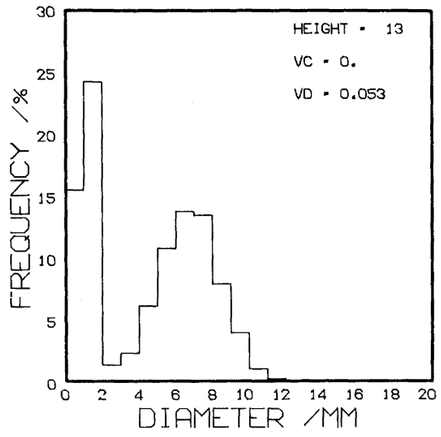

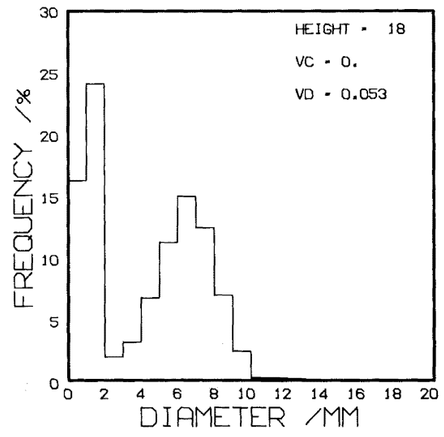

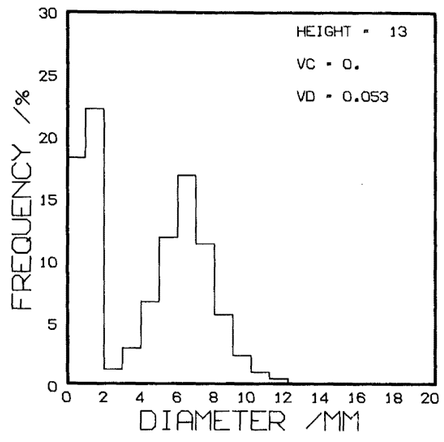

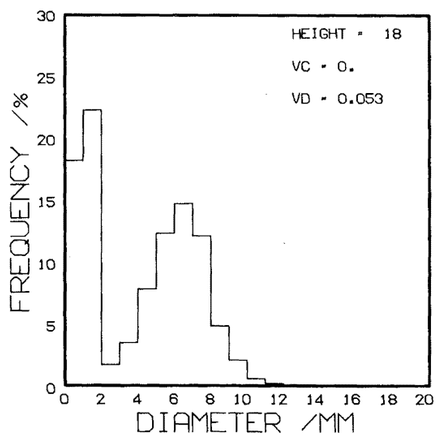

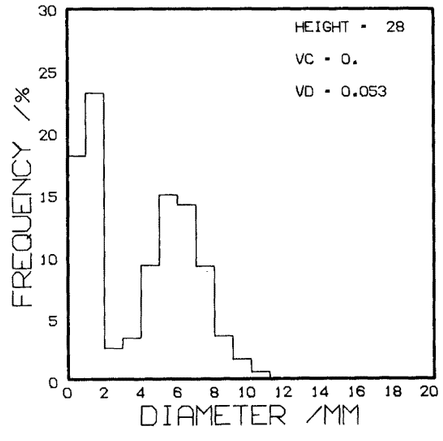

Impaction Only

Linear Breakup

Probability

40% Bypass

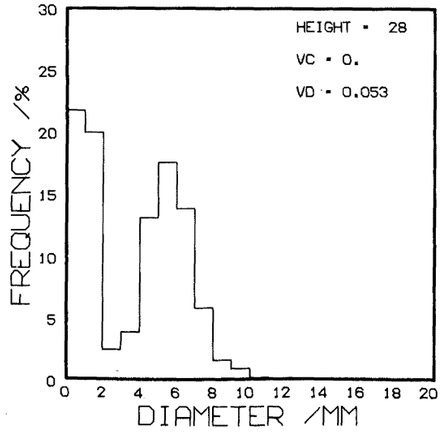

Impaction Only

Quadratic Breakup

Probability

40% Bypass

Droplet Pathlength

= 1.5 cm

FIGURE 9 - 4 INFLUENCE OF BREAKUP PROBABILITY AND DROPLET PATHLENGTH ON SIZE DISTRIBUTIONS

standard deviation of 0.33 for example. However, the differences are sufficiently small for the assumption of a uniform distribution to suffice.

(c) Secondary and Satellite Formation. The most obvious difference between the experimental distributions in figure 9 - 3 and most of the simulations shown is of course the absence of secondary droplets. Straight impaction produces just two daughter droplets with no secondary droplets or satellites. In the simulation however the formation of satellite droplets has been linked with impaction breakup. This has been done simply for computational convenience and to maximise efficiency in array handling. It is a relatively simple task to adjust the rate of formation of satellite droplets to correspond to secondary droplet formation rather than impaction breakup. Furthermore the volume of a satellite droplet is only about 0.1% of the volume of a droplet breaking up by impaction. Thus, associating satellite formation with impaction breakup is unlikely to influence the position of the main peak and need not imply that this mode of breakup is the actual source of the droplets.

(2) Breakup Rate

Slight differences can be seen in the rate of breakup - the experimental distribution changes more rapidly in the first few centimetres of packing than does the simulation and then somewhat more slowly than the simulation once the main peak reaches a size of about 6.5mm.

(a) Influence of Distributor. This could be a result of the influence of the distributor on the initial breakup. The distributor exit velocity for the distributions shown is 6.1cm s^{-1}, which is greater than the terminal velocity of droplets larger than 7.6mm in diameter. Continuity of flow means that this velocity will persist until the stream of droplets issuing from a nozzle has been dispersed.

Thus, there will be an enhanced tendency for larger droplets to breakup in the first few cent imetres of packing. The simulation tries to match the distributions by assuming an average rate of breakdown over the packed height.

(b) Approximations in the Impaction Model. Another possible reason for the slowdown in rate as the droplet size decreases is the increasing importance of the assumption that the droplet impacts upon a thin baffle. Ramshaw and Thornton (1967), found that the critical droplet diameter increased by 5% upon changing from 0.1mm thick to a 1.1mm thick baffle. The minimum baffle size in the column will be the wall thickness of a packing element which is approximately 2mm. Furthermore, many of the projections will have a greater effective width due to the orientation of the packing element. Thus, the critical droplet size may be 5 - 10% greater than that calculated using the equation of Ramshaw and Thornton (equation 7-34).

(c) Influence of Path Length and Probability Function. The influence of the path length and breakup probability function over the first 30cm of packing are shown in figure 9 - 4. The effect of changing to a linear probability function, i.e.

$$P = B\,(d - d_{crit})$$

appears to be slight - figure 9 - 4(a). The droplet path length used for figure 9 - 2 was 1.5cm for the first 10cm, 5cm for the next 10cm, and 10cm for packing heights greater than 20cm. Thus, only a slight enhancement of breakup can be detected when a uniform path length of $\bar{s}$ = 1.5cm is used instead of incrementing $\bar{s}$ to 5cm at a packing height of 10cm - figure 9 - 4(b). Two factors contribute to the apparent independence of the distributions of these parameters. Firstly, most of the droplet breakup appearing in the distributions shown is of relatively large droplets for which there is little difference between the linear and quadratic probability functions. The differences become more apparent

as the packing height, and thus the number of potential breakup sites increases. Decreasing the path length would thus be expected to have some influence by increasing the number of potential breakup sites. Thus, there is no change in the distributions below 10cm where the path length is the same. Between 10 and 20cm the smaller path length results in approximately three times the number of potential breakups. This results in a slight enhancement of the breakup rate. Above 20cm the increase in the number of breakup sites is approximately seven times and a more pronounced difference can be seen between the distributions at 18 and 28cm. Secondly, it could be noted that the responses shown are heavily damped by the amount of droplet bypassing occuring. The switching of droplets between the secondary and preferential channels means that the number of impactions in the preferential channels must be greater to achieve the same degree of breakup.

(3) Bypassing

The importance of bypassing is shown in figure 9 - 5. In figure 9 - 5(a) there is no bypassing and practically the entire inlet distribution has been reduced to the impaction equilibrium droplet diameter. In figure 9 - 5(b) however, 40% of all droplets greater than the impaction equilibrium size are allowed to bypass the main channels on any one cycle of free rise. This results in a considerable increase in the number of droplets in the 6 - 7mm range surviving after 140cm of packing and a small tail of larger diameter droplets extending from 7 - 10mm.

(a) Physical Model. The model used to simulate the interaction between the preferential and secondary channels is obviously a very simple one. For any cycle of free rise followed by movement through a restriction a random selection of droplets move into the secondary channels where no breakup occurs, and rejoin the main channel droplets at the end of the cycle. It seems unlikely however, that either the

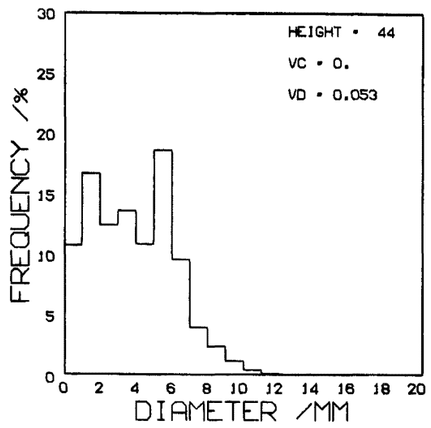

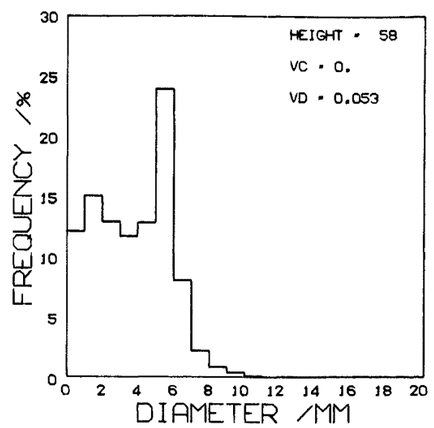

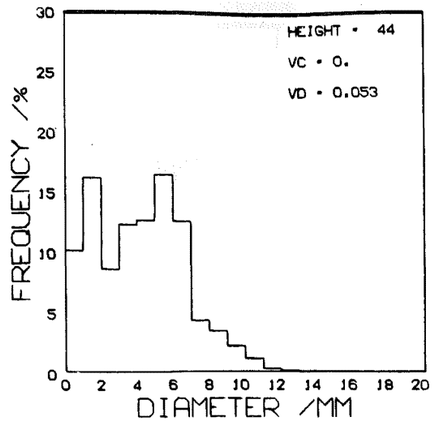

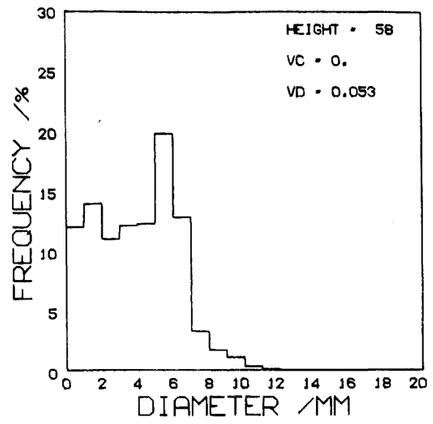

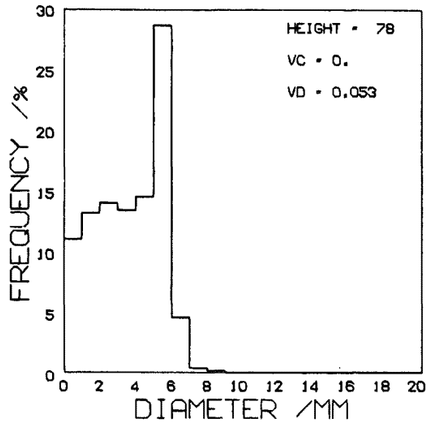

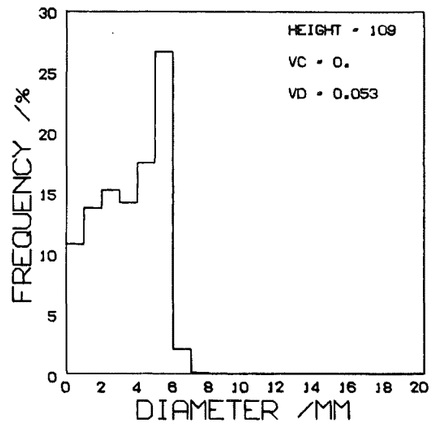

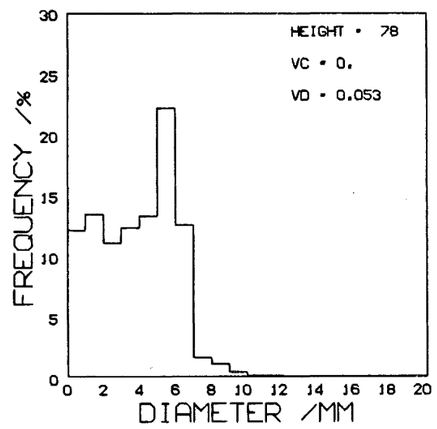

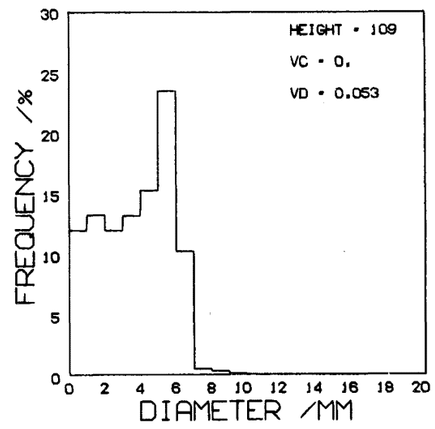

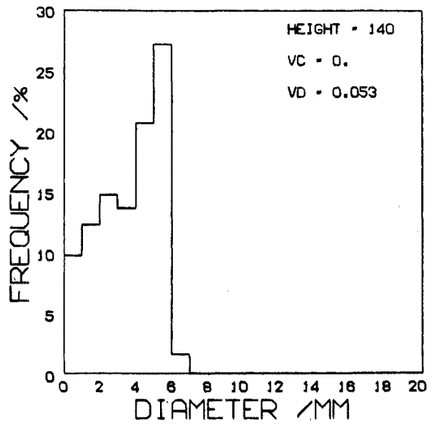

Impaction and Secondary Formation Quadratic Breakup Probability Zero Bypass

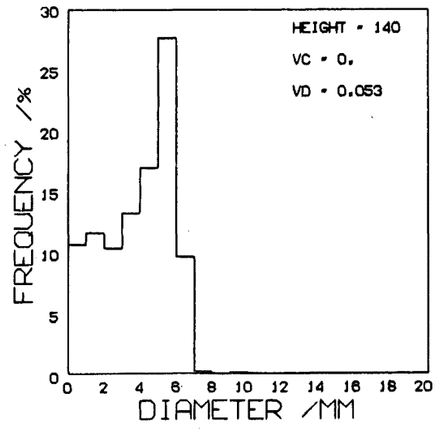

Impaction and Secondary Formation Quadratic Breakup 40% Bypass

FIGURE 9 - 5 INFLUENCE OF BYPASSING ON SIZE DISTRIBUTIONS

distance travelled or the droplet velocity within the secondary channels, will correspond to that within the preferential channels. Thus the droplet distribution within the secondary channels could persist for considerably longer than occurs with the bypassing of a different random selection of droplets over each cycle. Also ignored is the droplet behaviour within the secondary channel. By assuming that no change occurs in the distribution the finite rates of breakup and coalescence are neglected, since this assumption is not equivalent to equating the rates of the two processes.

(b) Influence of Packing Height. It seems physically unrealistic to expect any bypassing to occur in the first few centimetres of packing. In this region the droplets are moving under the influence of the distributor within well defined streams. It is not until these streams have been broken up and the droplets move independently of one another that bypassing can occur. Thus in figure 9 - 6 the effect of bypassing in the initial region is shown. A substantial number of droplets remain unchanged in the 9 - 11mm range while the droplets breaking up by impaction form a separate peak in the 7 - 9mm range. The model of bypassing assumed means that the two peaks get rejoined in a relatively short time. Thus, after 8cm there is a single peak again. Figure 9 - 3 shows that the experimental distributions dont support such behaviour however.

II RESTRICTION BREAKUP

(1) General Features

As a first step towards modelling the droplet behaviour at restrictions figure 9 - 7 shows the effects of assuming that a droplet at a restriction breaks into a droplet of secondary size and the residual remains unchanged. This results in the appearance of a secondary peak in the 3 - 5mm range. The secondary droplet has been

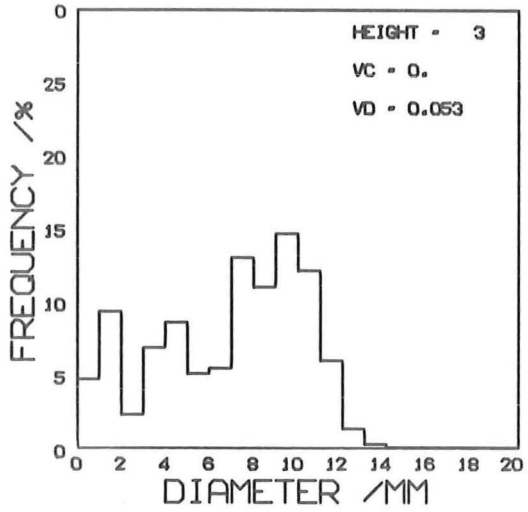

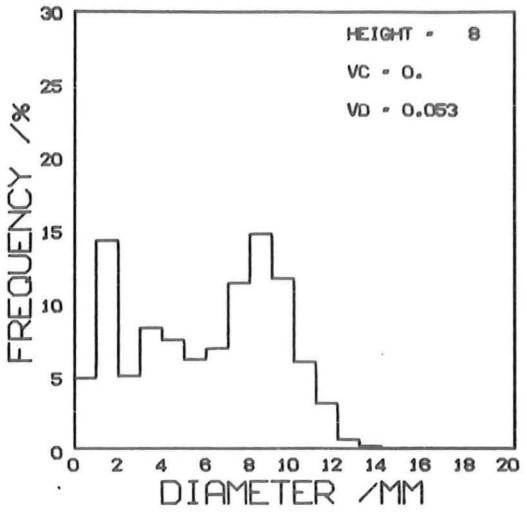

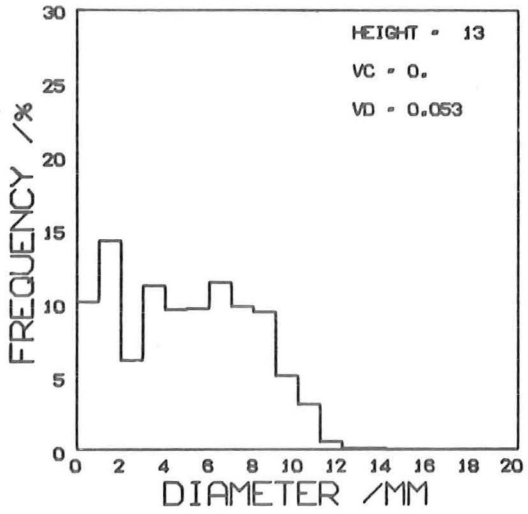

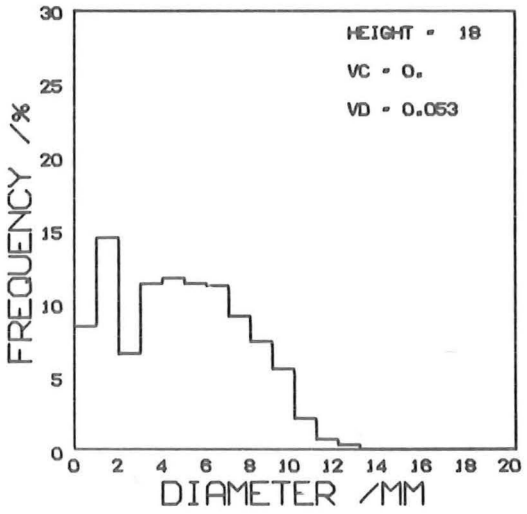

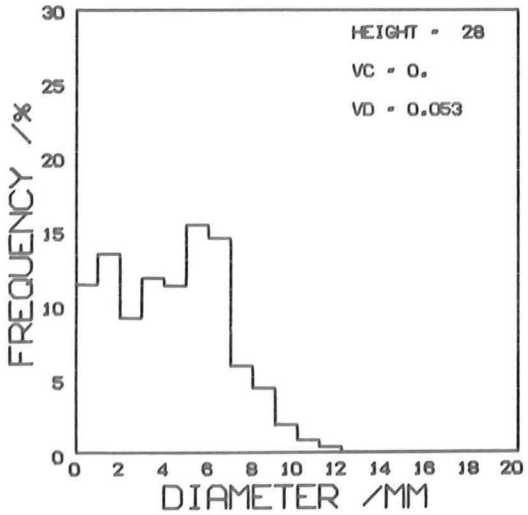

Impaction and Secondary Formation

Quadratic Breakup Probability

40% Bypass

FIGURE 9 – 6 INFLUENCE OF BYPASSING ON THE INITIAL BREAKUP RATE

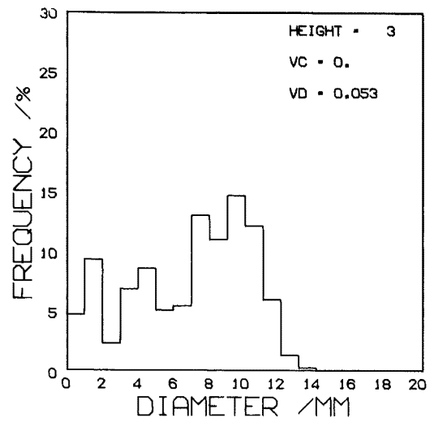

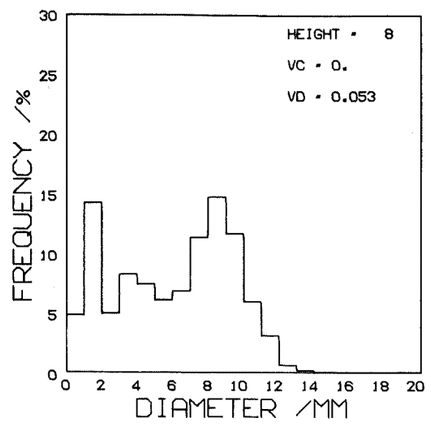

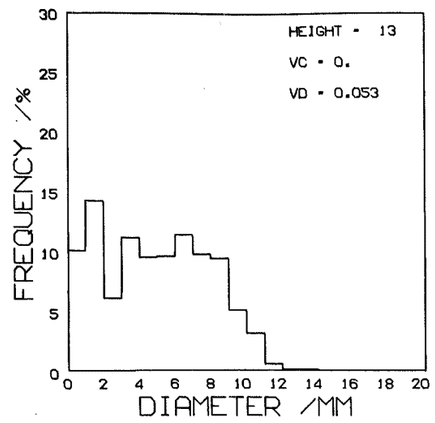

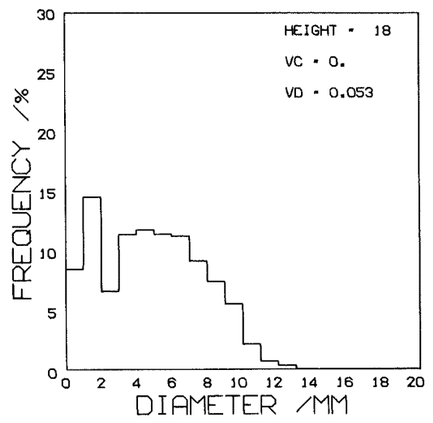

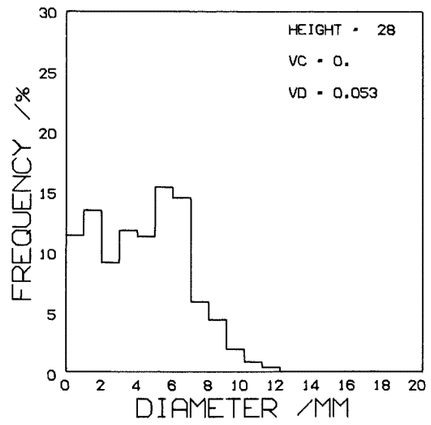

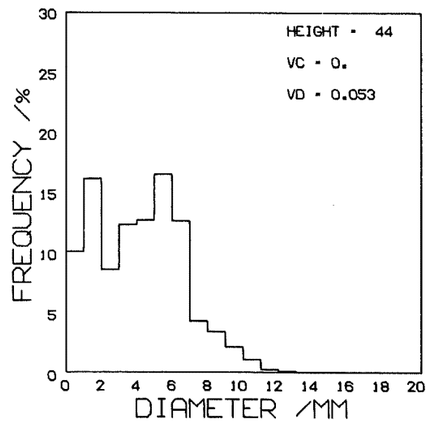

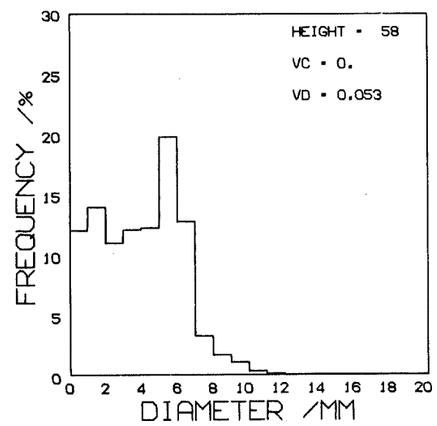

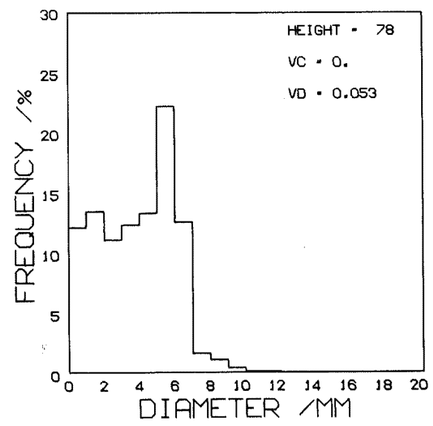

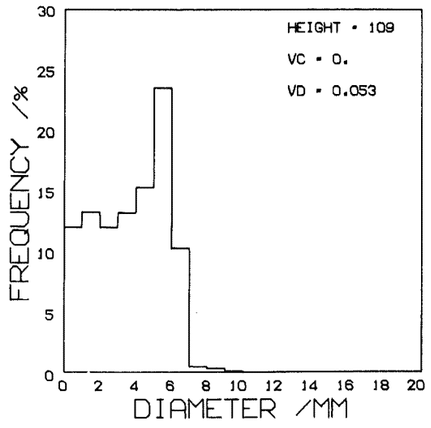

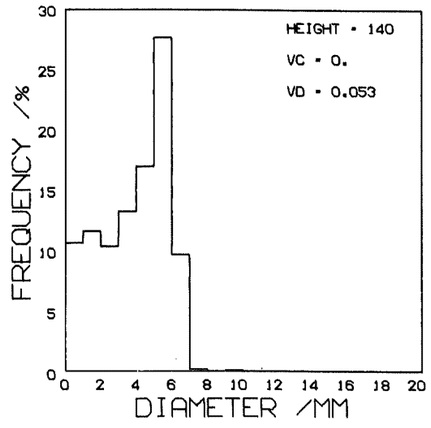

Impaction

Secondary Formation by

Instability Breakup

No Force Balance Breakup

No Residual Volume

Breakup

FIGURE 9 – 7 INFLUENCE OF RESTRICTION BREAKUP ON SIZE DISTRIBUTION

modelled as being proportional in volume to the parent droplet. The broadness of the main peak in the 10 - 20cm packed height range means that a wide spectrum of droplet sizes are formed. This causes some blurring of the distinctions between the individual peaks and finds a parallel in the behaviour of the experimental distributions at the same heights. The rate of secondary droplet formation is somewhat less than the experimental rate as shown by the distributions from 28cm packed height upwards. Two factors contribute to this lower rate of formation. Firstly, the number of droplets formed has been set at one per parent droplet. If the droplets are being distorted into long threads which break up by an instability mechanism, as in figures 7 - 2 to 7 - 5, then it is likely that two, three, or more droplets form from the unstable thread. Secondly, the assumed proportionality between secondary and parent volumes causes the position of the secondary peak to move towards lower diameters as the main peak decreases in diameter, and eventually merges with the satellite peak.

(2) Physical Model

The experimental distributions show that the behaviour is a great deal more complex than is indicated by the simple model used in figure 9 - 7. The volume dependence used produces a peak in the right range for the first few centimetres. There is also an initial movement of the experimental secondary peak as the main peak decreases in size. The number of droplets in the 2 - 3mm range continues to increase as the packed height increases. However, the number of droplets in the 3.5 - 5mm range also increases and goes through a maximum at a height of 30cm. This suggests that more than one breakup mechanism is operative at restrictions. With the large droplets present initially only a limited number (say two) can occupy the restriction at one time. The lower ratio of surface forces to buoyancy forces means that these large droplets can be relatively easily distorted into long jets or

threads. As the droplet size decreases however two things occur. Firstly, the ratio of surface forces to buoyancy forces increases reducing the tendency of the droplets to form long threads. Secondly, the number of droplets occupying the restriction increases. Thus, instead of forming a long thread which will tend to break up into a number of daughter droplets, the parent droplet will tend to break into just two daughter droplets by a force balance mechanism. The stable drop size for this form of breakup will be strongly dependent upon the number of droplets occupying the nozzle and the buoyancy head beneath the restriction. Thus, the position of the main peak will be dependent upon the dispersed phase flowrate as indicated in figure 8 - 7. Figure 9 - 8 shows the effects of including this form of breakup by assuming that 10% of all droplets in the range d_{crit} - 0.65mm break into two daughter droplets with a uniformly distributed volume ratio. It can be seen that this results in a slightly better agreement with the experimental results but the rate of formation is still somewhat low. The final distribution agrees well with the experimental distribution on the satellite peak and the position of the main peak but has a slightly smaller large diameter tail. This probably results from the simple model used to represent bypassing.

(3) Simultaneous Force Balance and Instability Breakup

The simulated distributions shown in figures 9 - 7 and 9 - 8 assume that when distortion of a droplet at a restriction occurs a droplet is formed from the thread but the remainder of the volume remains unchanged. For a large droplet (say 10mm) the volume of the undistorted remainder is up to four times greater than that of the thread. If the droplet is passing through a small restriction, or is occupying a larger restriction simultaneously with a similar sized droplet, then a force balance breakup of the remaining volume may occur. The breakup process is sensitive to the distribution of restriction diameters used. This is neccessarily rather arbitary and is

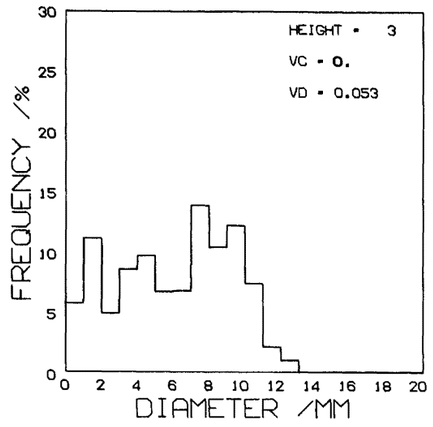

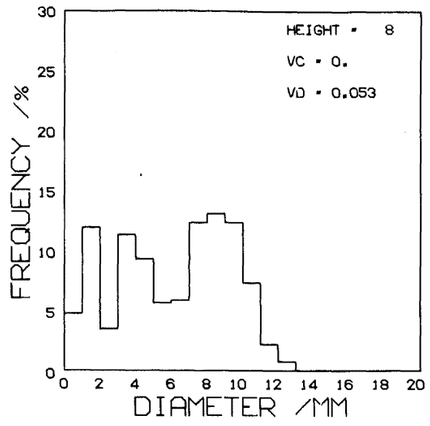

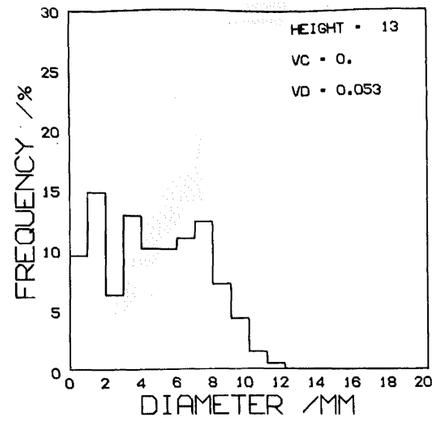

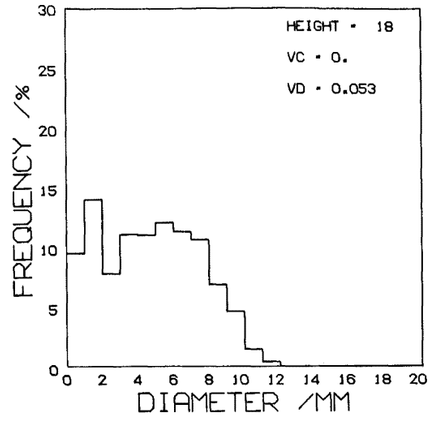

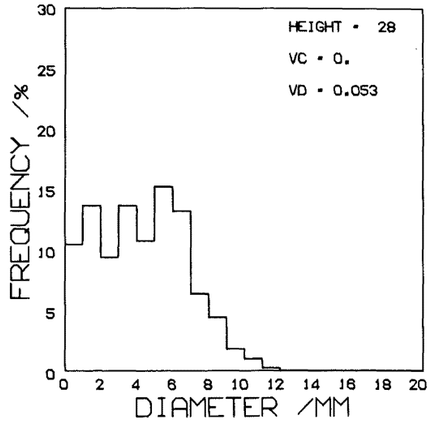

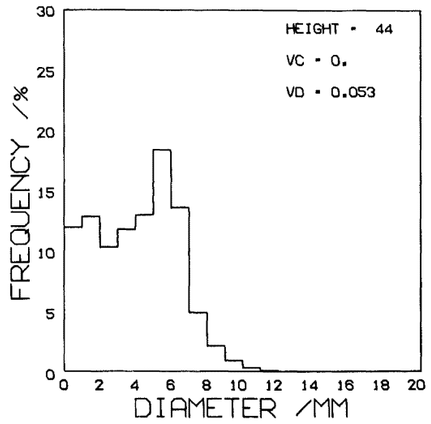

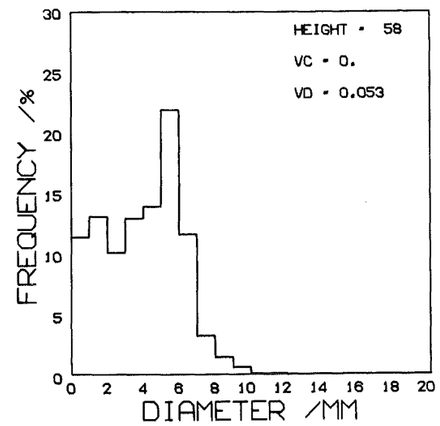

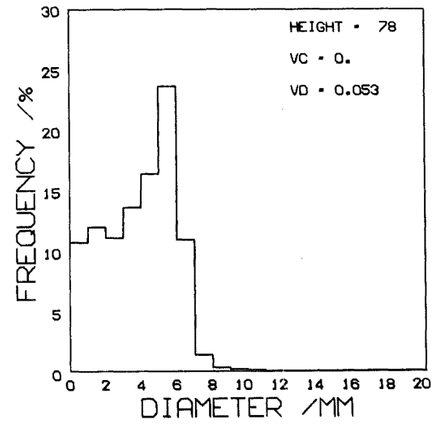

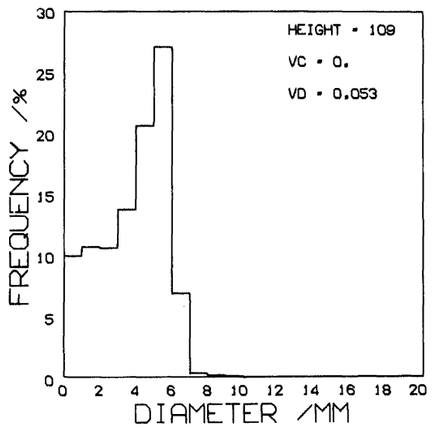

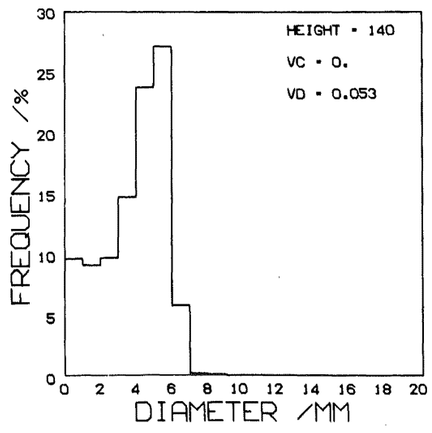

Impaction

Secondary Formation by

Instability Breakup

10%Force Balance Breakup

for $d_{crit} < d < 0.65$

No Residual Volume

Breakup

FIGURE 9 – 8 MODIFIED RESTRICTION BREAKUP

complicated by the effects of multiple occupation of the restriction. The effects of two distributions are compared in figure 9 - 9. The first assumes a normal distribution of restriction diameters with a mean of 5mm. The result is an enhanced rate of breakup for the larger droplets and a persistant peak in the vicinity of 8 - 9mm which is the approximate Scheele - Meister diameter for a 5mm restriction. Similar behaviour can be found in the experimental distribution for some corresponding packed heights. The second distribution shown assumes a uniform distribution of restriction diameters between the minimum value of 2.5mm (Wilkinson et al, 1975) and the internal diameter of a packing element, 12mm. This distribution results in only a slight enhancement of the breakup rate of the larger droplets. This is due to the fact that much of the range of restriction diameters would results in Scheele - Meister diameters which are larger than most of the parent droplets present.

This discussion of the influence of the restriction diameter is made much more doubtful by the influence of multiple occupation. The program assumes the droplet is occupying an equivalent diameter nozzle. Thus an apparently reasonable assumption about the restriction diameter distribution based on the packing dimensions may differ greatly from the actual behaviour. The degree of multiple occupation of the restriction is dependent upon the droplet size. Thus, as pointed out earlier, a maximum could exist in the rate of droplet breakup by a force balance mechanism.

III INFLUENCE OF A THIRD COMPONENT

(1) Physical Properties

The changes in physical properties resulting from the addition of a third component to the phase results in some changes in the simulations. The direct changes, and the indirect ones through the

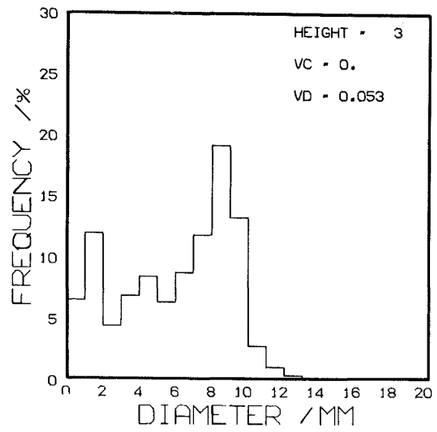

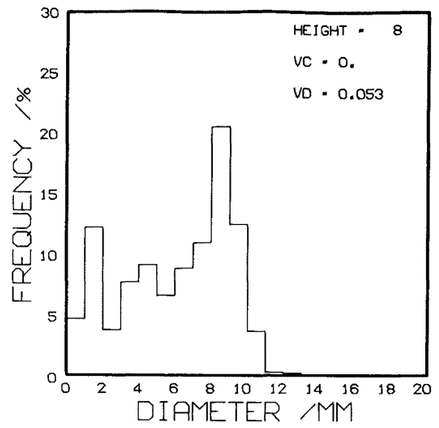

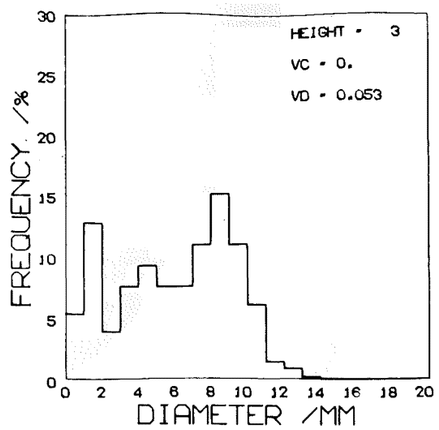

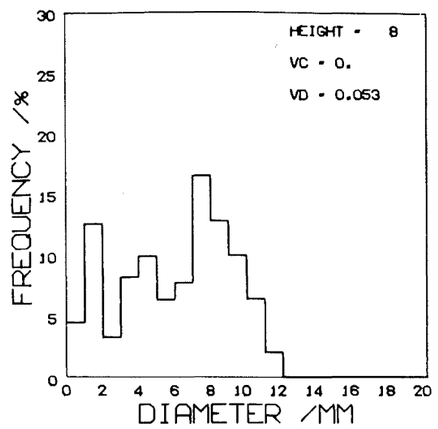

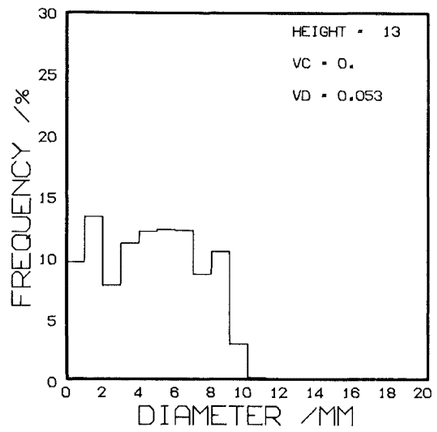

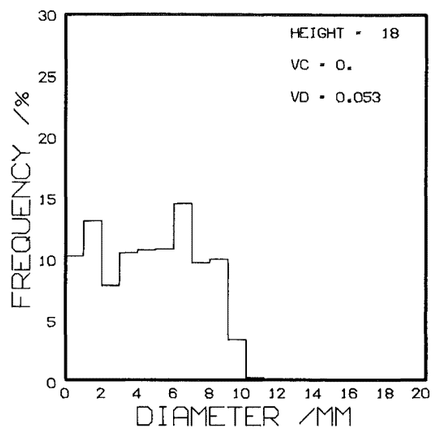

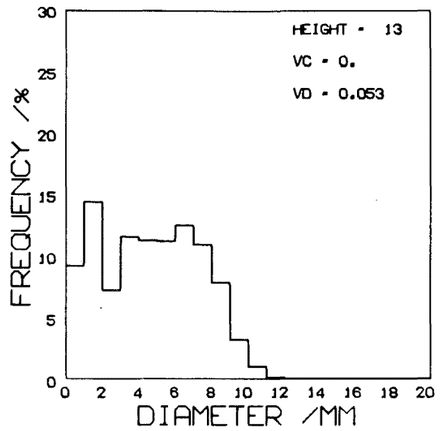

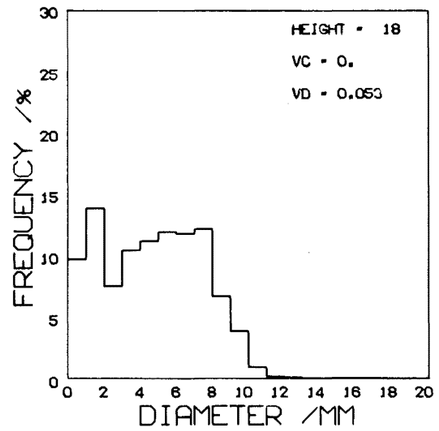

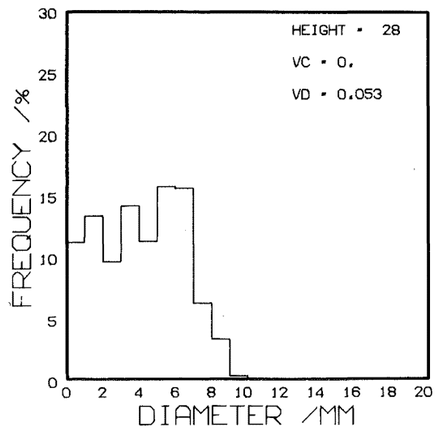

Impaction

Instability Breakup

Residual Volume Breakup

$D = 0.5 + 0.08\,Z$

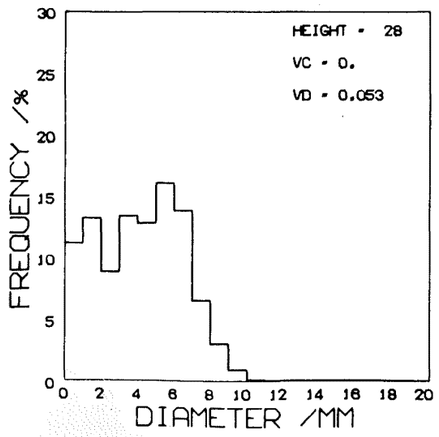

Impaction

Instability Breakup

Residual Volume Breakup

$D = 0.25 + 0.95\,X$

FIGURE 9 – 9 INFLUENCE OF RESTRICTION DIAMETER ON BREAKUP OF RESIDUAL VOLUME

terminal velocity result in reductions in the impaction critical diameter. The resulting distributions after 140cm of packing are shown in figure 9 - 10 when the same model as in figure 9 - 8 is used. Both distributions are very similar to the pure phases distribution.

The distribution for transfer into the dispersed phase has a slightly narrower peak in the range 4 - 5mm as opposed to the pure phases peak of 4 - 5.5mm. There is little change in either the number of satellite droplets or the large diameter tail. This behaviour agrees with the experimental behaviour.

The simulated distribution for the saturated phases shows a slight increases in the number of droplets in the 3 - 4mm range and a slight decrease in the large diameter tail. The agreement with the experimental distribution is not quite as good as for the other two cases. The measured distribution has a much broader peak in the range 3.5 - 5.5mm. Also, the number of droplets in the range 2 - 3mm has increased so that a separate satellite peak does not exist as such. There is also a slight reduction in the large diameter tail as predicted by the simulation.

The changes in physical properties are reflected by the simulation only in the changes in the impaction mechanism. The simulated rate of breakdown by jetting and force balance mechanisms does not alter. The increase in the number of smaller diameter droplets in the experimental saturated phases distribution thus suggests that some enhancement of the rate of breakup at restrictions has occured. As the critical impaction diameter is reduced the degree of multiple occupation of the nozzle increases. Thus for the same buoyancy head beneath the restriction this would tend to increase the force balance breakup. This is offset by the greater forces required to break the smaller droplets in two. The rate of instability formation should also be enhanced however since the lower interfacial tension will make the distortion of the medium sized droplets easier.

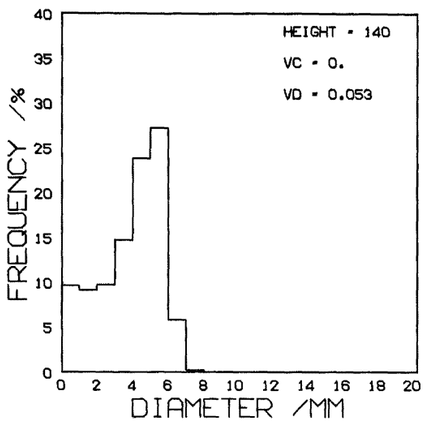

a Pure Phases

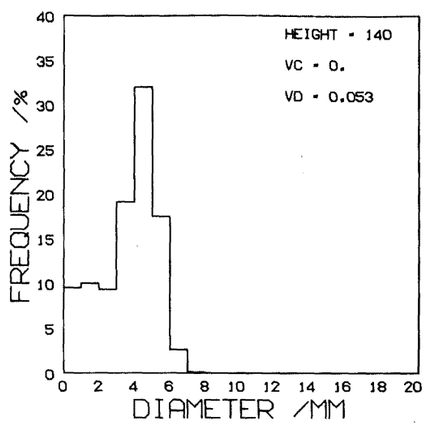

c Mass Transfer

Water to Toluene

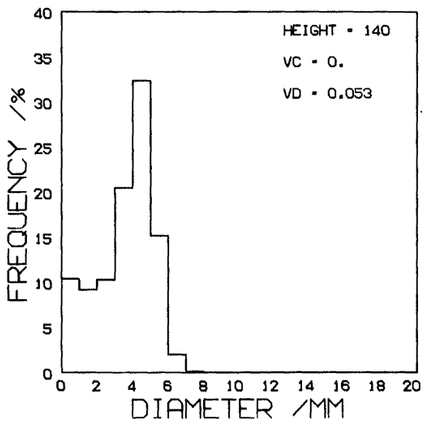

c Saturated Phases

Impaction

Instability Breakup

10% Force Balance Breakup

No Residual Volume Breakup

SIMULATED DISTRIBUTIONS

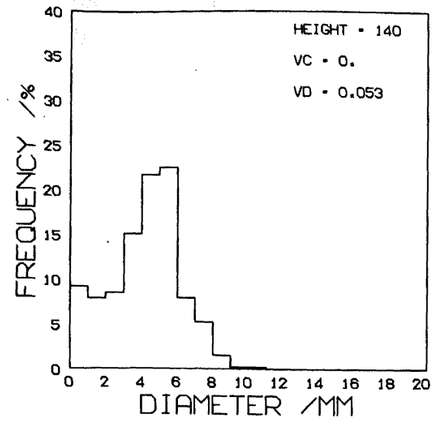

a Pure Phases

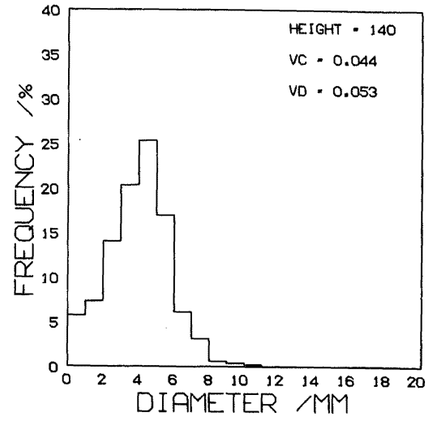

b Mass Transfer

Water to Toluene

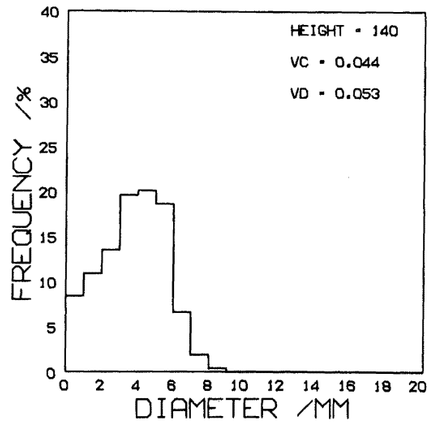

c Saturated Phases

EXPERIMENTAL DISTRIBUTIONS

FIGURE 9 – 10 INFLUENCE OF PHYSICAL PROPERTIES ON SIZE DISTRIBUTION

(2) Coalescence

The behaviour in the simulations considered so far has been determined solely by breakup criteria. However, one major effect of mass transfer is to enhance the coalescence rate between droplets when transfer is out of the dispersed phase. Figure 9 - 11 shows the distribution obtained when there is competition between coalescence and breakup. The main peak centred upon the equilibrium breakup diameter is very much reduced, and a second peak in the range 6 - 8mm has appeared. The satellite peak has more than doubled in size and now comprises about 45% of the total droplets. There is also an increase in the large diameter tail, which now stretches up to 13mm.

The coalescence model used in these simulations assumes that any droplet greater than the satellite size has a chance of single coalescence while it is beneath a restriction. Thus figure 9 - 11(a) is based on a 40% probability of coalescence, and figure 9 - 11(b) on a 100% probability of coalescence, if another droplet is present. The result of this is to broaden the larger diameter peak and to increase the large diameter tail. There is a slight reduction in the smaller diameter peak and the satellite peak is virtually unchanged.

Comparison of these distributions with the experimental distribution in figure 8 - 10 shows a number of differences. The most obvious difference is the number of satellite droplets which are formed. The experimental satellite peak comprises 75% of the total droplets compared with 45% for the simulation. Thus the remainder of the droplets form correspondingly smaller fractions of the total number. There could be a number of reasons for the larger number of experimental satellite droplets. Firstly, the experimental distributions show relatively larger numbers of larger diameter droplets in the 9 - 13mm range. The larger the droplet, the greater is the tendency for a satellite droplet to be formed during force balance breakup. Secondly, the number of satellite droplets formed during instability breakup is determined by

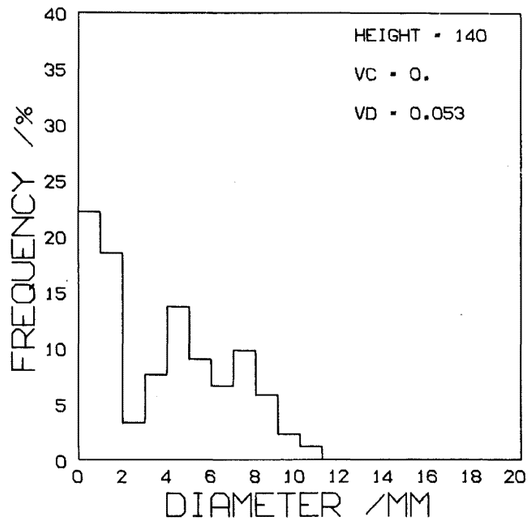

Impaction

No Secondary Formation

Force Balance Breakup

40 % Probability of

Coalescence

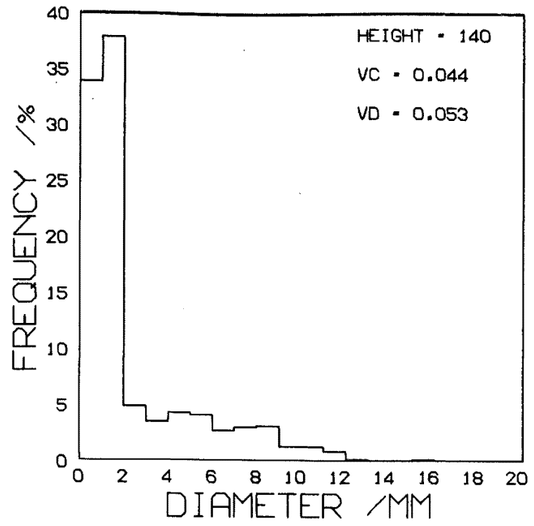

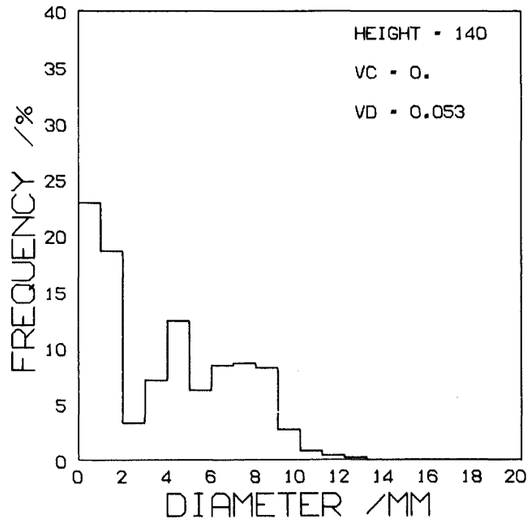

Impaction

No Secondary Formation

Force Balance Breakup

100 % Probability of

Coalescence

SIMULATED DISTRIBUTIONS

EXPERIMENTAL DISTRIBUTION

FIGURE 9 – 11 INFLUENCE OF COALESCENCE ON THE SIZE DISTRIBUTIONS

by the length of the cylindrical links connecting successive protruberances in the jet. If these increase with droplet size then an increase in the number of satellites would result. Finally, in chapter eight it was shown that the mass transfer process would increase the instability of jets when transfer was out of the dispersed phase. Thus, smaller droplets would be expected to form more satellites as well.

The middle section of the simulation from 3 - 9mm agrees reasonably well with the experimental distributions. The peak centred upon the equilibrium impaction size is a little broader than the simulation. The upper end of the simulations from 9mm upwards has somewhat less droplets than the experimental distributions. In particular, no droplets larger than 13mm are formed whereas droplets of up to 16mm diameter were found experimentally. Three factors contribute to this. Firstly, the model of bypassing used assumes that nothing happens to the bypassing droplets whereas coalescence could result in the formation of large droplets with a reduced probability of breakup. Secondly, the distribution of restriction diameters used, whilst having little effect when breakup only was occuring, becomes increasingly important as the droplet size increases. Lastly, the model of coalescence used assumes that only a single coalescence occurs beneath a restriction. Figure 9 - 12 shows the distributions obtained when it is assumed that 40% or 80% of the droplets beneath a restriction coalesce at one time. The 6 - 8mm peak increases at the expense of the 3 - 5mm peak. There is also an increase in the number of droplets in the region from 9mm upwards, although there is still no droplets larger than 13mm. The small increase in satellite formation which occurs suggests that mass transfer results in an enhancement of the formation rate directly rather than by simply maintaining a large diameter droplet population by coalescence.

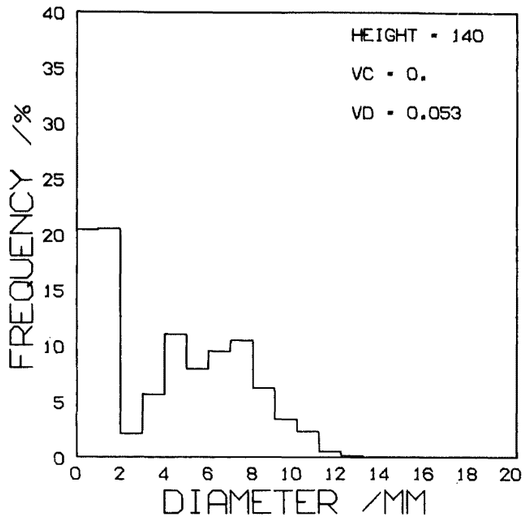

Impaction

No Secondary Formation

Force Balance Breakup

Coalescence of 40 % of

Volume at a Restriction

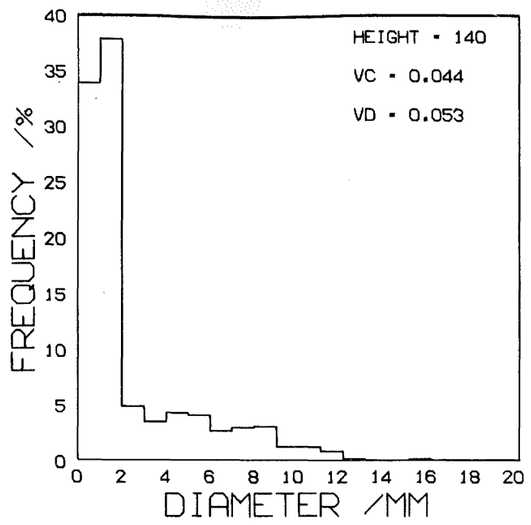

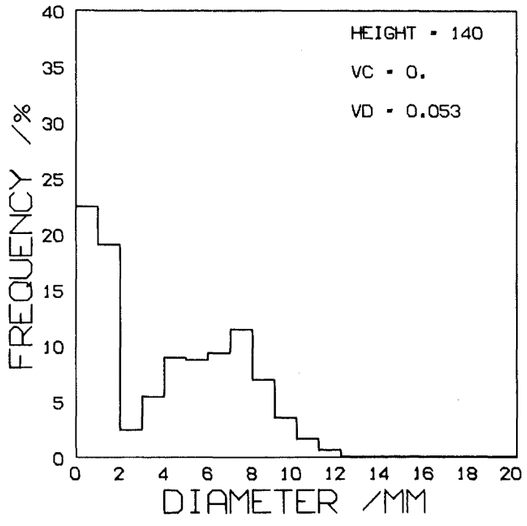

Impaction

No Secondary Formation

Force Balance Breakup

Coalescence of 80 % of

Volume at a Restriction

SIMULATED DISTRIBUTIONS

EXPERIMENTAL DISTRIBUTION

FIGURE 9 – 12 INFLUENCE OF COALESCENCE ON THE SIZE DISTRIBUTIONS

IV SIMULATION PARAMETERS

The parameters used in the simulations are as follows:

Droplet free rise path length = 1.5 cm up to 10 cm packed height.

= 5 cm between 10 and 20 cm packed height.

= 10 cm greater than 20 cm packed height.

The probability of impaction breakup is given by:

$$P = 3 (d - d_{crit})^2$$

where d_{crit} is given by equation (8-8) and

$$P_{max} = 0.80$$

Satellite formation is set at one satellite per breakup for $d < 0.65$. Then

$$d_{sat} = 0.15\ d\ x^{\frac{1}{3}}$$

The remaining volume is then uniformly distributed

$$V_1 / V_2 = x$$

Breakup by an instability mechanism was given by:

$$d_{sec} = 0.5\ d\ x^{\frac{1}{3}}$$

If breakup of the remaining volume by a force balance mechanism occured the following equation was used:

$$d = (6.3 \frac{\sigma}{\Delta \rho g} R)^{\frac{1}{3}}$$

where the restriction diameter R is given by:

$$R = 0.25 + 0.95\ x$$

In 10% of cases for $d_{crit} < d < 0.65$ instability and force balance breakup were replaced by:

$$V_1 / V_2 = x$$

A zero coalescence rate was used except when mass transfer was out of the dispersed phase. Then it was assumed either that all droplets greater than 2mm had a 40% or 100% chance of a single coalescence at a restriction, or that 40% or 80% of the droplet volume beneath a restriction coalesced.

At the end of the free rise interval 40% of all droplets bypassed the breakup steps and rejoined the distribution at the start of the next free rise interval.

V GENERAL CONSIDERATION

(1) Program Validation

It is readily apparent that errors in the simulation would not be immediately obvious. To check that the computer program was in fact carrying out the simulation intended a number of audited runs were made. Examination of the flow chart - figure 9 - 1, shows that four separate paths through the logic paths are possible. Flags were put on these paths. Tripping a flag at any point caused the printout of the parent distribution, the product distribution, breakup and coalescence functions, and book-keeping indices. Thus both overall and step by step mass balances could be done. This procedure resulted in a rapid debugging of the book-keeping and logic routines.

(2) Digital Simulation

The dispersed nature of the phase means that breakup and coalescence processes and book-keeping processes are best suited to a digital operation. However, the simultaneous movement of the droplets, especially relative to one another, is essentially a continuous operation and would be better suited by an analogue simulation. Thus,

the overall simulation might be better suited to a hybrid computer than a digital computer.

(3) Extension to Mass Transfer Simulation

The extension of the dispersed phase simulation to a model of the mass transfer processes in the column would require some additional steps. The interfacial area in the column is determined both by the droplet size distribution and by the holdup. Thus, a more explicit link between flowrates, holdup and queue behaviour would be required. This thus allows a close relationship between simulated and real time. Secondly a flow model for the continuous phase would be required, to account for the large degree of backmixing which occurs in that phase as a result of entrainment by the dispersed phase. Then, all that would be required would be to provide mass transfer coefficients for the two phases.

CONCLUSIONS

The simulation results confirm a number of proposals made in chapter eight about droplet behaviour in a packed column. It is shown that the final distribution evolves from the initial distribution by a complex interaction between a number of different breakup mechanisms and in some cases, the competing mechanism of coalescence.

Breakup of the initial distribution which was normal and centred upon 10mm is described well by the impaction mechanism of Ramshaw and Thornton (1967), (figure 9 - 2), whereby a parent droplet breaks into two daughter droplets upon impacting on a packing element. The rate of breakup is dependent upon the difference between the droplet diameter and the critical impaction diameter as defined by equation (8-8). No significant difference was found over the first 30cm between assuming a linear dependence on this group or a quadratic dependence. The number of breakup sites within the packing depends upon the droplet path length. Thus assuming a constant path length of 1.5cm results in an enhancement of the breakup rate (figure 9 - 4(b).

The simulations confirm the fact that the large diameter tail is a result of different flow regimes within the packing. Assuming that all droplets are subject to a breakup process results in a rapid breakup of all droplets greater than the critical diameter (figure 9 - 5(a)), whereas assuming the existence of secondary flow regions, where no breakup occurs, results in a large diameter tail (figure 9 - 5(b)). The rate of breakup of this tail is then dependent upon the model assumed for interchange between the secondary and preferential channels.

Instability breakup at restrictions was found to result in the formation of a secondary peak (figure 9 - 7). However, the simulations revealed that the behaviour found probably resulted from the interaction of two different mechanisms. Firstly, some droplets are distorted into long cylindrical threads which breakup by an instability

mechanism. Secondly, as the droplets become smaller the amount of multiple occupation of the restrictions increases and the rate of force balance breakup goes through a maximum (figure 9 - 8).

The changes in the critical impaction diameter resulting from changes in the physical properties were found to give a good fit to the distribution when transfer was into the dispersed phase. The effect was not great enough to explain the changes in the saturated phases distribution however. This indicated that there was an additional cahnge occuring in the behaviour at restrictions.

Reasonable agreement with the case of mass transfer out of the dispersed phase was obtained by superimposing a finite coalescence rate upon the breakup processes (figure 9 - 11). This resulted in a broadening of the distribution with two peaks appearing and a large diameter tail extending up to 13mm. The satellite peak doubled in size but was still considerably smaller than the experimental satellite peak. Whilst a number of explanations were proposed for this, the simulations suggest that a direct enhancement of the formation rate by the mass transfer process was the most likely.

The simulations had relatively fewer droplets with diameters greater than 10mm than did the experimental distributions. This resulted partly from the simple model of secondary flow used and partly from the distribution of restriction diameters assumed.

NOMENCLATURE

A,B,C - constants (-)

d - droplet diameter (cm)

d_{crit} - critical impaction diameter (cm)

D - restriction diameter (cm)

D_{jet} - jet diameter (cm)

g - gravitational acceleration ($cm\ s^{-2}$)

H - Harkins-Brown factor (-)

P - probability of droplet breakup (-)

q - arbitary parameter

$\bar{s}$ - free rise path length (cm)

$\bar{t}$ - time of free rise (s)

u - velocity through a restriction ($cm\ s^{-1}$)

V - droplet volume (cm^3)

V_r - droplet velocity ($cm\ s^{-1}$)

V_{sat} - satellite volume (cm^3)

V_{sec} - secondary droplet volume (cm^3)

V_t - droplet terminal velocity ($cm\ s^{-1}$)

x - random variable in range $0 \leqslant x \leqslant 1$ (-)

ϱ - density ($g\ cm^{-3}$)

$\Delta\varrho$ - phase density difference ($g\ cm^{-3}$)

Subscripts

1,2 - daughter droplet

d - dispersed phase

Sat - satellite

sec - secondary

SM - Scheele-Meister

RECOMMENDATIONS

A number of areas have been found where further work is required. These are as follows:

I A new model of droplet behaviour in packed columns has been proposed. It would be desirable to obtain more detailed information on those parameters in the model for which values were assumed, e.g. droplet path lengths and restriction diameters. This would require detailed information about the movements of individual droplets. To obtain this using conventional ceramic, plastic, or steel packing would require the use of radioactive tracers and one or more mobile scintillation counters. Alternatively, if a dispersed phase which did not wet glass was used, then a glass packing and a dye tracer could be used. Matching the refractive index of glass by using dimethyl phtallate as the continuous phase would completely eliminate distortion, but would introduce uncertainties due to the change in physical properties. To obtain the desired information requires that single tagged droplets can be inserted into the column under normal operating conditions. Thus a hypodermic attachment at the distributor, or at suitable points up the column would be needed.

II The characteristic velocity $\overline{V}_o$ has been shown to be strongly dependent upon the droplet size distribution in the first 30cm of packing. The average droplet size formed at the nozzle centre can be predicted. However, a layer of packing over the distributor tends to modify this action. It would be desirable to collect more information upon this effect and upon the effect of mass transfer on the distribution formed at the distributor. Secondly, more information is needed on the effect of both phase flowrates upon the distributions in the first 30cm of packing in order to verify the equation proposed in chapter six relating queue velocity to dispersed phase flowrate

(equation 6-25). It could also be determined from this information whether the splitting of the slip velocity function with changes in continuous phase flowrate could be correlated with the changes in droplet distribution occuring.

III It was pointed out that flooding was indicated in the first 30cm of packing. Further attention to the dependence of the flooding point on the droplet size distribution would be valuable.

IV The model developed is based upon results for a single packed column and system. Further data is required on the effects of column diameter, packing type and size, and of different systems. In particular, a low interfacial tension system with a high coalescence rate might be expected to have somewhat different behaviour.

REFERENCES

(1) Allerton J., Strom B.D., Treybal R.E., Trans.A.I.Ch.E. 361 - 384 (1943).

(2) American National Fire Protection Association, Fire Protection Guide on Hazardous Materials, 5th Ed., (1973).

(3) Appel F.J., Elgin J.C., Ind.Eng.Chem. 29(4), 451 - 459 (1937).

(4) Baird M.H.I., Lane S.J., Chem.Eng.Sci. 28, 947 - 957 (1973).

(5) Baranayev M.K., Teverovski E.V., Tregubova E.L., Doklady Akad. Nauk. S.S.S.R. 5 821 (1949)

(6) Barnea E., Mizrahi J., Chem.Eng.J. 5 171 - 189 (1973).

(7) Barnea E., Mizrahi J., Can.J.Chem.Eng. 53 461 - 468 (1975).

(8) Bashforth F., Adams J.C., An Attempt to Test the Theories of Capilliary Action, Cambridge Unv.Press, (1883).

(9) Basset A.B., Phil.Trans.Roy.Soc.(Lond). 179A 43 (1888).

(10) Basset A.B., Quart.J.Math. 41 369 - 381 (1910).

(11) Bayens C., Ph.D. Thesis. John Hopkins University (1967).

(12) Bayens C.A., Laurence R.L., Ind.Eng.Chem.Fund. 763 521 - 522 (1968).

(13) Bayens C.A., Laurence R.L., Ind.Eng.Chem.Fund. 861 71 - 77 (1969).

(14) Beek W.J., Symposium on Two Phase Flow, (University of Exeter) 2 F401 - F416 (1965)

(15) Berkholder H.C., Berg J.C., A.I.Ch.E.J. 20(5) 863 - 880 (1974).

(16) Beyaert B.O., Lapidus L., Elgin J.C., A.I.Ch.E.J. 7 46 - 48 (1961).

(17) Bondarenko V.S., Zhur.Fiz.Khim. 35 1374 (1961).

(18) Bridge A.C., Ph.D. Thesis Princeton University (1962).

(19) Brodkey R.S., The Phenomena of Fluid Motions, Addison Wesley Publ.Co. Chapt.17 (1967).

(20) Cavers S.D., Ewanchyna J.E., Can.J.Chem.Eng. 35 113 - 128 (1957).

(21) Charles G.E., Mason S.G., J.Coll.Sci. 15 105, 236 (1960).

(22) Chartres R.H., Korchinsky W.J., Trans.I.Ch.E. 53 247 - 254 (1975).

(23) Chen H.T., Middleman S., A.I.Ch.E.J. 13 989 - 995 (1967).

(24) Christiansen R.M., Hixon A.N., Ind.Eng.Chem. 49(6) 1017 - 1024 (1957).

(25) Collins S.B., Knudsen J.G., A.I.Ch.E.J. 16(6) 1072 - 1080 (1970).

(26) Curl R.L., A.I.Ch.E.J. 9(2) 175 - 181 (1963).

(27) Davies G.A., Jeffreys G.V., Azfal M., Brit.Chem.Eng.& Proc. Tech. 17(9) 709 - 714 (1972).

(28) Duffy J.P., Kadlec R.H., Can.J.Chem.Eng. 53 621 - 627 (1975).

(29) Dunn I.J., Ph.D. Thesis. Princeton University (1963).

(30) Edgerton H.E., Hauser E.A., Tucker W.B., J.Phys.Chem. 41 1017 - 1028 (1937).

(31) Esso Research and Engineering Company. Fluidised Bed Operation (1967) British Patent No. 1087355.

(32) Freedman W., Davidson J.F., Trans.I.Ch.E. 47 251 - 262 (1969).

(33) Gal-Or B., Hoelscher H.E., A.I.Ch.E.J. 12(3) 499 - 508 (1966).

(34) Garner F.H., Ellis S.R.M., Hill J.W., Trans.I.Ch.E. 34 223 - 234 (1956)

(35) Gayler R., Pratt H.R.C., Trans.I.Ch.E. 29 110 - 125 (1951).

(36) Gayler R., Pratt H.R.C., Trans.I.Ch.E. 31 69 - 77 (1953).

(37) Gayler R., Pratt H.R.C., Trans.I.Ch.E. 31 78 - 93 (1953).

(38) Gayler R., Pratt H.R.C., Trans.I.Ch.E. 35 267 - 272 (1957).

(39) Gayler R., Pratt H.R.C., Trans.I.Ch.E. 35 273 - 291 (1957).

(40) Gayler R., Roberts N.W., Pratt H.R.C., Trans.I.Ch.E. 31 57 - 68 (1953).

(41) Gier T.E., Hougen J.O., Ind.Eng.Chem. 45(6) 1362 - 1370 (1953).

(42) Gillespie T., Rideal E.K., Trans.Faraday Soc. 52 173 (1956)

(43) Goldsmith H.L., Mason S.G., J.Coll.Sci. 18 237 - 261 (1963)

(44) Goren S.L., J.Coll.Sci. 19 81 - 86 (1964).

(45) Graham E.E., Chan K.K., Fifth Australasian Conf. on Hydraulics and Fluid Mechanics.University of Canterbury (1974).

(46) Groothius H., Zuiderweg F.J., Chem.Eng.Sci. 12 288 - 289 (1960).

(47) Hanson C., Recent Advances in Liquid-Liquid Extraction, Editor, Pergamon Press (1971).

(48) Hanson C., Brown A.H., Symposium on Liquid-Liquid Extraction. Newcastle-upon-Tyne 57 - 62 (1967).

(49) Harkins W.D., Brown F.E., J.Am.Chem.Soc. 41 499 - 524 (1919).

(50) Harmathy T.Z., A.I.Ch.E.J. 6(2) 281 - 288 (1960).

(51) Hartland S., Chem.Eng.Sci. 24 987 - 985 (1969).

(52) Hasson D., Orell A., Fink M., Symposium on Two Phase Flow, (University of Exeter) A5 1 - 16 (1965).

(53) Hauser E.A., Edgerton H.E., Holt B.M., Cox J.T., J.Phys.Chem. 40 973 - 988 (1936).

(54) Haynes L.G., Himmelblau D.M., Schechter R.S., I.& EC.Proc.Des. & Dev. 7(14) 508 - 511 (1968).

(55) Hayworth C.B., Treybal R.E., I.&EC. 1174 - 1181 (1950).

(56) Heertjes P.M., de Nie L.H., in Recent Advances in Liquid-Liquid Extraction. Editor C.Hanson. Pergamon Press. Chapt.10 (1971).

(57) Heertjes P.M., de Nie L.H., de Vrie H.J., Chem.Eng.Sci. 26 441 - 459 (1971).

(58) Higbie R., Trans.A.I.Ch.E. 31 365 - 389 (1935).

(59) Hinze J.D., A.I.Ch.E.J. 1(3) 289 - 295 (1955).

(60) Ho B.P., Leal L.G., J.Fluid Mech. 71 361 - 383 (1975).

(61) Hu S., Kintner R.C., A.I.Ch.E.J. 1(1) 42 - 48 (1955).

(62) Hughes R.R., Gilliland E.R., Chem.Eng.Progress 48(10) 497 - 504 (1952).

(63) Izard J.A., A.I.Ch.E.J. 18(3) 634 - 638 (1972).

(64) Jeffreys G.V., Davies G.A., Filtration and Separation 6 349 (1969).

(65) Jeffreys G.V., Davies G.A., in Recent Advances in Liquid-Liquid Extraction. Editor C.Hanson. Pergamon Press. Chapt. 14. (1971).

(66) Jeffreys G.V., Hawksley J.L., A.I.Ch.E.J. 11 413 - 424 (1965).

(67) Jeffreys G.V., Lawson G., Trans.I.Ch.E. 43 294 - 298 (1965).

(68) Jeffreys G.V., Lawson G., International Solvent Extraction Conference. The Hague. 4 (1971).

(69) Johnson A.I., Lavergne E.A.L., Can.J.Ch.E. 39 37 - 41 (1961).

(70) Johnson H.F., Bliss H., Trans.A.I.Ch.E. 42 331 - 358 (1946).

(71) Johnson T.R., Pierce R.D., Teats F.G., Johnston E.F., A.I.Ch.E.J. 17(1) 14 - 18 (1971).

(72) Karam H.J., Bellinger J.C., Ind.Eng.Chem.Fund. 7 576 - 581 (1968).

(73) Kattan A., Adler R.J., A.I.Ch.E.J. 11 580 - 585 (1967).

(74) Kolmogorov A.N., Doklady Akad. Nauk. S.S.S.R. 66 825 (1949).

(75) Lamb H., Hydrodynamics. Dover Publications, New York. (1945).

(76) Lapidus L., Elgin J.C., A.I.Ch.E.J. 3 63 - 68 (1957).

(77) Lewis J.B., Jones I., Pratt H.R.C., Trans.I.Ch.E. 29 126 - 148 (1951).

(78) Lewis J.B., Pratt H.R.C., Nature (London). 171 1155 (1953).

(79) Lockett M.J., Kirkpatrick R.D., Trans.I.Ch.E. 53 267 - 273 (1975).

(80) Logsdail D.H., Lowes L., in Recent Advances in Liquid-Liquid Extraction. Editor C.Hanson. Pergamon Press. Chapt. 5. (1971).

(81) Logsdail D.H., Thornton J.D., Trans.I.Ch.E. 35 331 - 342 (1957).

(82) Logsdail D.H., Thornton J.D., Pratt H.R.C., Trans.I.Ch.E. 35 301 - 315 (1957).

(83) McAvoy R.M., Kintner R.C., J.Coll.Sci. 20 188 (1965).

(84) MacKay G.D.H., Mason S.G., Can.J.Ch.E. 41 203 - 212 (1963).

(85) Marangoni C., Annln.Phys. 137 337 (1871).

(86) Maraschino M.J., Treybal R.E., A.I.Ch.E.J. 17(5) 1174 -1180 (1971).

(87) Markas S.E., Beckmann R.B., A.I.Ch.E.J. 3(2) 223 - 229 (1957).

(88) Marsh B.D., Sleicher C.A., Heideger W.J., Paper presented to the 57th annual meeting of A.I.Ch.E. Philadelphia. (1965).

(89) Meister B.J., Scheele G.F., A.I.Ch.E.J. 13(4) 682 - 688 (1967).

(90) Meister B.J., Scheele G.F., A.I.Ch.E.J. 15(5) 689 - 699 (1969).

(91) Meister B.J., Scheele G.F., A.I.Ch.E.J. 15(5) 700 - 706 (1969).

(92) Mikami T., Cox R.C., Mason S.G., Int.J.Multi Phase Flow 2(2) 113 - 138 (1975).

(93) Misek T., Marek J., Brit.Chem.Eng. 15(2) 202 - 207 (1970).

(94) Mockros L.F., Lai R.Y.S., J.Eng.Mech.Div.Am.Soc.Civ.Engrs. 95 629 (1969).

(95) Moorman R.W., Ph.D. Thesis. University of Iowa (1955).

(96) Morello V.S., Beckmann R.B., Ind.Chem.Eng. 42 1078 - 1087 (1950).

(97) Mugele R.A., Evans H.O., Ind.Chem.Eng. 43(6) 1317 - 1324 (1951).

(98) Null H.R., Johnson H.F., A.I.Ch.E.J. 4 273 - 281 (1958).

(99) N.Z.Standard 379. Specifications for Electrical Switches in Hazardous Atmospheres.

(100) Odell M.H., Project Report. Dept. of Chem.Eng. University of Canterbury, (1975).

(101) Olney R.B., A.I.Ch.E.J. 10(6) 827 - 835 (1964).

(102) Ooi K.L., Unpublished work in this department.

(103) Paul H.I., Sleicher C.A., Chem.Eng.Sci. 20 57 - 59 (1965)

(104) Price B.G., Lapidus L., Elgin J.C., A.I.Ch.E.J. 5 93 - 97 (1959).

(105) Princen H.M., J.Coll.Sci. 18 178 (1963).

(106) Princen H.M., Mason S.G., J.Coll.Sci. 20 156 (1965).

(107) Ramkrishna D., Borwanker J.D., Chem.Eng.Sci. 28 1423 - 1435 (1973).

(108) Ramkrishna D., Borwanker J.D., Chem.Eng.Sci. 29 1711 - 1721 (1974).

(109) Ramkrishna D., Shah B.H., Borwanker J.D., Chem.Eng.Sci. 31 435 - 442 (1976).

(110) Ramshaw C., Thornton J.D., Symposium on Liquid-Liquid Extraction. Newcastle-upon-Tyne 73 - 87 (1967).

(111) Rao D.P., Dunn I.J., Chem.Eng.Sci. 25 1275 - 1282 (1970).

(112) Rao E.V.L.N., Kumar R., Kuloor N.R., Chem.Eng.Sci. 21 867 - 880 (1966).

(113) Rayleigh Lord, Proc.London Math.Soc. 10 4 (1879).

(114) Rayleigh Lord, Phil.Mag. 34 177 (1892).

(115) Richardson J.F., Meikle R.A., Trans.I.Ch.E. 39 348 - 356 (1961).

(116) Row S.B., Koffolt J.H., Withrow J.R., Trans.A.I.Ch.E. 37 559 - 594 (1941).

(117) Rumscheidt F.D., Mason S.G., J.Coll.Sci. 16 238 - 261 (1961).

(118) Rushton J.H., Costrich E.W., Everett H.J., Chem.Eng.Progress. 46 395 and 467 (1950).

(119) Sakiadis B.C., Johnson A.I., Ind.Eng.Chem. 46(6) 1229 - 1239 (1954).

(120) Sawistowski H., in Recent Advances in Liquid-Liquid Extraction Editor C.Hanson. Pergamon Press. Chapt.9. (1971).

(121) Sawistowski H., Chemie-Ing-Tech. 45(18) 1093 - 1098 (1973).

(122) Scheele G.F., Meister B.J., A.I.Ch.E.J. 14(1) 9 - 19 (1968).

(123) Scriven L.E., Sternling C.V., Nature.(London). 171 1155 (1953).

(124) Sehrt B., Linde H., Proc.IIIrd Int.Conf. on Surface Active Materials, Akademie Verlag, Berlin. (1967).

(125) Shinner R.J., J.Fluid Mech. 10 259 (1961).

(126) Sitaramayya T., Laddha G.S., Chem.Eng.Sci. 13 263 - 267 (1961).

(127) Sleicher C.A., A.I.Ch.E.J. 8(4) 471 - 477 (1962).

(128) Smith D.V., Davies G.A., Can.J.Ch.E. 48 628 - 637 (1970).

(129) Spielman L.A., Levenspiel O., Chem.Eng.Sci. 20 247 - 254 (1965).

(130) Sprow B., Chem.Eng.Sci. 22 435 - 442 (1967).

(131) Steinour H.H., Ind.Eng.Chem. 36(7) 618 - 624 (1944).

(132) Sternling C.V., Scriven L.E., A.I.Ch.E.J. 5 514 - 523 (1959).

(133) Strand C.P., Olney R.B., Ackerman G.H., A.I.Ch.E.J. 8(2) 252 - 260 (1962).

(134) Strom J.R., Kintner R.C., A.I.Ch.E.J. 4 153 - 156 (1958).

(135) Struve D., Lapidus L., Elgin J.C., Can.J.Ch.E. 36 141 - 152 (1958).

(136) Taylor G.I., Proc.Roy.Soc.(London) 138A 41 - 48 (1932).

(137) Taylor G.I., Proc.Roy.Soc.(London) 146A 501 - 523 (1934).

(138) Thiessen D.Z., Physik.Chem. 223 218 (1963).

(139) Thomas R.J., Mumford C.J., International Solvent Extraction Conference. The Hague. 3(5c) 16 - 23 (1971).

(140) Thomas W.J., Weng P.K.J., J.Appl.Chem. 20 48 - 57 (1970).

(141) Thomson J., Phil.Mag. 10(4) 330 (1855).

(142) Thornton J.D., Trans.I.Ch.E. 35 316 - 330 (1957).

(143) Thornton J.D., Pratt H.R.C., Trans.I.Ch.E. 31 289 - 306 (1953).

(144) Tomotika S., Proc.Roy.Soc.(London) A150 322 - 337 (1935).

(145) Tomotika S., Proc.Roy.Soc.(London) A153 302 - 318 (1936).

(146) Torobin L.B., Gauvin W.H., Can.J.Ch.E. 37 224 - 236 (1959).

(147) Treybal R.E., Liquid Extraction McGraw - Hill. (1963).

(148) Uno S., Kintner R.C., A.I.Ch.E.J. 2 420 - 425 (1956).

(149) Valentas K.J., Amundson N.R., Ind.Eng.Chem.Fund. 5(4) 533 - 542 (1966).

(150) Valentas K.J., Amundson N.R., Ind.Eng.Chem.Fund. 7(1) 66 - 72 (1968).

(151) Valentas K.J., Bilous O., Amundson N.R., Ind.Eng.Chem.Fund. 5(2) 271 - 279 (1966).

(152) Vermeulen T., Williams G.M., Langlois G.S., Chem.Eng.Progress. 51 85F - 94F (1955).

(153) Ward J.P., Knudsen J.G., A.I.Ch.E.J. 13(2) 356 - 365 (1967).

(154) Wark I.W., Cox A.B., Nature (London) 136 182 (1935).

(155) Watson J.S., McNeese L.E., A.I.Ch.E.J. 19(2) 230 - 237 (1973).

(156) Watson J.S., McNeese L.E., Day J., Carroad P.A., A.I.Ch.E.J. 21(6) 1080 - 1086 (1975).

(157) Weaver R.E.C., Lapidus L., Elgin J.C., A.I.Ch.E.J. 5 533 - 539 (1959)

(158) Weber C., Z.Angew.Math.Cech. 11 136 (1931).

(159) Wicks C.E., Beckmann R.B., A.I.Ch.E.J. 1(4) 426 - 433 (1955).

(160) Wilke C.R., Chang P., A.I.Ch.E.J. 1 264 - 270 (1955).

(161) Wilkinson D., Mumford C.J., Jeffreys G.V., A.I.Ch.E.J. 21(5) 910 - 917 (1975).

(162) Zabel T., Hanson C., Ingham J., Trans.I.Ch.E. 51 162 - 164 (1973).

(163) Zeitlin M.A., Tavlarides L.L., Can.J.Ch.E. 50 207 - 215 (1972).

APPENDIX I

SYSTEM PROPERTIES

(1) PHYSICAL PROPERTIES

NOMENCLATURE

a - b - c

a - drum number

b - system number:

1 - pure phases

2 - mass transfer: toluene to water

3 - mass transfer: water to toluene

4 - saturated phases

c - run number

Density - g/cm^3

Feed concentration - moles / litre

Interfacial tension - dynes / cm

Temperature - C

Viscosity - centipoise

(2) INTERFACIAL TENSION-CONCENTRATION GRADIENT

(3) SCHEELE-MEISTER PARAMETERS

1 PHYSICAL PROPERTIES

RUN	FEED CONC.	INTER FACIAL TENSION	CONT. PHASE DENSITY	DISP. PHASE DENSITY	PHASE DENSITY DIFFERENCE
1-1	-	27.2	0.9990	0.8720	0.1270
2-1	-	30.1	0.9990	0.8720	0.1270
2-2- 1	0.0360	25.4	0.9983	0.8715	0.1268
2-2- 2	0.0395	25.2	0.9975	0.8696	0.1279
2-2- 3	0.0372	24.9	0.9970	0.8690	0.1280
2-2- 4	0.0395	25.0	0.9974	0.8698	0.1276
2-2- 5	0.0425	26.0	0.9988	0.8698	0.1290
2-2- 6	0.0425	25.8	0.9985	0.8700	0.1285
2-2- 7	0.0406	22.9	0.9985	0.8705	0.1280
2-2- 8	0.0417	27.4	0.9990	0.8695	0.1295
2-2- 9	0.0395	25.4	0.9993	0.8698	0.1295
2-2-10	0.0406	26.7	0.9988	0.8693	0.1295
2-3- 1	0.0091	27.3	0.9970	0.8678	0.1292
2-3- 2	0.0086	27.4	0.9965	0.8695	0.1270
2-3- 3	0.0095	26.8	0.9963	0.8688	0.1275
2-3- 4	0.0086	25.6	0.9970	0.8693	0.1277
2-3- 5	0.0098	22.5	0.9940	0.8675	0.1265
2-3- 6	0.0091	24.1	0.9950	0.8695	0.1255
2-3- 7	0.0109	25.5	0.9943	0.8690	0.1253
2-3- 8	0.0091	24.1	0.9948	0.8688	0.1260
2-3- 9	0.0086	25.5	0.9945	0.8693	0.1252
2-3-10	0.0086	26.3	0.9953	0.8693	0.1260
2-4	0.0255	24.4	0.9988	0.8693	0.1295

RUN	CONT. PHASE VISCOSITY	DISP. PHASE VISCOSITY	TEMP.	PH
1-1	1.02	0.62	16.0	7.62
2-1	0.98	0.60	17.0	7.42
2-2- 1	0.97	0.59	15.0	7.78
2-2- 2	-	-	16.0	-
2-2- 3	0.97	0.57	15.5	7.66
2-2- 4	-	-	15.0	-
2-2- 5	0.99	0.59	15.0	7.54
2-2- 6	-	-	14.0	-
2-2- 7	0.96	0.57	14.0	7.70
2-2- 8	-	-	14.0	-
2-2- 9	0.97	0.57	14.0	7.48
2-2-10	-	-	15.0	-
2-3- 1	0.97	0.59	17.0	7.56
2-3- 2	-	-	17.0	7.56
2-3- 3	-	-	17.5	7.56
2-3- 4	0.96	0.58	17.0	7.56
2-3- 5	-	-	17.5	7.56
2-3- 6	-	-	16.0	7.56
2-3- 7	0.98	0.59	16.5	7.56
2-3- 8	-	-	17.0	7.56
2-3- 9	0.96	0.59	16.0	7.56
2-3-10	-	-	16.0	7.56
2-4	0.95	0.56	15.0	7.58

(2) INTERFACIAL TENSION-CONCENTRATION GRADIENT

The interfacial tension of the toluene - acetone - water system was measured when the acetone was in the toluene phase.

Solute Concentration / mole l^{-1}	Interfacial Tension / dyne cm^{-1}
0	31.7 ± 0.2
0.0049	28.8
0.0097	25.8
0.0286	19.0
0.0467	16.4
0.0892	10.9

Linear regression of $\frac{1}{\sigma}$ against concentration yields the expression:

$$\sigma' = \frac{1}{0.666\ C + 0.032}$$

$$\sigma' = \frac{1.5}{C + 0.05}$$

Thus:

$$\frac{d\sigma'}{dc} = \frac{-1.5}{(C + .05)^2}$$

$$= \frac{-\sigma'^2}{1.5}$$

(3) SCHEELE-MEISTER PARAMETERS

The Scheele-Meister equation for droplet formation at a nozzle is:

$$V = H\left[\frac{\pi \sigma D}{g \Delta \rho} + \frac{20 \mu Q D}{d^2 g \Delta \rho} - \frac{4 \rho_d Q U}{3 g \Delta \rho} + 4.5\left(\frac{Q^2 D^2 \rho_d \sigma}{(g \Delta \rho)^2}\right)^{\frac{1}{3}}\right]$$

If the Harkins-Brown factor is taken as 1.0 and the drag term is neglected this equation simplifies to:

$$V = A_{SM} D + D^2 (C_{SM} U^{\frac{2}{3}} - B_{SM} U^2)$$

The values of the parameters A_{SM}, B_{SM}, C_{SM} are as follows:

	A_{SM}	B_{SM}	C_{SM}
(1) Pure Phases	0.759	0.00733	0.456
(2) Mass Transfer Toluene to Water	0.634	0.00721	0.427
(3) Mass Transfer Water to Toluene	0.650	0.0733	0.433
(4) Saturated Phases	0.604	0.00716	0.414

APPENDIX II

HOLDUP DATA

NOMENCLATURE

V_c - superficial continuous phase velocity $(cm^3\ s^{-1}/cm^2)$

V_d - superficial dispersed phase velocity $(cm^3\ s^{-1}/cm^2)$

V_s - slip velocity $= V_d + \frac{x}{1-x} V_c$ $(cm\ s^{-1})$

X - dispersed phase free holdup (-)

DRUM(1) - SURFACTANT CASE

PACKING HEIGHT = 1.40 METRES

RUN	VC	VD	X	X(1-X)	VS
1-1- 1	0.000	0.054	0.029	0.028	0.054
1-1- 2	0.000	0.097	0.048	0.046	0.097
1-1- 3	0.000	0.141	0.066	0.062	0.141
1-1- 4	0.000	0.186	0.085	0.078	0.186
1-1- 5	0.000	0.236	0.105	0.094	0.236
1-1- 6	0.000	0.269	0.122	0.107	0.269
1-1- 7	0.000	0.334	0.154	0.130	0.334
1-1- 8	0.000	0.381	0.191	0.155	0.381
1-1- 9	0.043	0.054	0.030	0.029	0.055
1-1-10	0.044	0.097	0.045	0.043	0.099
1-1-11	0.044	0.142	0.062	0.058	0.145
1-1-12	0.043	0.187	0.085	0.078	0.191
1-1-13	0.043	0.234	0.106	0.095	0.239
1-1-14	0.044	0.269	0.130	0.113	0.276
1-1-15	0.044	0.333	0.166	0.138	0.342
1-1-16	0.043	0.377	0.236	0.180	0.390
1-1-17	0.118	0.054	0.031	0.030	0.058
1-1-18	0.118	0.097	0.047	0.045	0.103
1-1-19	0.116	0.185	0.087	0.079	0.196
1-1-20	0.118	0.236	0.117	0.103	0.252
1-1-21	0.117	0.270	0.141	0.121	0.289
1-1-22	0.116	0.334	0.260	0.192	0.375
1-1-23	0.118	0.381	0.546	0.248	0.523

DRUM(1) -SURFACTANT CASE

PACKING HEIGHT = 1.40 METRES

RUN	VC	VD	X	X(1-X)	VS
1-1-24	0.200	0.054	0.033	0.032	0.061
1-1-25	0.200	0.097	0.050	0.047	0.108
1-1-26	0.200	0.141	0.073	0.068	0.157
1-1-27	0.200	0.187	0.096	0.087	0.208
1-1-28	0.200	0.234	0.125	0.109	0.263
1-1-29	0.199	0.269	0.211	0.166	0.322
1-1-30	0.200	0.333	0.629	0.233	0.672
1-1-31	0.229	0.054	0.036	0.035	0.063
1-1-32	0.229	0.097	0.056	0.053	0.111
1-1-33	0.229	0.141	0.074	0.069	0.159
1-1-34	0.229	0.186	0.100	0.090	0.211
1-1-35	0.229	0.234	0.130	0.113	0.268
1-1-36	0.229	0.269	0.299	0.210	0.367
1-1-37	0.227	0.301	0.357	0.230	0.427
1-1-38	0.287	0.054	0.035	0.034	0.064
1-1-39	0.286	0.097	0.051	0.048	0.112
1-1-40	0.286	0.141	0.076	0.070	0.165
1-1-41	0.283	0.185	0.106	0.095	0.219
1-1-42	0.286	0.235	0.241	0.183	0.326
1-1-43	0.283	0.269	0.558	0.247	0.626

DRUM(1) -SURFACTANT CASE

PACKING HEIGHT = 1.40 METRES

RUN	VC	VD	X	X(1-X)	VS
1-1-44	0.400	0.053	0.041	0.039	0.070
1-1-45	0.400	0.096	0.060	0.056	0.122
1-1-46	0.400	0.141	0.078	0.072	0.175
1-1-47	0.400	0.186	0.177	0.146	0.272
1-1-48	0.400	0.220	0.329	0.221	0.416

DRUM(2) - PURE PHASES

PACKING HEIGHT = 1.40 METRES

RUN	VC	VD	X	X(1-X)	VS
2-1- 1	0.000	0.053	0.039	0.037	0.053
2-1- 2	0.000	0.097	0.059	0.056	0.097
2-1- 3	0.000	0.141	0.086	0.079	0.141
2-1- 4	0.000	0.234	0.146	0.125	0.234
2-1- 5	0.000	0.333	0.230	0.177	0.333
2-1- 6	0.044	0.053	0.040	0.038	0.055
2-1- 7	0.044	0.097	0.060	0.056	0.100
2-1- 8	0.044	0.141	0.085	0.078	0.145
2-1- 9	0.044	0.234	0.144	0.123	0.241
2-1-10	0.225	0.053	0.048	0.046	0.064
2-1-11	0.225	0.097	0.072	0.067	0.114
2-1-12	0.225	0.141	0.113	0.100	0.170
2-1-13	0.225	0.234	0.454	0.248	0.421
2-1-14	0.400	0.053	0.069	0.064	0.083
2-1-15	0.400	0.097	0.119	0.105	0.151

DRUM(2) - MASS TRANSFER : TOLUENE TO WATER

PACKING HEIGHT = 1.40 METRES

RUN	VC	VD	X	X(1-X)	VS
2-2- 1	0.044	0.053	0.027	0.026	0.054
2-2- 2	0.044	0.097	0.037	0.036	0.099
2-2- 3	0.044	0.141	0.059	0.056	0.144
2-2- 4	0.044	0.234	0.082	0.075	0.238
2-2- 5	0.229	0.053	0.029	0.028	0.060
2-2- 6	0.229	0.097	0.041	0.039	0.107
2-2- 7	0.229	0.234	0.096	0.087	0.258
2-2- 8	0.400	0.053	0.030	0.029	0.065
2-2- 9	0.400	0.097	0.050	0.047	0.118
2-2-10	0.400	0.234	0.101	0.091	0.279

DRUM(2) - MASS TRANSFER : WATER TO TOLUENE

PACKING HEIGHT = 1.40 METRES

RUN	VC	VD	X	X(1-X)	VS
2-3- 1	0.044	0.053	0.033	0.032	0.055
2-3- 2	0.044	0.097	0.054	0.051	0.100
2-3- 3	0.044	0.141	0.080	0.074	0.145
2-3- 4	0.044	0.234	0.154	0.130	0.242
2-3- 5	0.229	0.053	0.039	0.037	0.062
2-3- 6	0.229	0.097	0.057	0.054	0.111
2-3- 7	0.229	0.141	0.088	0.080	0.163
2-3- 8	0.400	0.053	0.044	0.042	0.071
2-3- 9	0.400	0.097	0.074	0.069	0.129

DRUM(2) -SATURATED PHASES

PACKING HEIGHT = 1.40 METRES

RUN	VC	VD	X	X(1-X)	VS
2-4- 1	0.000	0.053	0.034	0.033	0.053
2-4- 2	0.000	0.097	0.047	0.045	0.097
2-4- 3	0.000	0.141	0.075	0.069	0.141
2-4- 4	0.000	0.234	0.133	0.115	0.234
2-4- 5	0.044	0.053	0.038	0.037	0.055
2-4- 6	0.044	0.097	0.058	0.055	0.100
2-4- 7	0.044	0.141	0.081	0.074	0.145
2-4- 8	0.044	0.234	0.134	0.116	0.241
2-4- 9	0.229	0.053	0.041	0.039	0.063
2-4-10	0.229	0.097	0.064	0.060	0.113
2-4-11	0.229	0.141	0.101	0.091	0.167
2-4-12	0.229	0.234	0.285	0.204	0.325
2-4-13	0.400	0.053	0.051	0.048	0.074
2-4-14	0.400	0.097	0.078	0.072	0.131
2-4-15	0.400	0.141	0.225	0.174	0.257

APPENDIX III

MEAN DIAMETER DATA

NOMENCLATURE

D_{32} - Sauter mean diameter = $\sum_{i=1}^{\infty} n_i d_i^3 / \sum_{i=1}^{\infty} n_i d_i^2$ (cm)

D_{43} - mean diameter = $\sum_{i=1}^{\infty} n_i d_i^4 / \sum_{i=1}^{\infty} n_i d_i^3$ (cm)

H - packing height (cm)

N - sample size

V_c - superficial continuous phase velocity ($cm^3 s^{-1}/cm^2$)

V_d - superficial dispersed phase velocity ($cm^3 s^{-1}/cm^2$)

DRUM(1) - SURFACTANT CASE

PACKING HEIGHT = 1.40 METRES

RUN	VC	VD	D43	D32	N
1-1- 1	0.000	0.054	0.555	0.505	375
1-1- 2	0.000	0.097	0.585	0.519	633
1-1- 3	0.000	0.141	0.558	0.495	866
1-1- 4	0.000	0.186	0.518	0.467	796
1-1- 5	0.000	0.236	0.489	0.427	915
1-1- 6	0.000	0.269	0.562	0.496	1528
1-1- 7	0.000	0.334	0.579	0.500	1279
1-1-31	0.229	0.054	0.641	0.572	343
1-1-32	0.229	0.097	0.561	0.502	656
1-1-34	0.229	0.186	0.605	0.527	746
1-1-35	0.229	0.234	0.613	0.529	1017
1-1-36	0.229	0.269	0.689	0.604	696
1-1-37	0.227	0.301	0.709	0.633	804
1-1-38	0.287	0.054	0.564	0.509	437
1-1-39	0.286	0.097	0.586	0.521	599
1-1-40	0.286	0.141	0.552	0.493	855
1-1-41	0.283	0.185	0.559	0.492	1085
1-1-42	0.286	0.235	0.602	0.521	1270
1-1-43	0.283	0.269	0.708	0.610	1101
1-1-44	0.400	0.053	0.587	0.537	270
1-1-45	0.400	0.096	0.570	0.502	764
1-1-46	0.400	0.141	0.610	0.521	1073
1-1-47	0.400	0.186	0.619	0.550	1130
1-1-48	0.400	0.220	0.710	0.617	952

DRUM(1) -SURFACTANT CASE

RUN	VC	VD	D43	D32	N	H
1-1-49	0.000	0.053	0.921	0.910	47	0
1-1-50	0.000	0.097	0.921	0.910	189	0
1-1-51	0.000	0.053	1.064	1.037	97	3
1-1-52	0.000	0.097	1.074	1.019	82	3
1-1-53	0.000	0.053	0.913	0.845	94	5
1-1-54	0.000	0.097	0.915	0.857	188	5
1-1-55	0.000	0.053	1.102	1.050	275	10
1-1-56	0.000	0.097	0.845	0.768	269	10
1-1-57	0.000	0.053	0.846	0.775	318	15
1-1-58	0.000	0.097	0.779	0.726	257	15
1-1-59	0.000	0.053	0.852	0.741	382	20
1-1-60	0.000	0.097	0.762	0.683	356	20
1-1-61	0.000	0.053	0.722	0.670	418	30
1-1-62	0.000	0.097	0.714	0.659	379	30
1-1-63	0.000	0.053	0.715	0.619	283	45
1-1-64	0.000	0.097	0.606	0.559	494	45
1-1-65	0.000	0.053	0.636	0.570	388	61
1-1-66	0.000	0.053	0.630	0.582	426	81

DRUM(2) - PURE PHASES

PACKING HEIGHT = 1.40 METRES

RUN	VC	VD	D43	D32	N
2-1- 1	0.000	0.053	0.615	0.573	455
2-1- 2	0.000	0.097	0.604	0.557	516
2-1- 6	0.044	0.053	0.622	0.585	510
2-1- 7	0.044	0.097	0.580	0.537	485
2-1-14	0.400	0.053	0.659	0.613	516
2-1-15	0.400	0.097	0.658	0.600	474

DRUM(2) - MASS TRANSFER : TOLUENE TO WATER

PACKING HEIGHT = 1.40 METRES

RUN	VC	VD	D43	D32	N
2-2- 1	0.044	0.053	0.890	0.771	754
2-2- 2	0.044	0.097	0.922	0.748	954
2-2- 5	0.229	0.053	0.879	0.768	662
2-2- 6	0.229	0.097	0.896	0.773	750
2-2- 8	0.400	0.053	1.044	0.852	649
2-2- 9	0.400	0.097	0.971	0.847	555

DRUM(2) - MASS TRANSFER : WATER TO TOLUENE

PACKING HEIGHT = 1.40 METRES

RUN	VC	VD	D43	D32	N
2-3- 1	0.000	0.053	0.582	0.533	478
2-3- 8	0.400	0.053	0.572	0.536	464

DRUM(2) -SATURATED PHASES

PACKING HEIGHT = 1.40 METRES

RUN	VC	VD	D43	D32	N
2-4- 5	0.044	0.053	0.553	0.515	570
2-4- 6	0.044	0.097	0.511	0.473	531
2-4- 9	0.229	0.053	0.544	0.505	638
2-4-10	0.229	0.097	0.541	0.500	562
2-4-13	0.400	0.053	0.596	0.545	577
2-4-14	0.400	0.097	0.564	0.517	525

APPENDIX IV

DROPLET SIZE DISTRIBUTION DATA

(1) DISTRIBUTIONS

NOMENCLATURE

C - cumulative numerical frequency (%)

CV - cumulative volume frequency (%)

D - droplet diameter (cm)

N - numerical frequency (%)

V - volume frequency (%)

(2) DISTRIBUTION EQUATIONS

DRUM(1) - SURFACTANT CASE

PACKING HEIGHT = 1.40 METRES

RUN	D	N	C	V	CV
1-1- 1	0.05	0.083	0.083	0.0001	0.0001
	0.15	0.163	0.246	0.0070	0.0072
	0.25	0.131	0.377	0.0262	0.0333
	0.35	0.211	0.588	0.1156	0.1489
	0.45	0.206	0.794	0.2398	0.3888
	0.55	0.128	0.922	0.2721	0.6609
	0.65	0.056	0.978	0.1965	0.8574
	0.75	0.016	0.994	0.0862	0.9436
	0.85	0.003	0.997	0.0235	0.9671
	0.95	0.003	1.000	0.0329	1.0000
1-1- 2	0.05	0.079	0.079	0.0001	0.0001
	0.15	0.144	0.223	0.0061	0.0063
	0.25	0.163	0.386	0.0322	0.0385
	0.35	0.239	0.625	0.1296	0.1681
	0.45	0.191	0.816	0.2202	0.3883
	0.55	0.112	0.928	0.2357	0.6241
	0.65	0.046	0.974	0.1598	0.7839
	0.75	0.016	0.990	0.0854	0.8693
	0.85	0.000	0.990	0.0000	0.8693
	0.95	0.008	0.998	0.0868	0.9561
	1.05	0.003	1.000	0.0439	1.0000

DRUM(1) -SURFACTANT CASE

PACKING HEIGHT = 1.40 METRES

RUN	D	N	C	V	CV
1-1- 3	0.05	0.118	0.118	0.0002	0.0002
	0.15	0.217	0.335	0.0118	0.0120
	0.25	0.150	0.485	0.0377	0.0497
	0.35	0.191	0.676	0.1316	0.1813
	0.45	0.173	0.849	0.2534	0.4347
	0.55	0.107	0.956	0.2861	0.7208
	0.65	0.023	0.979	0.1015	0.8223
	0.75	0.013	0.992	0.0881	0.9104
	0.85	0.003	0.995	0.0296	0.9401
	0.95	0.003	0.998	0.0413	0.9814
	1.05	0.001	1.000	0.0186	1.0000
1-1- 4	0.05	0.246	0.246	0.0006	0.0006
	0.15	0.152	0.398	0.0099	0.0105
	0.25	0.138	0.536	0.0416	0.0521
	0.35	0.182	0.718	0.1507	0.2029
	0.45	0.158	0.876	0.2781	0.4810
	0.55	0.090	0.966	0.2892	0.7702
	0.65	0.018	0.984	0.0955	0.8656
	0.75	0.013	0.997	0.1059	0.9716
	0.85	0.001	0.998	0.0119	0.9834
	0.95	0.001	1.000	0.0166	1.0000

DRUM(1) -SURFACTANT CASE

PACKING HEIGHT = 1.40 METRES

RUN	D	N	C	V	CV
1-1- 5	0.05	0.131	0.131	0.0003	0.0003
	0.15	0.201	0.332	0.0144	0.0148
	0.25	0.199	0.531	0.0662	0.0809
	0.35	0.248	0.779	0.2262	0.3072
	0.45	0.121	0.900	0.2346	0.5417
	0.55	0.063	0.963	0.2230	0.7647
	0.65	0.031	0.994	0.1811	0.9459
	0.75	0.004	0.998	0.0359	0.9818
	0.85	0.000	0.998	0.0000	0.9818
	0.95	0.001	1.000	0.0182	1.0000
1-1- 6	0.05	0.129	0.129	0.0003	0.0003
	0.15	0.202	0.331	0.0108	0.0110
	0.25	0.177	0.508	0.0438	0.0548
	0.35	0.182	0.690	0.1235	0.1784
	0.45	0.166	0.856	0.2395	0.4178
	0.55	0.090	0.946	0.2370	0.6549
	0.65	0.036	0.982	0.1565	0.8114
	0.75	0.011	0.993	0.0735	0.8849
	0.85	0.002	0.995	0.0194	0.9043
	0.95	0.003	0.998	0.0407	0.9450
	1.05	0.003	1.000	0.0550	1.0000

DRUM(1) -SURFACTANT CASE

PACKING HEIGHT = 1.40 METRES

RUN	D	N	C	V	CV
1-1- 7	0.05	0.124	0.124	0.0003	0.0003
	0.15	0.235	0.359	0.0135	0.0138
	0.25	0.195	0.554	0.0520	0.0658
	0.35	0.166	0.720	0.1215	0.1873
	0.45	0.152	0.872	0.2365	0.4238
	0.55	0.082	0.954	0.2329	0.6568
	0.65	0.026	0.980	0.1219	0.7787
	0.75	0.010	0.990	0.0720	0.8507
	0.85	0.003	0.993	0.0315	0.8822
	0.95	0.004	0.997	0.0586	0.9407
	1.05	0.003	1.000	0.0593	1.0000
1-1-31	0.05	0.125	0.125	0.0002	0.0002
	0.15	0.157	0.282	0.0056	0.0057
	0.25	0.137	0.419	0.0225	0.0282
	0.35	0.175	0.594	0.0789	0.1071
	0.45	0.175	0.769	0.1676	0.2747
	0.55	0.117	0.886	0.2046	0.4793
	0.65	0.055	0.941	0.1587	0.6380
	0.75	0.026	0.967	0.1153	0.7533
	0.85	0.020	0.987	0.1291	0.8824
	0.95	0.009	0.996	0.0811	0.9635
	1.05	0.003	1.000	0.0365	1.0000

DRUM(1) -SURFACTANT CASE

PACKING HEIGHT = 1.40 METRES

RUN	D	N	C	V	CV
1-1-32	0.05	0.181	0.181	0.0004	0.0004
	0.15	0.175	0.356	0.0092	0.0095
	0.25	0.117	0.473	0.0284	0.0379
	0.35	0.206	0.679	0.1371	0.1749
	0.45	0.175	0.854	0.2475	0.4224
	0.55	0.085	0.939	0.2195	0.6419
	0.65	0.035	0.974	0.1492	0.7910
	0.75	0.018	0.992	0.1178	0.9089
	0.85	0.003	0.995	0.0286	0.9375
	0.95	0.002	0.997	0.0266	0.9641
	1.05	0.002	1.000	0.0359	1.0000
1-1-34	0.05	0.079	0.079	0.0001	0.0001
	0.15	0.232	0.311	0.0107	0.0108
	0.25	0.186	0.497	0.0396	0.0504
	0.35	0.181	0.678	0.1057	0.1561
	0.45	0.135	0.813	0.1676	0.3237
	0.55	0.107	0.920	0.2425	0.5663
	0.65	0.046	0.966	0.1721	0.7384
	0.75	0.021	0.987	0.1207	0.8591
	0.85	0.007	0.994	0.0586	0.9176
	0.95	0.003	0.997	0.0350	0.9527
	1.05	0.003	1.000	0.0473	1.0000

DRUM(1) -SURFACTANT CASE

PACKING HEIGHT = 1.40 METRES

RUN	D	N	C	V	CV
1-1-35	0.05	0.121	0.121	0.0002	0.0002
	0.15	0.215	0.336	0.0102	0.0105
	0.25	0.165	0.501	0.0264	0.0469
	0.35	0.165	0.666	0.0999	0.1468
	0.45	0.166	0.832	0.2137	0.3605
	0.55	0.104	0.936	0.2444	0.6049
	0.65	0.035	0.971	0.1358	0.7407
	0.75	0.017	0.988	0.1013	0.8420
	0.85	0.006	0.994	0.0520	0.8940
	0.95	0.002	0.996	0.0242	0.9182
	1.05	0.002	0.998	0.0327	0.9509
	1.15	0.001	0.999	0.0215	0.9724
	1.25	0.001	1.000	0.0276	1.0000
1-1-36	0.05	0.070	0.070	0.0001	0.0001
	0.15	0.154	0.224	0.0045	0.0046
	0.25	0.152	0.376	0.0205	0.0251
	0.35	0.165	0.541	0.0612	0.0863
	0.45	0.175	0.716	0.1380	0.2243
	0.55	0.142	0.858	0.2044	0.4287
	0.65	0.070	0.928	0.1663	0.5950
	0.75	0.030	0.958	0.1095	0.7046
	0.85	0.017	0.975	0.0903	0.7949
	0.95	0.016	0.991	0.1187	0.9136
	1.05	0.003	0.994	0.0300	0.9436
	1.15	0.003	0.997	0.0395	0.9831
	1.25	0.001	1.000	0.0169	1.0000

DRUM(1) -SURFACTANT CASE

PACKING HEIGHT = 1.40 METRES

RUN	D	N	C	V	CV
1-1-37	0.05	0.117	0.117	0.0001	0.0001
	0.15	0.203	0.320	0.0058	0.0060
	0.25	0.147	0.467	0.0196	0.0255
	0.35	0.116	0.583	0.0424	0.0679
	0.45	0.133	0.716	0.1033	0.1712
	0.55	0.115	0.831	0.1630	0.3342
	0.65	0.070	0.901	0.1638	0.4980
	0.75	0.045	0.946	0.1617	0.6597
	0.85	0.027	0.973	0.1413	0.8010
	0.95	0.021	0.994	0.1534	0.9544
	1.05	0.002	0.996	0.0197	0.9741
	1.15	0.002	1.000	0.0259	1.0000
1-1-38	0.05	0.211	0.211	0.0004	0.0004
	0.15	0.172	0.383	0.0093	0.0098
	0.25	0.130	0.513	0.0327	0.0425
	0.35	0.176	0.689	0.1214	0.1639
	0.45	0.140	0.829	0.2053	0.3692
	0.55	0.103	0.932	0.2758	0.6450
	0.65	0.055	0.987	0.2431	0.8881
	0.75	0.011	0.998	0.0747	0.9627
	0.85	0.000	0.998	0.0000	0.9627
	0.95	0.000	0.998	0.0000	0.9627
	1.05	0.002	1.000	0.0373	1.0000

DRUM(1) -SURFACTANT CASE

PACKING HEIGHT = 1.40 METRES

RUN	D	N	C	V	CV
1-1-39	0.05	0.130	0.130	0.0002	0.0002
	0.15	0.172	0.302	0.0081	0.0083
	0.25	0.154	0.456	0.0335	0.0418
	0.35	0.202	0.658	0.1205	0.1623
	0.45	0.167	0.825	0.2117	0.3740
	0.55	0.104	0.929	0.2407	0.6147
	0.65	0.042	0.971	0.1605	0.7752
	0.75	0.025	0.996	0.1467	0.9219
	0.85	0.000	0.996	0.0000	0.9219
	0.95	0.003	0.999	0.0358	0.9577
	1.05	0.000	0.999	0.0000	0.9577
	1.15	0.002	1.000	0.0423	1.0000
1-1-40	0.05	0.163	0.163	0.0004	0.0004
	0.15	0.214	0.377	0.0142	0.0146
	0.25	0.163	0.540	0.0499	0.0645
	0.35	0.148	0.688	0.1244	0.1889
	0.45	0.173	0.861	0.3091	0.4981
	0.55	0.093	0.954	0.3034	0.8015
	0.65	0.003	0.957	0.0162	0.8177
	0.75	0.011	0.968	0.0910	0.9087
	0.85	0.002	0.970	0.0241	0.9327
	0.95	0.004	1.000	0.0673	1.0000

DRUM(1) -SURFACTANT CASE

PACKING HEIGHT = 1.40 METRES

RUN	D	N	C	V	CV
1-1-41	0.05	0.132	0.132	0.0003	0.0003
	0.15	0.230	0.362	0.0132	0.0135
	0.25	0.181	0.543	0.0482	0.0618
	0.35	0.172	0.715	0.1258	0.1875
	0.45	0.141	0.856	0.2191	0.4067
	0.55	0.091	0.947	0.2582	0.6649
	0.65	0.039	0.986	0.1827	0.8475
	0.75	0.008	0.994	0.0576	0.9051
	0.85	0.001	0.995	0.0105	0.9156
	0.95	0.004	0.999	0.0585	0.9741
	1.05	0.000	0.999	0.0000	0.9741
	1.15	0.001	1.000	0.0259	1.0000
1-1-42	0.05	0.161	0.161	0.0003	0.0003
	0.15	0.261	0.422	0.0144	0.0148
	0.25	0.141	0.563	0.0361	0.0509
	0.35	0.154	0.717	0.1083	0.1592
	0.45	0.132	0.849	0.1972	0.3564
	0.55	0.088	0.937	0.2401	0.5965
	0.65	0.032	0.969	0.1441	0.7406
	0.75	0.017	0.986	0.1176	0.8582
	0.85	0.004	0.990	0.0403	0.8985
	0.95	0.003	0.993	0.0422	0.9407
	1.05	0.001	0.994	0.0190	0.9597
	1.15	0.000	0.994	0.0000	0.9597
	1.25	0.000	0.994	0.0000	0.9597
	1.35	0.001	1.000	0.0403	1.0000

DRUM(1) -SURFACTANT CASE

PACKING HEIGHT = 1.40 METRES

RUN	D	N	C	V	CV
1-1-43	0.05	0.148	0.148	0.0002	0.0002
	0.15	0.264	0.412	0.0097	0.0099
	0.25	0.138	0.550	0.0235	0.0333
	0.35	0.127	0.677	0.0592	0.0926
	0.45	0.103	0.780	0.1021	0.1946
	0.55	0.094	0.874	0.1701	0.3647
	0.65	0.068	0.942	0.2031	0.5678
	0.75	0.036	0.978	0.1652	0.7330
	0.85	0.005	0.983	0.0334	0.7664
	0.95	0.009	0.992	0.0839	0.8503
	1.05	0.004	0.996	0.0504	0.9007
	1.15	0.004	1.000	0.0662	0.9668
	1.25	0.000	1.000	0.0000	0.9668
	1.35	0.000	1.000	0.0000	0.9668
	1.45	0.001	1.000	0.0332	1.0000
1-1-44	0.05	0.096	0.096	0.0001	0.0001
	0.15	0.104	0.200	0.0037	0.0038
	0.25	0.126	0.326	0.0208	0.0247
	0.35	0.181	0.507	0.0821	0.1068
	0.45	0.248	0.755	0.2391	0.3458
	0.55	0.152	0.907	0.2675	0.6134
	0.65	0.056	0.963	0.1627	0.7761
	0.75	0.022	0.985	0.0982	0.8742
	0.85	0.004	0.989	0.0260	0.9002
	0.95	0.011	1.000	0.0998	1.0000

DRUM(1) -SURFACTANT CASE

PACKING HEIGHT = 1.40 METRES

RUN	D	N	C	V	CV
1-1-45	0.05	0.137	0.137	0.0003	0.0003
	0.15	0.254	0.391	0.0138	0.0141
	0.25	0.143	0.534	0.0361	0.0502
	0.35	0.156	0.690	0.1080	0.1582
	0.45	0.165	0.855	0.2427	0.4009
	0.55	0.097	0.952	0.2605	0.6614
	0.65	0.030	0.982	0.1330	0.7944
	0.75	0.008	0.990	0.0545	0.8489
	0.85	0.004	0.994	0.0397	0.8886
	0.95	0.004	0.998	0.0554	0.9439
	1.05	0.003	1.000	0.0561	1.0000
1-1-46	0.05	0.158	0.158	0.0003	0.0003
	0.15	0.233	0.391	0.0122	0.0125
	0.25	0.141	0.532	0.0341	0.0465
	0.35	0.171	0.703	0.1134	0.1599
	0.45	0.150	0.853	0.2114	0.3713
	0.55	0.088	0.941	0.2264	0.5977
	0.65	0.035	0.976	0.1487	0.7464
	0.75	0.013	0.989	0.0848	0.8312
	0.85	0.005	0.994	0.0475	0.8787
	0.95	0.004	0.998	0.0530	0.9317
	1.05	0.000	0.998	0.0000	0.9317
	1.15	0.000	0.998	0.0000	0.9317
	1.25	0.001	0.999	0.0302	0.9619
	1.35	0.001	1.000	0.0381	1.0000

DRUM(1) -SURFACTANT CASE

PACKING HEIGHT = 1.40 METRES

RUN	D	N	C	V	CV
1-1-47	0.05	0.247	0.247	0.0005	0.0005
	0.15	0.237	0.484	0.0127	0.0131
	0.25	0.116	0.600	0.0287	0.0418
	0.35	0.124	0.724	0.0841	0.1260
	0.45	0.104	0.828	0.1500	0.2759
	0.55	0.090	0.918	0.2369	0.5129
	0.65	0.048	0.966	0.2086	0.7214
	0.75	0.023	0.989	0.1535	0.8750
	0.85	0.004	0.993	0.0389	0.9138
	0.95	0.005	0.998	0.0678	0.9817
	1.05	0.001	1.000	0.0183	1.0000
1-1-48	0.05	0.202	0.202	0.0003	0.0003
	0.15	0.296	0.498	0.0117	0.0120
	0.25	0.100	0.598	0.0183	0.0304
	0.35	0.096	0.694	0.0483	0.0787
	0.45	0.101	0.795	0.1080	0.1867
	0.55	0.091	0.886	0.1777	0.3644
	0.65	0.054	0.940	0.1740	0.5384
	0.75	0.032	0.972	0.1584	0.6968
	0.85	0.013	0.985	0.0937	0.7905
	0.95	0.009	0.994	0.0906	0.8811
	1.05	0.004	0.998	0.0543	0.9354
	1.15	0.002	1.000	0.0357	0.9711
	1.25	0.000	1.000	0.0000	0.9711
	1.35	0.001	1.000	0.0289	1.0000

DRUM(1) -SURFACTANT CASE

PACKING HEIGHT = 0.00 METRES

RUN	D	N	C	V	CV
1-1-49	0.05	0.000	0.000	0.0000	0.0000
	0.15	0.000	0.000	0.0000	0.0000
	0.25	0.000	0.000	0.0000	0.0000
	0.35	0.000	0.000	0.0000	0.0000
	0.45	0.000	0.000	0.0000	0.0000
	0.55	0.000	0.000	0.0000	0.0000
	0.65	0.064	0.064	0.0243	0.0243
	0.75	0.149	0.213	0.0871	0.1114
	0.85	0.277	0.489	0.2355	0.3469
	0.95	0.425	0.915	0.5058	0.8527
	1.05	0.064	0.979	0.1024	0.9551
	1.15	0.021	1.000	0.0449	1.0000
1-1-50	0.05	0.264	0.264	0.0001	0.0001
	0.15	0.158	0.422	0.0022	0.0023
	0.25	0.021	0.443	0.0014	0.0037
	0.35	0.016	0.459	0.0028	0.0064
	0.45	0.000	0.459	0.0000	0.0064
	0.55	0.032	0.491	0.0216	0.0280
	0.65	0.158	0.649	0.1770	0.2050
	0.75	0.231	0.880	0.3975	0.6026
	0.85	0.053	0.933	0.1328	0.7353
	0.95	0.035	0.968	0.1238	0.8592
	1.05	0.016	0.984	0.0751	0.9342
	1.15	0.011	1.000	0.0658	1.0000

DRUM(1) -SURFACTANT CASE

PACKING HEIGHT = 0.03 METRES

RUN	D	N	C	V	CV
1-1-51	0.05	0.021	0.021	0.0000	0.0000
	0.15	0.021	0.041	0.0001	0.0001
	0.25	0.021	0.062	0.0003	0.0004
	0.35	0.021	0.082	0.0009	0.0013
	0.45	0.041	0.124	0.0040	0.0053
	0.55	0.000	0.124	0.0000	0.0053
	0.65	0.021	0.144	0.0060	0.0113
	0.75	0.041	0.185	0.0184	0.0297
	0.85	0.113	0.299	0.0736	0.1032
	0.95	0.289	0.588	0.2615	0.3647
	1.05	0.217	0.804	0.2648	0.6295
	1.15	0.124	0.928	0.1988	0.8283
	1.25	0.041	0.969	0.0850	0.9133
	1.35	0.021	0.990	0.0535	0.9668
	1.45	0.010	1.000	0.0332	1.0000
1-1-52	0.05	0.146	0.146	0.0000	0.0000
	0.15	0.146	0.293	0.0008	0.0008
	0.25	0.024	0.317	0.0006	0.0014
	0.35	0.012	0.329	0.0008	0.0022
	0.45	0.012	0.341	0.0018	0.0040
	0.55	0.024	0.366	0.0064	0.0104
	0.65	0.037	0.402	0.0159	0.0263
	0.75	0.073	0.476	0.0487	0.0750
	0.85	0.207	0.683	0.2009	0.2759
	0.95	0.110	0.793	0.1485	0.4244
	1.05	0.037	0.829	0.0669	0.4913
	1.15	0.085	0.915	0.2049	0.6962
	1.25	0.049	0.964	0.1504	0.8466
	1.35	0.024	0.988	0.0947	0.9413
	1.45	0.012	1.000	0.0587	1.0000

DRUM(1) -SURFACTANT CASE

PACKING HEIGHT = 0.05 METRES

RUN	D	N	C	V	CV
1-1-53	0.05	0.160	0.160	0.0001	0.0001
	0.15	0.075	0.234	0.0007	0.0008
	0.25	0.032	0.266	0.0014	0.0022
	0.35	0.075	0.341	0.0092	0.0114
	0.45	0.085	0.426	0.0223	0.0337
	0.55	0.075	0.500	0.0356	0.0693
	0.65	0.117	0.617	0.0924	0.1617
	0.75	0.128	0.745	0.1549	0.3166
	0.85	0.128	0.873	0.2255	0.5420
	0.95	0.064	0.936	0.1573	0.6993
	1.05	0.032	0.968	0.1062	0.8054
	1.15	0.000	0.968	0.0000	0.8054
	1.25	0.021	0.990	0.1196	0.9250
	1.35	0.011	1.000	0.0750	1.0000
1-1-54	0.05	0.213	0.213	0.0001	0.0001
	0.15	0.101	0.314	0.0010	0.0011
	0.25	0.053	0.367	0.0025	0.0037
	0.35	0.048	0.415	0.0063	0.0099
	0.45	0.069	0.484	0.0192	0.0291
	0.55	0.080	0.564	0.0405	0.0696
	0.65	0.069	0.633	0.0579	0.1275
	0.75	0.133	0.766	0.1711	0.2986
	0.85	0.064	0.830	0.1195	0.4181
	0.95	0.080	0.910	0.2087	0.6269
	1.05	0.048	0.958	0.1691	0.7959
	1.15	0.037	0.995	0.1725	0.9684
	1.25	0.005	1.000	0.0316	1.0000

DRUM(1) -SURFACTANT CASE

PACKING HEIGHT = 0.10 METRES

RUN	D	N	C	V	CV
1-1-55	0.05	0.135	0.135	0.0001	0.0001
	0.15	0.153	0.287	0.0018	0.0019
	0.25	0.084	0.371	0.0047	0.0066
	0.35	0.091	0.462	0.0139	0.0204
	0.45	0.058	0.520	0.0189	0.0393
	0.55	0.076	0.596	0.0453	0.0847
	0.65	0.131	0.727	0.1281	0.2128
	0.75	0.116	0.844	0.1750	0.3878
	0.85	0.047	0.891	0.1035	0.4914
	0.95	0.044	0.935	0.1332	0.6246
	1.05	0.026	0.960	0.1052	0.7299
	1.15	0.018	0.978	0.0987	0.8285
	1.25	0.011	0.989	0.0759	0.9044
	1.35	0.011	1.000	0.0956	1.0000
1-1-56	0.05	0.156	0.156	0.0001	0.0001
	0.15	0.186	0.342	0.0030	0.0031
	0.25	0.119	0.461	0.0088	0.0119
	0.35	0.048	0.509	0.0099	0.0218
	0.45	0.093	0.602	0.0403	0.0621
	0.55	0.071	0.673	0.0559	0.1180
	0.65	0.093	0.766	0.1215	0.2395
	0.75	0.093	0.859	0.1867	0.4263
	0.85	0.063	0.922	0.1847	0.6110
	0.95	0.041	0.963	0.1665	0.7774
	1.05	0.011	0.974	0.0612	0.8386
	1.15	0.022	1.000	0.1614	1.0000

DRUM(1) -SURFACTANT CASE

PACKING HEIGHT = 0.15 METRES

RUN	D	N	C	V	CV
1-1-57	0.05	0.126	0.126	0.0001	0.0001
	0.15	0.154	0.280	0.0022	0.0023
	0.25	0.091	0.371	0.0060	0.0083
	0.35	0.104	0.475	0.0189	0.0272
	0.45	0.082	0.557	0.0314	0.0586
	0.55	0.101	0.657	0.0706	0.1291
	0.65	0.104	0.761	0.1202	0.2492
	0.75	0.076	0.837	0.1343	0.3835
	0.85	0.060	0.896	0.1545	0.5380
	0.95	0.055	0.951	0.1970	0.7350
	1.05	0.041	0.992	0.1991	0.9341
	1.15	0.006	0.998	0.0404	0.9745
	1.25	0.003	1.000	0.0255	1.0000
1-1-58	0.05	0.117	0.117	0.0001	0.0001
	0.15	0.163	0.280	0.0026	0.0026
	0.25	0.074	0.354	0.0054	0.0080
	0.35	0.070	0.424	0.0140	0.0220
	0.45	0.124	0.549	0.0529	0.0750
	0.55	0.070	0.619	0.0544	0.1293
	0.65	0.132	0.751	0.1695	0.2988
	0.75	0.109	0.860	0.2147	0.5135
	0.85	0.086	0.945	0.2454	0.7589
	0.95	0.043	0.988	0.1713	0.9302
	1.05	0.008	0.996	0.0422	0.9723
	1.15	0.004	1.000	0.0277	1.0000

DRUM(1) -SURFACTANT CASE

PACKING HEIGHT = 0.20 METRES

RUN	D	N	C	V	CV
1-1-59	0.05	0.246	0.246	0.0002	0.0002
	0.15	0.230	0.477	0.0052	0.0054
	0.25	0.071	0.547	0.0074	0.0128
	0.35	0.060	0.607	0.0173	0.0302
	0.45	0.107	0.715	0.0656	0.0959
	0.55	0.065	0.780	0.0730	0.1688
	0.65	0.097	0.877	0.1786	0.3474
	0.75	0.047	0.924	0.1334	0.4808
	0.85	0.031	0.956	0.1294	0.6102
	0.95	0.026	0.982	0.1508	0.7610
	1.05	0.005	0.987	0.0404	0.8014
	1.15	0.000	0.987	0.0000	0.8014
	1.25	0.005	0.992	0.0682	0.8695
	1.35	0.008	1.000	0.1305	1.0000
1-1-60	0.05	0.272	0.272	0.0003	0.0003
	0.15	0.222	0.494	0.0063	0.0066
	0.25	0.104	0.598	0.0137	0.0204
	0.35	0.053	0.652	0.0194	0.0397
	0.45	0.090	0.742	0.0693	0.1091
	0.55	0.065	0.806	0.0910	0.2001
	0.65	0.084	0.891	0.1960	0.3960
	0.75	0.045	0.935	0.1603	0.5564
	0.85	0.034	0.969	0.1752	0.7316
	0.95	0.017	0.986	0.1226	0.8542
	1.05	0.011	0.997	0.1097	0.9640
	1.15	0.003	1.000	0.0360	1.0000

DRUM(1) -SURFACTANT CASE

PACKING HEIGHT = 0.30 METRES

RUN	D	N	C	V	CV
1-1-61	0.05	0.077	0.077	0.0001	0.0001
	0.15	0.160	0.237	0.0031	0.0031
	0.25	0.089	0.325	0.0078	0.0109
	0.35	0.112	0.438	0.0272	0.0381
	0.45	0.103	0.541	0.0529	0.0910
	0.55	0.153	0.694	0.1437	0.2347
	0.65	0.127	0.821	0.1965	0.4312
	0.75	0.093	0.914	0.2221	0.6533
	0.85	0.060	0.974	0.2072	0.8606
	0.95	0.019	0.993	0.0924	0.9530
	1.05	0.007	1.000	0.0470	1.0000
1-1-62	0.05	0.215	0.215	0.0002	0.0002
	0.15	0.151	0.365	0.0032	0.0033
	0.25	0.090	0.455	0.0087	0.0120
	0.35	0.096	0.551	0.0254	0.0374
	0.45	0.156	0.707	0.0884	0.1258
	0.55	0.101	0.809	0.1045	0.2303
	0.65	0.139	0.948	0.2367	0.4670
	0.75	0.078	1.026	0.2047	0.6717
	0.85	0.038	1.064	0.1435	0.8151
	0.95	0.035	1.000	0.1849	1.0000

DRUM(1) -SURFACTANT CASE

PACKING HEIGHT = 0.45 METRES

RUN	D	N	C	V	CV
1-1-63	0.05	0.152	0.152	0.0002	0.0002
	0.15	0.198	0.350	0.0058	0.0060
	0.25	0.095	0.445	0.0130	0.0190
	0.35	0.127	0.572	0.0475	0.0665
	0.45	0.113	0.686	0.0898	0.1564
	0.55	0.138	0.823	0.1998	0.3562
	0.65	0.113	0.936	0.2707	0.6270
	0.75	0.042	0.979	0.1559	0.7829
	0.85	0.004	0.982	0.0187	0.8016
	0.95	0.014	0.996	0.1054	0.9070
	1.05	0.000	0.996	0.0000	0.9070
	1.15	0.000	0.996	0.0000	0.9070
	1.25	0.000	0.996	0.0000	0.9070
	1.35	0.000	0.996	0.0000	0.9070
	1.45	0.004	1.000	0.0930	1.0000
1-1-64	0.05	0.109	0.109	0.0001	0.0001
	0.15	0.180	0.290	0.0060	0.0061
	0.25	0.101	0.391	0.0156	0.0217
	0.35	0.148	0.539	0.0624	0.0842
	0.45	0.160	0.698	0.1436	0.2278
	0.55	0.130	0.828	0.2125	0.4402
	0.65	0.138	0.966	0.3727	0.8129
	0.75	0.016	0.982	0.0674	0.8803
	0.85	0.014	0.996	0.0859	0.9662
	0.95	0.004	1.000	0.0338	1.0000

DRUM(1) -SURFACTANT CASE

PACKING HEIGHT = 0.61 METRES

RUN	D	N	C	V	CV
1-1-65	0.05	0.162	0.162	0.0002	0.0002
	0.15	0.143	0.305	0.0051	0.0053
	0.25	0.134	0.439	0.0221	0.0275
	0.35	0.167	0.606	0.0757	0.1032
	0.45	0.179	0.785	0.1725	0.2757
	0.55	0.069	0.854	0.1214	0.3970
	0.65	0.071	0.925	0.2062	0.6032
	0.75	0.050	0.975	0.2231	0.8263
	0.85	0.016	0.991	0.1039	0.9302
	0.95	0.005	0.996	0.0453	0.9755
	1.05	0.002	1.000	0.0245	1.0000

PACKING HEIGHT = 0.81 METRES

1-1-66	0.05	0.136	0.136	0.0002	0.0002
	0.15	0.198	0.334	0.0063	0.0064
	0.25	0.103	0.437	0.0151	0.0215
	0.35	0.095	0.532	0.0382	0.0598
	0.45	0.169	0.701	0.1445	0.2043
	0.55	0.116	0.817	0.1811	0.3853
	0.65	0.106	0.923	0.2732	0.6585
	0.75	0.056	0.979	0.2217	0.8802
	0.85	0.018	0.997	0.1037	0.9839
	0.95	0.002	1.000	0.0161	1.0000

DRUM(2) - PURE PHASES

PACKING HEIGHT = 1.40 METRES

RUN	D	N	C	V	CV
2-1- 1	0.05	0.092	0.092	0.0001	0.0001
	0.15	0.079	0.171	0.0022	0.0023
	0.25	0.085	0.256	0.0108	0.0131
	0.35	0.151	0.407	0.0527	0.0658
	0.45	0.217	0.624	0.1605	0.2263
	0.55	0.225	0.849	0.3050	0.5313
	0.65	0.079	0.928	0.1760	0.7074
	0.75	0.053	0.980	0.1802	0.8875
	0.85	0.015	0.996	0.0764	0.9639
	0.95	0.002	0.998	0.0153	0.9793
	1.05	0.002	1.000	0.0207	1.0000
2-1- 2	0.05	0.092	0.092	0.0001	0.0001
	0.15	0.067	0.159	0.0020	0.0021
	0.25	0.126	0.285	0.0175	0.0196
	0.35	0.189	0.473	0.0721	0.0917
	0.45	0.212	0.686	0.1723	0.2640
	0.55	0.159	0.845	0.2359	0.4999
	0.65	0.086	0.931	0.2115	0.7114
	0.75	0.057	0.988	0.2143	0.9257
	0.85	0.010	0.998	0.0536	0.9794
	0.95	0.000	0.998	0.0000	0.9794
	1.05	0.002	1.000	0.0206	1.0000

DRUM(2) - PURE PHASES

PACKING HEIGHT = 1.40 METRES

RUN	D	H	C	V	CV
2-1- 6	0.05	0.075	0.075	0.0001	0.0001
	0.15	0.088	0.163	0.0021	0.0022
	0.25	0.088	0.252	0.0099	0.0121
	0.35	0.118	0.369	0.0363	0.0485
	0.45	0.208	0.578	0.1365	0.1850
	0.55	0.212	0.790	0.2539	0.4389
	0.65	0.112	0.902	0.2212	0.6600
	0.75	0.073	0.975	0.2205	0.8806
	0.85	0.022	0.996	0.0954	0.9760
	0.95	0.004	1.000	0.0240	1.0000
2-1- 7	0.05	0.093	0.093	0.0001	0.0001
	0.15	0.112	0.205	0.0039	0.0040
	0.25	0.106	0.311	0.0169	0.0209
	0.35	0.176	0.487	0.0775	0.0984
	0.45	0.240	0.727	0.2248	0.3232
	0.55	0.164	0.890	0.2795	0.6027
	0.65	0.075	0.965	0.2101	0.8128
	0.75	0.023	0.988	0.0988	0.9116
	0.85	0.008	0.996	0.0523	0.9639
	0.95	0.004	1.000	0.0361	1.0000

DRUM(2) - PURE PHASES

PACKING HEIGHT = 1.40 METRES

RUN	D	N	C	V	CV
2-1-14	0.05	0.116	0.116	0.0001	0.0001
	0.15	0.101	0.217	0.0024	0.0025
	0.25	0.085	0.302	0.0094	0.0119
	0.35	0.111	0.413	0.0334	0.0452
	0.45	0.186	0.599	0.1193	0.1646
	0.55	0.196	0.795	0.2292	0.3938
	0.65	0.080	0.874	0.1537	0.5475
	0.75	0.089	0.963	0.2646	0.8122
	0.85	0.025	0.988	0.1090	0.9211
	0.95	0.008	0.996	0.0471	0.9682
	1.05	0.004	1.000	0.0318	1.0000
2-1-15	0.05	0.118	0.118	0.0001	0.0001
	0.15	0.128	0.246	0.0036	0.0037
	0.25	0.114	0.360	0.0148	0.0186
	0.35	0.139	0.499	0.0497	0.0682
	0.45	0.179	0.678	0.1360	0.2042
	0.55	0.135	0.813	0.1869	0.3911
	0.65	0.103	0.916	0.2364	0.6274
	0.75	0.057	0.973	0.1998	0.8273
	0.85	0.017	0.989	0.0860	0.9133
	0.95	0.008	0.998	0.0601	0.9734
	1.05	0.000	0.998	0.0000	0.9734
	1.15	0.002	1.000	0.0266	1.0000

RUN(2) - MASS TRANSFER : TOLUENE TO WATER

PACKING HEIGHT = 1.40 METRES

RUN	D	H	C	V	CV
2-2- 1	0.05	0.338	0.338	0.0004	0.0004
	0.15	0.378	0.716	0.0132	0.0136
	0.25	0.048	0.764	0.0077	0.0213
	0.35	0.034	0.798	0.0151	0.0364
	0.45	0.042	0.840	0.0398	0.0763
	0.55	0.040	0.880	0.0681	0.1443
	0.65	0.026	0.906	0.0735	0.2178
	0.75	0.029	0.934	0.1247	0.3425
	0.85	0.030	0.964	0.1904	0.5329
	0.95	0.012	0.977	0.1090	0.6419
	1.05	0.012	0.989	0.1471	0.7890
	1.15	0.008	0.997	0.1289	0.9179
	1.25	0.001	0.999	0.0283	0.9461
	1.35	0.000	0.999	0.0000	0.9461
	1.45	0.000	0.999	0.0000	0.9461
	1.55	0.001	1.000	0.0539	1.0000
2-2- 2	0.05	0.422	0.422	0.0008	0.0008
	0.15	0.291	0.714	0.0144	0.0152
	0.25	0.077	0.790	0.0175	0.0327
	0.35	0.048	0.839	0.0302	0.0629
	0.45	0.061	0.899	0.0811	0.1440
	0.55	0.028	0.928	0.0689	0.2129
	0.65	0.017	0.944	0.0675	0.2804
	0.75	0.022	0.966	0.1358	0.4162
	0.85	0.016	0.982	0.1411	0.5573
	0.95	0.002	0.984	0.0263	0.5836
	1.05	0.004	0.988	0.0711	0.6548
	1.15	0.003	0.992	0.0690	0.7237
	1.25	0.004	0.996	0.1200	0.8438
	1.35	0.003	0.999	0.1116	0.9554
	1.45	0.001	1.000	0.0446	1.0000

ORUN(2) - MASS TRANSFER : TOLUENE TO WATER

PACKING HEIGHT = 1.40 METRES

RUN	D	H	C	V	CV
2-2- 5	0.05	0.425	0.425	0.0005	0.0005
	0.15	0.246	0.672	0.0081	0.0086
	0.25	0.058	0.730	0.0088	0.0174
	0.35	0.035	0.765	0.0146	0.0320
	0.45	0.049	0.813	0.0431	0.0752
	0.55	0.056	0.869	0.0911	0.1662
	0.65	0.038	0.907	0.1016	0.2679
	0.75	0.029	0.936	0.1188	0.3866
	0.85	0.026	0.962	0.1543	0.5410
	0.95	0.017	0.979	0.1395	0.6804
	1.05	0.012	0.991	0.1376	0.8180
	1.15	0.003	0.994	0.0444	0.8624
	1.25	0.003	0.997	0.0571	0.9195
	1.35	0.002	0.998	0.0359	0.9555
	1.45	0.002	1.000	0.0445	1.0000
2-2- 6	0.05	0.542	0.542	0.0009	0.0009
	0.15	0.237	0.778	0.0112	0.0121
	0.25	0.040	0.819	0.0088	0.0209
	0.35	0.027	0.846	0.0161	0.0370
	0.45	0.024	0.870	0.0308	0.0678
	0.55	0.046	0.915	0.1063	0.1741
	0.65	0.024	0.940	0.0929	0.2670
	0.75	0.020	0.960	0.1191	0.3861
	0.85	0.011	0.971	0.0927	0.4787
	0.95	0.012	0.983	0.1450	0.6237
	1.05	0.007	0.989	0.1084	0.7321
	1.15	0.004	0.993	0.0850	0.8171
	1.25	0.007	1.000	0.1829	1.0000

DRUM(2) - MASS TRANSFER : TOLUENE TO WATER

PACKING HEIGHT = 1.40 METRES

RUN	D	N	C	V	CV
2-2- 8	0.05	0.472	0.472	0.0005	0.0005
	0.15	0.219	0.690	0.0060	0.0065
	0.25	0.041	0.731	0.0052	0.0117
	0.35	0.035	0.766	0.0121	0.0237
	0.45	0.038	0.804	0.0279	0.0517
	0.55	0.049	0.852	0.0659	0.1175
	0.65	0.063	0.915	0.1404	0.2579
	0.75	0.028	0.943	0.0971	0.3550
	0.85	0.025	0.969	0.1258	0.4808
	0.95	0.005	0.973	0.0328	0.5136
	1.05	0.011	0.984	0.1035	0.6171
	1.15	0.006	0.991	0.0779	0.6950
	1.25	0.002	0.992	0.0254	0.7204
	1.35	0.002	0.994	0.0320	0.7524
	1.45	0.002	0.995	0.0397	0.7920
	1.55	0.002	0.997	0.0484	0.8404
	1.65	0.000	0.997	0.0000	0.8404
	1.75	0.000	0.997	0.0000	0.8404
	1.85	0.003	1.000	0.1596	1.0000
2-2- 9	0.05	0.497	0.497	0.0006	0.0006
	0.15	0.234	0.731	0.0071	0.0077
	0.25	0.044	0.775	0.0062	0.0139
	0.35	0.038	0.814	0.0148	0.0287
	0.45	0.020	0.834	0.0165	0.0452
	0.55	0.038	0.872	0.0576	0.1028
	0.65	0.026	0.898	0.0634	0.1662
	0.75	0.037	0.934	0.1392	0.3054
	0.85	0.026	0.960	0.1418	0.4472
	0.95	0.009	0.969	0.0703	0.5176
	1.05	0.015	0.984	0.1524	0.6699
	1.15	0.004	0.987	0.0507	0.7207
	1.25	0.006	0.993	0.0969	0.8175
	1.35	0.006	0.998	0.1220	0.9396
	1.45	0.000	0.998	0.0000	0.9396
	1.55	0.002	1.000	0.0604	1.0000

DRUM(2) - MASS TRANSFER : WATER TO TOLUENE

PACKING HEIGHT = 1.40 METRES

RUN	D	N	C	V	CV
2-3- 1	0.05	0.056	0.056	0.0001	0.0001
	0.15	0.073	0.130	0.0026	0.0026
	0.25	0.140	0.270	0.0228	0.0254
	0.35	0.203	0.473	0.0904	0.1159
	0.45	0.253	0.726	0.2398	0.3556
	0.55	0.170	0.895	0.2932	0.6488
	0.65	0.061	0.956	0.1733	0.8221
	0.75	0.031	0.988	0.1377	0.9598
	0.85	0.006	1.000	0.0402	1.0000
2-3- 8	0.05	0.097	0.097	0.0001	0.0001
	0.15	0.067	0.164	0.0021	0.0023
	0.25	0.106	0.270	0.0157	0.0180
	0.35	0.166	0.436	0.0677	0.0857
	0.45	0.261	0.697	0.2264	0.3121
	0.55	0.179	0.876	0.2835	0.5956
	0.65	0.076	0.951	0.1974	0.7930
	0.75	0.045	0.996	0.1819	0.9749
	0.85	0.004	1.001	0.0251	1.0000
	0.95	0.000	1.001	0.0000	1.0000
	1.05	0.000	1.000	0.0000	1.0000

DRUM(2) -SATURATED PHASES

PACKING HEIGHT = 1.40 METRES

RUN	D	M	C	V	CV
2-4- 5	0.05	0.084	0.084	0.0001	0.0001
	0.15	0.109	0.193	0.0041	0.0043
	0.25	0.135	0.328	0.0238	0.0280
	0.35	0.196	0.524	0.0948	0.1228
	0.45	0.201	0.725	0.2070	0.3298
	0.55	0.186	0.911	0.3482	0.6780
	0.65	0.067	0.977	0.2059	0.8839
	0.75	0.019	0.997	0.0918	0.9758
	0.85	0.004	1.000	0.0242	1.0000
2-4- 6	0.05	0.099	0.099	0.0004	0.0004
	0.15	0.110	0.209	0.0113	0.0117
	0.25	0.181	0.390	0.0855	0.0971
	0.35	0.219	0.608	0.2839	0.3811
	0.45	0.127	0.736	0.3517	0.7328
	0.55	0.034	0.770	0.1724	0.9052
	0.65	0.011	1.000	0.0948	1.0000

DRUM(2) -SATURATED PHASES

PACKING HEIGHT = 1.40 METRES

RUN	D	N	C	V	CV
2-4- 9	0.05	0.160	0.160	0.0003	0.0003
	0.15	0.119	0.279	0.0054	0.0056
	0.25	0.130	0.410	0.0272	0.0329
	0.35	0.179	0.589	0.1026	0.1354
	0.45	0.192	0.780	0.2332	0.3686
	0.55	0.148	0.928	0.3282	0.6968
	0.65	0.055	0.983	0.2015	0.8983
	0.75	0.016	0.998	0.0885	0.9869
	0.85	0.002	1.000	0.0131	1.0000
2-4-10	0.05	0.154	0.154	0.0003	0.0003
	0.15	0.149	0.303	0.0071	0.0073
	0.25	0.145	0.449	0.0320	0.0393
	0.35	0.153	0.601	0.0921	0.1314
	0.45	0.193	0.794	0.2480	0.3794
	0.55	0.144	0.938	0.3364	0.7157
	0.65	0.041	0.979	0.1577	0.8735
	0.75	0.021	1.000	0.1265	1.0000

DRUM(2) -SATURATED PHASES

PACKING HEIGHT = 1.40 METRES

RUN	D	N	C	V	CV
2-4-13	0.05	0.110	0.110	0.0001	0.0001
	0.15	0.135	0.245	0.0048	0.0050
	0.25	0.133	0.378	0.0220	0.0270
	0.35	0.169	0.547	0.0770	0.1040
	0.45	0.188	0.735	0.1818	0.2858
	0.55	0.138	0.872	0.2437	0.5295
	0.65	0.091	0.964	0.2666	0.7960
	0.75	0.026	0.990	0.1160	0.9121
	0.85	0.007	0.997	0.0450	0.9571
	0.95	0.002	0.998	0.0155	0.9725
	1.05	0.000	0.998	0.0000	0.9725
	1.15	0.002	1.000	0.0275	1.0000
2-4-14	0.05	0.156	0.156	0.0003	0.0003
	0.15	0.175	0.331	0.0080	0.0083
	0.25	0.133	0.464	0.0282	0.0365
	0.35	0.131	0.595	0.0764	0.1129
	0.45	0.198	0.793	0.2446	0.3575
	0.55	0.133	0.926	0.3007	0.6582
	0.65	0.051	0.977	0.1913	0.8495
	0.75	0.015	0.992	0.0871	0.9366
	0.85	0.008	1.000	0.0634	1.0000

(2) DISTRIBUTION EQUATIONS

(a) Rosin-Rammler Equation

The cumulative volume form of this equation is:

$$1 - V = \exp\left(- \left(\frac{d}{\bar{d}} \right)^{\alpha} \right)$$

where $\bar{d}$ is a size parameter and α is a distribution parameter. It is normally plotted as

$$\ln \ln \left(\frac{1}{1-V} \right) = \alpha \left(\ln d - \ln \bar{d} \right)$$

(b) Log-Normal Equation

$$V = \frac{1}{\sqrt{\pi}} \int_{-\infty}^{y\alpha} e^{-u^2} \, d u$$

where $y = \ln \left(d / \bar{d} \right)$

The integral may be evaluated using standard tables or the function may be plotted directly onto log-probability paper.

(c) Upper Limit Equation

Instead of using $y = \ln \left(d / \bar{d} \right)$ a bounded function is used:

$$y = \ln \frac{a d^s}{d_m^{\,s} - d^s}$$

where a is a constant, $s = 1, 2,$ or 3 and d_m is the maximum droplet size.

(d) Bayens Function

A normalised gamma distribution function is proposed:

$$f (d, \alpha) = \frac{16}{\pi \bar{a}_v^{\,3}} \; a^2 \exp \left[- \left(\frac{4}{\sqrt{\pi} \, \bar{a}_v^{\,3}} \right)^{\frac{2}{3}} a^2 \right]$$

where

$$\bar{a}_v = \sqrt[3]{\frac{\Sigma n_i \, a_i^{\,3}}{\Sigma n_i}}$$

APPENDIX V

DROPLET HISTOGRAMS

DRUM 1 SURFACTANT CASE

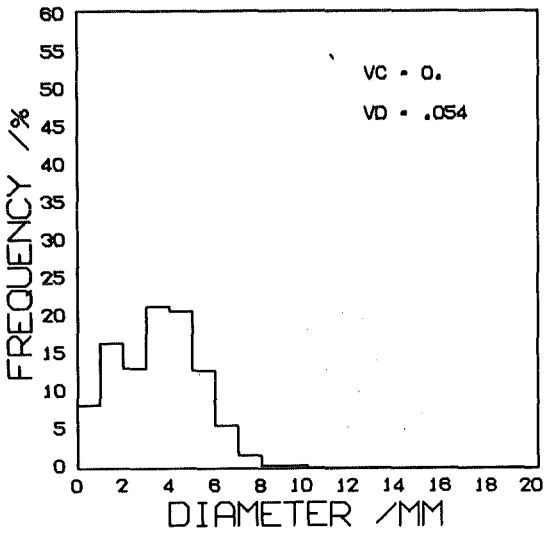

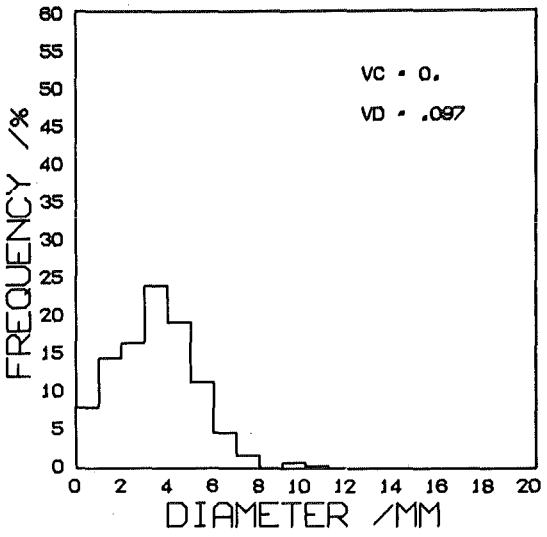

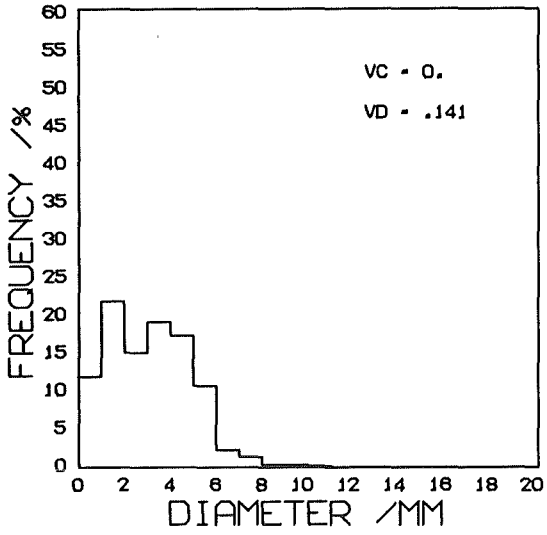

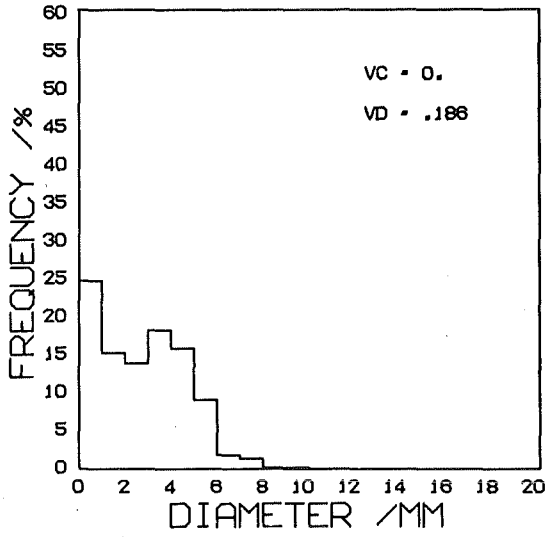

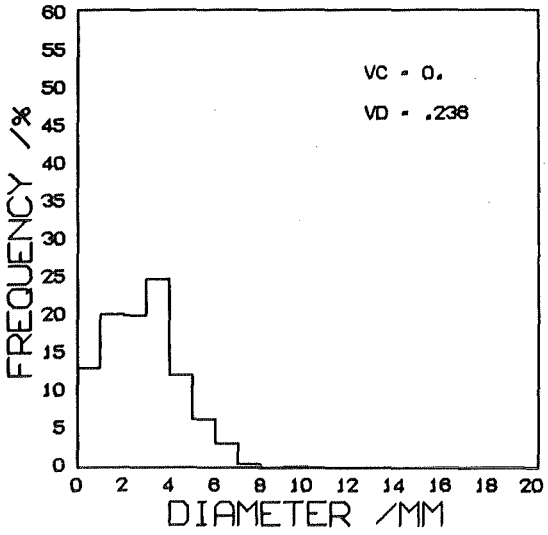

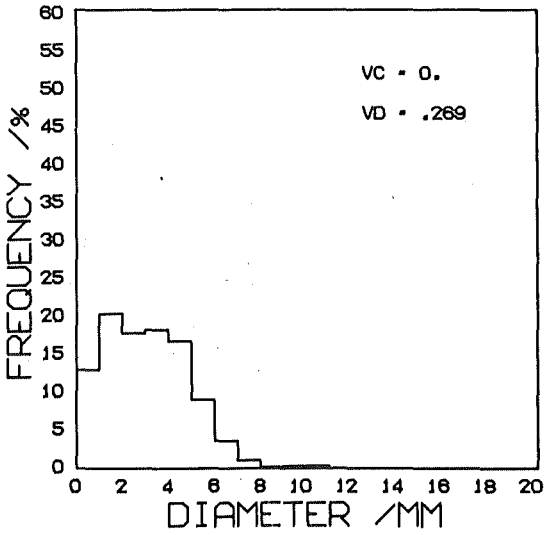

DRUM 1 SURFACTANT CASE

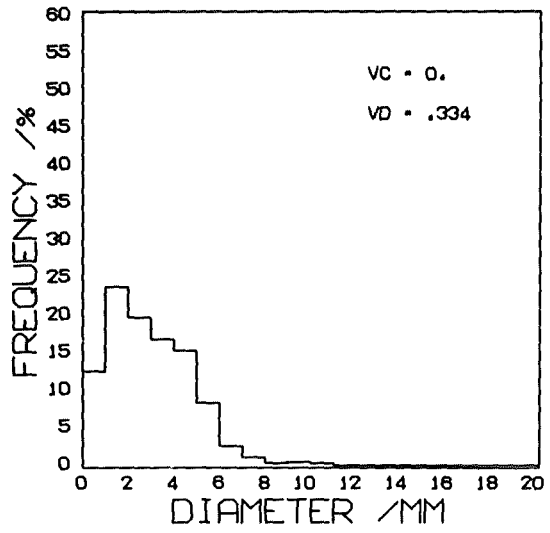

DRUM 1 SURFACTANT CASE

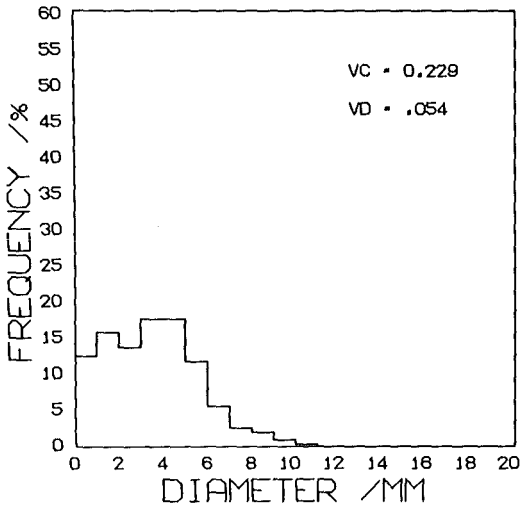

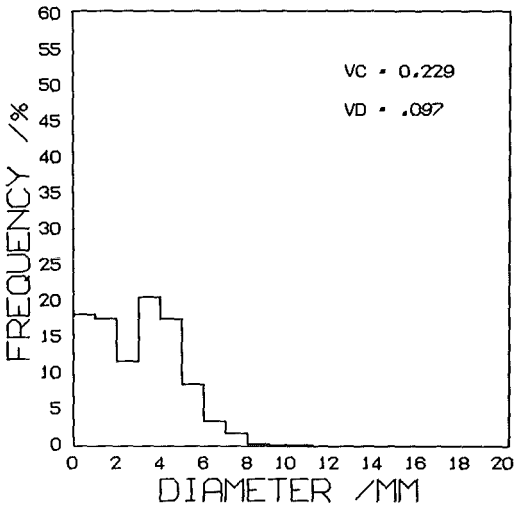

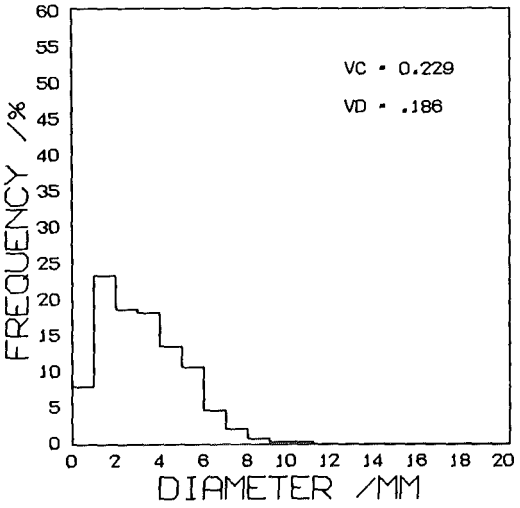

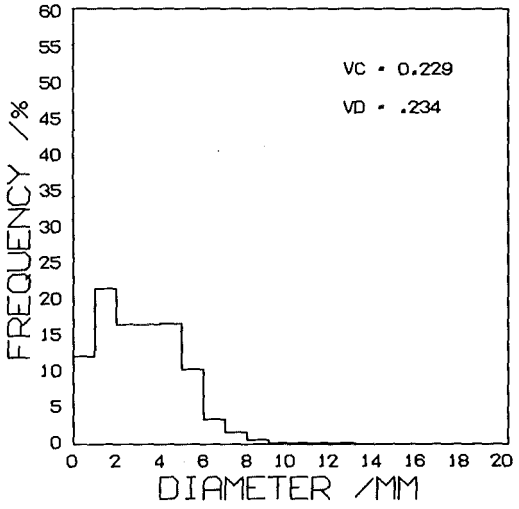

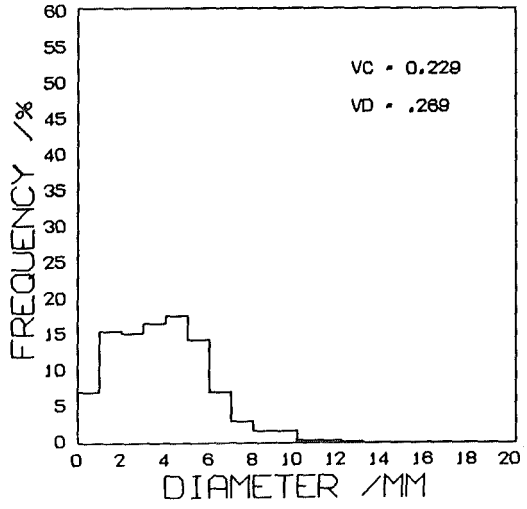

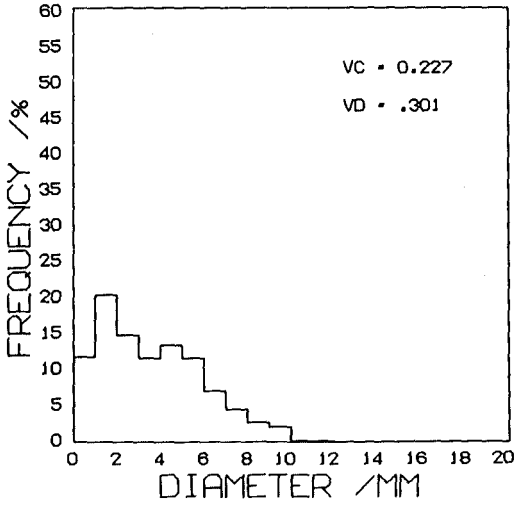

DRUM 1 SURFACTANT CASE

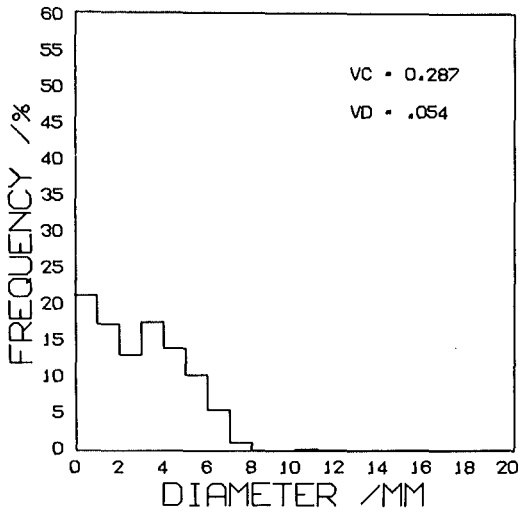

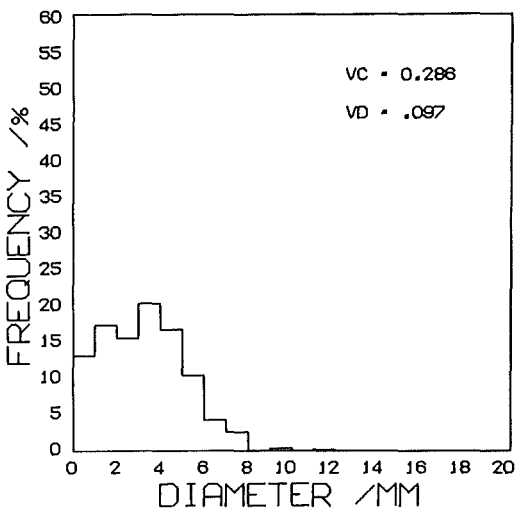

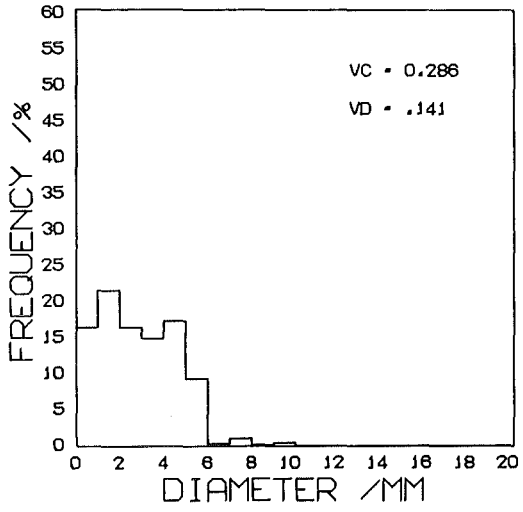

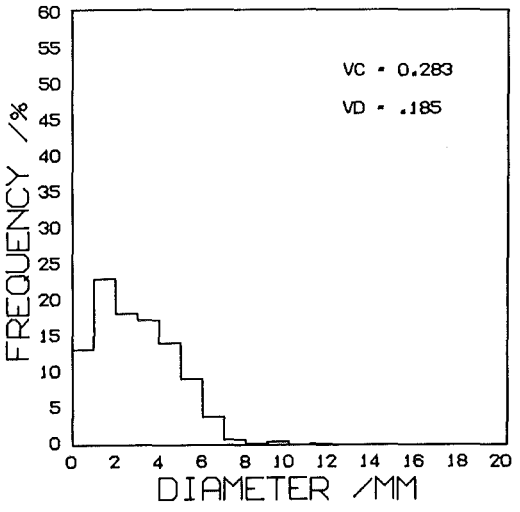

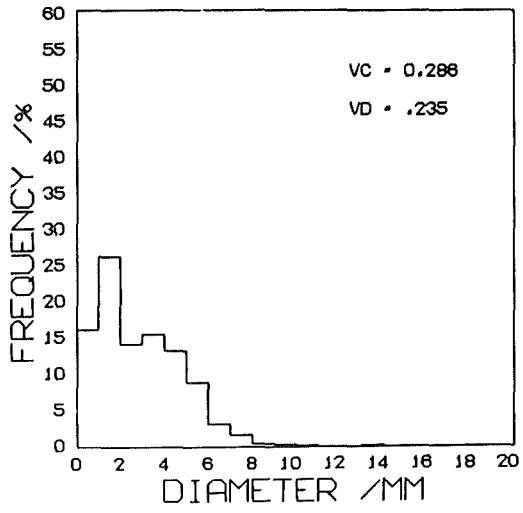

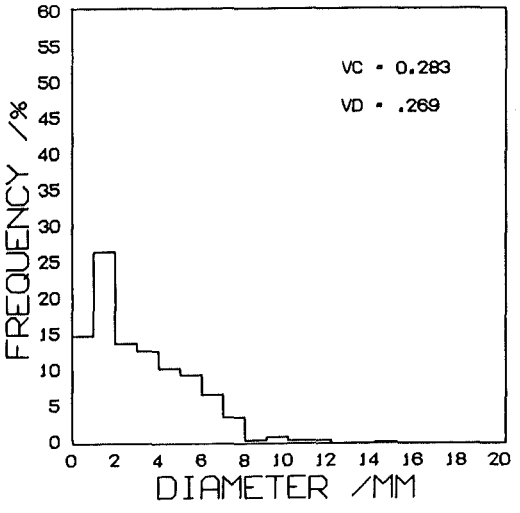

DRUM 1 SURFACTANT CASE

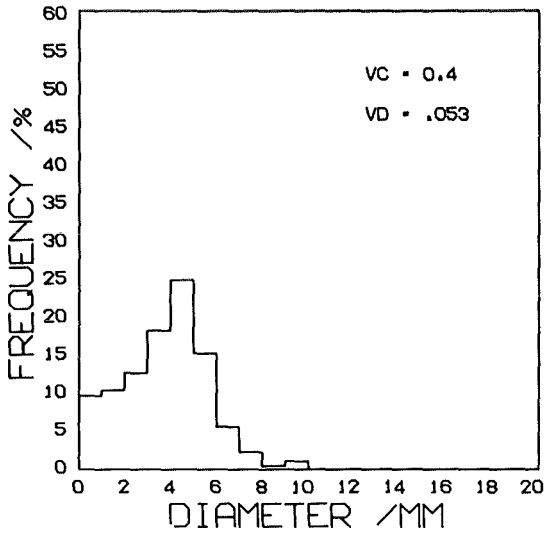

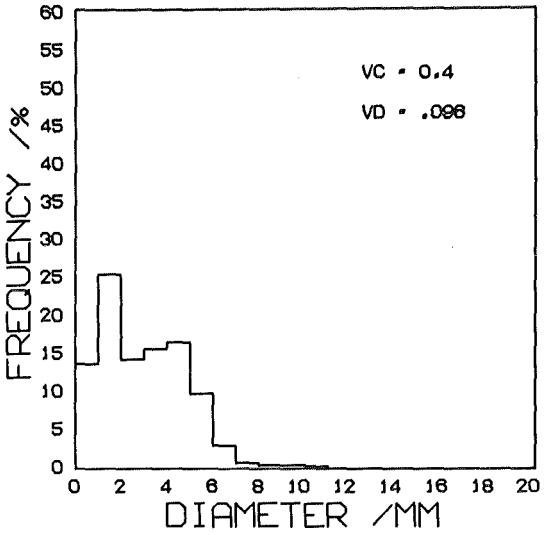

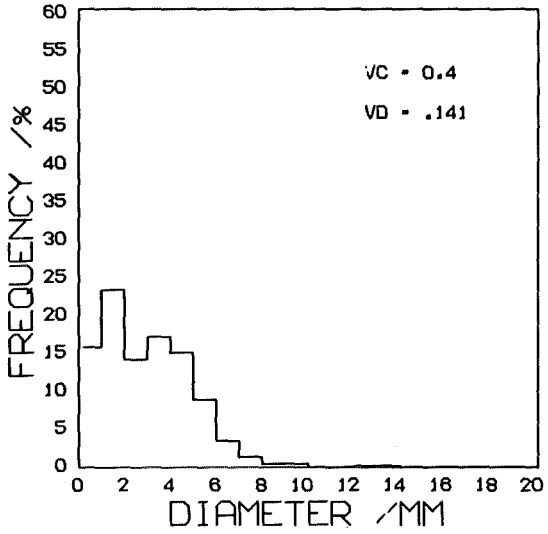

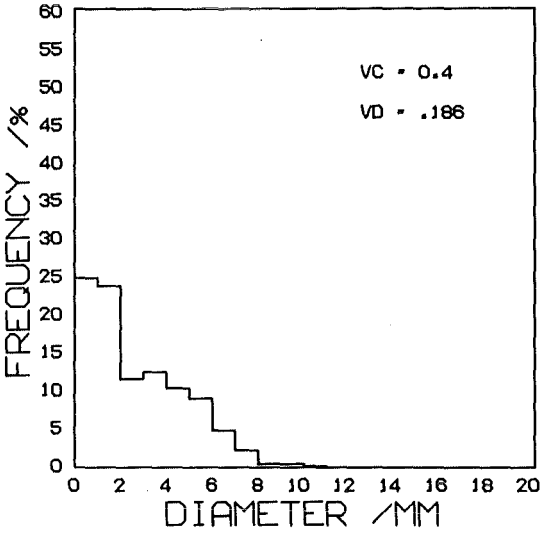

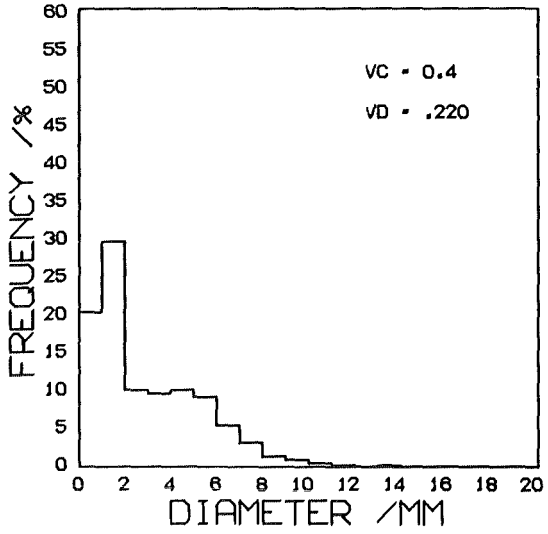

DRUM 1 SURFACTANT CASE

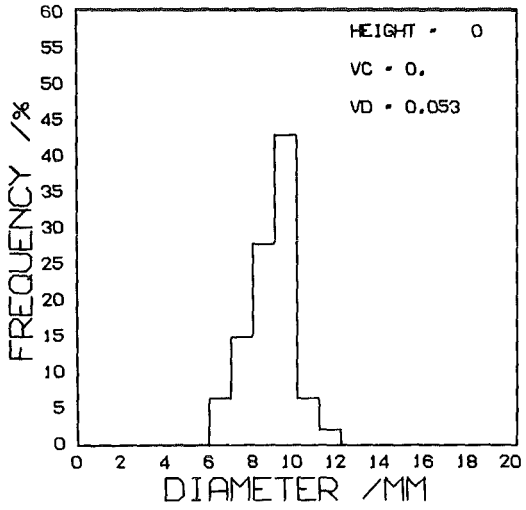

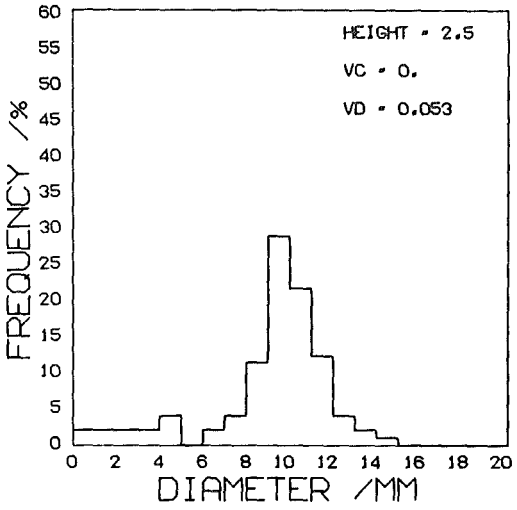

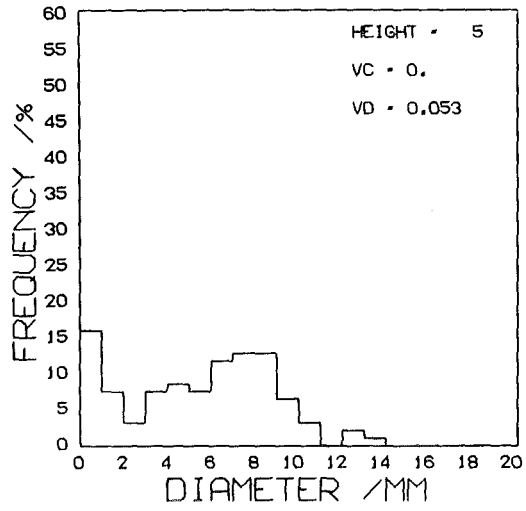

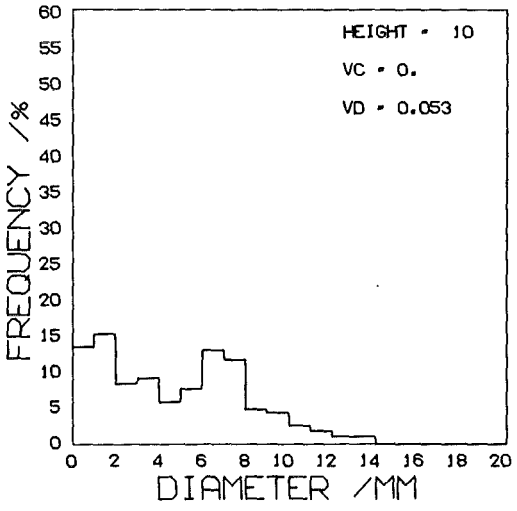

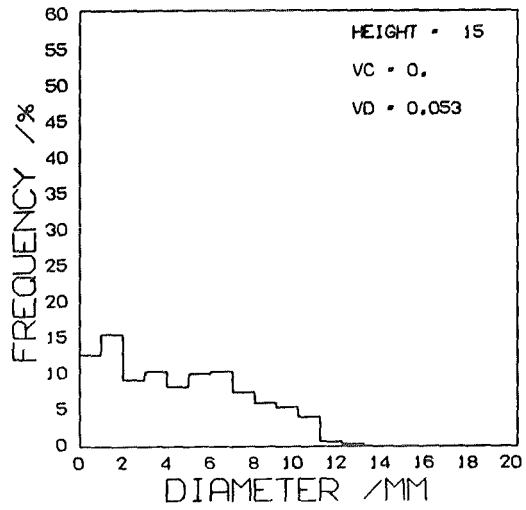

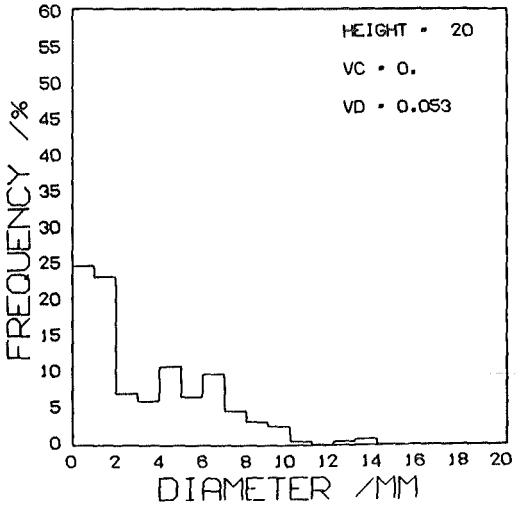

DRUM 1 SURFACTANT CASE

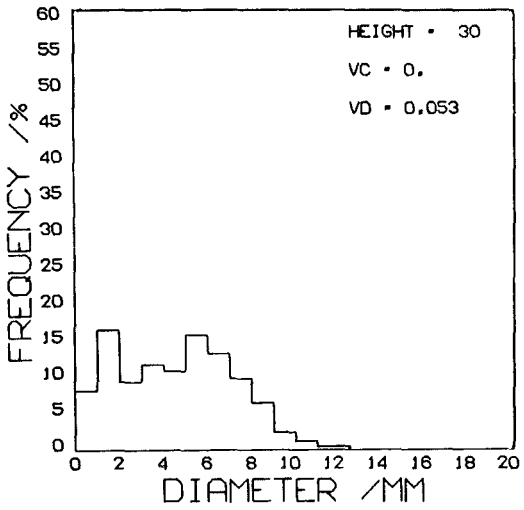

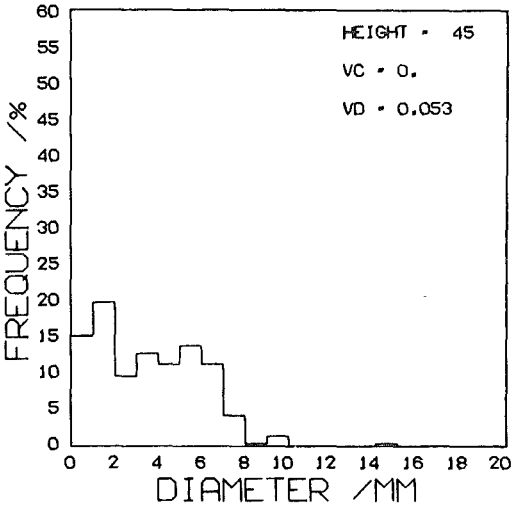

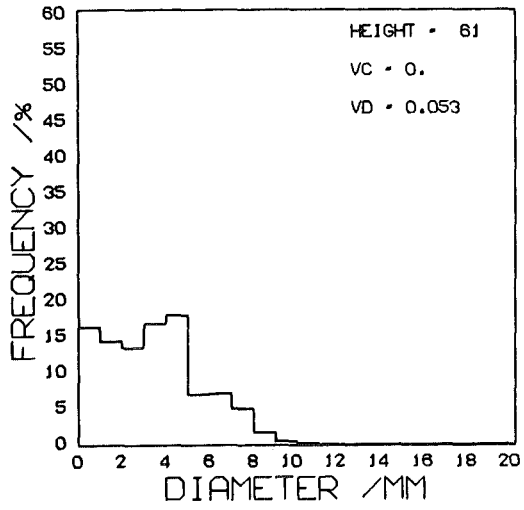

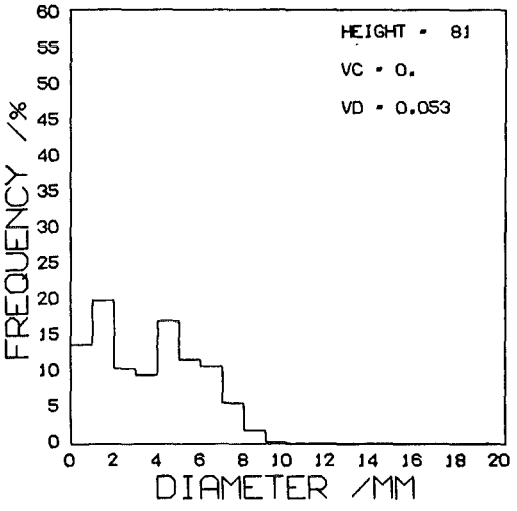

DRUM 1 SURFACTANT CASE

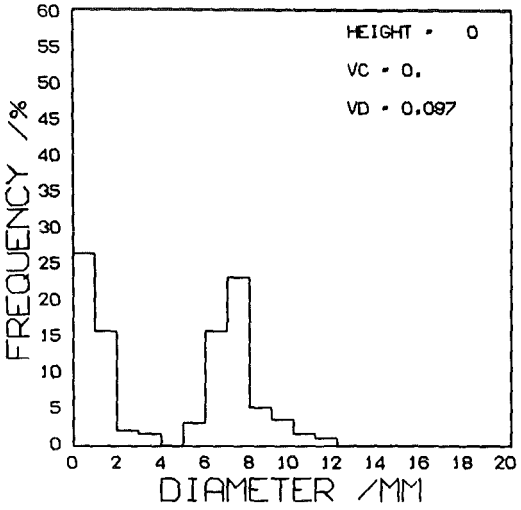

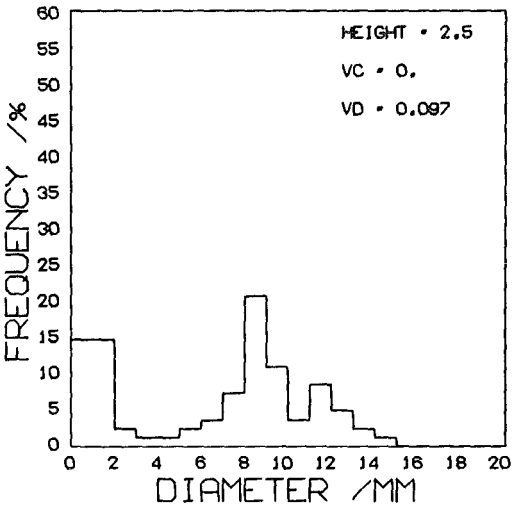

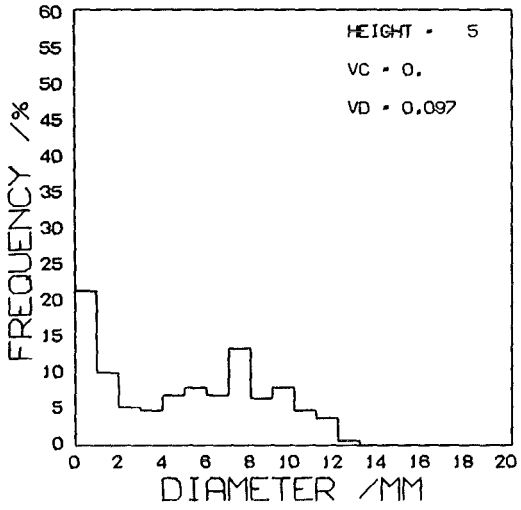

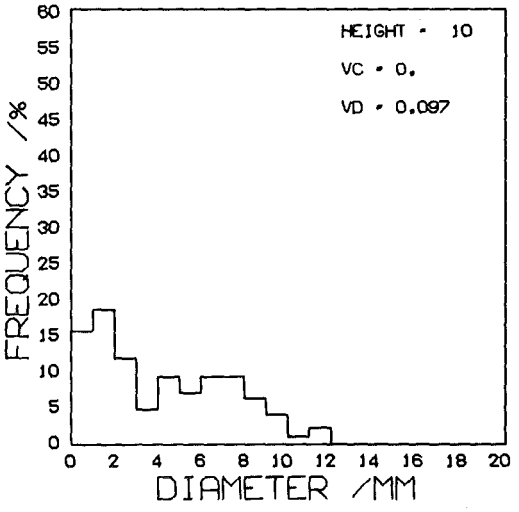

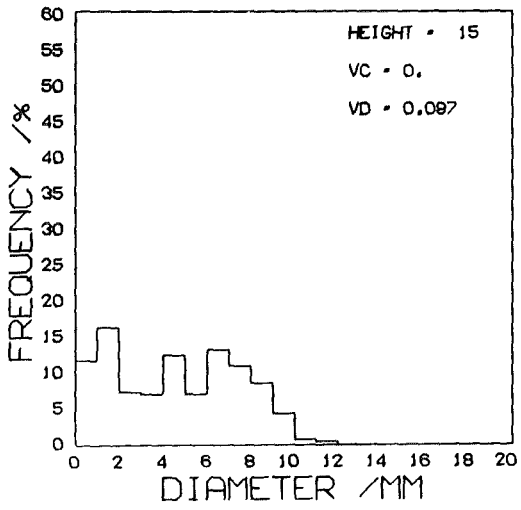

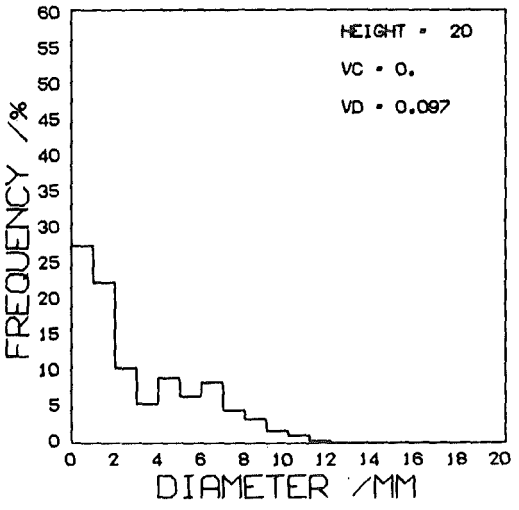

DRUM 1 SURFACTANT CASE

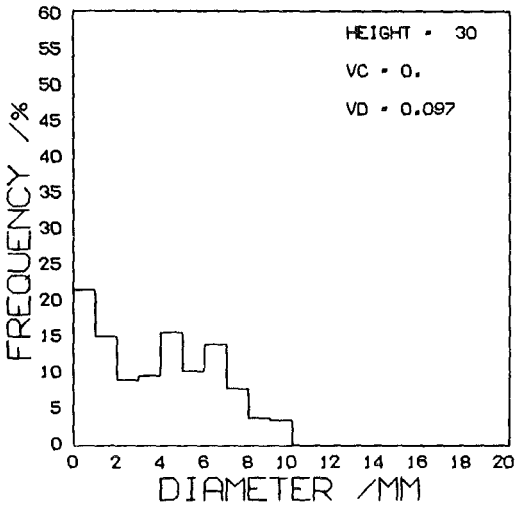

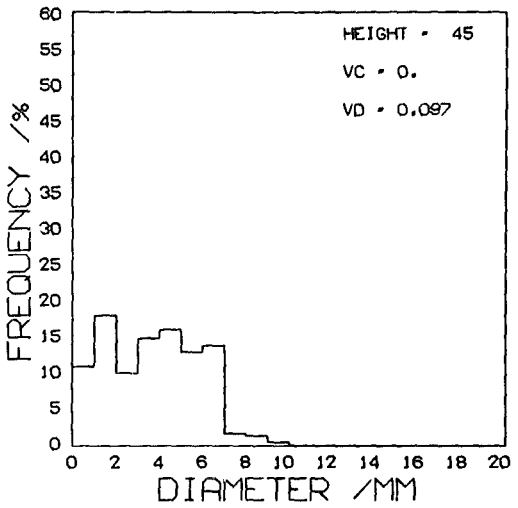

DRUM 2 PURE PHASES

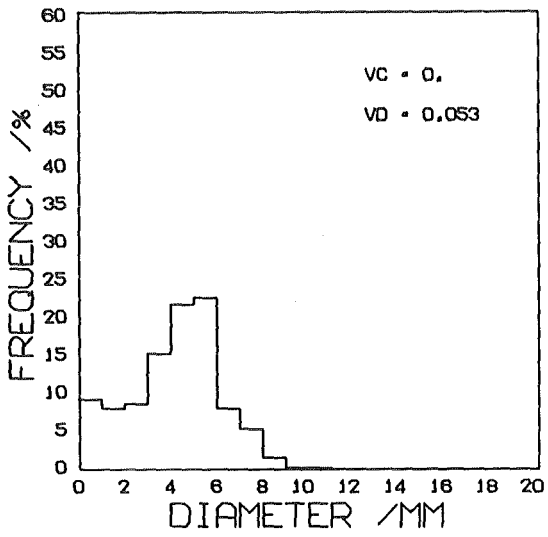

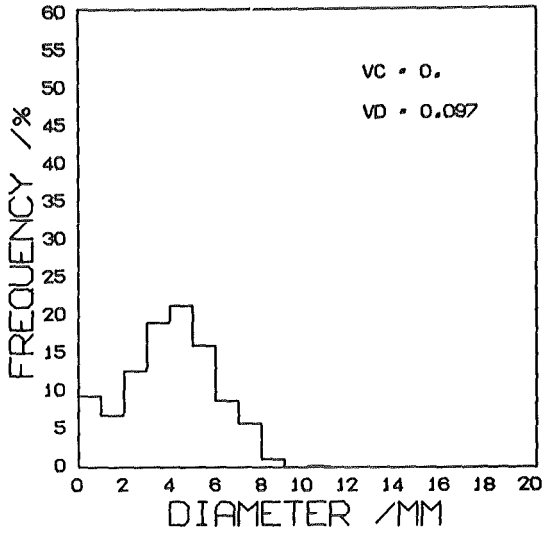

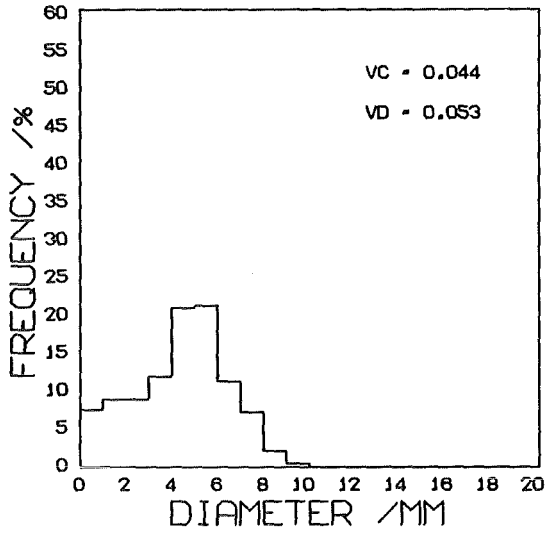

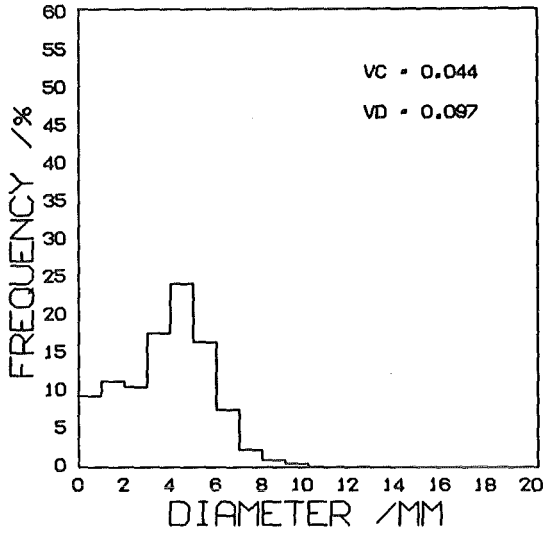

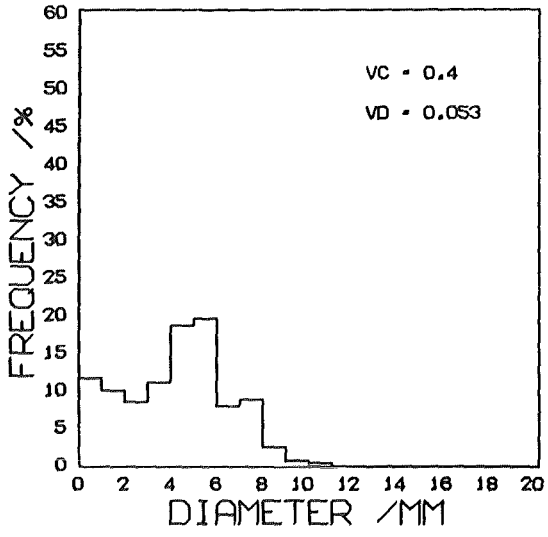

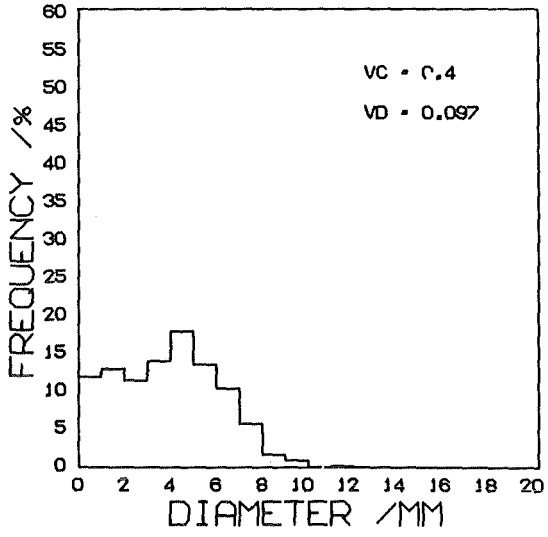

DRUM 2 MASS TRANSFER Toluene to Water

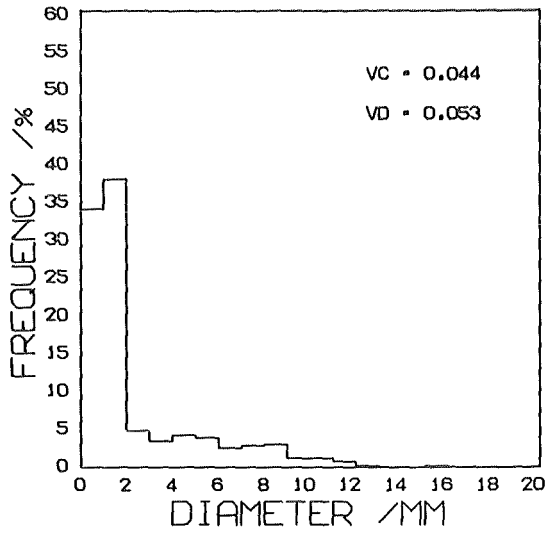

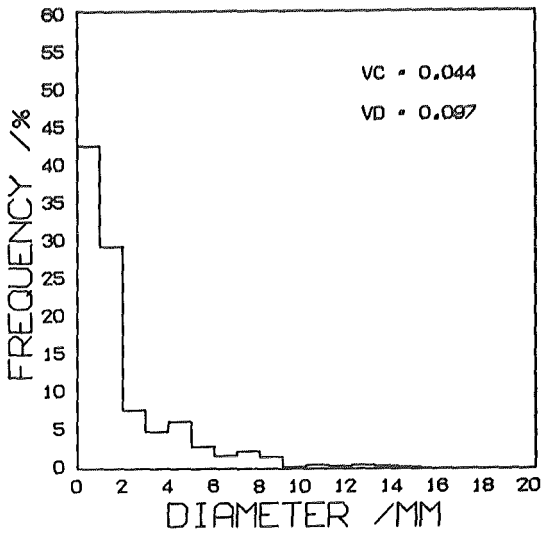

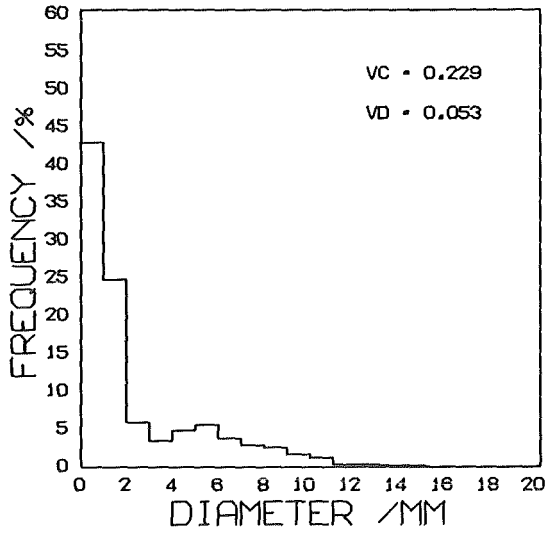

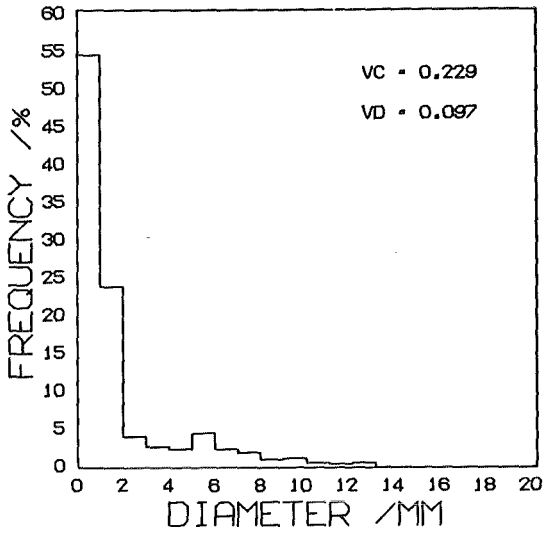

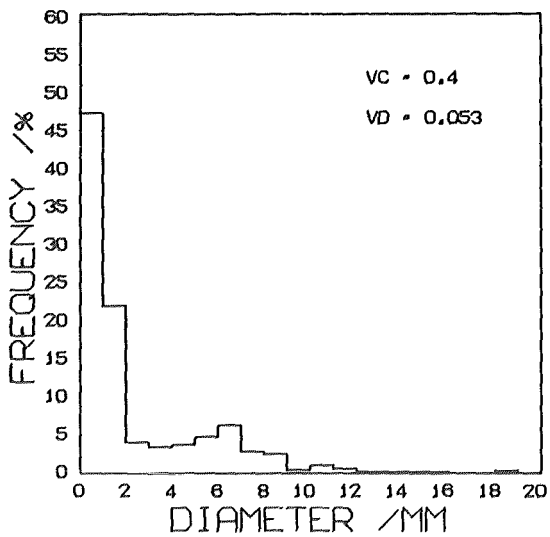

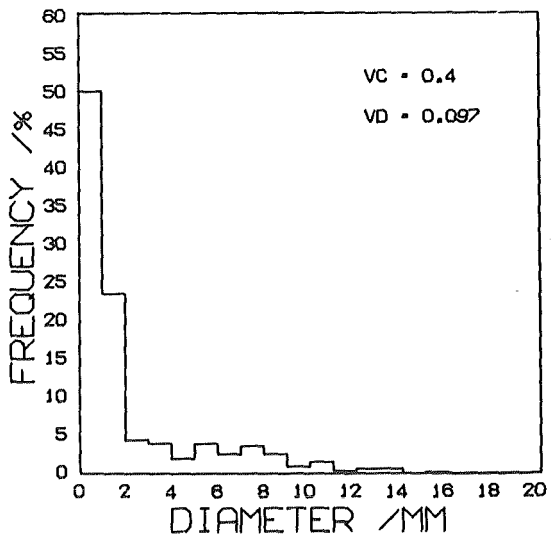

DRUM 2 MASS TRANSFER Water To Toluene

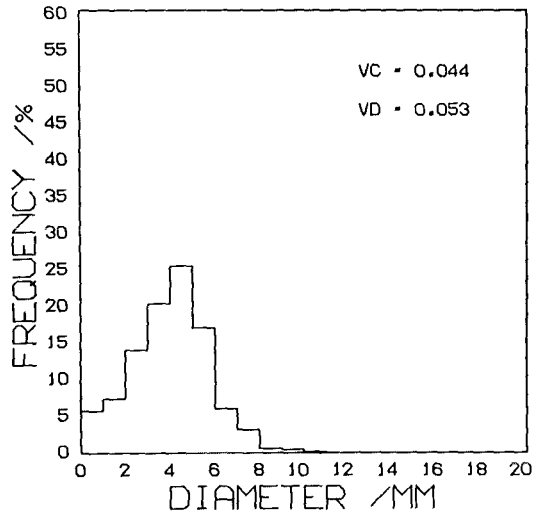

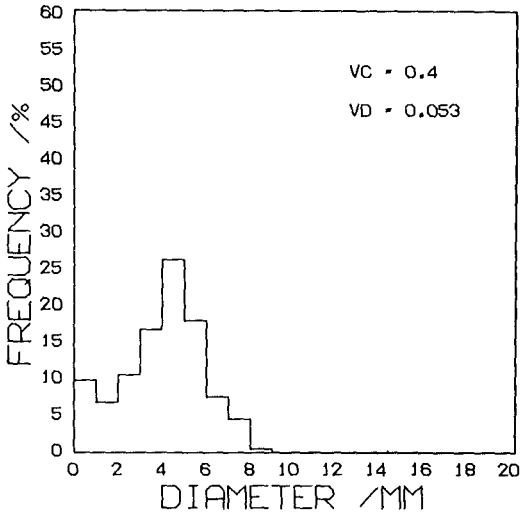

DRUM 2 SATURATED PHASES

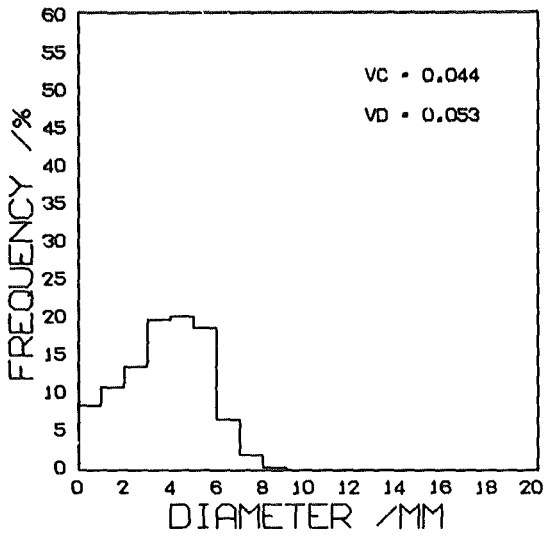

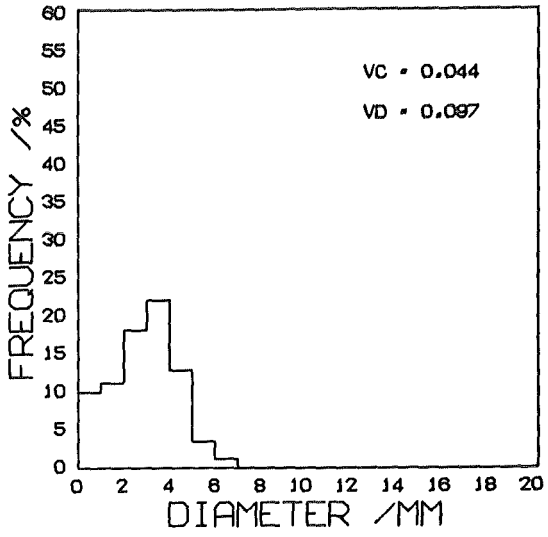

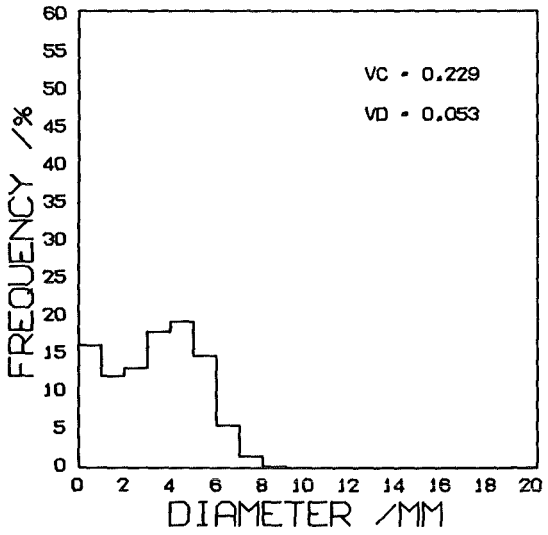

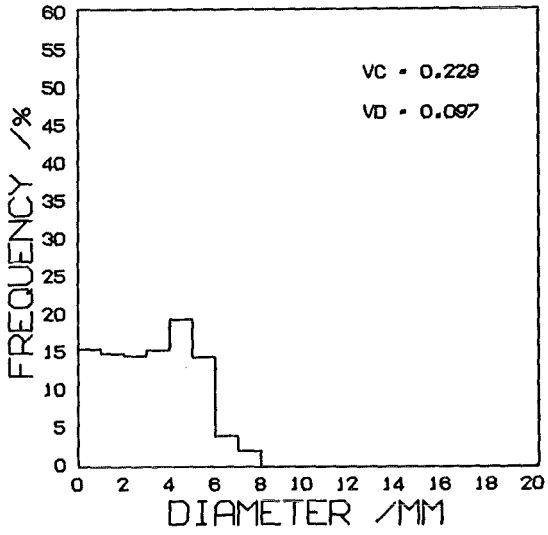

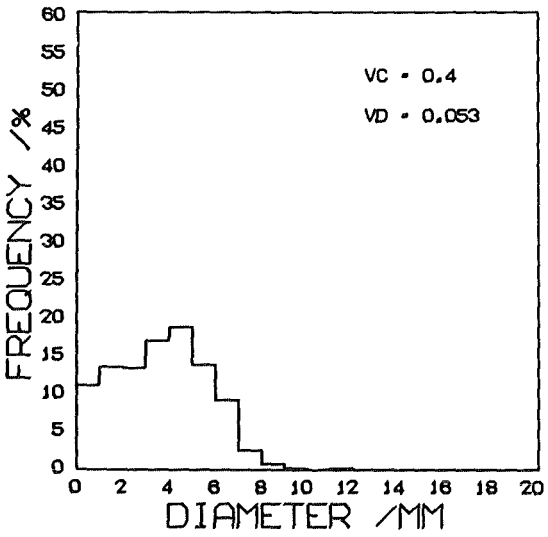

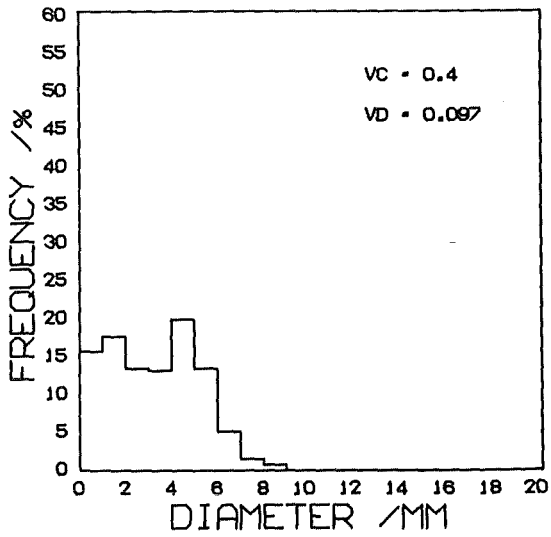

APPENDIX VI

COMPUTER PROGRAM FOR THE SIMULATION OF THE DROPLET DISTRIBUTION

```
C*************************************************************************** 00001000  C
C                                                                           00002000  C
C PROGRAM FLOSYM                                                            00003000  C
C                                                                           00004000  C
C                                                                           00005000  C
C PURPOSE : TO SIMULATE THE EVOLUTION OF THE DISPERSED PHASE DROPLET         00006000  C
C SIZE DISTRIBUTION IN A COLUMN PACKED WITH 16MM OD RASCHIG RINGS            00007000  C
C                                                                           00008000  C
C                                                                           00009000  C
C                                                                           00010000  C
C METHOD : A NORMAL DISTRIBUTION OF DROPLETS IS GENERATED AT THE BASE OF     00011000  C
C THE PACKING.A MONTE CARLO TECHNIQUE IS USED TO CONTROL THE RATE OF         00012000  C
C BREAKUP AND COALESCENCE OF THIS DISTRIBUTION OVER PACKED HEIGHTS OF UP     00013000  C
C TO 1.40 METRES                                                            00014000  C
C THE BREAKUP MECHANISMS EMPLOYED ARE :                                     00015000  C
C 1 IMPACTION - REFERENCE RAMSHAW AND THORNTON (1967)                       00016000  C
C 2 INSTABILITY BREAKUP                                                     00017000  C
C 3 FORCE BALANCE BREAKUP                                                   00018000  C
C COALESCENCE BETWEEN DROPLETS MAY OCCUR AT SIMULATED RESTRICTIONS IN        00019000  C
C THE PACKING                                                               00020000  C
C MOTION UP THE COLUMN IS CYCLIC OVER THE DROPLET PATHLENGTH WHICH IS        00021000  C
C INCREASED IN DISCRETE STEPS UP THE COLUMN.A CYCLE CONSISTS OF FREE         00022000  C
C RISE FOLLOWED BY IMPACTION,THEN MOVEMENT THROUGH A RESTRICTION.ON ANY     00023000  C
C ONE CYCLE SOME DROPLETS MAY BYPASS THE BREAKUP SITES.                     00024000  C
C                                                                           00025000  C
C                                                                           00026000  C
C                                                                           00027000  C
C SUBROUTINES USED                                                          00028000  C
C VEL - CALULATES DROPLET TERMINAL VELOCITY USING HU-KINTER OR               00029000  C
C KLEE-TREYBAL EQUATIONS                                                    00030000  C
C OUTPUT - SORTS DROPLET PRODUCT VECTOR AT TOP OF PACKING INTO               00031000  C
C DISTRIBUTIONS AND CALULATES MEAN DIAMETERS.WRITES OUTPUT OR CALLS          00032000  C
C SUBROUTINE BTPLOT                                                         00033000  C
C BTPLOT - PLOTS DISTRIBUTIONS USING RESIDENT PLOTTING SUBROUTINES ON        00034000  C
C B6718                                                                     00035000  C
C                                                                           00036000  C
C                                                                           00037000  C
C                                                                           00038000  C
C NOMENCLATURE                                                              00039000  C
C A - PARAMETER USED IN EVALUATING DCRIT                                    00040000  C
C AMAJ - INTERNAL UPDATE REGISTER OF NUMBER OF DROPLETS ON ANY PACKING       00041000  C
C      HEIGHT                                                               00042000  C
C AMAZ - INTERNAL UPDATE REGISTER OF DROPLET DIAMETERS ON ANY PACKING        00043000  C
C      HEIGHT                                                               00044000  C
C AMBJ - INTERNAL CURRENT REGISTER OF NUMBER OF DROPLETS ON ANY PACKING      00045000  C
C      HEIGHT                                                               00046000  C
C AMBZ - INTERNAL CURRENT REGISTER OF DROPLET DIAMETERS ON ANY PACKING       00047000  C
C      HEIGHT                                                               00048000  C
C B - DROPLET POPULATION                                                    00049000  C
C BOND - BOND NUMBER                                                        00050000  C
C BREAK - IMPACTION BREAKUP PROBABILITY                                     00051000  C
C CA - PARAMETER USED IN EVALUATING DCRIT                                   00052000  C
C CNR - PARAMETER USED IN EVALUATING FREE RISE TIME                         00053000  C
C COALP - COALESCENCE PROBABILITY                                           00054000  C
C CODROP - DROPLET SELECTED FOR COALESCENCE                                 00055000  C
C CRITWE - CRITICAL WEBER NUMBER                                            00056000  C
C CUBE - CUBE OF DROPLET DIAMETER                                           00057000  C
C D - DROPLET DIAMETER                                                      00058000  C
C DC - CONTINUOUS PHASE DENSITY                                             00059000  C
C DCRIT - CRITICAL IMPACTION DIAMETER                                       00060000  C
C DD - PHASE DENSITY DIFFERENCE                                             00061000  C
C DELTA - TOLERANCE TESTER                                                  00062000  C
C EPS - TOLERANCE                                                           00063000  C
C I - DO LOOP PARAMETER                                                     00064000  C
C IC - DO LOOP PARAMETER                                                    00065000  C
C ICO - COALESCENCE COUNTER                                                 00066000  C
C ICOUNT - ITERATION COUNTER                                                00067000  C
C IH - PACKING HEIGHT                                                       00068000  C
C IHEIGH - NUMBER OF PACKING HEIGHTS TO BE SIMULATED                        00069000  C
C IJK - BREAKUP FLAG                                                        00070000  C
C IK - DO LOOP PARAMETER                                                    00071000  C
C INITZ - INITIAL PACKING HEIGHT                                            00072000  C
C INR - ITERATION COUNTER                                                   00073000  C
C IOUT - FORMAT PARAMETER                                                   00074000  C
C IPFORM - FORMAT PARAMETER                                                 00075000  C
C IPUNCH - PARAMETER FOR OPTIONAL CARD PUNCHING                             00076000  C
C ISAVE - DO LOOP PARAMETER                                                 00077000  C
C ISUP - FORMAT PARAMETER                                                   00078000  C
C ITER - SAMPLING FREQUENCY                                                 00079000  C
C ITERD - ITERATION COUNTER                                                 00080000  C
C J - DO LOOP PARAMETER                                                     00081000  C
C JA - INDEX                                                                00082000  C
C JB - INDEX                                                                00083000  C
C JAA - INDEX                                                               00084000  C
C JPC - INDEX                                                               00085000  C
C JSAVE - DO LOOP PARAMETER                                                 00086000  C
C K - PROGRAM ITERATION COUNTER                                             00087000  C
```

```
C  M - NUMBER OF PROGRAM ITERATIONS                                          00088000  C
C  NCOAL - NUMBER OF COALESCENCES                                           00089000  C
C  NODE - BREAKUP STORAGE PARAMETER                                         00090000  C
C  NR - BREAKUP STORAGE PARAMETER                                           00091000  C
C  OLD - PARAMETER USED IN WEGSTEIN NUMERICAL EQUATION SOLUTION TECHNIQUE   00092000  C
C  OPDATA - VECTOR CONTAINING FREQUENCY DISTRIBUTIONS FOR PLOTTING          00093000  C
C  P - PARAMETER USED IN EVALUATING FREE RISE TIME                          00094000  C
C  PC - OUTPUT PRODUCT VECTOR                                               00095000  C
C  PIH - PARAMETER TO ADJUST INITIAL BREAKUP RATE                           00096000  C
C  POINT - GIVES TYPE OF LAST BREAKUP                                       00097000  C
C  PRF - BYPASS COEFFICIENT                                                 00098000  C
C  PROD - BREAKUP PRODUCT  STORAGE VECTOR                                   00099000  C
C  R - RESTRICTION DIAMETER                                                 00100000  C
C  REN - RESIDUAL VOLUME                                                    00101000  C
C  S - OUTPUT FLAG                                                          00102000  C
C  SMCO - SCHEELE-MEISTER COEFFICIENT                                       00103000  C
C  ST - INTERFACIAL TENSION                                                 00104000  C
C  TL - PARAMETER USED IN EVALUATING FREE RISE TIME                         00105000  C
C  TOBM - TIME OF DROPLET MOTION                                            00106000  C
C  TNR - PARAMETER USED IN EVALUATING FREE RISE TIME                        00107000  C
C  U - CONTINUOUS PHASE VISCOSITY                                           00108000  C
C  V - DROPLET TERMINAL VELOCITY                                            00109000  C
C  VA - TERMINAL VELOCITY CORRECTED FOR WALL DRAG                           00110000  C
C  WE - WEBER NUMBER                                                        00111000  C
C  X - RANDOM VARIABLE IN RANGE 0 - 1                                       00112000  C
C  Z - DROPLET HEIGHT                                                       00113000  C
C  ZH - DISTANCE OF DROPLET MOTION                                          00114000  C
C  ZPL - DROPLET PATH LENGTH                                                00115000  C
C  ZPLC - DROPLET HEIGHT                                                    00116000  C
C                                                                           00117000  C
C                                                                           00118000  C
C*************************************************************************  00119000  C


      DIMENSION V(200),PC(200),OPDATA(20)                                   00120000  C
      DIMENSION AMAZ(140,120),AMBZ(140,120),AMAJ(140),AMBJ(140)             00121000  C
      DIMENSION NR(8),PROD(10),POINT(8),ZH(8,120),D(8,120),TOBM(8,120)      00122000  C
      DIMENSION IL(10)                                                      00123000  C
      DIMENSION PD(10)                                                      00124000  C
      COMMON IOUT,ISUP,IPFORM                                               00125000  C
C*************************************************************************  00126000  C
C                                                                           00127000  C
C                                                                           00128000  C
C  INPUT PARAMETERS AND PHYSICAL PROPERTIES                                 00129000  C
      READ(5,104)M,INITZ                                                    00130000  C

  104 FORMAT(I2,I3)                                                         00131000  C
      READ(5,130)IHEIGH                                                     00132000  C
  130 FORMAT(I3)                                                            00133000  C
      READ(5,120)(IL(I),I=1,IHEIGH)                                         00134000  C
  120 FORMAT(10I3)                                                          00135000  C
      READ(5,135) COALP                                                     00136000  C
  135 FORMAT(F4.2)                                                          00137000  C
      READ(5,140)BREAK                                                      00138000  C
  140  FORMAT(F4.2)                                                         00139000  C
      READ(5,145)PRF                                                        00140000  C
  145 FORMAT(F4.2)                                                          00141000  C
      READ(5,150)PIH                                                        00142000  C
  150 FORMAT(F4.2)                                                          00143000  C
      READ(5,110)IOUT,IPFORM,ITER,IPUNCH                                    00144000  C
  110 FORMAT(4I2)                                                           00145000  C
      READ(5,100)N,B                                                        00146000  C
  100 FORMAT(I3,F5.1)                                                       00147000  C
      IF(INITZ.EQ.1) GO TO 1025                                             00148000  C
 1025 READ(5,102)ST,DC,DD,U                                                 00149000  C
  102 FORMAT(F4.1,3F5.3)                                                    00150000  C
      X=389556557536                                                        00151000  C
      K=1                                                                   00152000  C
      EPS=0.0005                                                            00153000  C
      AMBJ(1)=9.                                                            00154000  C
C                                                                           00155000  C
C                                                                           00156000  C
C     OUTPUT INITIAL CONDITIONS                                             00157000  C
C                                                                           00158000  C
      IF(IOUT) 32,32,33                                                     00159000  C
   32 WRITE(6,200)                                                          00160000  C

  200 FORMAT(18H SYSTEM PROPERTIES/1X,17('*')//23H SYSTEM : TOLUENE-WATE    00161000  C
     3R/)                                                                   00162000  C
      WRITE(6,201)ST,U,DC,DD                                                00163000  C
  201 FORMAT(22H INTERFACIAL TENSION =,F4.1,9H DYNES/CM,5X,12H VISCOSITY    00164000  C
     1 =,F5.3,6H POISE//22H CONT. PHASE DENSITY =,F4.2,5H G/CC,9X,21H DE    00165000  C
     2NSITY DIFFERENCE =,F4.2,5H G/CC/)                                     00166000  C
      WRITE(6,209)CRITWE                                                    00167000  C
  209 FORMAT(24H CRITICAL WEBER NUMBER =,F5.2/)                             00168000  C
      WRITE(6,265)                                                          00169000  C
  265 FORMAT(1X,////22H SIMULATION PARAMETERS/1X,21('*')/)                   00170000  C
      WRITE(6,235)                                                          00171000  C
```

```
  235 FORMAT(21H BREAK = (D-DCRIT)**2/)                                  00172000  C
      WRITE(6,240)COALP                                                  00173000  C
  240 FORMAT(9H COALP = ,F4.2/)                                          00174000  C
      WRITE(6,245)PRF                                                    00175000  C
  245 FORMAT(7H PRF = ,F4.2/)                                            00176000  C
      WRITE(6,250)PIH                                                    00177000  C
  250 FORMAT(23H BY-PASS COEFFICIENT = ,F4.2/)                           00178000  C
      WRITE(6,260)                                                       00179000  C
  260 FORMAT(29H PATHLENGTH = 5. FOR IH LE 20/13X,15H 10. FOR IH >20/)   00180000  C
   33 ISUP=1                                                             00181000  C
C CALULATE BOND NUMBER AND SCHEELE-MEISTER COEFFICIENT                   00182000  C
C                                                                        00183000  C
C                                                                        00184000  C
      BOND=-(DC-DD)*1765.8/ST                                            00185000  C
      SMCO=6.3*ST/(DD*981.)                                              00186000  C
      ICOUNT=1                                                           00187000  C
C                                                                        00188000  C
C                                                                        00189000  C
C     FIND VELOCITY DISTRIBUTION USING HU-KINTNER CORRELATION            00190000  C
      CALL VEL(DC,DD,U,ST,V,N)                                           00191000  C
C                                                                        00192000  C
C                                                                        00193000  C
C CALULATE CRITICAL IMPACTION DIAMETER USING RAMSHAW-THORNTON EQUATION    00194000  C
      ITERD=0                                                            00195000  C
      DCRIT=0.5                                                          00196000  C
      A=(DC-DD)/(1.8*DD*981.)                                            00197000  C
      B=3.12*ST/(1.8*DD*981.)                                            00198000  C
 1060 J=DCRIT*100                                                        00199000  C
      OLDDC=DCRIT                                                        00200000  C
C                                                                        00201000  C
C CORRECT TERMINAL VELOCITY FOR WALL DRAG                                00202000  C
      VA=V(J)*(-DCRIT*DCRIT/1.44+1.)**1.43                               00203000  C
      CA=A*VA*VA                                                         00204000  C
      DCRIT=(SQRT(CA*CA+4.*B)-CA)/2.                                     00205000  C
      DELTA=ABS(OLDDC-DCRIT)                                             00206000  C
      ITERD=ITERD+1                                                      00207000  C
      IF(DELTA.LE.0.005) GO TO 1061                                      00208000  C
      IF(ITERD.GE.10) GO TO 1062                                         00209000  C
      GO TO 1060                                                         00210000  C
 1062 WRITE(6,230)                                                       00211000  C
  230 FORMAT(24H DCRIT FAILS TO CONVERGE/)                               00212000  C
      GO TO 20                                                           00213000  C
C                                                                        00214000  C
C                                                                        00215000  C
C SIMULATE ONE OR MORE PACKING HEIGHTS                                   00216000  C
 1061 DO 1050 IK=1,IHEIGH                                                00217000  C
C                                                                        00218000  C
C SET PACKING HEIGHT                                                     00219000  C
      IZ=IL(IK)                                                          00220000  C
C                                                                        00221000  C
C                                                                        00222000  C
C SET INITIAL DISTRIBUTION                                               00223000  C
   30 DO 61 I=1,9                                                        00224000  C
      Z=SQRT(-2.*ALOG(1.-RANDOM(X)))*COS(6.28318*RANDOM(X))              00225000  C
   61 AMBZ(1,I)=Z*13.+100.                                               00226000  C
C                                                                        00227000  C
C                                                                        00228000  C
 1029 DO 62 IH=INITZ,IZ                                                  00229000  C
      N=AMBJ(IH)                                                         00230000  C
      IF(N.EQ.0) GO TO 62                                                00231000  C
C                                                                        00232000  C
C                                                                        00233000  C
C ITERATE OVER NUMBER OF DROPLETS IN EACH CM OF PACKING                  00234000  C
      DO 63 I=1,N                                                        00235000  C
C                                                                        00236000  C
C                                                                        00237000  C
C SET INITIAL MOVEMENT AND BREAKUP PARAMETERS FOR EACH DROPLET           00238000  C
      J=AMBZ(IH,I)                                                       00239000  C
      IF(J.EQ.0) J=1                                                     00240000  C
      VA=V(J)                                                            00241000  C
      NODE=1                                                             00242000  C
      NR(NODE)=1                                                         00243000  C
      ZH(NODE,1)=0.                                                      00244000  C
      D(NODE,1)=J/100.                                                   00245000  C
      TOBM(NODE,1)=0.                                                    00246000  C
C                                                                        00247000  C
C                                                                        00248000  C
C BEGIN CYCLE FOR EACH DROPLET                                           00249000  C
   74 Z=SQRT(-2.*ALOG(1.-RANDOM(X)))*COS(6.28318*RANDOM(X))              00250000  C
      INDEZ=1                                                            00251000  C
      NS=1                                                               00252000  C
      IJK=2                                                              00253000  C
C                                                                        00254000  C
C                                                                        00255000  C
C SET PATHLENGTH                                                         00256000  C
      ZPL=1.5                                                            00257000  C
      IF(IH.GT.10) ZPL=5.                                                00258000  C
      IF(IH.GT.20) ZPL=10.                                               00259000  C
```

```
C                                                                       00260000  C
C                                                                       00261000  C
C CORRECT TERMINAL VELOCITY FOR WALL DRAG                               00262000  C
      JB=D(NODE,1)*100                                                  00263000  C
      IF(JB.LT.1) JB=1                                                  00264000  C
      IF(D(NODE,1).LT.1.2) GO TO 31                                     00265000  C
      VA=3.                                                             00266000  C
      GO TO 34                                                          00267000  C
   31 VA=V(JB)*(-D(NODE,1)*D(NODE,1)/1.44+1.)**1.43                     00268000  C
      IF(VA.LT.3.) VA=3.                                                00269000  C
   34 IF(D(NODE,1).LE.DCRIT) GO TO 35                                   00270000  C
C                                                                       00271000  C
C                                                                       00272000  C
C CALULATE FREE RISE AND CYCLE TIME                                     00273000  C
   35 CNR=ZPL/VA                                                        00274000  C
      P=VA/173.117647                                                   00275000  C
      INR=0                                                             00276000  C
      TL=0.1                                                            00277000  C
   19 TNR=(CNR+P*(1.-(1.+TL/P)*EXP(-TL/P)))/(1.-EXP(-TL/P))             00278000  C
      INR=INR+1                                                         00279000  C
      DELTA=ABS(TNR-TL)                                                 00280000  C
      IF(DELTA.LE.EPS) GO TO 22                                         00281000  C
      IF(INR.GE.10) GO TO 18                                            00282000  C
      TL=TNR                                                            00283000  C
      GO TO 19                                                          00284000  C
   18 WRITE(6,402)                                                      00285000  C
  402 FORMAT(32H NUMBER OF ITERATIONS EXCEEDS 10)                       00286000  C
      GO TO 20                                                          00287000  C
C                                                                       00288000  C
C                                                                       00289000  C
C CALULATE VELOCITY AND POSITION                                        00290000  C
   22 TOBM(NODE,1)=TNR+TOBM(NODE,1)                                     00291000  C
      VA=VA*(1.-EXP(-TNR/P))                                            00292000  C
      ZH(NODE,1)=ZH(NODE,1)+ZPL                                         00293000  C
      ZPLC=ZH(NODE,1)+IH                                                00294000  C
      IF(ZPLC.GT.IZ) TOBM(NODE,1)=5.                                    00295000  C
   39 IF(TOBM(NODE,1).GE.5.) GO TO 73                                   00296000  C
C                                                                       00297000  C
C                                                                       00298000  C
C DETERMINE BYPASSING                                                   00299000  C
   65 RA=RANDOM(X)                                                      00300000  C
      Z=RANDOM(X)                                                       00301000  C
      IF(D(NODE,1).GT.DCRIT.AND.Z.GE.PIH.AND.IH.GT.10) GO TO 21         00302000  C
      IF(D(NODE,1).LE.DCRIT) GO TO 21                                   00303000  C
C DETERMINE IMPACTION BREAKUP                                           00304000  C
      BREAK=3.*(D(NODE,1)-DCRIT)*(D(NODE,1)-DCRIT)                      00305000  C
      IF(BREAK.GE.0.8) BREAK=0.8                                        00306000  C
      Z=RANDOM(X)                                                       00307000  C
 1046 IF(Z.GT.BREAK) GO TO 1022                                         00308000  C
      IF(Z.GT.PRF) GO TO 1022                                           00309000  C
      GO TO 17                                                          00310000  C
C                                                                       00311000  C
C DETERMINE COALESCENCES                                                00312000  C
 1022 JA=ZPLC                                                           00313000  C
      NCOAL=AMBJ(JA)*COALP                                              00314000  C
      ICOAL=0                                                           00315000  C
      IF(NCOAL.GE.1) GO TO 1016                                         00316000  C
C PERFORM INSTABILITY AND FORCE BALANCE BREAKUPS                         00317000  C
 1055 CUBE=D(NODE,1)*D(NODE,1)*D(NODE,1)                                00318000  C
      ICO=0                                                             00319000  C
      R=1.5*RANDOM(X)+0.25                                              00320000  C
      IF(R.GT.1.2) R=1.2                                                00321000  C
      REM=SMCO*R+0.5*R*R*R                                              00322000  C
      JA=0                                                              00323000  C
      Z=RANDOM(X)                                                       00324000  C
      IF(Z.GE.0.9.AND.D(NODE,1).LE.0.65) GO TO 1075                     00325000  C
      IF(CUBE.LE.REM) GO TO 1047                                        00326000  C
 1030 JA=JA+1                                                           00327000  C
      PROD(JA)=SMCO*R                                                   00328000  C
      CUBE=CUBE-PROD(JA)                                                00329000  C
      PROD(JA)=(PROD(JA))**0.3333                                       00330000  C
      IF(JA.GE.7) GO TO 1047                                            00331000  C
      IF(CUBE.GT.REM) GO TO 1030                                        00332000  C
 1047 JA=JA+1                                                           00333000  C
      PROD(JA)=CUBE**0.3333                                             00334000  C
      IF(JA.GT.3) NS=JA-2                                               00335000  C
      IJK=5                                                             00336000  C
      IF(JA.EQ.1) IJK=2                                                 00337000  C
      GO TO 21                                                          00338000  C
 1075 Z=RANDOM(X)                                                       00339000  C
      PROD(1)=CUBE/(1.+Z)                                               00340000  C
      PROD(2)=Z*PROD(1)                                                 00341000  C
      PROD(2)=(PROD(2))**0.3333                                         00342000  C
      PROD(1)=PROD(1)**0.3333                                           00343000  C
      IJK=5                                                             00344000  C
      GO TO 21                                                          00345000  C
C PERFORM COALESCENCES                                                  00346000  C
 1016 JB=AMBJ(JA)*RANDOM(X)                                             00347000  C
```

```
      IF(D(NODE,1).LE.0.2) GO TO 1055                                          00348000  C
      ICO=ICO+1                                                                00349000  C
      IF(ICO.GE.AMBJ(JA)) GO TO 1055                                           00350000  C
      IF(JB.EQ.0) GO TO 1016                                                   00351000  C
      IF(AMBZ(JA,JB).LE.0.2) GO TO 1016                                        00352000  C
      CODROP=AMBZ(JA,JB)/100.                                                  00353000  C
      D(NODE,1)=D(NODE,1)*D(NODE,1)*D(NODE,1)+CODROP*CODROP*CODROP             00354000  C
      IF(D(NODE,1).LE.8.) GO TO 1091                                           00355000  C
      D(NODE,1)=D(NODE,1)-CODROP*CODROP*CODROP                                 00356000  C
      D(NODE,1)=(D(NODE,1))**0.3333                                            00357000  C
      GO TO 1016                                                               00358000  C
 1091 D(NODE,1)=(D(NODE,1))**0.3333                                            00359000  C
      AMBZ(JA,JB)=0.                                                           00360000  C
      JB=AMBJ(JA)                                                              00361000  C
      JAA=0                                                                    00362000  C
      DO 1017 IC=1,JB                                                          00363000  C
 1018 JAA=JAA+1                                                                00364000  C
      IF(AMBZ(JA,JAA).EQ.0.0.AND.JAA.LT.AMBJ(JA)) GO TO 1018                   00365000  C
 1017 AMBZ(JA,IC)=AMBZ(JA,JAA)                                                 00366000  C
      AMBJ(JA)=AMBJ(JA)-1.                                                     00367000  C
      ICOAL=ICOAL+1                                                            00368000  C
      IF(ICOAL.LE.NCOAL) GO TO 1016                                            00369000  C
      GO TO 1055                                                               00370000  C
C                                                                              003/1000  C
C COMPARE WEBER NUMBER WITH CRITICAL WEBER NUMBER                              00372000  C
   17 WE=VA*VA*D(NODE,1)*DC/ST                                                 00373000  C
      CRITWE=BOND*D(NODE,1)*D(NODE,1)+3.12                                     00374000  C
      IF(WE.GT.CRITWE) GO TO 27                                                00375000  C
C                                                                              00376000  C
C                                                                              00377000  C
   51 DO 53 JB=1,5                                                             00378000  C
   53 PROD(JB)=0.                                                              00379000  C
      IJK=2                                                                    00380000  C
      GO TO 21                                                                 00381000  C
C                                                                              00382000  C
C                                                                              00383000  C
C PERFORM IMPACTION BREAKUPS                                                   00384000  C
   27 DIS=(ALF*WE/12.+1.)**3                                                   00385000  C
      PROD(3)=0.15*D(NODE,1)*(RANDOM(X))**0.3333                               00386000  C
      IF(D(NODE,1).LE.0.65) PROD(3)=0.                                         00387000  C
      CUBE=D(NODE,1)*D(NODE,1)*D(NODE,1)-PROD(3)*PROD(3)*PROD(3)               00388000  C
      Z=RANDOM(X)                                                              00389000  C
      PROD(1)=CUBE/(1.+Z)                                                      00390000  C
      PROD(2)=Z*PROD(1)                                                        00391000  C
      PROD(2)=(PROD(2))**0.3333                                                00392000  C
      PROD(1)=PROD(1)**0.3333                                                  00393000  C
   38 IJK=1                                                                    00394000  C
      TOBM(NODE,1)=TOBM(NODE,1)+0.125                                          00395000  C
      ZH(NODE,1)=ZH(NODE,1)+D(NODE,1)                                          00396000  C
      GO TO 1054                                                               00397000  C
C                                                                              00398000  C
C                                                                              00399000  C
C CALULATE POSITION AND CYCLE TIME                                             00400000  C
   21 TOBM(NODE,1)=TOBM(NODE,1)+1.6                                            00401000  C
      ZH(NODE,1)=ZH(NODE,1)+1.5                                                00402000  C
 1054 ZPLC=ZH(NODE,1)+IH                                                       00403000  C
      IF(ZPLC.GT.IZ) TOBM(NODE,1)=5.                                           00404000  C
   59 INDEZ=NS+2                                                               00405000  C
      IF(PROD(3).LE.0.) INDEZ=INDEZ-1                                          00406000  C
      IF(PROD(2).LE.0.) INDEZ=INDEZ-1                                          00407000  C
C                                                                              00408000  C
C                                                                              00409000  C
   85 IF(IJK.EQ.5) IJK=1                                                       00410000  C
      JB=D(NODE,1)*100.                                                        00411000  C
      IF(JB.EQ.0) JB=1                                                         00412000  C
      VA=V(JB)                                                                 00413000  C
      IF(TOBM(NODE,1).GE.5.0.AND.IJK.EQ.1) GO TO 91                            00414000  C
      IF(TOBM(NODE,1).GE.5.) GO TO 73                                          00415000  C
      IF(IJK.NE.1) GO TO 74                                                    00416000  C
C                                                                              00417000  C
C                                                                              00418000  C
C STORE BREAKUP PRODUCTS                                                       00419000  C
   91 JB=NODE+1                                                                00420000  C
      DO 77 JA=1,INDEZ                                                         00421000  C
      ZH(JB,JA)=ZH(NODE,1)                                                     00422000  C
   77 TOBM(JB,JA)=TOBM(NODE,1)                                                 00423000  C
      DO 84 JA=1,NR(NODE)                                                      00424000  C
      JB=JA+1                                                                  00425000  C
      D(NODE,JA)=D(NODE,JB)                                                    00426000  C
      ZH(NODE,JA)=ZH(NODE,JB)                                                  00427000  C
   84 TOBM(NODE,JA)=TOBM(NODE,JB)                                              00428000  C
      NR(NODE)=NR(NODE)-1                                                      00429000  C
      S=1                                                                      00430000  C
      NODE=NODE+1                                                              00431000  C
      NR(NODE)=INDEZ                                                           00432000  C
      DO 50 JB=1,INDEZ                                                         00433000  C
   50 D(NODE,JB)=PROD(JB)                                                      00434000  C
      IF(TOBM(NODE,1).GE.5.) GO TO 73                                          00435000  C
```

```
      JB=PROD(1)*100                                                    00436000  C
      IF(JB.LT.1) JB=1                                                  00437000  C
      VA=V(JB)                                                          00438000  C
      IF(POINT(NODE).EQ.1) GO TO 65                                     00439000  C
      GO TO 74                                                          00440000  C
C                                                                       00441000  C
C                                                                       00442000  C
   73 ZH(NODE,1)=ZH(NODE,1)*5./TOBM(NODE,1)+0.5                         00443000  C
      J=IH+ZH(NODE,1)                                                   00444000  C
      IF(IJK.EQ.5) IJK=1                                                00445000  C
      IF(IJK.EQ.1) GO TO 78                                             00446000  C
      IF(J.GT.IZ) GO TO 86                                              00447000  C
C UPDATE INTERNAL DISTRIBUTION VECTOR                                   00448000  C
      JA=AMAJ(J)+1                                                      00449000  C
      AMAJ(J)=JA                                                        00450000  C
      AMAZ(J,JA)=D(NODE,1)*100.                                         00451000  C
      S=2                                                               00452000  C
      GO TO 79                                                          00453000  C
C                                                                       00454000  C
C INCREMENT OUTPUT  DISTRIBUTION VECTOR IF HEIGHT EXCEEDS PACKING HEIGHT 00455000  C
   86 IF(K.LT.20) GO TO 79                                              00456000  C
      JB=D(NODE,1)*100                                                  00457000  C
      IF(JB.LT.1) JB=1                                                  00458000  C
      JPC=JPC+1                                                         00459000  C
      PC(JB)=PC(JB)+1.                                                  00460000  C
      S=3                                                               00461000  C
      GO TO 79                                                          00462000  C
C                                                                       00463000  C
C                                                                       00464000  C
   78 IF(J.GT.IZ) GO TO 87                                              00465000  C
C UPDATE INTERNAL DISTRIBUTION VECTOR                                   00466000  C
      DO 90 JA=1,INDEZ                                                  00467000  C
      JB=AMAJ(J)+1                                                      00468000  C
      AMAJ(J)=JB                                                        00469000  C
      S=4                                                               00470000  C
   90 AMAZ(J,JB)=D(NODE,JA)*100.                                        00471000  C
      GO TO 79                                                          00472000  C
C                                                                       00473000  C
C INCREMENT OUTPUT  DISTRIBUTION VECTOR IF HEIGHT EXCEEDS PACKING HEIGHT 00474000  C
   87 IF(K.LT.20) GO TO 79                                              00475000  C
      DO 92 JA=1,INDEZ                                                  00476000  C
      JB=D(NODE,JA)*100                                                 00477000  C
      IF(JB.LT.1) JB=1                                                  00478000  C
      JPC=JPC+1                                                         00479000  C
      S=5                                                               00480000  C
   92 PC(JB)=PC(JB)+1                                                   00481000  C
C                                                                       00482000  C
C                                                                       00483000  C
C RESET BREAKUP PRODUCT VECTORS                                         00484000  C
   79 IF(NR(NODE).GT.1) GO TO 82                                        00485000  C
   88 DO 81 JA=1,INDEZ                                                  00486000  C
      TOBM(NODE,JA)=0.                                                  00487000  C
      ZH(NODE,JA)=0.                                                    00488000  C
      NR(NODE)=0                                                        00489000  C
   81 D(NODE,JA)=0.                                                     00490000  C
      DO 1056 JA=1,8                                                    00491000  C
 1056 PROD(JA)=0.                                                       00492000  C
      POINT(NODE)=0.                                                    00493000  C
      S=6                                                               00494000  C
      IF(NODE.EQ.1) GO TO 63                                            00495000  C
      NODE=NODE-1                                                       00496000  C
      IF(NR(NODE).GE.1) GO TO 89                                        00497000  C
      GO TO 88                                                          00498000  C
C                                                                       00499000  C
C                                                                       00500000  C
C HANDLE REMAINING BREAKUP PRODUCTS                                     00501000  C
   82 IF(IJK.EQ.1.AND.TOBM(NODE,1).GE.5.) GO TO 88                      00502000  C
      NR(NODE)=NR(NODE)-1                                               00503000  C
      DO 83 JA=1,NR(NODE)                                               00504000  C
      JB=JA+1                                                           00505000  C
      D(NODE,JA)=D(NODE,JB)                                             00506000  C
      ZH(NODE,JA)=ZH(NODE,JB)                                           00507000  C
   83 TOBM(NODE,JA)=TOBM(NODE,JB)                                       00508000  C
      IF(D(NODE,1).EQ.0.) GO TO 82                                      00509000  C
   89 JB=D(NODE,1)*100                                                  00510000  C
      IF(JB.LT.1) JB=1                                                  00511000  C
      VA=V(JB)                                                          00512000  C
      S=7                                                               00513000  C
      IF(POINT(NODE).EQ.1) GO TO 65                                     00514000  C
      GO TO 74                                                          00515000  C
C                                                                       00516000  C
C                                                                       00517000  C
   63 CONTINUE                                                          00518000  C
   62 CONTINUE                                                          00519000  C
C                                                                       00520000  C
C                                                                       00521000  C
C RESET INTERNAL DISTRIBUTION VECTORS                                   00522000  C
```

```
      JA=INITZ+1                                                        00523000  C
      DO 64 I=JA,IZ                                                     00524000  C
      N=AMAJ(I)                                                         00525000  C
      DO 66 J=1,N                                                       00526000  C
   66 AMBZ(I,J)=AMAZ(I,J)                                               00527000  C
      AMBJ(I)=AMAJ(I)                                                   00528000  C
   64 AMAJ(I)=0.                                                        00529000  C
C                                                                       00530000  C
C                                                                       00531000  C
      IF(ICOUNT.NE.ITER) GO TO 72                                       00532000  C
C                                                                       00533000  C
C                                                                       00534000  C
C SET DROPLET POPULATION                                                00535000  C
      B=JPC                                                             00536000  C
      IF(B.EQ.0.) GO TO 72                                              00537000  C
C                                                                       00538000  C
C                                                                       00539000  C
C CALL OUTPUT IF SAMPLING PARAMETER EQUALS SAMPLE FREQUENCY              00540000  C
      N=200                                                             00541000  C
      IF(ICOUNT.EQ.ITER) CALL OUTPUT(B,N,PC,K,OPDATA,M,IZ)              00542000  C
      IF(IPUNCH.NE.1.OR.K.NE.M) GO TO 72                                00543000  C
C                                                                       00544000  C
C INCREMENT LOOP COUNTER                                                00545000  C
   72 K=K+1                                                             00546000  C
      ICOUNT=ICOUNT+1                                                   00547000  C
C     REPEAT THE BREAKUP LOOP                                           00548000  C
      IF(ICOUNT.GT.ITER) ICOUNT=1                                       00549000  C
      IF(K.LE.M) GO TO 30                                               00550000  C
C                                                                       00551000  C
C                                                                       00552000  C
C ZERO VECTORS IF ANOTHER PACKING HEIGHT IS TO BE SIMULATED             00553000  C
      DO 1048 ISAVE=1,IZ                                                00554000  C
      AMAJ(ISAVE)=0.                                                    00555000  C
      AMBJ(ISAVE)=0.                                                    00556000  C
      DO 1049 JSAVE=1,50                                                00557000  C
      AMAZ(ISAVE,JSAVE)=0.                                              00558000  C
 1049 AMBZ(ISAVE,JSAVE)=0.                                              00559000  C
 1048 CONTINUE                                                          00560000  C
      DO 1051 ISAVE=1,200                                               00561000  C
 1051 PC(ISAVE)=0.                                                      00562000  C
      K=1                                                               00563000  C
      ICOUNT=1                                                          00564000  C
      AMBJ(1)=9.                                                        00565000  C
      JPC=0                                                             00566000  C
 1050 CONTINUE                                                          00567000  C
   15 K=K/ITER+1                                                        00568000  C
      IF(IOUT.GE.0) WRITE(6,206)K                                       00569000  C
  206 FORMAT(26H DATA HAS BEEN PLOTTED ON ,I2,11H HISTOGRAMS/)          00570000  C
      YST=TIME(2)/60.                                                   00571000  C
      DELTAT=YST-YINT                                                   00572000  C
      WRITE(6,600)DELTAT                                                00573000  C
  600 FORMAT(10H DELTAT = ,F5.1/)                                       00574000  C
      WRITE(6,216)X                                                     00575000  C
  216 FORMAT(1X//12H LAST X WAS ,113/)                                  00576000  C
   20 STOP                                                              00577000  C
      END                                                               00578000  C
```

```
      SUBROUTINE VEL(DC,DD,U,S,V,N)                                          00579000  C
C*************************************************************************** 00580000  C
C PURPOSE - CALULATES DROPLET TERMINAL VELOCITY FOR 0.1MM INCREMENTS          00581000  C
C IN THE RANGE 0 - 2.0CM USING THE HU-KINTNER OR KLEE-TREYBAL EQUATIONS      00582000  C
C*************************************************************************** 00583000  C
      DIMENSION V(N)                                                         00584000  C
      DO 40 J=1,N                                                            00585000  C
      D=J/100.                                                               00586000  C
      P=(S*S*S*DC*DC)/(981.*DD*(U**4))                                       00587000  C
      P15=P**0.15                                                            00588000  C
      Y=(4.*DD*D*D*981.*P15)/(3.*S)                                          00589000  C
      IF(Y.LE.2.) GO TO 45                                                   00590000  C
      IF(Y.GT.70.) GO TO 50                                                  00591000  C
C HU-KINTNER EQUATION                                                        00592000  C
      X=(0.75*Y)**0.7843                                                     00593000  C
      V(J)=(X-0.75)*U*P15/(D*DC)                                             00594000  C
   40 CONTINUE                                                               00595000  C
      IF(J.GE.N) GO TO 55                                                    00596000  C
   50 X=(Y/0.045)**0.4219                                                    00597000  C
      V(J)=(X-0.75)*U*P15/(D*DC)                                             00598000  C
      GO TO 40                                                               00599000  C
C KLEE-TREYBAL EQUATION                                                      00600000  C
   45 V(J)=38.3*(DD**0.58)*(D**0.7)/((DC**0.45)*(U**0.11))                   00601000  C
      GO TO 40                                                               00602000  C
   55 RETURN                                                                 00603000  C
      END                                                                    00604000  C
```

```
      SUBROUTINE OUTPUT(B,N,C,K,OPDATA,M,IZ)                                 00605000  C
C*************************************************************************** 00606000  C
C PURPOSE - TO SORT OUTPUT PRODUCT VECTOR INTO DISTRIBUTIONS AND TO          00607000  C
C CALULATE MEAN DIAMETERS                                                    00608000  C
C DATA MAY BE WRITTEN ONLY ,PLOTTED ONLY OR BOTH BY SETTING THE              00609000  C
C PARAMETER IOUT TO -1,+1,OR 0 RESPECTIVELY                                  00610000  C
C*************************************************************************** 00611000  C
      DIMENSION C(N),OPDATA(20)                                              00612000  C
      COMMON IOUT,ISUP,IPFORM                                                00613000  C
      IF(IOUT) 24,24,25                                                      00614000  C
   24 D=-0.5                                                                 00615000  C
      I=1                                                                    00616000  C
      IF(ISUP.EQ.1)WRITE(6,213)K                                             00617000  C
  213 FORMAT(1X//21H DISTRIBUTION NUMBER ,I2/1X,22('*')/)                    00618000  C
      WRITE(6,230)IZ                                                         00619000  C
  230 FORMAT(9H HEIGHT =,I3,21H CM ABOVE DISTRIBUTOR/)                       00620000  C
C REDUCE 0.1MM INCREMENTS TO 1MM INCREMENTS                                   00621000  C
      DO 65 J=1,N                                                            00622000  C
      OUT=OUT+C(J)                                                           00623000  C
      I=I+1                                                                  00624000  C
      IF(I.GE.10)GO TO 80                                                    00625000  C
   65 CONTINUE                                                               00626000  C
C CALCULATE MEAN DIAMETERS                                                   00627000  C
   80 D=D+1.                                                                 00628000  C
      TOT=TOT+D*OUT                                                          00629000  C
      DSQR=DSQR+D*D*OUT                                                      00630000  C
      TOTCUB=TOTCUB+OUT*D*D*D                                                00631000  C
      TOTFOR=TOTFOR+OUT*D*D*D*D                                              00632000  C
      OUT=0.                                                                 00633000  C
      I=0                                                                    00634000  C
      IF(J.LT.N)GO TO 65                                                     00635000  C
      WRITE(6,214)B                                                          00636000  C
  214 FORMAT(14H SAMPLE SIZE =,I4/)                                          00637000  C
      ARITH=TOT/B                                                            00638000  C
      DVS=TOTCUB/DSQR                                                        00639000  C
      D43=TOTFOR/TOTCUB                                                      00640000  C
      STDEV=SQRT(DSQR/B-(TOT/B)*(TOT/B))                                     00641000  C
      WRITE(6,215)D43,DVS,ARITH,STDEV                                        00642000  C
  215 FORMAT(6H D43 =,F6.3//14H SAUTER MEAN =,F6.3//18H ARITHMETIC MEAN       00643000  C
     6=,F6.3//21H STANDARD DEVIATION =,F8.5/)                                00644000  C
      WRITE(6,212)                                                           00645000  C
  212 FORMAT(67H DIAMETER   FREQUENCY     CUM. FREQ.    VOL. FREQ.    CU     00646000  C
     4MVOL. FREQ./)                                                          00647000  C
C ARRANGE DISTRIBUTIONS                                                      00648000  C
   25 D=-0.5                                                                 00649000  C
      I=1                                                                    00650000  C
      DO 70 J=1,N                                                            00651000  C
      OUT=OUT+C(J)                                                           00652000  C
      I=I+1                                                                  00653000  C
```

```
      IF(I.GE.10)GO TO 85                                                    00654000  C
   70 CONTINUE                                                               00655000  C
   85 D=D+1.                                                                 00656000  C
      IJ=IJ+1                                                                00657000  C
      FREQ=OUT/B                                                             00658000  C
      OPDATA(IJ)=FREQ                                                        00659000  C
      IF(IOUT) 26,26,28                                                      00660000  C
   26 VFREQ=OUT*D*D*D/TOTCUB                                                 00661000  C
      CFREQ=CFREQ+FREQ                                                       00662000  C
      CVFREQ=CVFREQ+VFREQ                                                    00663000  C
      WRITE(6,205)D,FREQ,CFREQ,VFREQ,CVFREQ                                  00664000  C
  205 FORMAT(1X,F4.1,4(8X,F6.4)/)                                            00665000  C
   28 OUT=0.                                                                 00666000  C
      I=0                                                                    00667000  C
      IF(CFREQ.GE.1.0.OR.J.GE.N) GO TO 90                                    00668000  C
      GO TO70                                                                00669000  C
C PLOT DATA IF DESIRED                                                       00670000  C
   90 IF(IOUT) 29,31,31                                                      00671000  C
   31 CALL BTPLOT(OPDATA,K,M)                                                00672000  C
   29 RETURN                                                                 00673000  C
      END                                                                    00674000  C
```

```
      SUBROUTINE BTPLOT(OPDATA,K,M)                                          00675000  C
C*************************************************************************** 00676000  C
C                                                                            00677000  C
C                                                                            00678000  C
C PURPOSE - TO PLOT DISTRIBUTIONS USING RESIDENT PLOTTING SUBROUTINES ON      00679000  C
C B6718                                                                      00680000  C
C DISTRIBUTIONS MAY BE PLOTTED SINGLY OR OVERPLOTTED BY SETTING THE          00681000  C
C PARAMETER IPFORM TO 1 OR 0 RESPECTIVELY                                    00682000  C
C                                                                            00683000  C
C                                                                            00684000  C
C*************************************************************************** 00685000  C
      DIMENSION OPDATA(15,M),X(15),Y(15)                                     00686000  C
      COMMON IOUT,ISUP,IPFORM                                                00687000  C
      REAL ALABX(2)/'DIAMETER/MM '/                                          00688000  C
      REAL ALABY(4)/'NUMERICAL FREQUENCY $K$ '/                              00689000  C
      REAL ALABI(4)/'INITIAL DISTRIBUTION    '/                              00690000  C
      REAL ALABH(4)/'DISTRIBUTION NUMBER     '/                              00691000  C
C                                                                            00692000  C
C                                                                            00693000  C
C STORE X AND Y COORDINATES                                                  00694000  C
      X(1)=0.                                                                00695000  C
      Y(1)=0.                                                                00696000  C
      DO 19 J=2,15                                                           00697000  C
      JI=J-1                                                                 00698000  C
      D=J-1.5                                                                00699000  C
      X(J)=D                                                                 00700000  C
   19 Y(J)=OPDATA(JI,K)                                                      00701000  C
C                                                                            00702000  C
C                                                                            00703000  C
C CALL PLOTTING SUBROUTINES                                                  00704000  C
      IF(IPFORM.GT.0) GO TO 36                                               00705000  C
      IF(ISUP.GT.0) GO TO 35                                                 00706000  C
   36 CALL AINIT(1500)                                                       00707000  C
      CALL ASPEED(0)                                                         00708000  C
      CALL AORIG(200,150)                                                    00709000  C
      CALL AGRID(0,0,16,9,50,100)                                            00710000  C
      CALL ASPEED(3)                                                         00711000  C
      CALL ASCA(-125,0,0,100,0,5,9,2,2)                                      00712000  C
      CALL ASCA(-80,-45,50,0,0,1,16,2,2)                                     00713000  C
      CALL ALAB(250,-125,ALABX,11,3,2)                                       00714000  C
      CALL ALAB(-95,150,ALABY,23,3,4)                                        00715000  C
      IF(IPFORM.EQ.0) GO TO 35                                               00716000  C
      IF(ISUP.EQ.0) CALL ALAB(525,875,ALABI,20,1,2)                          00717000  C
      IF(ISUP.GT.0) CALL ALAB(525,875,ALABH,20,1,2)                          00718000  C
      IF(ISUP.GT.0) CALL ASCA(695,875,0,0,K,0,1,1,2)                         00719000  C
   35 CALL ASPEED(0)                                                         00720000  C
      CALL ALINE(X,Y,15,0,0,2,.05)                                           00721000  C
      IF(IPFORM.GT.0) GO TO 37                                               00722000  C
      IF(K.LT.M) GO TO 38                                                    00723000  C
   37 CALL AEND                                                              00724000  C
   38 RETURN                                                                 00725000  C
      END                                                                    00726000  C
```